hydrophobic PDMS inner layer might serve as a reservoir for entrapment of hydrophobic entities. PDMS was synthesized *via* acid-catalyzed ring opening copolymerization of D_4 and D_4H. This reaction was designed such that the as-synthesized PDMS possessed Si-H bonds in the chain for further functionalization and subsequently coupling with MNP surface. After the immobilization of the PDMS on the MNP surface, it was then used as a macroinitiator for ATRP of PPEGMA. According to the kinetic studies, the propagating rate of PPEGMA was constant during first 7 h of the reaction. Increasing time periods of ATRP of PPEGMA further enhanced the percentage of the polymer in the complex, resulting in the enhancement in its dispersibility in water. These novel magnetic field-guidable complexes might be used as nano-vehicles for loading hydrophobic entities, such as drugs, fluorophores and biomolecules, by partitioning to the hydrophobic inner shell on the particle surface.

Acknowledgement

The authors thank the Thailand Research Fund (TRF) and Naresuan University (DBG5380001) for financial funding. The Center of Excellence for Innovation in Chemistry (PERCH-CIC), Commission on Higher Education, Ministry of Education is also gratefully acknowledged for financial support.

References

Astete CE, Kumar CSSR, Sabliov CM (2007) Size control of poly(d,l-lactide-co-glycolide) and poly(d,l-lactide-co-glycolide)-magnetite nanoparticles synthesized by emulsion evaporation technique. Colloids Surf. 299:209-216.

Bica D, Vékás L, Avdeev MV, Marinica O, Socoliu V, Balasoiu M, Garamus VM (2007) Sterically stabilized water based magnetic fluids: Synthesis, structure and properties. J Magn Magn Mater 311:17-21.

Brestovac B, Harnett GB, Smith DW, Frost F, Shellam GR (2005) Multiplex nested PCR (MNP) assay for the detection of 15 high risk genotypes of human papillomavirus. J Clin Virol 33:116-122.

Brown DA, Price GJ (2001) Preparation and thermal properties of block copolymers of PDMS with styrene or methyl methacrylate using ATRP. Polymer 42:4767-4771.

Cao H, He J, Deng L, Gao X (2009) Fabrication of cyclodextrin-functionalized superparamagnetic Fe_3O_4/amino-silane core-shell nanoparticles via layer-by-layer method. Appl Surf Sci 255:7974-7980.

Chorny M, Hood E, Levy RJ, Muzykantov VR (2010) Endothelial delivery of antioxidant enzymes loaded into non-polymeric magnetic nanoparticles. J Control Release 146:144-151.

Fan Q-L, Neoh K-G, Kang E-T, Shuter B, Wang S-C (2007) Solvent-free atom transfer radical polymerization for the preparation of poly(poly(ethyleneglycol) monomethacrylate)-grafted Fe_3O_4 nanoparticles: Synthesis, characterization and cellular uptake. Biomaterials 28: 5426-5436.

Galeotti F, Bertini F, Scavia G, Bolognesi A (2011) A controlled approach to iron oxide nanoparticles functionalization for magnetic polymer brushes. J Colloid Interf Sci 360:540-547.

Harris LA, Goff JD, Carmichael AY, Riffle JS, Harburn JJ, Pierre TG, Saunders M (2003) Magnetite nanoparticle dispersions stabilized with triblock copolymers. Chem Mater 15:1367-1377.

Hong RY, Feng B, Chen LL, Liu GH, Li HZ, Zheng Y, Wei DG (2008) Synthesis, characterization and MRI application of dextran-coated Fe_3O_4 magnetic nanoparticles. Biochem Eng J 42:290-300.

Jaffer FA, Libby P, Weissleder R (2006) Molecular and cellular imaging of atherosclerosis: emerging applications. J Am Coll Cardiol 47:1328-1338.

Jain TK, Foy SP, Erokwu B, Dimitrijevic S, Flask CA, Labhasetwar V (2009) Magnetic resonance imaging of multifunctional pluronic stabilized iron-oxide nanoparticles in tumor-bearing mice. Biomaterials 30:6748-6756.

Jiang J, Lu X, Lu Y (2008) Stereospecific preparation of polyacrylamide with low polydispersity by ATRP in the presence of Lewis acid. Polymer 49:1770-1776.

Kralj S, Makovec D, Campelj S, Drofenik M (2010) Producing ultra-thin silica coatings on iron-oxide nanoparticles to improve their surface reactivity. J Magn Magn Mater 322:1847-1853.

Lee K, Park C, Moon H-Y, Ahn E, Park HE, Ihm S-H, Seung K-B, Yoon T-J, Chang K, Lee C, Cheong C, Hong KS (2009) Magnetic resonance tracking of multifunctional nanoparticle-labeled mouse mesenchymal stem cells in a mouse model of myocardial infarction. Curr Appl Phys 9:12-14.

Meerod S, Tumcharern G, Wichai U, Rutnakornpituk M (2008) Magnetite nanoparticles stabilized with polymeric bilayer of poly(ethylene glycol) methyl ether-poly(ε-caprolactone) copolymers. Polymer 49:3950-3956.

Moisescu C, Bonneville S, Tobler D, Ardelean I, Benning LG (2008) Controlled biomineralization of magnetite (Fe_3O_4) by Magnetospirillum gryphiswaldense. Mineral Mag 72:333–336.

Monge S, Haddleton DM (2004) Synthesis of precursors of poly(acryl amides) by copper mediated living radical polymerization in DMSO. Eur Polym J 40:37-45.

Neugebauer D (2007) Graft copolymers with hydrophilic and hydrophobic polyether side chains. Polymer 48:4966-4973.

Öisjöen F, Schneiderman JF, Astalan AP, Kalabukhov A, Johansson C, Winkler D (2009) A new approach for bioassays based on frequency- and time-domain measurements of magnetic nanoparticles. Biosens Bioelectron 25:1008-1013.

Okassa LN, Marchais H, Douziech-Eyrolles L, Hervé K, Cohen-Jonathan S, Munnier E, Soucé M, Linassier C, Dubois P, Chourpa I (2007) Optimization of iron oxide nanoparticles encapsulation within poly(d,l-lactide-co-glycolide) sub-micron particles. Eur J Pharm Biopharm 67:31-38.

Park NH, Park JK, Choi Y, Yoo C-I, Lee CR, Lee H, Kim HK, Kim S-R, Jeong T-H, Park J, Yoon CS, Kim Y (2003) Whole blood manganese correlates with high signal intensities on T1-weighted MRI in patients with liver cirrhosis. NeuroToxicology 24:909-915.

Pei W, Kumada H, Natusme T, Saito H, Ishio S (2007) Study on magnetite nanoparticles synthesized by chemical method. J Magn Magn Mater 310:2375-2377.

Pich A, Bhattacharya S, Boyko V, Adler H-JP (2004) Temperature-sensitive hybrid microgels with magnetic properties. Langmuir 20:10706-10711.

Prai-in Y, Tankanya K, Rutnakornpituk B, Wichai U, Montembault V, Pascual S, Fontaine L, Rutnakornpituk M (2012) Azlactone functionalization of magnetic nanoparticles using ATRP and their bioconjugation. Polymer 53:113-120.

Qiang R, Fanghong G, Bibiao J, Dongliang Z, Jianbo F, Fudi G (2006) Preparation of hyperbranched copolymers of maleimide inimer and styrene by ATRP. Polymer 47:3382-3389.

Ragheb RT, Riffle JS (2008) Synthesis and characterization of poly(lactide-b-siloxane-b-lactide) copolymers as magnetite nanoparticle dispersants. Polymer 49:5397-5404.

Reining B, Keul H, Hcker H (2002) Amphiphilic block copolymers comprising poly(ethylene oxide) and poly(styrene) blocks: synthesis and surface morphology. Polymer 43:7145-7154.

Rutnakornpituk M, Meerod S, Boontha B, Wichai U (2009) Magnetic core-bilayer shell nanoparticle: A novel vehicle for entrapmentof poorly water-soluble drugs. Polymer 50:3508-3515.

Rutnakornpituk M, Puangsin N, Theamdee P, Rutnakornpituk B, Wichai U (2011) Poly(acrylic acid)-grafted magnetic nanoparticle for conjugation with folic acid. Polymer 52:987-995.

Semsarzadeh MA, Mirzaei A, Vasheghani-Farahani E, Nekoomanesh Haghighi M (2003) Atom transfer radical polymerization of (meth)acrylates and their novel block copolymers with vinyl acetate. Eur Polym J 39:2193-2201.

Storm PB, Moriarity JL, Tyler B, Burger PC, Brem H, Weingart J (2002) Polymer delivery of camptothecin against 9L gliosarcoma: release, distribution, and efficacy. J Neuro-Oncol 6:209-217.

Sun Y, Ding X, Zheng Z, Cheng X, Hu X, Peng Y (2007) Surface initiated ATRP in the synthesis of iron oxide/polystyrene core/shell nanoparticles. Eur Polym J 43:762-772.

Wootthikanokkhan J, Peesan M, Phinyocheep P (2001) Atom transfer radical polymerizations of (meth)acrylic monomers and isoprene. Eur Polym J 37: 2063-2071.

Yi Z, Pan K, Jiang L, Zhang J, Dan Y (2007) Copper-based reverse ATRP process of styrene in mixed solvents. Eur Polym J 43:2557-2563.

Yin M, Habicher WD, Voit B (2005) Preparation of functional poly(acrylates and methacrylates) and block copolymers formation based on polystyrene macroinitiator by ATRP. Polymer 46:3215-3222.

Zhang Y, Zhang J (2005) Surface modification of monodisperse magnetite nanoparticles for improved intracellular uptake to breast cancer cells. J Colloid Interf Sci 283:352-357.

Supporting Information

(A) Synthesis of tris-[2-(dimethylamino)ethyl]amine (Me_6Tren) (Figure S1)

Tris-(2-aminoethyl)amine (Tren) (10 ml, 0.33 mol, 1 equiv.) was slowly dropped into the mixture of formic acid (64 ml, 6.67 mol, 20 equiv.) and formaldehyde (54 ml, 3.34 mol, 10 equiv.) at 0^oC in an ice bath. The mixture was heated to 120^oC and stirred under reflux overnight. Unreacted formic acid and formaldehyde were removed by rotary evaporation. Then, the resulting orange oil was adjusted to pH 10 with saturated sodium

hydroxide solution. The oil layer was extracted into diethyl methyl ether (four times), and the volatiles were removed by rotary evaporation to leave a yellow oil. The resulting oil was distilled under reduced pressure to give a colorless liquid (84% yield).

Figure S1. Synthesis of tris-(2-(dimethylamino)ethyl)amine (Me_6Tren)

Figure S2B showed a ^1H NMR spectrum of Me_6Tren in comparison with that of Tren starting reagent (Figure S2A). The formation of Me_6Tren was identified by the presence of the methyl protons at 2.14 ppm (signal *a*). Also, the methylene protons of signal *b* (2.52 ppm) and signal *c* (2.28 ppm) confirmed the formation of Me_6Tren.

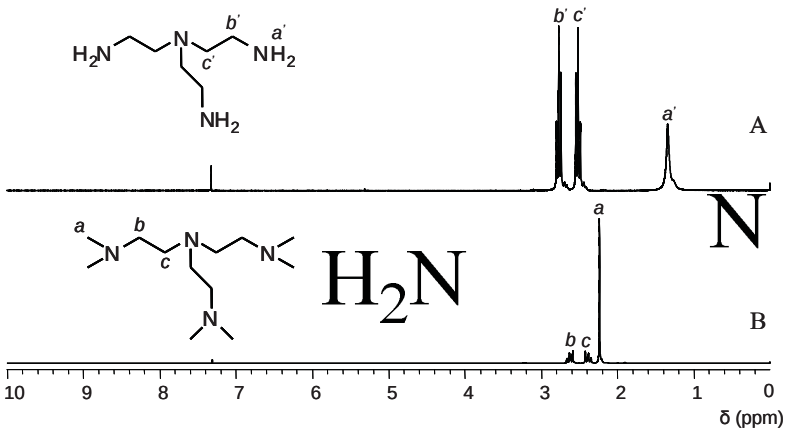

Figure S2. ^1H NMR spectra of (A) tris-(2-aminoethyl)amine (Tren) (solvent:$CDCl_3$), and tris-(2-(dimethylamino)ethyl)amine (Me_6Tren) (solvent: $CDCl_3$).

(B) Synthesis of oleic acid-coated MNP

In a typical procedure, iron (III) acetylacetonate ($Fe(acac)_3$) (5.0 g, 0.014 mole) and benzyl alcohol (90 ml) were thoroughly mixed by magnetic stirring with hexamethylene under nitrogen flow. The mixture was heated to 180°C for 48 h. During this process, the initial red-brown color of the mixture changed to black, indicating the formation of MNP.

The precipitants were removed from the dispersion using an external magnet and repetitively washed with ethanol and CH_2Cl_2. After a drying process *in vacuo*, the resultant products were obtained as fine black powder. To obtain MNP with oleic acid coating, an MNP dispersion (0.6 g MNP in 30 ml toluene) was sonicated for 1 h, followed by an addition of oleic acid (4 ml). It was then sonicated for another 3 h under nitrogen atmosphere. Finally, large aggregate that may arise was separated from the oleic acid-coated MNP by centrifugation at 5000 rpm for 15 min.

FTIR spectrum of the as-synthesized MNP indicated a characteristic absorption peak of the Fe-O bond at 574 cm^{-1} without the presence of the signal of organic component (Figure S3A). Bare MNP were subsequently coated with oleic acid to form dispersible MNP in toluene. After the solution was separated from MNP precipitant by centrifugation and dried *in vacuo*, the resultant black solid was characterized by FTIR to elucidate its functional groups (Figure S3B). FT-IR (KBr disc) υ_{max} : 3369 cm^{-1} (O-H stretching), 2920 cm^{-1} (C-H stretching), 1403 cm^{-1} (CH_2 stretching) and 589 cm^{-1} (Fe-O stretching).

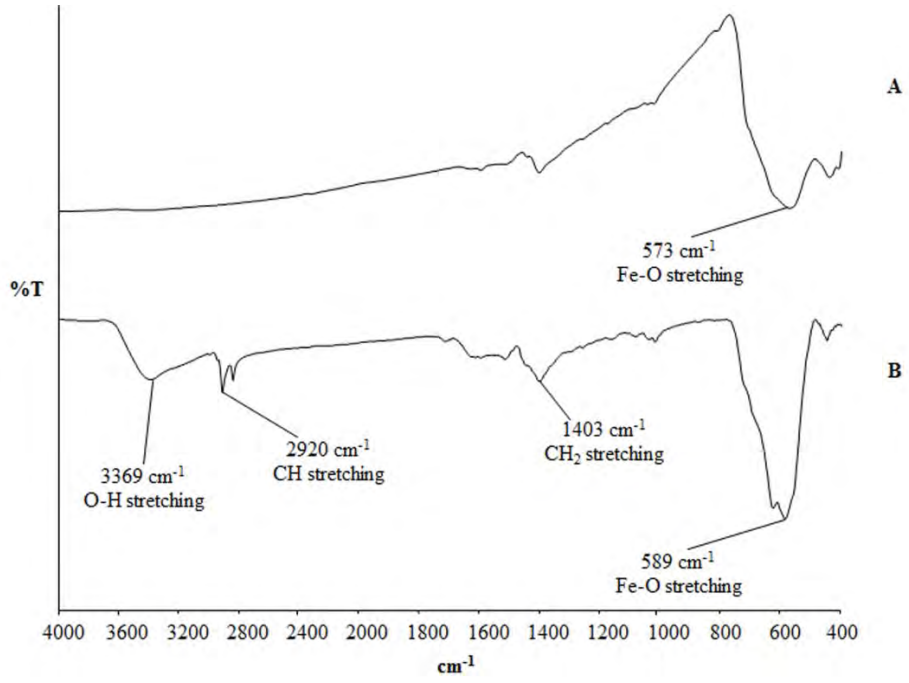

Figure S3. FTIR spectra of (A) bare MNP and (B) oleic acid-coated MNP

(C) Synthesis of dialkyl bromide-terminated disiloxane (dialkyl bromide disiloxane) as a free initiator in ATRP reaction

The dialkyl bromide disiloxane was synthesized for use as a free initiator in the ATRP reaction in competitive with those of the PDMS-coated MNP having alkyl bromide on

its surface. To synthesize the dialkyl bromide disiloxane, BIBB (2 ml, 0.013 mole) was slowly added into the mixture of disiloxane diol (1.23 g, 5.91 mmole) and TEA (2 ml, 0.013 mole) dissolved in anhydrous toluene (10 ml) at 0^{o}C under nitrogen atmosphere. A white precipitate was formed upon the addition. The reaction was set at room temperature for 24 h. The mixture was passed through a filter paper to remove salts and the filtrate was evaporated to remove TEA under reduced pressure. The resultant product appeared as yellow oil with 88% yield.

Figure S4C shows ^{1}H NMR spectrum of the resultant dialkyl bromide disiloxane in comparison with those of BIBB and disiloxane diol (Figure S4A and S4B, respectively). The shift of methylene protons at 3.50 ppm of disiloxane diol (peak *d*, Figure S4A) to 4.20 ppm of dialkyl bromide disiloxane (peak *d*', Figure S4C) indicated the occurrence of this coupling reaction. Also, the presence of the signal at 1.96 ppm corresponding to -C(C$\underline{H}_3)_2$Br (peak *f*', Figure S4C) signified the formation of dialkyl bromide disiloxane. In good agreement with ^{1}H NMR, FTIR spectra (Figure S5) exhibited characteristic absorption signals of dialkyl bromide disiloxane; 1737 cm^{-1} (-O-C=O stretching), 2959 cm^{-1} (CH stretching), 1411 cm^{-1} (CH_2 stretching), 1259 cm^{-1} (Si-CH_3 stretching), 1051 cm^{-1} (Si-O stretching) and 799 cm^{-1} (Si-C stretching). ^{1}H NMR (400 MHz, $CDCl_3$) δ_H : 0.06 [m, 12H, Si-C$\underline{H}_3$], 0.60 [t, 4H, Si-C$\underline{H}_2$-CH_2], 1.60 [m, 4H, CH_2-C$\underline{H}_2$-CH_2], 1.90[d, 12H, -C(C$\underline{H}_3)_2$Br] and 4.20 [t, 4H, C$\underline{H}_2$-O-(C=O)]. FTIR (thin film) υ_{max} : 2959 cm^{-1} (CH stretching), 1737 cm^{-1} (-C=O stretching), 1411 cm^{-1} (CH_2 stretching), 1259 cm^{-1} (Si-CH_3 stretching), 1051 cm^{-1} (Si-O stretching) and 799 cm^{-1} (Si-C stretching).

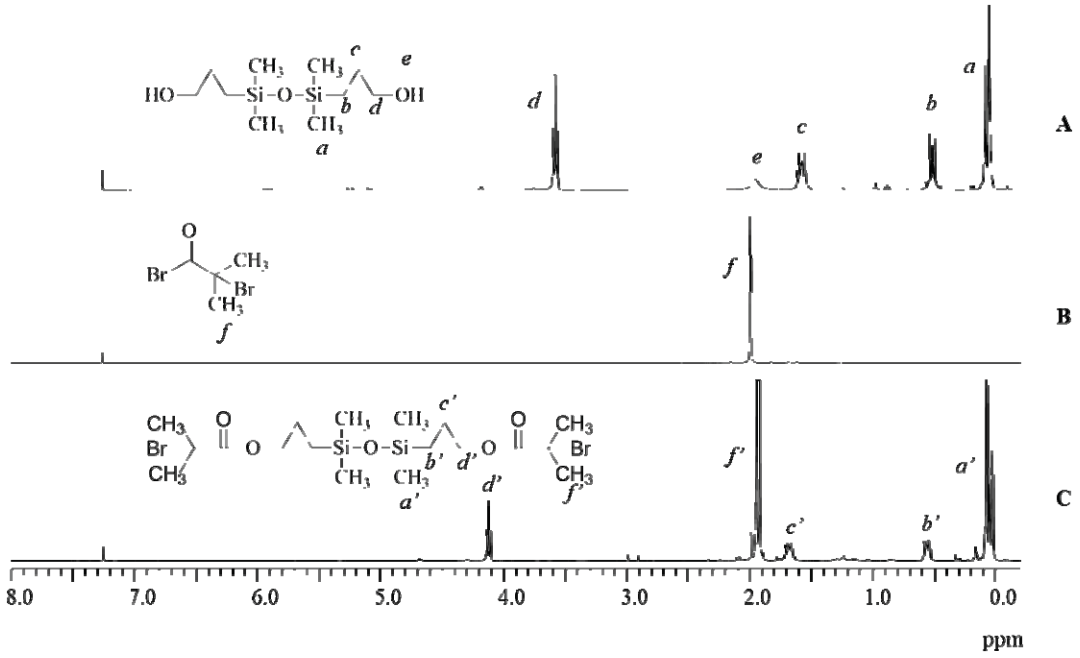

Figure S4 ^{1}H NMR spectra of (A) disiloxane diol, (B) BIBB and (C) dialkyl bromide disiloxane

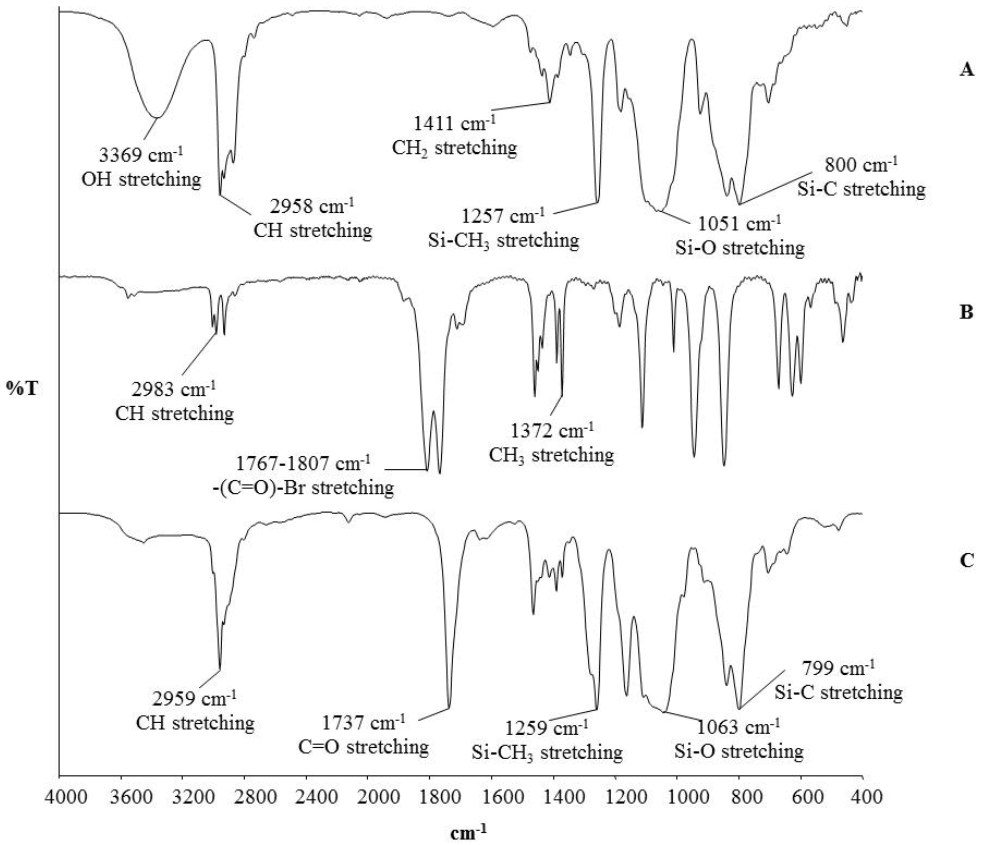

Figure S5 FTIR spectra of (A) disiloxane diol, (B) BIBB and (C) dialkyl bromide disiloxane

(D) ^{1}H NMR and FTIR spectra of disiloxane diol as an endcapper

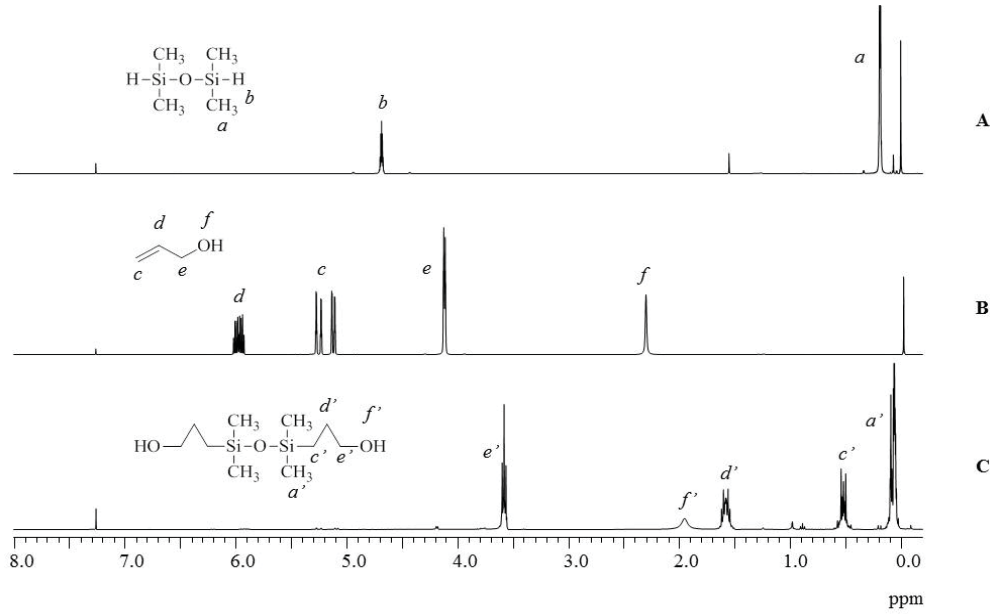

Figure S6 ^{1}H NMR spectra of (A) 1,1,3,3-tetramethylsiloxane, (B) allyl alcohol and (C) disiloxane diol

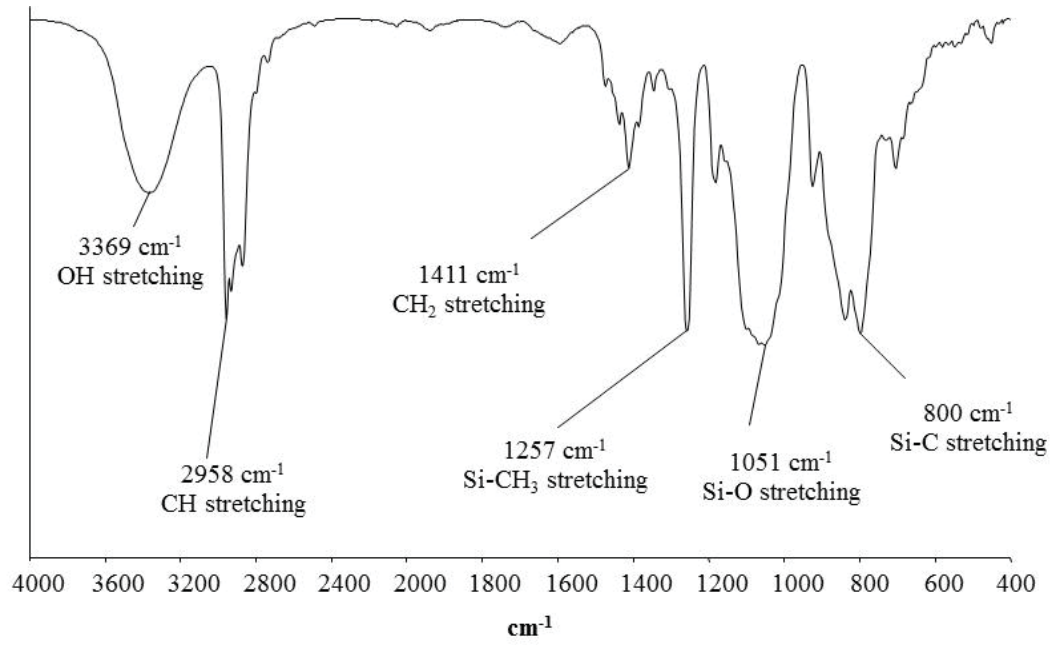

Figure S7 FTIR spectrum of disiloxane diol (an endcapper)

(E) ^{1}H NMR spectrum of PDMS-OH

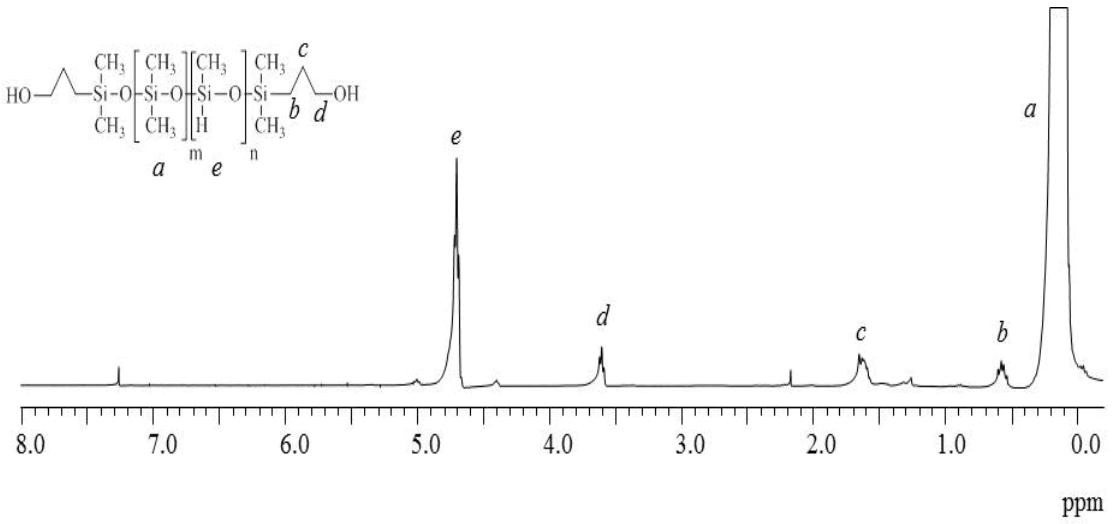

Figure S8 ^{1}H NMR spectrum of PDMS-OH

(F) ^{1}H NMR spectra of allyl-containing silane compound

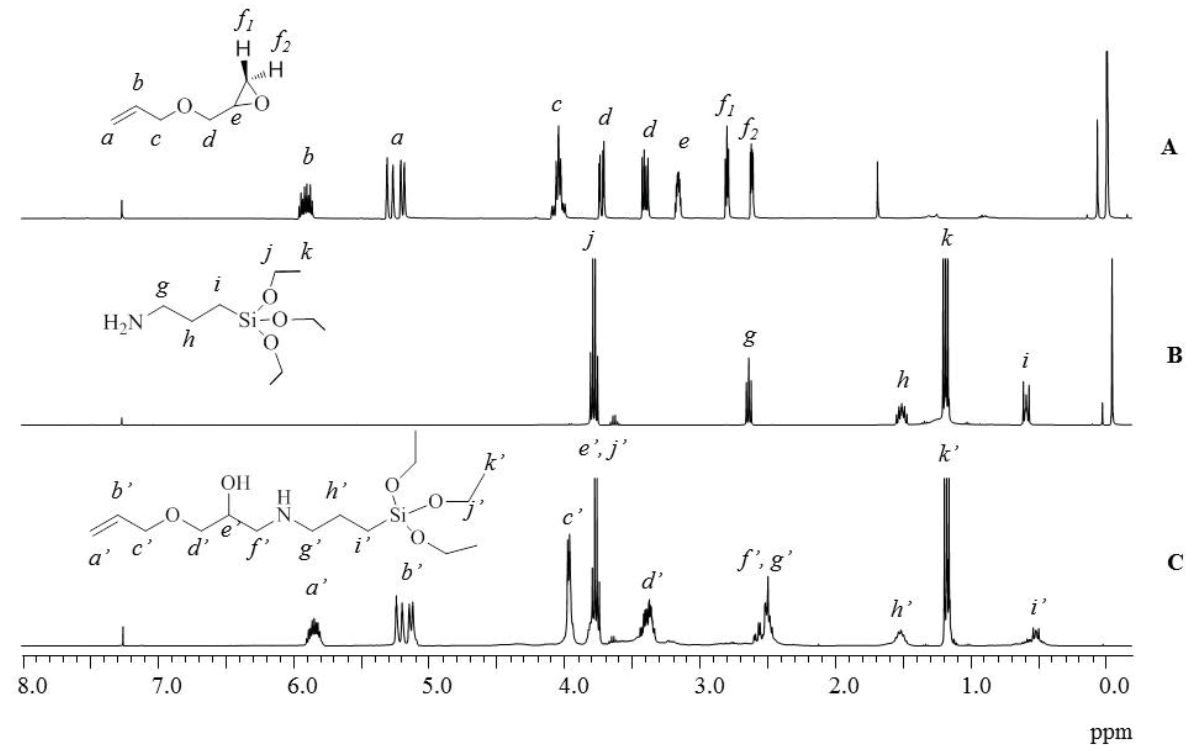

Figure S9 ^{1}H NMR spectra of (A) allyl glycidyl ether, (B) aminopropylsilane (APS) and (C) allyl-containing silane compound

(G) Determination of crystal structure of magnetite nanoparticles *via* SAED technique

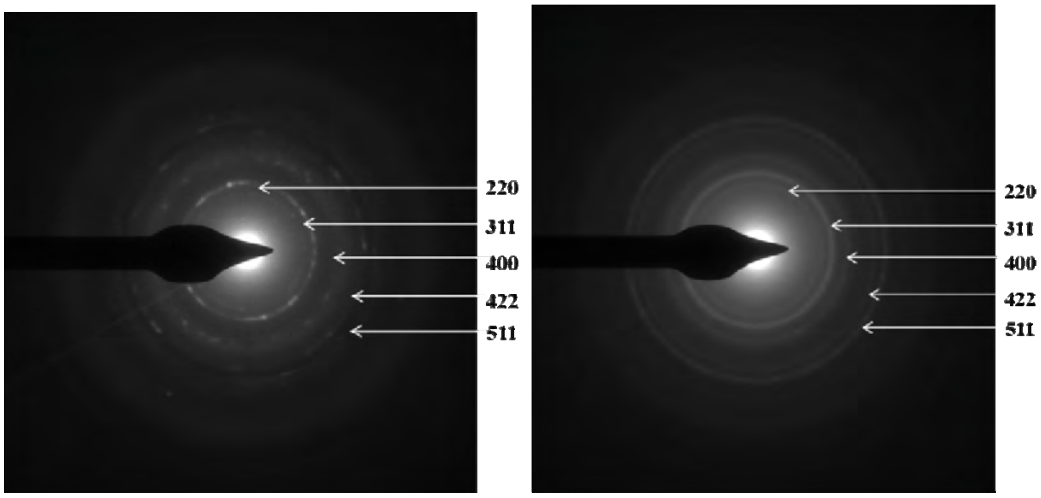

A) Bare MNP B) PDMS-coated MNP

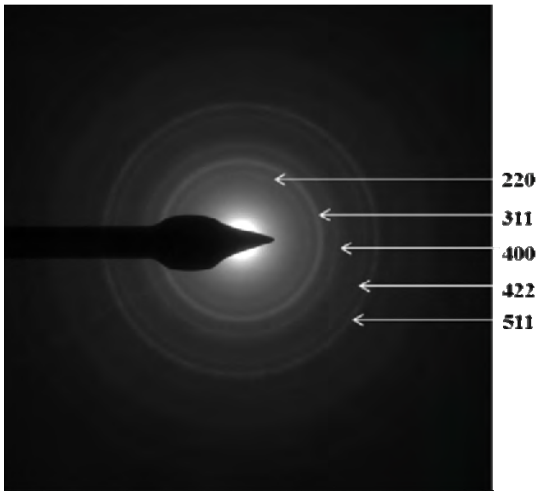

C) PPEGMA-coated MNP

Figure S10 Selected area electron diffraction (SAED) patterns of the particles obtaining from each step of the reactions

(H) Stability studies of PDMS-coated MNP (before ATRP) in toluene and PPEGMA-coated MNP (after ATRP) in water

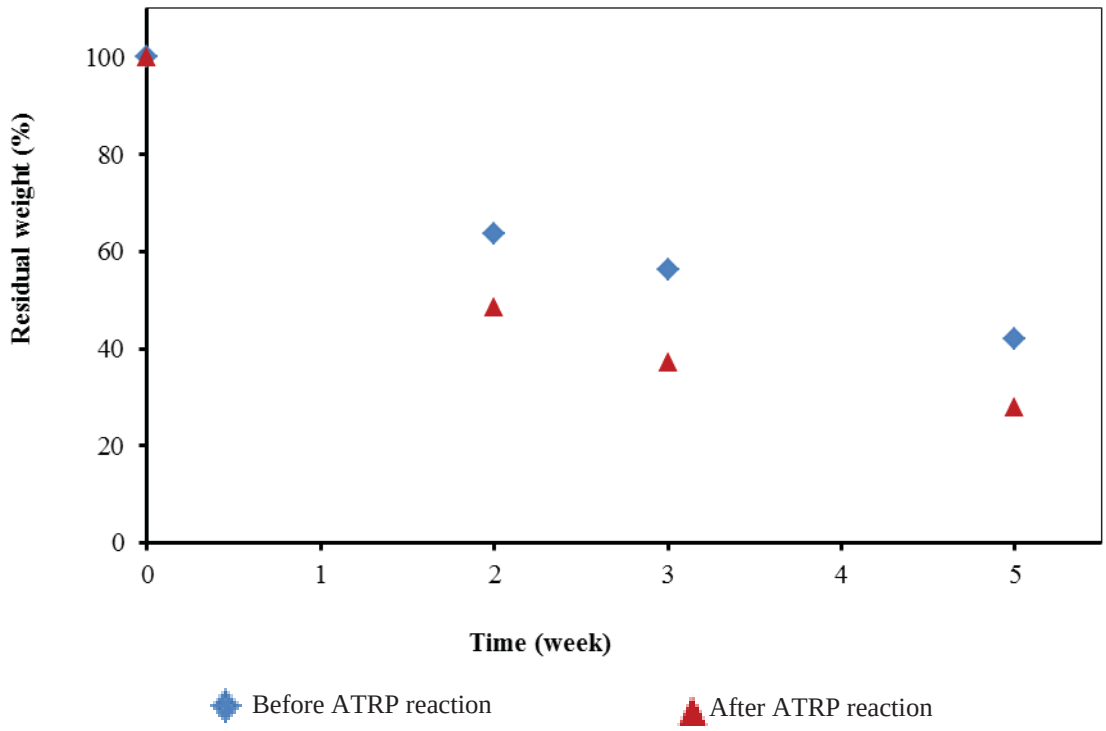

Figure S11 Percent residual weight of MNP remaining dispersible in the dispersions as a function of time. MNP before ATRP (PDMS-coated MNP) was dispersed in toluene and MNP after ATRP (PPEGMA-coated MNP) dispersed in water

(I) Calculation of indomethacin entrapment efficiency (%EE)

Table S1 Percent entrapment efficiency (%EE) determined *via* UV-visible spectrophotometry

Type of copolymer used	Wt of loaded drug (g)	Wt of the entrapped drug in complex (g)	% EE
PEGMA-coated MNP	8.40×10^{-4}	5.222×10^{-4}	62.17

Entrapment efficiency (%EE) was determined from the following equation:

$$\%\text{Entrapment Efficency}(\%EE) = \frac{\text{Weight of the entrapped drug in the complex}}{\text{Weight of loaded drug}} \times 100$$

Calculation of the weight of the loaded indomethacin

0.1 ml of the indomethacin-THF solution (0.01 g indomethacin/ml THF) was loaded into the dispersion of copolymer-magnetite complex in water. From the calibration curve of standard indomethacin curve, indomethacin purity was 84%.

Therefore, weight of loaded indomethacin $= \frac{(0.1ml).(0.01g/ml)(84)}{100} = 8.40\times10^{-4}$ g

Calculation of the excess drug in the solution

The weight of the entrapped drug in the complex was determined from the difference of the weights of the loaded drug and the excess of the drug remaining dispersible in the solution.

One ml of indomethacin-loaded particle dispersion was 44-time diluted with water.
The observed concentration of indomethacin from UV technique was 7.22 ppm.

Therefore, the weight of indomethacin in the solution $= \frac{(7.22\ mg)(1\ ml)(44)}{1000\ ml}$

$= 0.3178$ ml $= 3.178\times10^{-4}$ g

Calculation of the entrapped drug in the complex

The entrapped drug in the complex = The weight of the loaded drug - the excess of the drug in the solution

The entrapped drug in the complex $= (8.40\times10^{-4}\text{ g}) - (3.178\times10^{-4}\text{ g})$

$= 5.222\times10^{-4}$ g

Therefore, $\%EE = \frac{5.222\times10^{-4}\text{ g}}{8.40\times10^{-4}\ g} \times 100 = 62.17$ %w/w

(J) Calculation of drug (indomethacin) loading efficiency (%DLE)

Table S2 Percent drug (indomethacin) loading efficiency (%DLE) determined *via* UV-visible spectrophotometry

Type of copolymer used	Wt of nanoparticles (g)	Wt of the entrapped drug in complex (g)	% DLE
PEGMA-coated MNP	1.9×10^{-3}	5.2×10^{-4}	27.48

Drug (indomethacin) loading efficiency (%DLE) was determined from the following equation:

$$\%\text{Drug Loading Efficiency}(\%\text{DLE}) = \frac{\text{Weight of entrapped drug in the complex}}{\text{Weight of nanoparticles}} \times 100$$

The weight of the MNP complex = 1.9×10^{-3} g

Calculation of the entrapped indomethacin was illustrated in the above example of %EE. Thus,

$$\%\text{DLE} = \frac{(5.222\times10^{-4}\ \text{g})(100)}{1.9\times10^{-3}\ \text{g}} = 27.48\ \%\text{w/w}$$

RESEARCH OUTPUT

1. 4 international publications
2. 16 international presentations
3. 5 invited oral presentations
4. National awards and conference awards
5. International collaboration

1) 4 International publications

1.1) M. Rutnakornpituk, N. Puangsin, P. Theamdee, B. Rutnakornpituk, U. Wichai, “Poly(acrylic acid)-grafted magnetic nanoparticle for conjugation with folic acid”, *Polymer* 52, 987-995 (2011) (IF = 3.828)

1.2) Y. Prai-in, K. Tankanya, B. Rutnakornpituk, U. Wichai, V. Montembault, S. Pascual, L. Fontaine, M. Rutnakornpituk, “Azlactone functionalization of magnetic nanoparticles using ATRP and their bioconjugation”, *Polymer* 53, 113-120. (2012) (IF = 3.438)

1.3) P. Theamdee, R. Traiphol, B. Rutnakornpituk, U. Wichai, M. Rutnakornpituk, “Surface modification of magnetite nanoparticle with azobenzene-containing water dispersible polymer”, *Journal of Nanoparticle Research*, 13, 4463-4477 (2011). (IF = 3.25)

1.4) B. Thong-On, B. Rutnakornpituk, U. Wichai, M. Rutnakornpituk, “Magnetite nanoparticle coated with amphiphilic bilayer surfactant of polysiloxane and poly(poly(ethylene glycol) methacrylate)”, *Journal of Nanoparticle Research* 14, 953-964 (2012) (IF = 3.287)

2) 16 International presentations

2.1) PERCH-CIC Congress VIII, 5-8 May 2013, Jomtien Palm Beach& Resort, Pattaya, Chonbury, Thailand.

2.1.1) Pawinee Theamdeea and Metha Rutnakornpituk, Cysteine-conjugated magnetic nanoparticle

2.2) Pure and Applied Chemistry International Conference (PACCON2012), 11-13 January 2012, The Empress Hotel, Chiang Mai, Thailand

2.2.1) Bandit Thong-On and Metha Rutnakornpituk, Magnetite nanoparticle coated with amphiphilic bilayer stabilizer of PDMS and PEGMA

2.2.2) Siraprapa Meerod and Metha Rutnakornpituk, Smart magnetic nanocomposite of magnetite nanoparticle in thermal responsive polymer

2.2.3) Pawinee Theamdee, Metha Rutnakornpituk, Surface Modification of Magnetite Nanoparticle with External Stimuli-Responsive polymer *via* ATRP and Click Reaction

2.2.4) Yingrak Prai-in, Kritsada Tankanya, Boonjira Rutnakornpituk, Uthai Wichai, Véronique Montembault, Sagrario Pascual, Laurent Fontaine and Metha Rutnakornpituk, Hydrophilic azlactone functionalized magnetic nanoparticles and their application as scavengers

2.3) Pure and Applied Chemistry International Conference (PACCON 2011), 5-6 January 2011, The Miracle Grand Hotel, Bangkok, Thailand

2.3.1) Patcharin Kanhakeaw, Boonjira Rutnakornpituk, Uthai Wichai and Metha Rutnakornpituk, Synthesis of polyelectrolyte-grafted magnetite nanoparticle

2.3.2) Bandit Thong-On and Metha Rutnakornpituk, Polysiloxane-poly(ethylene glycol) methyl ether methacrylate amphiphilic block copolymer prepared *via* atom transfer radical polymerization

2.4) PERCH-CIC Congress VII, 4-7 May 2011, Jomtien Palm Beach& Resort, Pattaya, Chonbury, Thailand

2.4.1) Bandit Thong-On, and Metha Rutnakornpituk, Synthesis of amphiphilic block copolymer via atom transfer radical polymerization

2.4.2) Patcharin Kanhakeaw and Metha Rutnakornpituk, Water dispersible magnetite nanoparticle with pH sensitive surface

2.4.3) Pawinee Theamdee and Metha Rutnakornpituk, Surface Modification of Magnetite Nanoparticle with External Stimuli-Responsive Polymer via ATRP and Click Reaction

2.4.4) Siraprapa Meerod and Metha Rutnakornpituk, Magnetite nanoparticles stabilized with polydimethylsiloxane brush

2.5) Pure and Applied Chemistry International Conference 2009 (PACCON2009), Phitsanulok, Thailand, 14-16 January 2009

2.5.1) Nipaporn Puangsin, Uthai Wichai and Metha Rutnakornpituk, Surface Functionalization of Iron Oxide Nanoparticles Coated with Poly(acrylic acid), Oral presentation

2.5.2) Siraprapa Meerod, Uthai Wichai and Metha Rutnakornpituk, Magnetic core-shell nanoparticles : effect of amphiphilic block lengths on drug-released behavior, Oral presentation

2.5.3) Pawinee Theamdee, and Metha Rutnakornpituk, Atom transfer radical polymerization of poly (ethylene glycol) methyl ether methacrylate (PEGMA) brush on magnetic nanoparticle surface, Poster presentation

2.6. PERCH-CIC Congress VI, 3-6 May 2009, Jomtien Palm Beach& Resort, Pattaya, Chonbury, Thailand

2.6.1) Siraprapa Meerod, Uthai Wichai and Metha Rutnakornpituk, Indomethacin-loaded bilayer surface magnetite nanoparticles and its released behavior

2.6.2) Nipaporn Puangsin, Uthai Wichai and Metha Rutnakornpituk, Efficient immobilization of folic acid onto nanoparticle surface

2.1) PERCH-CIC Congress VIII, 5-8 May 2013, Jomtien Palm Beach& Resort, Pattaya, Chonbury, Thailand.

PERCH-CIC

CONGRESS VIII

Theme: Chemistry for Creative Economy

การประชุมวิชาการ

ศูนยความเป็นเลิศด้านนวัตกรรมทางเคมี ครั้งที่ 8

5-8 May 2013

Jomtien Palm Beach Hotel & Resort Pattaya, Chonburi, Thailand

PERCH-CIC
PERDO

Center of Excellence for Innovation in Chemistry

www.perch-cic.org

S3-P65

Cysteine-Conjugated Magnetic Nanoparticle

Pawinee Theamdee and Metha Rutnakornpituk

Department of Chemistry and Center of Excellence for Innovation in Chemistry, Faculty of Science, Naresuan University, Phitsanulok 65000, Thailand.

Introduction and Objective

Magnetite nanoparticles (MNPs) have been intensively studied for various applications such as hyperthermia treatment of tumors, magnetic field-guided drug delivery, biomolecular magnetic separation, diagnosis and magnetic resonance imaging [1]. Surface modification of MNPs with biomolecules such as amino acids, peptides and antibodies allows these particles even more practical and applicable in biomedical-related uses. In the current work, surface modification of MNPs with cysteine, a water-soluble and sulfur-containing amino acid, is herein reported [2]. Cysteine grafted on MNP surface hypothetically renders them to be hydrophilic, biocompatible and capable to specifically interact with silver nanoparticles, which might be then applicable in antibacterial applications.

Methods

MNPs were first synthesized via a thermal decomposition of $Fe(acac)_3$ precursor, and then modified with 3 aminopropyltrimethoxysilane (APS) to obtain particles with reactive amino groups ($-NH_2$) on their surface. Amino groups on the MNP were then reacted with succinic anhydride to obtain COOH-containing MNPs (COOH-MNPs). These particles were then coupled with amino groups of cysteine, leaving SH and COOH groups dangling out from the MNPs surface. The surface-modified MNPs with cysteine on their surface are anticipated to possess dual responsive properties due to the existence of both -COOH, a pH-responsive functional group, and –SH, which has a specific interaction with silver nanoparticle.

Results and Conclusion

FTIR of the cysteine-coated MNPs showed characteristic signals attributed to the Fe-O of MNP core at 586 cm^{-1} and a thiol-derived signal (S-H) of cysteine at 2076 cm^{-1}. Photocorrelation spectroscopy (PCS) indicated that, as increasing pH of the dispersions, their hydrodynamic diameter was decreased and their surface charge became more negative. It was rationalized that the formation of carboxylate (COO-) on their surface produced additional electrostatic repulsion force to the particles, leading to the improved dispersibility of the particle in water. It is hoped that these particles can attract a great attention in the biomedical field as a stimulus-sensitive material.

Keywords: magnetic nanoparticles (MNPs), cysteine

Selected References:

1. Boeun, L.; Sangkyun, K. *J. Ind. Eng.*, **2011**, *17*, 762-766.
2. Koichiro, H. *Chem. Mater.*, **2010**, *22*, 3768-3772.

Pawinee Theamdee (ภาวินี (พิมดี)) **Ph.D. Student**
b 1985 in Sukhothai, Thailand
Naresuan University, Thailand, Chemistry, B.Sc. 2006
Naresuan University, Thailand, Chemistry, M.Sc. 2009
Research field: nanoparticle and polymer synthesis

2.2) Pure and Applied Chemistry International Conference (PACCON2012), 11-13 January 2012, The Empress Hotel, Chiang Mai, Thailand

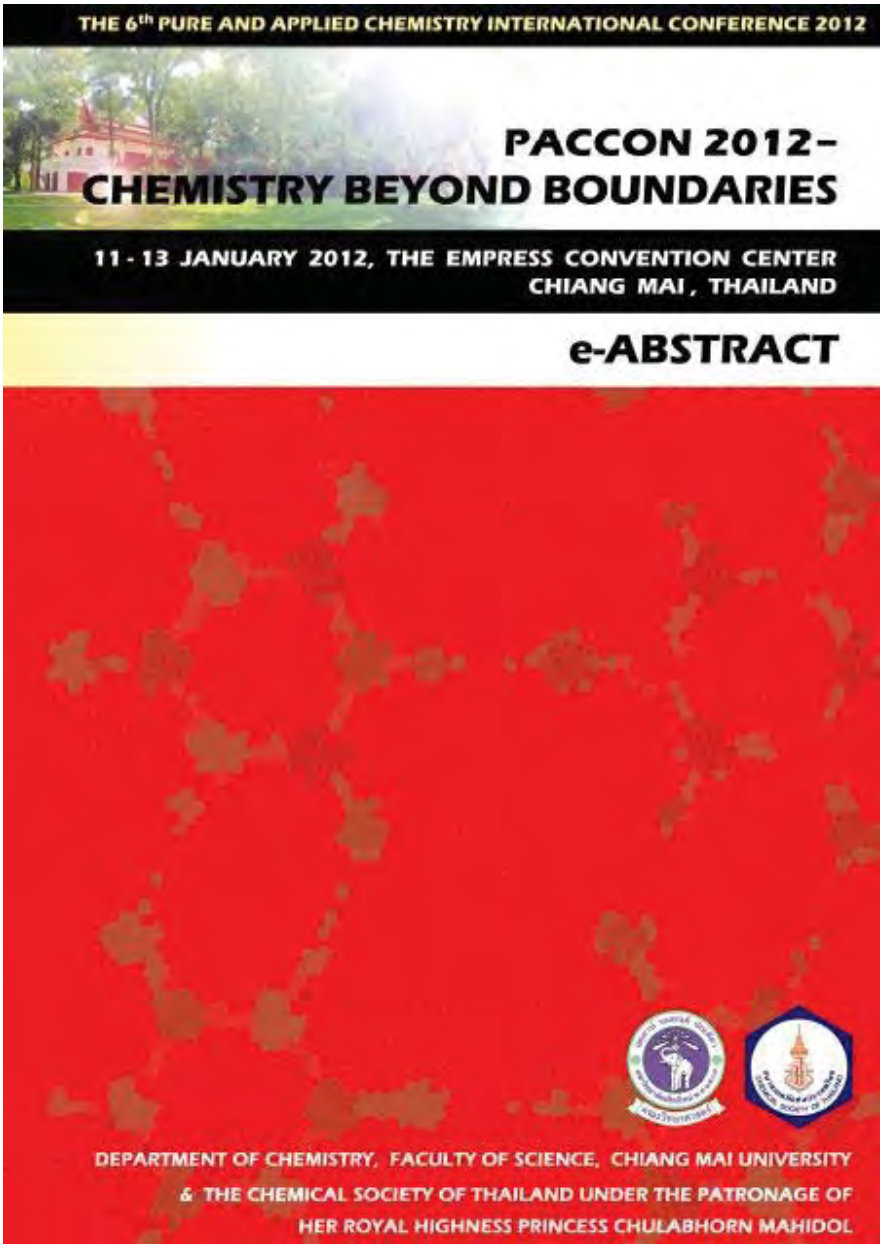

MNT-P-260

MAGNETITE NANOPARTICLE COATED WITH AMPHIPHILIC BILAYER STABILIZER OF PDMS AND PEGMA

Bandit Thong-on, Metha Rutnakornpituk*

Department of Chemistry and Center of Excellence for Innovation in Chemistry, Faculty of Science, Naresuan University, Phitsanulok, 65000 Thailand
**Corresponding Author : methar@nu.ac.th*

ABSTRACT

The surface modification of magnetite nanoparticle (MNP) with bilayer stabilizer of polydimethylsiloxane (PDMS) inner shell and poly(ethylene glycol) methyl ether methacrylate (PEGMA) corona is presented. PDMS was first prepared *via* acid-catalyzed ring-opening copolymerization of octamethylcyclotetrasiloxane (D_4) and tetramethylcyclotetrasiloxane (D_4H) using dihydroxypropyltetramethyl disiloxane as an end capping agent and to control its molecular weight. Copolymerization of D_4 and D_4H was performed to gain the polysiloxane containing Si-H bonds for further coupling on MNP surface. The molecular weight of PDMS, estimated from ^{1}H NMR spectrum, was approximately 2,254 g/mol (m=19, n=14). Immobilization of the PDMS on the MNP surface was carried out through the hydrosillylation between Si-H-containing PDMS and allyl-grafted MNP. The PDMS-grafted MNP then served as a reactive macroinitiator for ATRP of PEGMA. The ATRP reaction was performed at room temperature in toluene using CuBr/Me_6Tren catalytic complex. Kinetics studies *via* proton-nuclear magnetic resonance spectrometer (^{1}H NMR) indicated the constant consumption of PEGMA during first 7 h of the ATRP reaction. Transmission electron microscopy (TEM) showed the average particle size about 7 nm in diameter. Fourier transform infrared spectrophotometry (FTIR), thermogravimetric analysis (TGA) and vibrating sample magnetometry (VSM) indicated the increase of the copolymer in the complex when the ATRP reaction was prolonged.

Keywords Magnetite nanoparticle; PDMS; ATRP; Bilayer surfactant

Presentation Code	Presenter	Affiliation	Title
P3-MNT-014	A. Klinbumrung	CMU, Thailand	Phase characterization and optical properties of orthorhombic molybdenum oxide nanostructure synthesized by plasma microwave radiation
P3-MNT-015	A. Tikumpornban-jerd	KU, Thailand	Synthesis and characterization of nanoparticulate zinc oxide *via* an aqueous citric acid gelation route
P3-MNT-016	B. Thong-on	NU, Thailand	Magnetite nanoparticle coated with amphiphilic bilayer stabilizer of PDMS and PEGMA
P3-MNT-017	B. Mahapram	CMU, Thailand	Hydrophobicity enhancement of $SiCl_4$-treated cotton cloth modified by POTS and DMDCS
P3-MNT-018	B. Nuntapichedkul	CU, Thailand	Effect of propylene-ethylene copolymer on surface free energy of BOPP films
P3-MNT-019	B. Sukhummek	KMUTT, Thailand	Usage of water treatment sludge as reinforcing agent in natural rubber
P3-MNT-020	B. Phattanaphatta-nanon	BUU, Thailand	Affixation of propargyl alcohol ligand onto crosslinked poly(styrene-co-vinyl benzyl chloride) beads by "click" reaction and their adsorption properties for copper ions
P3-MNT-021	B. Khumpaitool	KKU, Thailand	Structure, microstructure and dielectric properties of Li and Cr-codoped NiO giant dielectric constant materials
P3-MNT-022	B. Somboon	MTEC , Thailand	Zinc oxide nanoparticles as light fastness improvers for printing of natural dyes on cotton fabrics
P3-MNT-023	B. Puangbuppha	KMUTT, Thailand	Assembly of graphene and nanographite sheets for sensing applications
P3-MNT-024	C. Junin	MTEC , Thailand	Effect of different morphology of TiO_2 films on cyanide degradation
P3-MNT-025	C. Inntam	UBU, Thailand	Ethanol dehydration over clinoptilolite: a density functional theory (DFT) study
P3-MNT-026	C. Samart	TU, Thailand	Organic-inorganic hybrid material for pH-responsive controlled release: physical and chemical study
P3-MNT-027	C. Sukyoo	KMUTT, Thailand	Study on structural properties and band-gap energy of zinc oxide doped with metal ions
P3-MNT-028	C. Mongkolkachit	MTEC, Thailand	Preparation of Al_2O_3/TiO_2 membrane supports

MNT-P-258

SURFACE MODIFICATION OF MAGNETITE NANOPARTICLES WITH THE TEMPERATURE-RESPONSIVE OF N-ISOPROPYLACRYLAMIDE

Siraprapa Meerod, Metha Rutnakornpituk*

Department of Chemistry and Center of Excellence for Innovation in Chemistry, Faculty of Science, Naresuan University, Phitsanulok 65000, Thailand
**Corresponding Author : methar@nu.ac.th*

ABSTRACT

Surface modification of magnetite nanoparticles (MNPs) with the temperature-responsive N-isopropylacrylamide stabilizer were developed for applications as drug release. The magnetite nanoparticles were prepared using the following method. Magnetic Iron oxide nanoparticles were successfully prepared by a coprecipitation method followed by modification with 3-aminopropyl triethoxysilane (APTES) and acryloyl chloride (AC) subsequently. Then the surface of modified nanoparticles was modified by free radical polymerization with N-isopropylacrylamide. The resulting magnetite nanoparticles were dispersed in an aqueous medium. The obtained nanoparticles were characterized by transmission electron microscopy (TEM), scanning electron microscopy (SEM), vibrating sample magnetometer (VSM), Fourier transform infrared (FT-IR) and thermogravimetric analysis (TGA).

Keywords Magnetite nanoparticles; N-isopropylacrylamide; Acryloyl chloride

Presentation Code	Presenter	Affiliation	Title
P4-MNT-189	S. Laksee	SU, Thailand	Iodide-doped TiO_2 photocatalyst for degradation of dye
P4-MNT-190	S. Samanman	PSU, Thailand	Label-free capacitive immunosensor signal: effect of the deposition of gold nanoparticles by a "Face-Up" and a "Face-Down" method
P4-MNT-191	S. Chairam	UBU, Thailand	A Green synthesis of gold nanoparticles using mung bean starch and its application
P4-MNT-192	S. Pongphot	CMU, Thailand	Synthesis of cordierite ceramics from talc, alumina and kaolinite
P4-MNT-193	S. Rattanaveeranon	KMUTT, Thailand	Fabrication of nanographite for electric double layer capacitor
P4-MNT-194	S. Taopen	CU, Thailand	Surface modification for protein adsorption
P4-MNT-195	S. Chotisuwan	PSU, Thailand	Porous calcium and magnesium oxide: preparation and characterization
P4-MNT-196	S. Thongbau	KU, Thailand	Synthesis and characterization of zinc oxide nanopowder *via* an aqueous acetate-succinate gelation method
P4-MNT-197	S. Parinyataramas	CU, Thailand	The preparation of spherical carbon powder by spray drying of resorcinol-formaldehyde gel
P4-MNT-198	S. Kraithong	SU, Thailand	Hg(II)-selective chemosensors based on rhodamine derivatives: utilization in the solutions and polymeric membranes
P4-MNT-199	S. Phiyanalinmat	CMU, Thailand	Nitrate removal by zinc-doped titanium dioxide photocatalyst
P4-MNT-200	S. Vuttivong	KMITL, Thailand	Sonochemical synthesis of barium titanate ($BaTiO_3$) nanoparticles
P4-MNT-201	S. Meerod	NU, Thailand	Surface modification of magnetite nanoparticles with the temperature-responsive of *N*-isopropylacrylamide
P4-MNT-202	S. Monchayapisut	CU, Thailand	Facile synthesis of tungsten oxide-multiwalled carbon nanotube hybrid material
P4-MNT-203	S. Wacharawicha-nant	SU, Thailand	Effects of surface-treated TiO_2 on mechanical and morphological properties of high density polyethylene/TiO_2 nanocomposites
P4-MNT-204	S. Alaksanasuwan	KMUTT, Thailand	Determination of total mass attenuation coefficients and effective atomic numbers of the Pb/Sn alloys

MNT-P-353

SURFACE MODIFICATION OF MAGNETITE NANOPARTICLE WITH EXTERNAL STIMULI-RESPONSIVE POLYMER *VIA* ATRP AND CLICK REACTION

Pawinee Theamdee, Metha Rutnakornpituk*

Department of Chemistry and Center of Excellence for Innovation in Chemistry, Faculty of Science, Naresuan University, Phitsanulok 65000, Thailand
**Corresponding Author : methar@nu.ac.th*

ABSTRACT

Magnetite nanoparticle (MNP) was surface modified with pH-responsive polymer, poly((2-(diethylamino) ethyl methacrylate (PDEAEMA), via the combination of atom transfer radical polymerization (ATRP) and Click reaction. MNP surface was first enriched with azido groups. In a separate aliquot, PDEAEMA with an alkyne functional groups at one end was synthesized via ATRP. The azido-functionalized MNP was then reacted with alkyne-functioanlized PDEAEMA via Cu(I)-catalyzed azido-alkyne-1,3-dipolar cycloaddition (CuAAC) reaction. The success of the surface functionalization was confirmed by fourier transform infrared spectroscopy (FTIR). The particles size and pH-responsive properties of PDEAEMA-modified MNP were investigated *via* transmission electron microscopy (TEM) and dynamic light scattering spectrophotometer (DLS), respectively. Thermogravimetric analysis (TGA) was used to estimate the content of linked organic compound.

Keywords Magnetic nanoparticles; ATRP; Click Reaction; DEAEMA

Presentation Code	Presenter	Affiliation	Title
P3-MNT-130	P. Chotmongkolsap	MU, Thailand	Transition metal functionalized metal-organic framework
P3-MNT-131	P. Amonphanpokin	MTEC, Thailand	Improvement in compatibility and mechanical properties of modified diatom frustule/polyethylene composites
P3-MNT-132	P. Ruenpakdan	MU, Thailand	Flame retardant property of cross-linked polypropylene in the presence of peroxide and sulfur
P3-MNT-133	P. Jaiban	CMU, Thailand	Characterization of compound with chemical formula $Bi_{0.5}Na_{0.5}ZrO_3$
P3-MNT-134	P. Waenkaew	CMU, Thailand	Effect of temperature on the morphology of titanium dioxide nanoparticles synthesized by the modified sol-gel method
P3-MNT-135	P. Boonchoo	CU, Thailand	Synthesis of polyisoprene/montmorillonite nanocomposites *via* differential microemulsion polymerization
P3-MNT-136	P. Siriprapa	CMU, Thailand	Doping content and sinterbility effects on crystal structure of Cr^{6+}-doped BLT ceramics
P3-MNT-137	P. Gonil	NANOTEC, Thailand	Novel fluorescent chitosan using naphthalene-2,3-dicarboxaldehyde as a fluorogenic reagent: synthesis and fluorescent property
P3-MNT-138	P. Changsuwan	NANOTEC, Thailand	Fabrication of calcium hydroxide pellets via freeze drying process
P3-MNT-139	P. Wongkhampral	MU, Thailand	The effect of green tea extract on the corrosion behaviour of C-steel in acid solution
P3-MNT-140	P. Theamdee	NU, Thailand	Surface modification of magnetite nanoparticle with external stimuli-responsive polymer *via* ATRP and click reaction
P3-MNT-141	P. Khemthong	NU, Thailand	Solvothermal synthesis and crystal structure of lanthanide Nd104 nanocluster
P3-MNT-142	P. Saowapa	CU, Thailand	Microencapsulation of *n*-octadecane with silica from sodium silicate by spray drying process.
P3-MNT-143	P. Kamkhou	KKU, Thailand	Effecs of calcination temperature on phase development and magnetic properties of (Li, Fe)-codoped NiO nanoparticle prepared by sol-gel process
P3-MNT-144	P. Chankachang	CMU, Thailand	Treatment of water from rubber processes by using TiO_2 nanopowder

MNT-P-346

HYDROPHILIC AZLACTONE FUNCTIONALIZED MAGNETIC NANOPARTICLES AND THEIR APPLICATION AS SCAVENGERS

Yingrak Prai-in[1], Kritsada Tankanya[1], Boonjira Rutnakornpituk[1], Uthai Wichai[1], Véronique Montembault[2], Sagrario Pascual[2], Laurent Fontaine[2], Metha Rutnakornpituk[1,*]

[1] *Department of Chemistry and Center of Excellence for Innovation in Chemistry, Faculty of Science, Naresuan University, Phitsanulok, 65000 Thailand*

[2] *UCO2M, LCOM-Chimie des Polymères, UMR CNRS 6011, Université du Maine, Avenue O. Messiaen, 72085 Le Mans Cedex 9, France*

**Corresponding Author : methar@nu.ac.th*

ABSTRACT

Surface modification of magnetite nanoparticle (MNP) with poly(ethylene glycol) methyl ether methacrylate (PEGMA)/2-vinyl-4,4-dimethylazlactone (VDM) copolymer via atom transfer radical polymerization (ATRP) and its application as a scavenger for thymine PNA monomer were presented. ATRP of PEGMA and VDM was first performed in a solution system to optimize the reaction condition. It was found that 1/0.2/0.2 molar ratio of [ethyl-2-bromoisobutyrate (EBiB)]$_0$/ [copper(I)bromide (CuBr)]$_0$/[tris-[2-(dimethylamino)ethyl]amine (Me_6Tren)]$_0$, respectively, led to a good control of the copolymerization; the resulting polymer has $\overline{M_n}$ close to the theoretical ones and relatively narrow polydispersity indices. The optimal reaction condition was also applicable in the surface-initiated ATRP of MNP. Fourier transform infrared spectroscopy (FTIR) and vibrating sample magnetometry (VSM) techniques indicated the presence of the copolymer in the MNP complexes. After immobilization step of thymine PNA monomer, thermogravimetric analysis (TGA) indicated that there was about 4 wt% of the PNA monomer in the complex (1.2 μmol/g complex). The existence of the PNA monomer in the complex was also confirmed via FTIR. The MNP complex with active surface might be efficiently used as magnetically guidable nanosolid support for PNA oligomers and other molecules containing affinity functional groups.

Keywords ATRP; Azlactone; Magnetite

Presentation Code	Presenter	Affiliation	Title
P4-MNT-294	Y. Pharat	CU, Thailand	Structural effects of bispyrenyl ureas linked by polyethylene glycol chain towards their anion binding abilities
P4-MNT-295	Y. Wattanodorn	MU, Thailand	Antimicrobial waterborne polyurethane
P4-MNT-296	Y. Prai-in	NU, Thailand	Hydrophilic azlactone functionalized magnetic nanoparticles and their application as scavengers
P4-MNT-297	Y. Poo-arporn	RLRI, Thailand	Time-resolved XAS beamline at SLRI: the advanced tool for *in situ* characterization of nanomaterials
P4-MNT-298	Y. Ngoenngam	CU, Thailand	Fabrication of porous alumina ceramic membrane by extrusion
P4-MNT-299	Y. Thathong	UBU, Thailand	Synthesis novel ruthenium complexes for dye-syntizing solar cell (DSC)

2.3) Pure and Applied Chemistry International Conference (PACCON 2011), 5-6 January 2011, The Miracle Grand Hotel, Bangkok, Thailand

PACCON

SWU 2011

January 5-7, 2011

Miracle Grand Hotel
Bangkok, Thailand

PACCON

PURE AND APPLIED CHEMISTRY INTERNATIONAL CONFERENCE 2011

ABSTRACTS

Sustainable Development: from Basic to Applied Chemistry

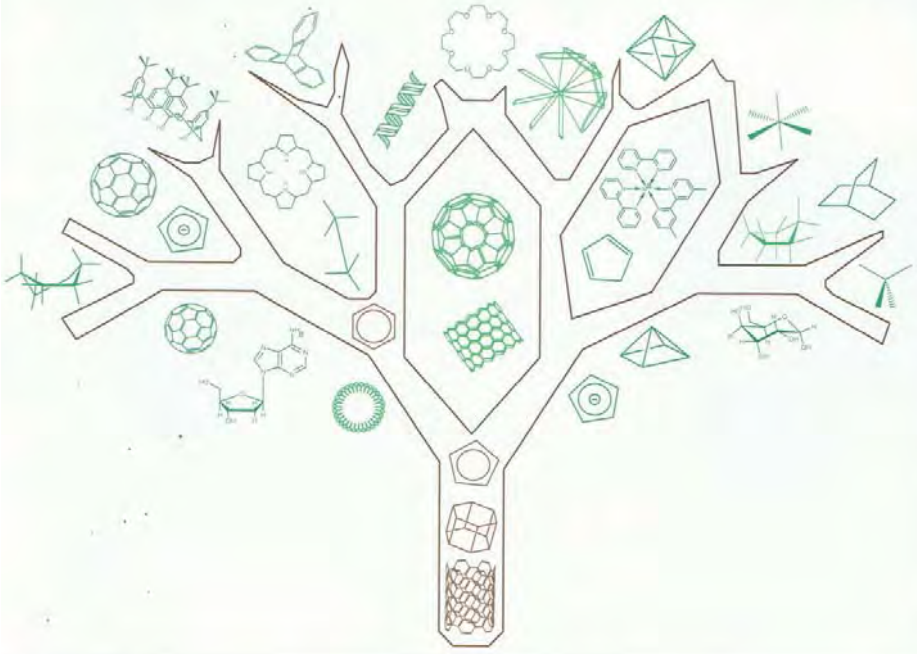

Organized by

Supported by

SHARP BRUKER NANOTEC THAILAND

morphology, optical properties and photocatalytic activity of deposited films were studied. XRD results show that all of doped and un-doped films prepared under pure Ar or mixture of Ar and O_2 gas consisted of only anatase phase. The sputtering gas had played an important parameter on the morphology of deposited films. It was demonstrated the difference in surface morphology and roughness of films sputtered under with and without O_2 gas characterized by FE-SEM and AFM. In addition, the sputtering gas showed an effect on the optical transmittance of deposited films. The film prepared under pure Ar gas had lower transparency than that of film prepared under mixture of Ar and O_2 in which its absorption edge slightly shifted towards longer wavelengths. The photocatalytic activity of produced films was evaluated by the degradation of a methylene blue solution under UV irradiation. It was demonstrated that the film prepared under pure Ar gas had better photocatalytic activity than that of film prepared under gas mixtures.

MN_M0017: Water dispersible magnetite nanoparticle with pH sensitive surface

Patcharin Kanhakeaw[1], and Metha Rutnakornpituk[1]*
[1]*Department of Chemistry, and Center of Excellence for Innovalation in Chemistry, Faculty of Science, Naresuan University, Phitsanulok, 65000 Thailand*
**E-mail:methar@nu.ac.th*

In this work, water dispersible magnetite nanoparticles (MNPs) with pH sensitive surface were synthesized. The particles were prepared by a thermal decomposition reaction of iron(III) acetylacetonate precursor in benzyl alcohol to obtain narrow-size distribution nanoparticles. They were then surface modified using a "grafting from" strategy *via* atom transfer radical polymerization (ATRP) of poly(ethylene glycol) methyl methacrylate (PEGMA)/*tert*-butyl acrylate(*t*-BA) copolymer, followed by deprotection of *t*-butyl groups of P(*t*-BA) in acidic dispersions to obtain PEGMA/poly(acrylic acid) (PAA)-coated MNPs. Molar ratio of PEGMA and PAA was tuned to obtain various degrees of negative charge on the particle surface. Fourier transform infrared spectroscopy (FTIR) was used to monitor the reaction progress in each step of the synthesis. Photocorrelation spectroscopy (PCS) indicated that, as increasing pH of the dispersions, their hydrodynamic diameter decreased while negative charge from zeta potential measurements was enhanced. These were attributable to the formation of negatively charge carboxylate ion on the particle surfaces, resulting in additional electrostatic stabilization. Transmission electron microscopy (TEM) revealed that they were about 8 nm in diameter with narrow size distribution. This copolymer-MNP complex with pH sensitive surface and magnetically guidable properties is warranted for further development for potential use in medical applications.

MN_M0018: Effects of electrospinning conditions on platinum and copper nanowire structures

Wittaya Yaipimai[1,2] and Rojana Pornpresertsuk[1,2]*
[1] *Research Unit of Advanced Ceramics, Department of Materials Science, Faculty of Science, Chulalongkorn University*
[2] *Research Unit of Advanced Ceramic and Polymeric Materials, National Center of Excellence for Petroleum, Petrochemical, and Advanced Material, Chulalongkorn University*
**E-mail: rojana.p@chula.ac.th*

Platinum (Pt) and Copper (Cu) nanowires were fabricated by electrospinning technique. The electrospinning conditions such as polymer concentration, water/ethanol ratio in the electrospinning solution and electric field strength were investigated in order to obtain platinum and copper nanowires with no bead formation. The precursor solutions were prepared by dissolving $H_2PtCl_6 \cdot xH_2O$ for Pt nanowires and $CuCl_2 \cdot 2H_2O$ for Cu nanowires in DI water and mixed with poly (vinylpyrrolidone) (PVP, Mw 1,300,000 g/mol) dissolved in ethanol. The microstructures, phases and chemical compositions of the metallic nanowires were subsequently investigated by Scanning Electron Microscopy (SEM), X-Ray Diffraction (XRD) and Transmission Electron Microscopy (TEM) techniques. The results that the suitable electrospinning conditions comprising of polymer concentration of more than 0.03 g/ml, a low water/ethanol ratio of 0.15, and a feeding rate of 0.1 ml/h

reflectance Fourier transform infrared (ATR-FTIR) spectroscopy. The mechanical property (peel strength) before and after surface treatment were studied by mechanical tensile testing. The water contact angle analysis proved an increase in hydrophilicity of the surface of plasma-modified polymer substrates due to the formation of hydrophilic groups on substrate surface verified by ATR-FTIR spectroscopy. Resulting effect of several kinds of gas plasma treatment on the wettability of polymer and mechanical property before and after the plasma treatment will be discussed.

PM_P0018: Accelerated weathering effects on mechanical properties and morphology of vetiver grass fiber/polyamide-6 composites

Khanitthakanya Munkid[1] Pattarapan Prasassarakich[2,3]
[1] *Program in Petrochemistry and Polymer Science, Faculty of Science, Chulalongkorn University, Bangkok 10330, Thailand*
[2] *Department of Chemical Technology, Faculty of Science, Chulalongkorn University, Bangkok 10330, Thailand*
[3] *Center for Petroleum, Petrochemicals and Advanced Materials, Chulalongkorn University, Bangkok 10330, Thailand*

The interest for the use of natural fibers as polymer reinforcement has recently increased because of their unique environmental and technological advantages. This research evaluates the use of natural fibers in polyamide-6 composites aiming to synthetic fiber replacement. Vetiver grass is one of natural fibers which have attracted attention because of their low cost compared with synthetic fibers such as glass, carbon etc. Shortcomings with respect to moisture stability and poor strength are resolved satisfactorily. The application of natural fiber as reinforcement in composite materials requires a strong adhesion between fiber and the synthetic matrix. In this work, the chemical treatment, mercerization (5 wt% NaOH) and silane coupling agent (1.0% w/w vinyltrietoxysilane and 0.5% w/w dicumyl peroxide) are used to improve this interface. Objective of this work is to study the preparation of Vetiver grass fibers reinforced polyamide-6 composites using twin screw extruders at various contents of Vetiver grass fibers (15 and 30%). The mechanical properties, morphology by scanning electron microscopy and long term stability of Vetiver grass fibers reinforced polyamide-6 composites are investigated for automotive application compared with glass fiber and talc reinforced composites. Polyamide-6 composites reinforced with fibers treated with silane coupling agent had improved properties compared with fibers treated by mercerization. Properties of polyamide-6 composites reinforced with fibers treated with silane coupling agent were slightly lower than glass fiber reinforced composites and about the same as talc reinforced composites.

PM_P0019: Synthesis of amphiphilic block copolymer *via* atom transfer radical polymerization

Bandit Thong-On, and Metha Rutnakornpituk*
Department of Chemistry and Center of Excellence for Innovation in Chemistry, Faculty of Science, Naresuan University, Phitsanulok, 65000 Thailand
**E-mail: mrutnako@hotmail.com*

We are here reporting the synthesis of amphiphilic ABA triblock copolymer of polysiloxane and poly(ethylene glycol) methyl ether methacrylate (PEGMA) *via* the combination of cationic ring opening polymerization and atom transfer radical polymerization (ATRP). Polysiloxane central block was first prepared *via* acid-catalyzed ring-opening polymerization of octamethylcyclotetrasiloxane (D_4) and tetramethylcyclotetrasiloxane (D_4H) using dihydroxypropyl tetramethyl disiloxane as an end capping agent and to control its molecular weight. 1:1 Molar ratio of D_4:D_4H was used to form poly(dimethyl-*ran*-methylhydro)siloxane copolymer. The telechelic polysiloxane was then functionalized with dialkyl bromide functional groups at both terminals and used as macroinitiator for ATRP of PEGMA. The ATRP reaction was performed at room temperature in toluene using CuBr catalyst and M_6Tren ligand. Kinetics studies of the ATRP reaction were also performed. Finally, allyl glycidyl ether was then hydrosillylated to Si-H bonds in the siloxane central of the copolymer. Chemical structures of the copolymer were characterized using proton-nuclear magnetic resonance spectrometer (^{1}H NMR) and its functional groups were studied using fourier transform infrared

spectrophotometer (FTIR). The epoxide rings distributed throughout the siloxane central block were thought to readily reactive toward any nucleophiles for further reactions. Hence, this ABA triblock copolymer is expected for use as amphiphilic surfactant for iron oxide nanoparticle through the reaction between the epoxide rings at the siloxane central block and the particle surfaces.

PM_P0020: Effect of modified calcium silicate on spinnability of PET fibres

Boonsri Kusuktham*
Division of Textile Chemistry Engineering, Faculty of Textile Industries, Rajamangala University of Technology Krungthep, Bangkok 10120, Thailand

* *E-mail: kuboonsri@yahoo.com*

The spinning of poly(ethylene terephthalate) (PET) filament in laboratory-scale was studied. The objective was to study the effect of modified calcium silicate (CS) with vinyltriethoxysilane (VTES) on the melt spinning of PET fibres. The CS was modified with VTES (2% v/v) in diethyl ether at room temperature for 24 h. The modification of CS with VTES improved agglomeration of CS, hydrophobic and heat resistance properties. These properties were expected that modified CS could be used as filler in melt spinning of PET. The incorporation of modified CS in PET was spinnable. Also, the addition of CS in PET improved its heat resistance.

PM_P0021: Effect of silica/carbon black hybrid filler on mechanical properties and morphology of styrene butadiene rubber/acrylonitrile butadiene rubber blends.

Jansamorn Ma-Iat[1*] Pattarapan Prasassarakich[2,3]
[1] *Program in Petrochemistry and Polymer Science, Faculty of Science, Bangkok 10330, Thailand*
[2] *Department of Chemical Technology, Faculty of Science, Chulalongkorn University, Bangkok 10330, Thailand*
[3] *Center for Petroleum, Petrochemicals and Advanced Materials, Chulalongkorn University, Bangkok 10330, Thailand*
Email: jansamorn@nok.co.th

Carbon black (CB) and silica have been used as the reinforcement fillers of rubber composites. As each filler possesses its own advantages, the use of silica/CB blends should increase the mechanical, dynamic properties, oil resistance and compression set. However, the appropriate silica/CB ratio giving rise to the optimum properties needs to be explicated. Blending of elastomers has been used to obtain an optimum number of desirable combinations, physical properties, processability and cost. In this work, the variables are blending ratio of SBR/NBR blends, filler content and ratio of silica/CB hybrid filler. The combination of sulfur and dicumyl peroxide as vulcanizing systems is employed. To improve interaction between silica and rubber matrix, 3 types of silane coupling agent, gamma-mercaptopropylmethoxysilane, gamma-glycidoxypropyltrimethoxysilane and vinyl-*tris*-(2-methoxyethoxy) silane are used. The effects of silica/CB hybrid filler and coupling agent in rubber compound on mechanical properties such as tensile strength, modulus, and compression set and oil resistance characterization are analyzed. The results revealed that the mechanical properties, oil resistance and compression set of SBR/NBR blend (30/70) reinforced with silica/CB hybrid filler and silane coupling agents were improved. Dispersion of silica/CB hybrid filler in rubber matrix was improved by silane coupling agent. The rubber blend (SBR/NBR = 30/70) reinforced with 50 phr of silica/CB (25/25) hybrid filler and gamma-mercaptopropylmethoxysilane exhibited the good mechanical properties, oil resistance and compression set and could be used as o-ring for motor oil medium resistance.

PM_P0028: Effect of HEMA on properties of polyester rope coated with epoxy resin

Phattharapa Joypod[1], Boonsri Kusuktham[2*]
[1] Division of Textile and Clothing, Faculty of Textile Industries, Rajamangala University of Technology Krungthep, Bangkok 10120, Thailand

[2]Division of Textile Chemical Engineering, Faculty of Textile Industries, Rajamangala University of Technology Krungthep, Bangkok 10120, Thailand

2.4) *PERCH-CIC Congress VII, 4-7 May 2011, Jomtien Palm Beach& Resort, Pattaya, Chonbury, Thailand*

S3-P97

Polysiloxane-poly(ethylene glycol) Methyl Ether Methacrylate Amphiphilic Block Copolymer Prepared *via* Atom Transfer Radical Polymerization

Bandit Thong-On and Metha Rutnakornpituk

Department of Chemistry and Center of Excellence for Innovation in Chemistry, Faculty of Science, Naresuan University, Phitsanulok, 65000 Thailand, Tel. +66 55 96 3464, Fax. +66 55 96 3401

Introduction and Objective

Atom transfer radical polymerization (ATRP) is one of a controlled radical polymerization method. ATRP has been applied for the polymerization of homo- and block copolymers because of a good control in their molecular weight and polydispersity. It can be used in a wide range of functional monomers such as styrene, (meth)acrylates and (meth)acrylamides [1,2].

Methods

In this work, amphiphilic triblock copolymer of polysiloxane central block and poly(ethylene glycol) methyl ether methacrylate (PEGMA) tail blocks were prepared *via* the combination of cationic ring-opening polymerization and ATRP. Polysiloxane central block was first prepared *via* acid-catalyzed ring-opening polymerization of octamethylcyclotetrasiloxane (D_4) and tetramethylcyclotetrasiloxane (D_4H). The polysiloxane was then functionalized with dialkyl bromide functional groups at both terminals and used as macroinitiator for ATRP of PEGMA. 1:1 Molar ratio of D_4:D_4H was used in the ring-opening reaction in acidic condition and using dihydroxypropyl tetramethyl disiloxane as an end capping agent and to control its molecular weight. The product was then reacted with 2-bromo-2-methylpropanoyl bromide (BIBB) to form polysiloxane macroinitiator (PDMS-Br) for ATRP of PEGMA monomer.

Results

The molecular weights of the polysiloxane central block determined by end group analysis from ^{1}H NMR spectra was about 2,100 g/mol with 19 units of poly(dimethyl siloxane) and 14 units of poly(hydromethyl siloxane). The ^{1}H NMR signal at 2.0 ppm of PDMS-Br corresponding to methyl protons of its terminal indicated the formation of telechelic polysiloxane with ATRP initiator. It was then used as a macroinitiator for ATRP of hydrophilic PEGMA. According to ^{1}H NMR, the rate of the reaction followed the first-order relationship during first 90 minutes of ATRP.

Conclusion

The deviation from linearity of its first-order plot was observed when the reaction was prolonged probably due to the decrease of monomer concentration, resulting in recombination of active radicals. FTIR also indicated the formation of amphiphilic block copolymer due to the existence of siloxane functional groups and PEGMA in the structure.

Keywords: polysiloxane, poly(ehtylene glycol) methyl ether acrylate (PEGMA), amphiphilic block copolymer, atom transfer radical polymerization(ATRP).

Selected References:

1. Kurjata, J. *J. Chojnowski, Polymer*, **2004**, *45*, 6111-6121.
2. Zheng-Hong, L.; Teng-Yun, H, *Reactive & Functional Polymers*, **2008**, *68*, 931-942.

Bandit Thong-On (บัณฑิต ทองอ่อน) **M.Sc. Student**
b 1986 in Kamphaengphet, Thailand
Naresurn University, Thailand, Chemistry, B.Sc. 2008
Research field: polymer

S3-P100

Synthesis of Polyelectrolyte-grafted Magnetite Nanoparticle

Patcharin Kanhakeaw, Boonjira Rutnakornpituk, Uthai Wichai and Metha Rutnakornpituk

Department of Chemistry and Center of Excellence for Innovation in Chemistry, Faculty of Science, Naresuan University, Phitsanulok 65000, Thailand.

Introduction and Objective

Polymers containing ionizable groups in their backbone can from polyelectrolytes in an aqueous system. Depending on their nature, polyelectrolyte can respond to external stimuli, such as pH, ionic strength or temperature [1]. Recently, two main methods have been used for surface modification of particle, including the so-called "grafting from" and "grafting to" methods.

In the present work, we focused on preparing PAA homopolymer and PAA/PEGMA copolymer polyelectrolyte coating on magnetite nanoparticle (MNP) *via* atom transfer radical polymerization (ATRP) using "grafting from" technique. The kinetics of polymerization and characterization of co- and homopolymer coated-MNP were also studied

Methods

A method to prepare magnetic nanoparticles with a covalently bonded PAA homopolymer and PAA/PEGMA copolymer polyelectrolyte by ATRP was reported. First, the initiator for ATRP was synthesized from the coupling reaction between triethoxysilane (APS) and 2-bromoisobutylryl bromide (BIBB). It was then coordinated on the oleic acid-coated MNP to obtain the particle with ATRP initiator on its surface. Then the surface-initiated ATRP of poly(*tert*-butyl acrylate) (P(*t*-BA) homopolymer and P(*t*-BA)/PEGMA copolymer polyelectrolyte mediated by a copper complex was carried out. Finally, the t-butyl groups on the particle surface was deprotected in acidic dispersion to obtain carboxylic group on its surface.

Results

Fourier transform infrared spectroscopy (FTIR) of the (co)polymer-coated MNP revealed the decrease of signals at 2929 cm^{-1} (CH-stretching), 1360 cm^{-1} and1390 cm^{-1} (CH-bending). Moreover, the carbonyl signal (1671 cm^{-1}) was observed as a broad signal which is the characteristics of carboxylic acid of PAA. Ethyl-2-bromoisobutyrate (EBIB) was used as a sacrificial initiator in the ATRP reaction to study the kinetics of the ATRP reactions *via* ^1H NMR. From the first order plot of homopolymer, it showed a linear relationship during the first 8 h of the reaction. In the case of the copolymerization, *t*-BA and PEGMA were consumed rapidly at the beginning period and slowly at the ending period during the copolymerization. Moreover, it was found that PEGMA would be consumed more quickly than P(*t*-BA) in the copolymerization.

Conclusion

MNPs coated with PAA homopolymer and PAA/PEGMA copolymer were successfully synthesized and well characterized. Kinetics studies of the ATRP reactions were also investigated. PEGMA in the copolymerization showed a rapid rate as compared to that of P(*t*-BA). It was envisioned that ATRP can be essentially applied for surface-initiated graft polymerization to obtain a well-packed polymer layer on the surface of MNP.

Keywords: magnetic nanoparticle, polyelectrolyte, ATRP

Selected Reference:

1. Mori, H.; Muller, A. H. E.; Klee, J. E. *J. Am. Chem. Soc.*, **2003**, *125*, 3712-3713.

Patcharin Kanhakeaw (พัชรินทร์ กันหาเขียว) **M.Sc. Student**
b 1986 in Petchaboon, Thailand
Naresurn University, Thailand, Chemistry, B.Sc. 2008
Research field: Polymer science

S3-P96

Surface Modification of Magnetite Nanoparticle with External Stimuli-responsive Polymer *via* ATRP and Click Reaction

Pawinee Theamdee and Metha Rutnakornpituk

Department of Chemistry and Center of Excellence for Innovation in Chemistry, Faculty of Science, Naresuan University, Phitsanulok 65000, Thailand.

Introduction and Objective

Surface modification of magnetite nanoparticle (MNP) is an important and challenging step for controlling chemical composition and function of the polymer on its surface. Atom transfer radical polymerization (ATRP) has recently become a good choice for coating organic polymeric shell to MNP core [1] because narrow molecular weight distribution of polymers was obtained. Moreover, 1,3-dipolar cycloaddition reaction, one of the popular 'click' reaction between azide and alkyne functional groups, has been demonstrated to be a versatile tool in organic, material and polymer syntheses [2].

In this work, we have adopted ATRP and Click reaction to modify MNP surface with an external stimuli responsive polymer. One of the most interesting "sensitive" polymer is *N*-isopropylacryamide (NIPAAM), a thermoresponsive, biocompatible and water soluble polymer. Because of these unique properties, PNIPAAm has been widely used in the synthesis of stimuli-responsive materials [3].

Methods

The overall of this work was divided into two parts: 1) azide-modified surface of MNP and 2) alkyne-terminated PNIPAAm. First, MNP were prepared *via* thermal decomposition reaction of $Fe(acac)_3$, and then surface coated with oleic acid and (3-chloropropyl) triethoxysilane (CPTES). The Cl groups at chain ends of CPTES-modified MNP were changed to an azide end group. In a separate aliquot, the initiator for ATRP was synthesized from the coupling reaction between α-bromoisobutyric acid (BIBB) and propargyl alcohol. The coupling product was then used as an initiator for ATRP of NIPAAm monomer to obtain alkyne-terminated PNIPAAm. Finally, the alkyne-functionalized NIPAAm was click coupled to the as-synthesized azide-modified surface of MNP.

Results

FTIR of azide-modified MNP showed a very strong absorbance at 2110 cm^{-1} of azide. The signal at 578 cm^{-1} corresponding to Fe-O bonds in MNPs was also observed. In the ATRP of PNIPAAm, the first-order reaction at initial stage of the reaction was observed.

Conclusion

The detailed studies of the "grafting-onto" of the alkyne-terminated PNIPAAm to azide-modified MNP are under investigation and will be reported in the future. It is hoped that these hybrid particles can attracted at great attention in the biomedical field as a stimulus-sensitive material.

Keywords: magnetic nanoparticles, ATRP, click reaction, NIPAAm

Selected References:

1. Zhoua, Y.; Wang, S.; Ding, B.; Yang, Z. *Chem. Eng. J.*, **2008**, *138*, 578-585.
2. Ranjan, R.; Brittain, W. J. *Macromolecules*, **2007**, *40*, 6217-6223.
3. Xu, F. J.; Zhong, S. P.; Yung, L. Y. L.; Kang, E. T.; Neoh, K. G. *Biomacromolecules*, **2004**, *5*, 2392-2403.

Pawinee Theamdee (ภาวินี เทียมดี) **Ph.D. Student**
b 1985 in Sukhothai, Thailand
Naresuan University, Thailand, Chemistry, B.Sc. 2006
Naresuan University, Thailand, Chemistry, M.Sc. 2009
Research field: nanoparticle and polymer synthesis

S3-P103

Magnetite Nanoparticles Stabilized with Polydimethylsiloxane Brush

Siraprapa Meerod and Metha Rutnakornpituk

Department of Chemistry and Center of Excellence for Innovation in Chemistry, Faculty of Science, Naresuan University, Phitsanulok 65000, Thailand.

Introduction and Objective

Magnetite nanoparticles (MNPs) is one of the most popular nanomaterial known for its biomedical applications such as magnetic resonance imaging , targeted drug delivery , gene delivery systems, and gene therapy as well as targeted hyperthermia of cancers. In all the above applications, it is preferable that MNPs are encapsulated with a polymer of interest in order to avoid its agglomeration for various biomedical applications [1]. The objective of this study is to synthesis of functionalized polydimethylsiloxane (PDMS) for use as polymeric surfactants of MNPs.

Methods

MNPs were synthesized *via* co-precipitation reaction between iron (III) and iron (II) in basic solution and coated with oleic acid to disperse the particle in toluene. In a separate aliquot, PDMS prepolymer was first prepared *via* a living anionic polymerization of hexamethylcyclotrisiloxane (D_3) using n-butyl lithium as an initiator. The reaction was performed at room temperature in CH_2Cl_2 for 24 h. The reaction progress was followed *via* ^{1}H NMR and terminated with allyl glycidyl ether to obtain epoxy-terminated PDMS with the molecular weight of 2,010 g/mol. Aminopropyl triethoxysilane (APS) was subsequently reacted with the epoxy-terminated PDMS to form the triethoxysilane-terminated PDMS for effective coupling with surface of MNP.

Results

After hydrosilylation of allyl glycidyl ether with PDMS prepolymer (H-terminated PDMS), the product was characterized by ^{1}H NMR. The peaks at 2.6, 2.8, 3.1 ppm were assigned to the signals of epoxide groups at PDMS chain end. In addition, the spectrum of the Si–H peak at 4.7 ppm disappeared, indicating the occurrence of epoxy-terminated PDMS. After the reaction of the epoxide-terminated PDMS with amino groups of APS, ^{1}H NMR and FTIR spectra indicated the formation of triethoxysilane-terminated PDMS from the absence of epoxide signals (2.8 and 3.1 ppm in ^{1}H NMR and 1,280 cm^{-1} in FTIR). After immobilization of the PDMS onto MNP surface, FTIR showed the characteristic absorption signals of both MNPs (582 cm^{-1}, Fe-O bond) and PDMS (1080-1013 cm^{-1}, Si-O stretching).

Conclusion

PDMS with an effective functional group for chemical conjugation onto MNP surface was prepared. Triethoxysilxane-terminated PDMS was synthesized through a living anionic ring-opening polymerization of D_3 monomer, followed by hydrosillylation and epoxide ring-opening reaction. It was successfully used as a hydrophobic steric stabilizer of magnetite nanoparticles.

Keywords: magnetite nanoparticle, polydimethyl siloxane

Selected Reference:

1. Babu, K.; Dhamodharan, R. I. *Nanoscale Res. Lett.*, **2009**, *4*, 1090-1102.

Siraprapa Meerod (ศิราประภา มีรอด) **Ph.D. Student**
b 1982 in Uttaradit, Thailand
Naresuan University, Thailand, Chemistry, B.Sc. 2005
Naresuan University, Thailand, Industrail Chemistry, M.Sc. 2008
Research field: Organic Polymer

2.5) *Pure and Applied Chemistry International Conference 2009 (PACCON2009), Phitsanulok, Thailand, 14-16 January 2009*

PACCON

Pure and Applied Chemistry International Conference 2009

Abstracts

JANUARY 14-16, 2009
NARESUAN UNIVERSITY, PHITSANULOK, THAILAND

PACCON 2009
ABSTRACTS

PURE AND APPLIED CHEMISTRY INTERNATIONAL CONFERENCE

Sustainable Development in Chemistry Based on Indigenous Knowledge

investigated so far in order to construct organophilic layered solids with novel chemical and physical properties. Among possible layered inorganic solids, smectite groups of layered clay minerals have extensively been used as host materials, since they provide various attractive features such as the swelling behavior, ion exchange property, adsorptive property and large surface area for organizing organic species. The immobilization of photoactive species, cadmium selenide (CdSe), on the surface of organophilic-smectite is a way to create novel photofunctional system. Solid-state intercalation of both nonionic and cationic guest species into the interlayer spaces of layered clay minerals has been reported so far. The intercalation of CdSe in the interlayer space of organically modified montmorillonite was prepared by solid-solid reaction between powder of hexadecyltrimethylammonium ($C_{16}H_{33}(CH_3)_3N^+$)-montmorillonite and CdSe at room temperature. The product was characterized by XRD, TG-DTG-DTA and FT-IR, UV-visible and photoluminescence spectroscopies. The basal spacings of the product were 3.92 and 2.1 nm, indicating the gallery heights of ca. 2.92 and 1.10 nm, respectively. According to the gallery heights (2.92 and 1.10 nm) of the product indicated the formation of CdSe was thought to be laying flate between the modified silicate layers with the hight of ca. 3 and/or 1 nm. The diffuse reflectance absorption onset exhibited at 639 nm. When the product was allowed to stand for 1 week, the diffuse reflectance absorption onset and emission peak appeared at 628 and 585 nm, respectively. The luminescence intensity of the product was weak, supporting that the impurities such as iron in montmorillonite quenched the luminescence of CdSe particles.

REFERENCES

1. Ogawa, M., 2004. *Photoprocess in clay-organic complexes. In: Auerbach, S.M., Carrado, K.A., Dutta, P.K. (Eds.), Handbook of Layered Materials.* Marcel Dekker, New York, 191-260.
2. Khaorapapong, N.; Ontam, A.; Khemprasit, J.; Ogawa, M. *Formation of MnS- and NiS-montmorillonites by solid-solid reactions. Appl. Clay Sci.*, in press. **2008**
3. Khaorapapong, N.; Ontam, A., Youngme, S.; Ogawa, M. *J. Phys. Chem. Solid.* **2008**, 69, 1107-1111.
4. Ogawa, M.; Hashizume, T.; Kuroda, K.; Kato, C. *Inorg. Chem.* **1991**, 30, 584-585.

S7-OR-41

Surface Functionalization of Iron Oxide Nanoparticles Coated with Poly(acrylic acid)

Nipaporn Puangsin, Uthai Wichai, Metha Rutnakornpituk*

Department of Chemistry and Center of Excellence for Innovation in Chemistry, Faculty of Science, Naresuan University, Phitsanulok, 65000 Thailand

**E-mail: methar@nu.ac.th, Tel: +66-55-261000-4 ext. 3464, Fax: +66-55-261025*

Folic acid is known as a low-molecular-weight targeting agent specifically recognizing to cancer cells becasue it can couple to the folate receptors overexpressed on cancer cell membranes. In this report, superparamagnetic magnetic nanoparticles were hence surface modified with poly(acrylic acid) (PAA) and folic acid, respectively, to offer improved ability to target specific cells. Magnetite nanoparticles were synthesized via a thermal decomposition reaction of iron (III) acetylacetonate precursor in benzyl alcohol to obtain narrow-size distribution nanoparticles. PAA was synthesized via a three-step reaction: 1) formation of atom transfer radical polymerization (ATRP) initiating sites from the nanoparticle surface, 2) ATRP of *t*-butyl acrylate monomers mediated by a copper complex to obtain poly(*t*-butyl acrylate)(poly(*t*-BA))-coated magnetite nanoparticles, and 3) hydrolysis of poly(*t*-BA) in acidic dispersions to obtain PAA-magnetite complex. Thermal gravimetric analysis (TGA) disclosed the composition ratio of iron oxide to polymer as a function of time in ATRP step. Subsequently, folic acid was successfully immobilized on the surfaces of magnetite nanoparticles. Fourier transform infrared spectroscopy (FTIR) was used to monitor the reaction progress in each step. Transmission electron micrographs (TEM) revealed that the particle size increased from 9 to 11 nm after coating with PAA. The nanoparticles coated with PAA shells were well dispersed in various organic solvents. Vibrating sample magnetometry (VSM) manifested that the magnetite nanoparticles were superparamagnetic. Intracellular uptake of the folic acid-immobilized nanoparticles into cancer cells is warranted to be studied.

REFERENCES

1. Pinna, N.; Grancharov, S.; Beato, P.; Bonville, P.; Antonietti, M.; Niederberger, M. *Chemical Material.* **2005**, *17*, 3044-3049.
2. Sun, Y.; Ding, X.; Zheng, Z.; Cheng, X.; Hu, X.; Peng, Y. *European Polymer Journal.* **2007**, *43*, 762-772.
3. Saez-Martinez, V.; Perez-Alvarez, L.; Merrero, M.T.; Hernaez, E.; Katime, I. *Macromolecular Nanotechnology.* **2008**, *44*, 1309-1322.

S7-OR-42

Effects of Blend Compositions and Additives on Physical and Mechanical Properties of LDPE/EVA Foams

Phansiri Suktha, Varun Taepaisitphongse*

Polymer Engineering Laboratory, Department of Chemical Engineering, Faculty of Engineering, Chulalongkorn University, Bangkok, 10330 Thailand

**E-mail: varun.t@chula.ac.th, Tel: +662-218-6878*

Polyolefin foams have been widely used in a variety of applications including packaging, thermal insulation, automotive, cushioning and others. But low density polyethylene (LDPE) foams have limited applications due to their good load bearing capability but low flexibility and compression recovery. Addition of the ethylene vinyl acetate copolymer (EVA) to LDPE to form polymer blend foam can increase flexibility, toughness and impact resistance. However, crosslinked polymer has higher tensile strength leading to hardness and stiffness. This paper studied the effects of addition of ethylene vinyl acetate copolymer and crosslinking agent into LDPE foam to improve its flexibility. Polymer blend foams were

S7-OR-30

Methanol Oxidation by Platinum–Ruthenium Electrocatalysts Supported on Carbon Nanotubes

Ratana Cheerapradit[1], Orawon Chailapakul[2], Parichatr Vanalabhpatana[2*]

[1]*Program in Petrochemistry and Polymer Science, Faculty of Science, Chulalongkorn University, Bangkok 10330 Thailand*
[2]*Department of Chemistry, Faculty of Science, Chulalongkorn University, Bangkok 10330 Thailand*
**E-Mail: parichatr.v@chula.ac.th, Tel: +66-2218-7615*

Platinum and platinum–ruthenium nanoparticles deposited on carbon nanotubes (Pt/CNT and Pt–Ru/CNT) were prepared by polyol process and served as electrocatalysts for methanol oxidation. The Pt/CNT and Pt–Ru/CNT catalysts were then characterized by X-ray diffraction (XRD) technique. Cyclic voltammetry was used to inspect the electro-oxidation of methanol by these Pt/CNT and Pt–Ru/CNT catalysts. Our results indicated that the Pt–Ru/CNT catalysts displayed higher current densities for methanol oxidation than the Pt/CNT catalyst. Among all of the prepared catalysts, the Pt_2–$Ru_{1.5}$/CNT demonstrated the best electrocatalytic activity. Furthermore, we have tried to co-deposit other metals with Pt and Ru on CNT to enhance the electrocatalytic activity for methanol oxidation.

REFERENCES

1. Gu, Y. J.; Wong, W. T. *Langmuir* **2006**, *22*, 11447–11452.
2. Liu, Z.; Ling, X. Y.; Guo, B.; Hong, L.; Lee, J. Y. *J. Power Sources* **2007**, *167*, 272–280.
3. Guo, D. J.; Li, H. L. *J. Power Sources* **2006**, *160*, 44–49.

S7-OR-31

Visible Light Responsive Titanium Dioxide Nanoparticle

Natee Sirisit, Siwaporn Meejoo*

Department of Chemistry, Faculty of Science, Mahidol University, Ratchathewi, Bangkok, Thailand 10400
**E-mail: scsmj@mahidol.ac.th, Tel: +66-2-201-5164*

In recent years, there has been an extensive interest in the use of semiconductor as photocatalyst to initiate photocatalytic reaction at their interface. Among various types of semiconductors, TiO_2 has been widely used because of its favourable properties like non-toxicity, chemical inertness, and stability over a wide pH range under irradiation conditions. Many applications using titania in photo reactions have been successfully developed, such as the purification of contaminated water and solar energy conversion. However, TiO_2 has some disadvantages i.e. wide band gap (E_g =3.2 eV). It can be only triggered by near UV radiation that encompass only about 4-5% of natural solar radiation. Therefore, a visible-light responsive photocatalyst becomes a great demand, in order to take full advantage of visible light region in the sunlight. In addition, the photoactivity of TiO_2 is largely enhanced when its size is decreased into the nanometre scale as a result of dramatically increase of surface-to-volume ratio. The TiO_2 nanoparticles obtained by literature synthesized method are typically amorphous so that a high-temperature calcinations process is followed to increase the crystallinity of the nanoparticles. However, there are new developed hydrothermal synthesis method to prepare crystalline TiO_2 nanoparticles without the postcalcination treatment. Such that method still has the agglomeration of nanoparticles, similar to that found in the crystallization via postcalcination. In this work, the incorporation of transition metals, Fe with TiO_2 was carried out and the photoactivities of both nanomaterials are compared with that of P25 Degussa TiO_2.

REFERENCES

1. Umebayashi, T.; Yamaki, T.; Itoh, H.; Asai, K. *J. Phys. Chem. Solids.* **2002**, *63*, 1909.
2. Wang, C.-C.; Zhang, Z.; Ying, J. Y. *Nanostruct. Mater.* **1997**, *9*, 583.
3. Inagaki, M.; Nonaka, R.; Tryba, B.; Morawski, A.W. *Chemosphere.* **2006**, *64*, 437-445.
4. Lin, J.; Lin, Y.; Liu, P.; Meziani, M.J.; Allard, L.F.; Sun, Y.-P. *J. Am. Chem. Soc.* **2002**, *124*, 11514-11518.

S7-OR-32

Magnetic Core-Shell Nanoparticles : Effect of Amphiphilic Block Lengths on Drug-Released Behavior

Siraprapa Meerod, Uthai. Wichai, Metha Rutnakornpituk*

Department of Chemistry and Center of Excellence for Innovation in Chemistry, Faculty of Science, Naresuan University, Phitsanulok, 65000 Thailand
**E-mail: methar@nu.ac.th, Tel: +66-55-261000-4 ext. 3464, Fax: +66-55-261025*

We here presents a synthesis of indomethacin-loaded bilayer-surface magnetite nanoparticles. The particles were first prepared by a co-precipitation method and stabilized with poly(ethylene glycol) methyl ether-poly(ε-caprolactone) (mPEG-PCL) amphiphilic block copolymer to form the particles having hydrophobic inner shell and hydrophilic corona. Hydrophobic PCL block is thought to physically adsorb onto the oleic acid-precoated particle surface and hydrophilic mPEG block provides steric stabilization in aqueous dispersions. mPEG-PCL copolymers with systematically varied molecular weights of each block (2,000-10,000 g/mol, 2,000-2,000 g/mol, 5,000-10,000 g/mol, 5,000-5,000 g/mol, respectively) were synthesized by a ring-opening polymerization of ε-caprolactone using mPEG as a macroinitiator and stannous octoate catalyst. The particles were about 9.0±1.1 nm in diameter and exhibited superparamagnetic behavior at room temperature with saturation magnetization (M_s) ranging between 21-35 emu/g magnetite. Approximately 6.8±0.5% of indomethacin model drug was effectively loaded in the complexes (drug loading efficiency = 68 μg/mg of magnetite). Entrapping efficiency of the drug was 27-32%, depending on the molecular weights of mPEG and PCL blocks; high

2.6) *PERCH-CIC Congress VI, 3-6 May 2009, Jomtien Palm Beach& Resort, Pattaya, Chonbury, Thailand*

PERCH-CIC

CONGRESS VI

Theme: Towards a Sustainable Future

การประชุมวิชาการ

ศูนย์ความเป็นเลิศด้านนวัตกรรมทางเคมี ครั้งที่ 6

3-6 May 2009

Jomtien Palm Beach Hotel & Resort Pattaya, Chonburi

PERCH-CIC **Center of Excellence for Innovation in Chemistry**

www.perch-cic.org

S3-O14

Indomethacin-loaded Bilayer-Surface Magnetite Nanoparticles Its Released Behavior

Siraprapa Meerod, Uthai Wichai and Metha Rutnakornpituk
Department of Chemistry and Center of Excellence for Innovation in Chemistry, Faculty of Science, Naresuan University, Phitsanulok, 65000 Thailand.

Core-shell magnetite nanoparticle having bilayer surface and loading with indomethacin have been presented. The particles were first prepared by a co-precipitation method and stabilized with poly(ethylene glycol) methyl ether-poly(ε-caprolactone) (mPEG-PCL) amphiphilic block copolymer to form the particles having hydrophobic inner shell and hydrophilic corona. Hydrophobic PCL block is thought to physically adsorb onto the oleic acid-precoated particle surface and hydrophilic mPEG block provides steric stabilization in aqueous dispersions. mPEG-PCL copolymers with systematically varied molecular weights of each block (2,000-10,000 g/mol, 2,000-2,000 g/mol, 5,000-10,000 g/mol, 5,000-5,000 g/mol, respectively) were synthesized by a ring-opening polymerization of ε-caprolactone using mPEG as a macroinitiator and stannous octoate catalyst. The particles were about 9.0±1.1 nm in diameter and exhibited superparamagnetic behavior at room temperature with saturation magnetization (M_s) ranging between 21-35 emu/g magnetite.

Approximately 6.8±0.5% of indomethacin model drug was effectively loaded in the complexes (drug loading efficiency = 68 μg/mg of magnetite). Entrapping efficiency of the drug was 27-32%, depending on the molecular weights of mPEG and PCL blocks; high molecular weight PCL in the complexes promoted their entrapping efficiency. Releasing profile of the complexes indicated that 23-55% of the entrapped drug in the complexes was gradually released and it reached the equilibrium within 24 h. Percent of released drug from the complexes at equilibrium decreased with increasing PCL block lengths. The releasing profile is hence hypothetically tunable by adjusting the molecular weights of mPEG and PLC blocks. This complex was theoretically possible to load any other hydrophobic drug by partitioning to the hydrophobic inner shell on the particle surface and they might be suitable for use as efficient drug delivery vehicles.

Keywords: water dispersible, magnetite, nanoparticle, bilayer stabilizer

Selected References:

1. Bergeman, C.; Schulte, M. D.; Oster, J.; Brassard, L.; Lubbe, S. A. *Magnetism Magnetic Materials* 1999, *194*, 45-52.
2. Nathan, K.; Glen, E.; Fryxell, Z.; Miqin, Z.. *American Chemical Society* 2004, *126*, 7206-7211.
3. Liu, G.; Yang, H.; Zhou, H. *Biomacromolecules* 2005, *6*, 1280-1288 *Encyclopedia of Spectroscopy and Spectrometry*, Academic Press, San Diego, 1999, pp. 1945-1954.
4. Harris, L. A.; Goff, J. D.; Carmichael, A. Y.; Riffle, J. S.; Harburn, J. J.; St. Pierre, T. G.; Saunders, M.. *Chem Mater* 2003, *15*, 1367.

S3-P48

Efficient Immobilization of Folic Acid onto Nanoparticle Surfaces

Nipaporn Puangsin, Uthai Wichai and Metha Rutnakornpituk
Department of Chemistry and Center of Excellence for Innovation in Chemistry, Faculty of Science, Naresuan University, Phitsanulok 65000, Thailand.

We are here reporting an efficient method to immobilize folic acid onto surfaces of magnetite nanoparticles. Folic acid is known as a low-molecular-weight compound that their corresponding folate receptor is overexpressed on many types of cancer cells. Therefore, to obtain specific cancer cell recognition and increased efficiency of nanoparticle intracellular uptake, folic acid has been coated on nanoparticles so that it can couple to the folate receptors on cancer cell membrane. Therefore magnetic nanoparticles were hence surface modified with poly(acrylic acid) (PAA) and folic acid, respectively, to offer improved ability to target specific cells. Magnetite nanoparticles were synthesized via a thermal decomposition reaction of iron (III) acetylacetonate precursor in benzyl alcohol to obtain narrow-size distribution nanoparticles. PAA-grafted nanoparticles were synthesized via a three-step reaction: 1) formation of atom transfer radical polymerization (ATRP) initiating sites from the nanoparticle surface, 2) ATRP of *t*-butyl acrylate monomers mediated by a copper complex to obtain poly(*t*-butyl acrylate)(poly(*t*-BA))-coated magnetite nanoparticles, and 3) hydrolysis of poly(*t*-BA) in acidic dispersions to obtain PAA-magnetite complex. Thermal gravimetric analysis (TGA) disclosed the composition ratio of iron oxide to polymer as a function of time in ATRP step. Subsequently, folic acid was successfully immobilized on the surfaces of magnetite nanoparticles. Fourier transform infrared spectroscopy (FTIR) was used to monitor the reaction progress in each step.

Transmission electron micrographs (TEM) revealed that the particle size 9 nm after coating with PAA. Vibrating sample magnetometry (VSM) manifested that the magnetite nanoparticles were superparamagnetic. Intracellular uptake of the folic acid-immobilized nanoparticles into cancer cells is warranted to be studied.

Keywords: magnetite nanoparticles, Atomic Transfer Radical Polymerization (ATRP), poly(acrylic acid), folic acid

Selected References:

1. Pinna, N.; Grancharov, S.; Beato, P.; Bonville, P.; Antonietti, M.; Niederberger, M. *Chem. Mater.* 2005, *17*, 3044-3049.
2. Sun, Y.; Ding, X.; Zheng, Z.; Cheng, X.; Hu, X.; Peng, Y. *Eur. Polym. J.* 2007, *43*, 762-772.
3. Saez-Martinez, V.; Perez-Alvarez, L.; Merrero, M. T.; Hernaez, E.; Katime, I. *Macromolecular Nanotechnology* 2008, *44*, 1309-1322.

3) 5 Invited oral presentations

3.1) The World Polymer Congress 2012 (MACRO2012), 24-29 June 2012, Blacksburg, Virginia Tech, USA,

Title: Azlactone functionalization of magnetite nanoparticles using ATRP and their bioconjugation

3.2) The 38th Congress on Science and Technology of Thailand (STT38th), 17-19 October 2012, The Empress Hotel, Chiang Mai, Thailand,

Title: Surface modification of magnetite nanoparticle with functional polymers

3.3) The 3rd Polymer Congress of Thailand (PCT3), 28-29 March 2013, Patumwan Princess Hotel, Bangkok, Thailand

Title: Surface functionalization of magnetic nanoparticle with polymers and its bioconjugation

3.4) The 2nd Taiwan-Thailand Bilateral Mini-symposium at Faculty of Science, Mahidol University, 17-18 January 2013

Title: Surface Modification of Magnetic Nanoparticles with Functional Polymers

3.5) The 1st Thai-Taiwan Colloquium on “Frontier Research in Science and Technology” 30 November 2012 and 25 January 2013 at Naresuan University

Title: Surface modification of magnetic nanoparticle with functional polymers

3.1) The World Polymer Congress 2012 (MACRO2012), 24-29 June 2012, Blacksburg, Virginia Tech, USA,

Title: Azlactone functionalization of magnetite nanoparticles using ATRP and their bioconjugation

Invitation to IUPAC MACRO 2012 at Virginia Tech

iupac [iupac@vt.edu]

ส่ง: 12 มกราคม 2012 23:01

ถึง: Metha Rutnakornpituk

Invitation to Lecture at the IUPAC MACRO 2012 World Polymer Congress at Virginia Tech

We formally invite you to lecture at the 44th International Symposium on Macromolecules (MACRO 2012) – IUPAC World Polymer Congress, which will take place June 24 through June 29, 2012, in Blacksburg, Virginia, USA at the Virginia Tech Campus. As part of this invitation, your registration fee of $599 for the conference is waived. You would need to pay your own travel, food, and lodging expenses. Information on travel options can be found at the conference website, www.macro2012.org.

We sincerely hope you will accept this invitation to attend the World Polymer Congress. We look forward to hearing your response. If you accept our invitation, we will give you a special link for conference registration. We invite you to submit an abstract for a lecture at the conference. Please designate your preferred symposium during the registration process, and we will attempt to ensure an oral presentation with the symposium organizer. Abstract submission is open in December 2011 at www.macro2012.org. Thank you for considering this invitation and please let us know by simply replying to this invitation (iupac@vt.edu).

I personally look forward to seeing you in Blacksburg next summer!

All the best, Tim

Timothy E. Long
Organizing Committee Chair
IUPAC MACRO 2012
Virginia Tech

Virginia Tech is hosting IUPAC MACRO 2012:
World Polymer Congress, June 24 - 29, 2012, MACRO2012.org

IUPAC
International Union of Pure and Applied Chemistry

World Polymer Congress
June 24–29, 2012

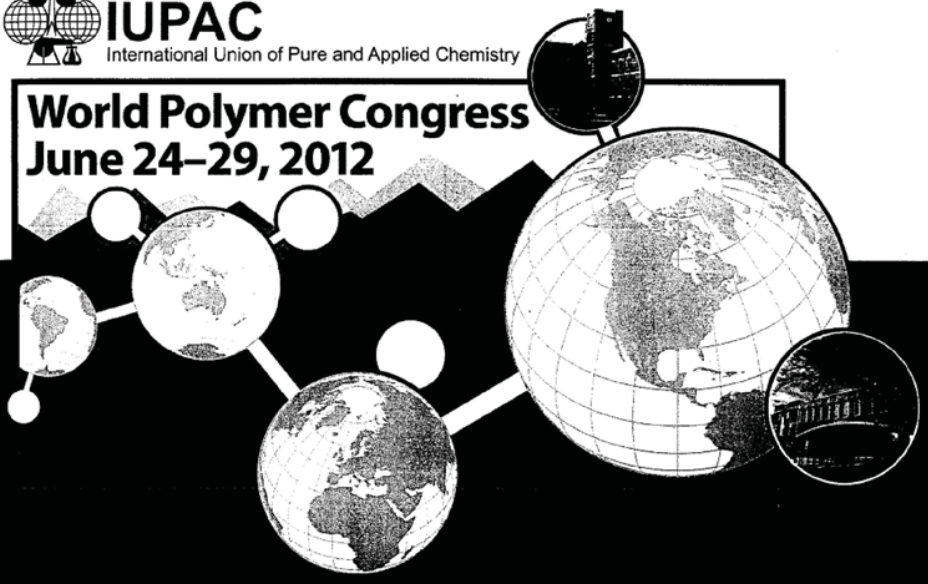

MACRO2012

Enabling Technologies for a Safe, Sustainable, Healthy World

VirginiaTech
Invent the Future®

Blacksburg, Virginia • USA

Abstract

AZLACTONE FUNCTIONALIZATION OF MAGNETITE NANOPARTICLES USING ATRP AND THEIR BIOCONJUGATION

Y.Prai-in[1], K.Tankanya[1], B.Rutnakornpituk[1], U.Wichai[1], V. Montembault[2], S.Pascual[2], L.Fontaine[2] and M.Rutnakornpituk[1]**

[1]Department of Chemistry and Center of Excellence for Innovation in Chemistry, Faculty of Science, Naresuan University, Phitsanulok, 65000 Thailand. [2]UCO2M, LCOM-Chimie des Polymères, UMR CNRS 6011, Université du Maine, Avenue O. Messiaen, 72085 Le Mans Cedex 9, France, *E-mail: methar@nu.ac.th, laurent.fontaine@univ-lemans.fr

Introduction

Recently, several groups have applied atom transfer radical polymerization (ATRP) based on a "grafting-from" method to prepare polymeric layers on surface of magnetite nanoparticle (MNP) [1-3]. The advantages of this method are that the as-synthesized polymer possesses low polydispersity index, controllable molecular weight, functionality, composition distribution and desired polymer architecture. In this work, we have applied a copper-mediated ATRP technique to synthesize grafted statistical copolymer of poly(ethylene glycol) methacrylate (PEGMA) and 2-vinyl-4,4-dimethylazlactone (VDM) onto MNP. The azlactone ring of 4,4-dimethyl-5-oxazolone displays a high reactivity towards a nucleophilic molecules by means of a ring-opening addition reaction without the use of catalysts. Water dispersibility of MNP should be greatly improved by introducing a thin layer of PEGMA to its surface and the presence of the azlactone rings of VDM serves as a site for immobilization of bioentities on its surface. In this work, thymine PNA monomer and folic acid (FA) were used as model compounds for immobilization onto the VDM-grafted particles.

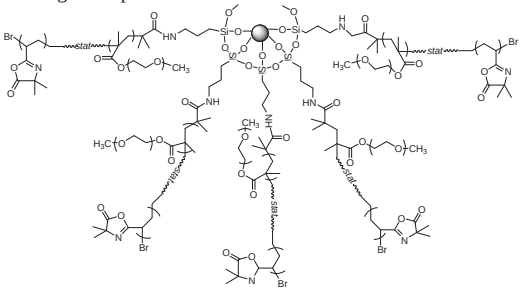

Figure 1. Surface modification of MNP with poly(PEGMA-*stat*-VDM) copolymer

Experimental

Synthesis of poly(PEGMA-*stat*-VDM)-coated MNP *via* ATRP. MNP coated with an ATRP initiator (BTPAm-coated MNP) dispersed in toluene was sonicated for 20 min in argon. This suspension was then added to a degassed Schlenk tube containing CuBr, PEGMA, VDM, EBiB (used as a free initiator), and DMF (used as an internal standard) *via* a cannula. Degassed Me_6Tren ligand was added to the above dispersion (*t=0*) and the mixture was set in an oil bath preheated at 30°C. The reaction progress was monitored via ^{1}H NMR. At the end of the copolymerization, the MNP were separated from the mixture by external magnet, precipitated into diethyl ether and dried *in vacuo*. The as-synthesized poly(PEGMA-*stat*-VDM)-coated MNP resulted as a fine black powder.

Immobilization of thymine PNA monomer or FA on the poly(PEGMA-*stat*-VDM)-coated MNP. Thymine PNA monomer or FA (10 mg) was added into a dispersion of poly(PEGMA-*stat*-VDM)-coated MNP (10 mg) in DMF (10 mL). The mixture was sonicated at room temperature for 6 h under argon The particle was then collected using an external magnet and washed with DMF repeatedly to remove ungrafted thymine PNA monomer or FA from the particle surface.

Results and Discussion

Fourier transform infrared spectroscopy (FTIR) indicated the presence of the copolymer in the MNP complexes. Poly(PEGMA-*stat*-VDM)-coated MNP exhibited a characteristic signal of azlactone rings of VDM units at 1816 cm^{-1} (-C=O stretching), 1203 cm^{-1} (C-O-C stretching) and that of PEGMA at 1722 cm^{-1} (-C=O stretching), indicating the presence of the copolymer in the complex. A broad and strong band of Fe-O from MNP cores was also observed at 578 cm^{-1}. After surface modification of the particle with poly(PEGMA-*stat*-VDM) in DMF, there was some nanoscale aggregation of about 30-50 particles/cluster (Figure 2). After immobilization of thymine PNA monomer on their surface, more aggregation of the particles was observed (about 100 particles/cluster). The presence of hydrophobic thymine PNA monomer units on surface of the complexes might promote the particle aggregation in the reaction solvent (DMF). Similar behavior was also observed in the case of FA-grafted MNP.

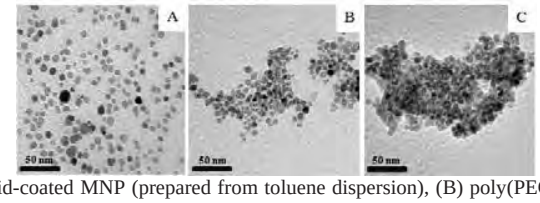

Figure 2. TEM images of (A) oleic acid-coated MNP (prepared from toluene dispersion), (B) poly(PEGMA-*stat*-VDM)-coated MNP (prepared from DMF dispersion) and (C) poly(PEGMA-*stat*-VDM)-coated MNP immobilized with thymine PNA monomer (prepared from DMF dispersion)

The ideal chemical structures of poly(PEGMA-*stat*-VDM)-coated MNP immobilized with thymine PNA monomer and folic acid are illustrated in Figure 3.

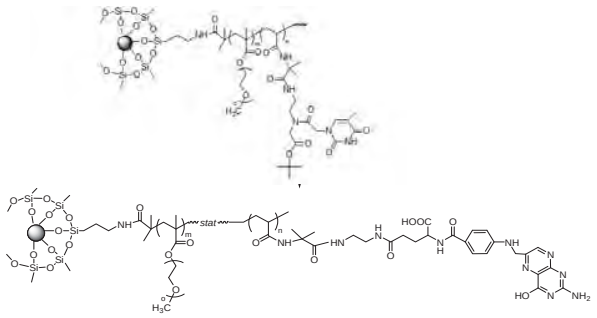

Figure 3. Poly(PEGMA-*stat*-VDM)-coated MNP immobilized with thymine PNA monomer (top) and folic acid (FA) (bottom)

Thermogravimetric analysis (TGA) results indicated that there were about 4 wt% and 10 wt% of the PNA monomer and FA, respectively, in the complexes. In addition, the existence of the PNA monomer and FA in the complex was also confirmed *via* FTIR and vibrating sample magnetometry (VSM). For example, the decreases of saturation magnetization (M_s) from 56 emu/g of bare MNP to 36 emu/g of poly(PEGMA-*stat*-VDM)-coated MNP and to 34 emu/g of poly(PEGMA-*stat*-VDM)-coated MNP immobilized with thymine PNA monomer were devoted to the decrease of MNP content in the complexes owing to the copolymer/thymine coating.

Conclusions

This work presented the surface modification of MNP with the statistical copolymer between PEGMA and VDM *via* ATRP to obtain the particles containing active functional groups on its surface. The nanosolid supports were successfully used for immobilization of thymine PNA monomers and folic acid on its surface. The results indicated the feasibility to functionalize the surface of these novel azlactone-based nanoparticles with a broad range of other nucleophilic scavengers such as hydroxyl- and thiol-containing compounds.

Acknowledgement. The authors thank the Thailand Research Fund (TRF) and Naresuan University (DBG5380001) and the Royal Golden Jubilee for financial funding.

References

(1) Marutani, E.; Yamamoto, S.; Ninjbadgar, T.; Tsujii, Y.; Fukuda, T.; Takano, M. *Polymer* **2004,***45*,2231.
(2) Zhou, Y.; Wang, S.; Ding, B.; Yang, Z. *Chem. Eng. J.* **2008**,*138*,578.
(3) Sun, Y.; Ding, X.; Zheng, Z.; Cheng, X.; Hu, X.; Peng, Y. *Eur. Polym. J.* **2007**,*43*,762.

3.2) The 38th Congress on Science and Technology of Thailand (STT38th), 17-19 October 2012, The Empress Hotel, Chiang Mai, Thailand,

Program Book

38th CONGRESS ON SCIENCE AND TECHNOLOGY OF THAILAND

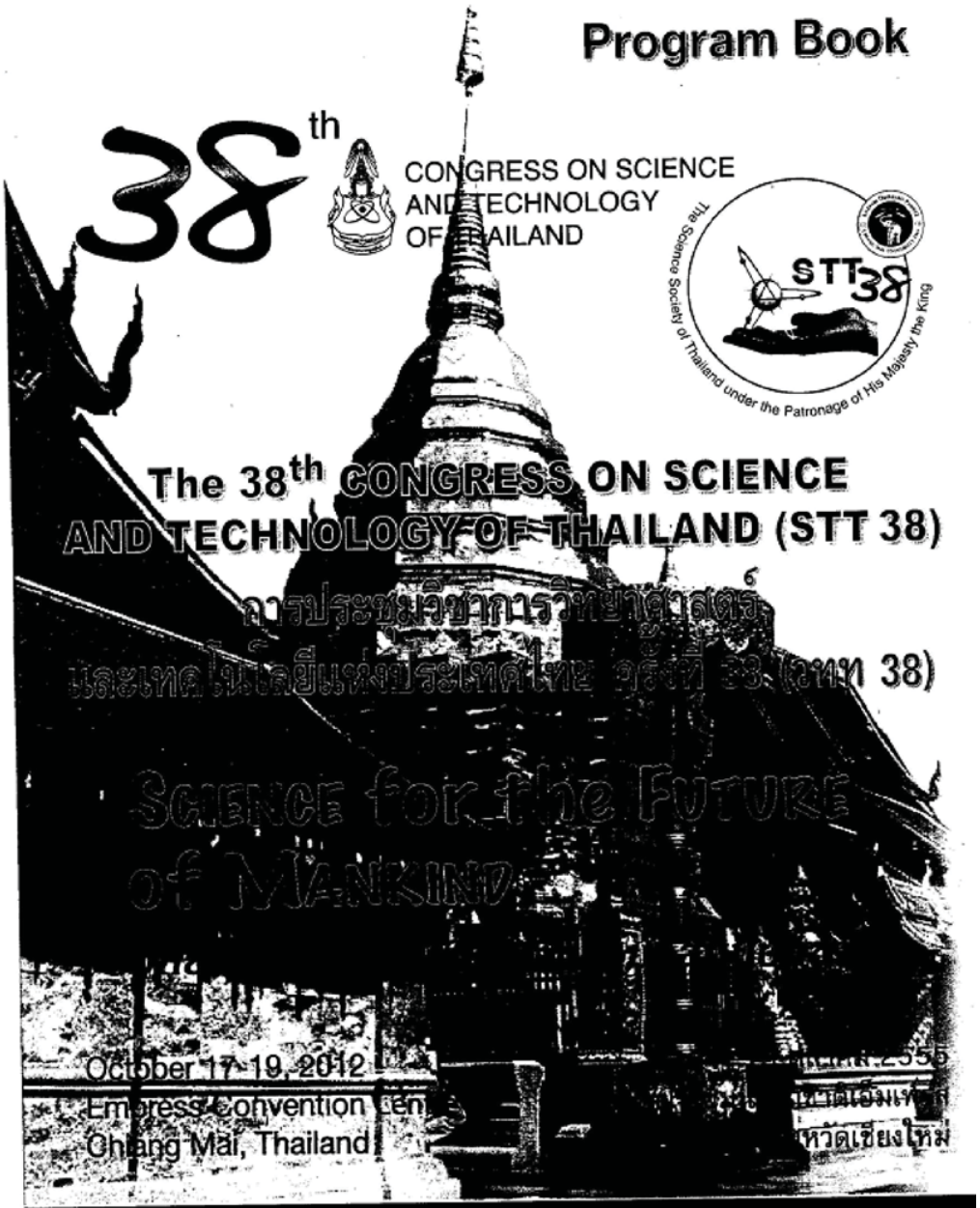

The 38th CONGRESS ON SCIENCE AND TECHNOLOGY OF THAILAND (STT 38)

การประชุมวิชาการวิทยาศาสตร์และเทคโนโลยีแห่งประเทศไทย ครั้งที่ 38 (สทท 38)

Science for the Future of Mankind

October 17-19, 2012
Empress Convention Center
Chiang Mai, Thailand

Organized by:
The Science Society of Thailand under the Patronage of His Majesty the King in association with the Faculty of Science, Chiang Mai University, Chiang Mai, Thailand

www.scisoc.or.th/stt38

PROGRAM FOR INVITED LECTURES AND ORAL PRESENTATIONS
19th October 2012

SESSION E (POLYMERS)
ROOM: ECC-Chiangmai 2

Chair Person: Taweechai Amornsakchai
Co-chair Person: Winita Punyodom

Time	ID	Title	Speaker	Language
13:00-13:30	E_INV001	SURFACE MODIFICATION OF MAGNETITE NANOPARTICLE WITH FUNCTIONAL POLYMERS	Metha Rutnakornpituk	English
13:30-13:50	E_E0021	SYNTHESIS OF CARBOXYMETHYLCHITOSAN HYDROGEL GRAFTED WITH THERMO-SENSITIVE POLY(*N*-ISOPROPYLACRYLAMIDE)	Rathanon Jankaew	English
13:50-14:10	E_E0017	KINETIC STUDIES OF THE BULK RING-OPENING POLYMERISATION OF L-LACTIDE USING A NOVEL SOLUBLE TIN(II) *n*-BUTOXIDE INITIATOR BY DIFFERENTIAL SCANNING CALORIMETRY	Montira Sriyai	English
14:10-14:30	E_E0018	ESTIMATION OF THE ACTIVATION PARAMETERS FOR RING OPENING POLYMERIZATION OF ε-CAPROLACTONE INITIATED BY STANNOUS OCTOATE USING DIFFERENTIAL SCANNING CALORIMETRY	Wanich Limwanich	English
14:30-15:00		coffee break		

Metha Rutnakornpituk

Department of Chemistry and Center for Innovation in Chemistry, Faculty of Science, Naresuan University, Phitsanulok 65000, Thailand

e-mail: methar@nu.ac.th

SURFACE MODIFICATION OF MAGNETITE NANOPARTICLE WITH FUNCTIONAL POLYMERS

Surface functionalization of magnetite nanoparticle (MNP) has recently attracted a great attention in the biotechnology and biomedical applications. We herein present various strategies for modification and functionalization of MNP surface and its corresponding applications briefly. MNP can be prepared *via* either a coprecipitation of the mixture of iron salts or a thermal decomposition of iron organic precursors. The particle was then surface modified with various kinds of polymers to obtain the MNP with desirable properties such as high magnetic saturation, biocompatibility, water dispersibility and containing interactive functions at the surface. Different strategies, such as "grafting to" and "grafting from" methods, have been applied to modify the particle surface. The stability in the dispersions and the availability for further functionalization of MNP have been improved after the polymeric coatings. For example, we have recently demonstrated the surface modification of MNP with azlactone functional groups for further attachments with bioentities. Surface functionalization of MNP with pH sensitive polymers, e.g. poly(4-vinyl pyridine) and poly(acrylic acid) or UV sensitive polymers, e.g. poly(azobenzene acrylate), have also been reported. These surface modified and functionalized MNPs exhibit a great potential for uses in many areas, including biomedical and biotechnology applications.

References: 1. Thong-On B., Rutnakornpituk B., Wichai U. and Rutnakornpituk M., *Journal of Nanoparticle Research* **2012**, *14*, 953-964.2. Prai-in Y., Tankanya K., Rutnakornpituk B., Wichai U., Montembault V., Pascual S., Fontaine L. and Rutnakornpituk M., *Polymer* **2012**, *53*, 113-120. 3. Rutnakornpituk B., Wichai U., Vilaivan T. and Rutnakornpituk M., *Journal of Nanoparticle Research* **2011**, *13*, 6847-6857. 4. Rutnakornpituk M., Puangsin N., Theamdee P., Rutnakornpituk B. and Wichai U., *Polymer* **2011**, *52*, 987-995. 5. Theamdee P., Traiphol R., Rutnakornpituk B., Wichai U. and Rutnakornpituk M., *Journal of Nanoparticle Research* **2011**, *13*, 4463-4477.

Dr. Metha received his Ph.D. in Chemistry from Virginia Tech, USA, in 2002. He is currently an associate professor at the Department of Chemistry, Faculty of Science, Naresuan University. His research theme mainly focuses on the design and synthesis of block and graft copolymers with functional groups and surface modification of nanoparticle via controlled radical and living anionic polymerizations.

3.3) The 3rd Polymer Congress of Thailand (PCT3), 28-29 March 2013, Patumwan Princess Hotel, Bangkok, Thailand

Title: Surface functionalization of magnetic nanoparticle with polymers and its bioconjugation

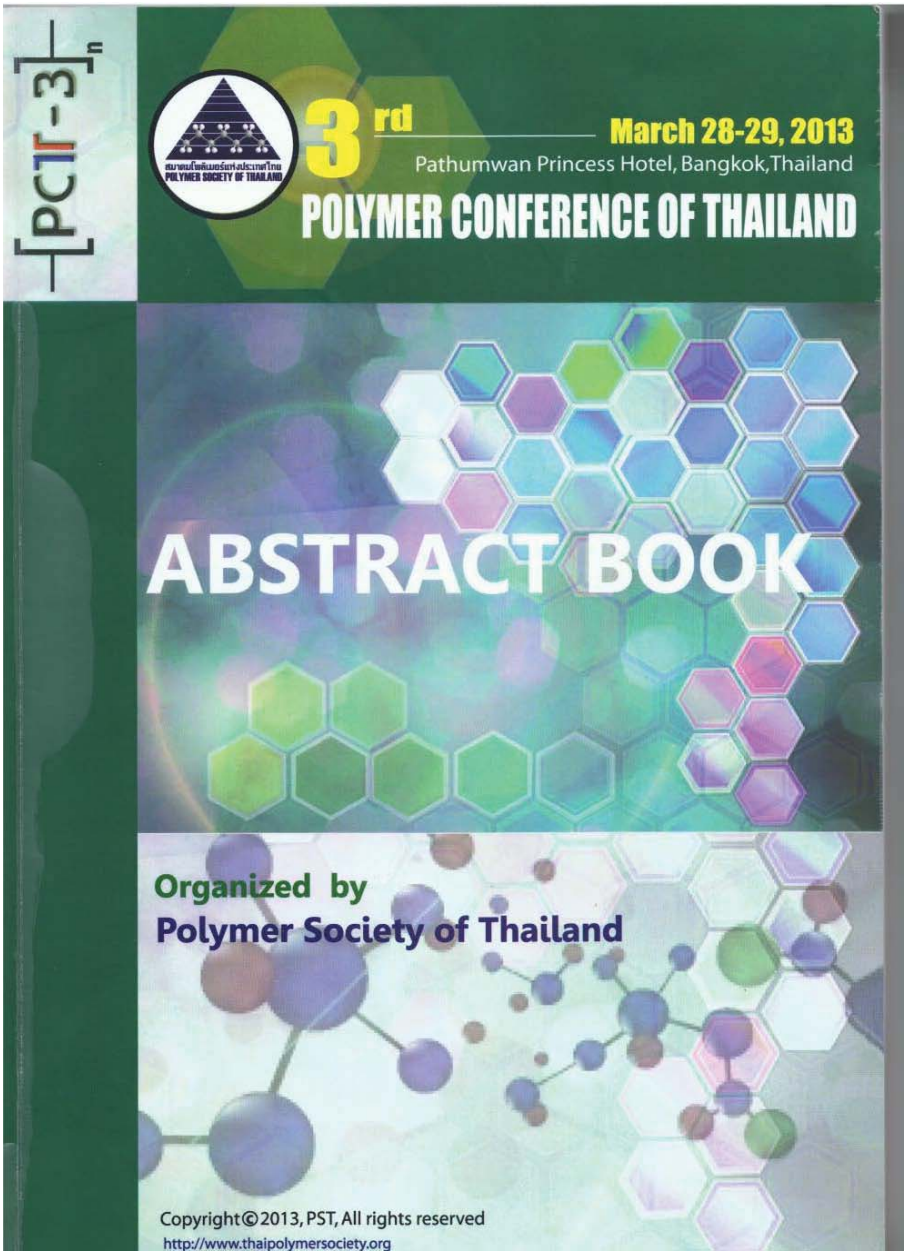

สมาคมโพลิเมอร์แห่งประเทศไทย
POLYMER SOCIETY OF THAILAND

24 March 2013

Subject: PCT-3 presentation schedule

Dear **Associate Professor Metha Rutnakornpituk**,

Polymer Society of Thailand and the organizing committee of The 3rd Polymer Conference of Thailand **[-PCT-3-]** is very grateful to have your honor as our **Keynote Speaker** in **session: Polymers for Health and Medicine (PHM)**. Your presentation is scheduled to be on **Thursday 28 March 2013, from 11:00-11:30 am** (25 min talk + 5 min Q&A), at **Jamjuree Room 1**, Floor M, Pathumwan Princess Hotel [www.pprincess.com].

The full presentation program is available at

http://www.thaipolymersociety.org/pct-3/pct-3_index.html

Thank you again and we are looking forward to meeting you in PCT-3.

Sincerely yours,

(Professor Suwabun Chirachanchai)

President of Polymer Society of Thailand

& Chairman of PCT-3

PROGRAM

The 3rd Polymer Conference of Thailand

March 28-29, 2013 @Pathumwan Princess Hotel, Bangkok

Thursday, March 28, 2013 (1st day)

08:00-09:00	***Registration*** *(M Floor)*				
Jamjuree Ballroom A & B					
09:00-09:20	**Opening Remarks by** ***Prof.Suwabun Chirachanchai*** *President of The Polymer Society of Thailand (PST)*				
09:20-10:10	**Plenary lecture I:** ***Prof.Yoshiki Chujo*** *Kyoto University, Japan* " Advanced luminescent materials based on organoboron polymers"				
Refreshment Break (10:10-10:30)					
Jamjuree Ballroom A & B		**Jamjuree Room 1**		**Jamjuree Room 2**	
Polymers for Energy & Environment (1)		Polymers for Health & Medicine (1)		Polymers for Industry (1)	
10:30-11:00	**KN1 (Miyata)**	10:30-11:00	**KN1 (Wanida)**	10:30-11:00	**KN1 (Piyarat)**
11:00-11:30	**KN2 (Yupaporn)**	11:00-11:30	**KN2 (Metha)**	11:00-11:20	**PIN-OP-01**(P011)
11:30-11:50	**PEN-OP-01 (Miyamoto)**	11:30-12:00	**KN3 (Panya)**	11:20-11:40	**PIN-OP-02**(P075)
11:50-12:10	**PEN-OP-02** (P015)			11:40-12:00	**PIN-OP-03**(P035)
Lunch (12:00-13:30) *@Ground Floor*					
13:30-14:20	**Plenary lecture II:** ***Pongdej Pantasanyakul*** *VP Maintenance and Engineering, PTT Phenol* "Challenge of doing petrochemical projects in Thailand"				
14:20-14:50	**BASF-PST lecture:** *hosted by* ***BASF*** ***Asst.Prof. Sumrit Wacharasindhu*** *Department of Chemistry, Faculty of Science, Chulalongkorn University* "Direct colorimetric chemical sensor from polydiacetylenes"				
Refreshment Break (14:50-15:10)					
Jamjuree Ballroom A		**Jamjuree Ballroom B**		**Jamjuree Room 1 & 2**	
Polymers for Health & Medicine (2)		Polymer for Industry (2)		Special Bioplastic Session	
15:10-15:40	**KN4 (Voravee)**	15:10-15:40	**KN3 (Anoma)**	15:10-15:40	**Dr. Wantanee Chongkum** *–NIA*
15:40-16:00	**PHM-OP-01** (P021)	15:40-16:00	**PIN-OP-04**(P023)	15:40-16:00	**Asst.Prof. Winita Punyodom** *–Chiangmai U.*
16:00-16:20	**PHM-OP-02** (P036)	16:00-16:20	**PIN-OP-05**(P038)	16:00-16:20	**Dr. Chaya Chandavasu** *-PTTGC*
16:20-16:40	**PHM-OP-03** (P053)	16:20-16:40	**PIN-OP-06**(P034)	16:20-16:40	**Dr. Phietoon Trivijitkasem** *-Thantawan*
		16:40-17:00	**PIN-OP-07**(P022)	16:40-18:00	**Panel Discussion** "Market drive technology push: What is the key factor of success?" Prof.Suwabun Chirachanchai *–PST & moderator* **Panelist:** Dr. Pipat Weerathaworn *-Thai Bioplastic Industrial Association* Dr. Pisuth Lertwilai *-Multibax* *Mrs.*Yannee Sirivong na Ayudhya *-Concept Tree* Dr. Thanawadee Leejarkpai *-National Metal and Materials Technology Center* Dr. Narin Kaabbuathong *-PTT Public Co. Ltd.* Dr. Suphakij Suttiruengwong *-Silpakorn University*
		17:00-17:20	**PIN-OP-08**(P013)		
		17:20-17:40	**PIN-OP-09**(P043)		
Jamjuree Ballroom A & B					
18:00-19:30	***Cocktail Reception*** *-Sponsor Acknowledgment* *-Company Profile Talk*				

3.4) The 2nd Taiwan-Thailand Bilateral Mini-symposium at Faculty of Science, Mahidol University, 17-18 January 2013

Title: Surface Modification of Magnetic Nanoparticles with Functional Polymers

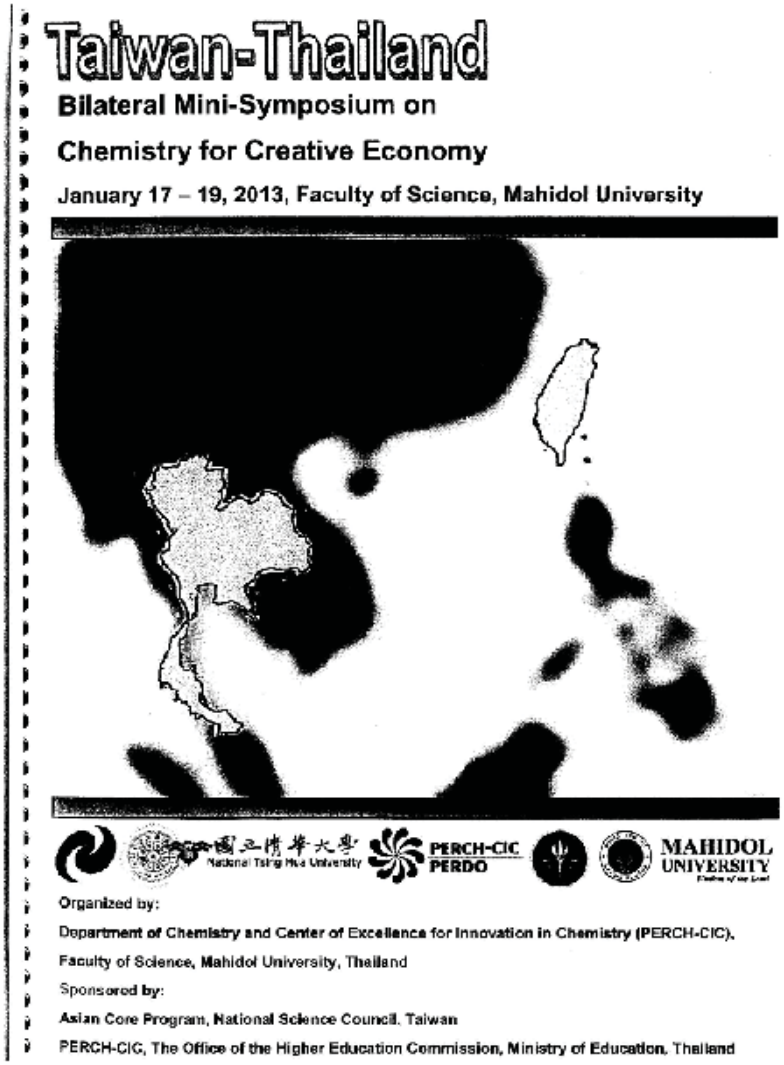

The 2nd Taiwan-Thailand Bilateral Mini-Symposium:

Chemistry for Creative Economy

17 - 18 January, 2013

Stang Mongkolsuk Building, Faculty of Science, Mahidol University, Thailand

Thursday January 17, 2013

08.00-08.45	Registration
08.45-09.00	Welcome Address: Prof. Vichai Reutrakul, Director, PERCH-CIC Opening Address: Prof. Skorn Mongkolsuk, Dean, Faculty of Science, Mahidol University
	Chairman: Vichai Reutrakul, Mahidol University
09.00-09.30	**IL-01: Recent Advances in the Chemistry of Masked *o*-Benzoquinones** (Chun-Chen Liao)
09.30-10.00	**IL-02: Vicinal Dianions of Succinic Acid Derivatives: Syntheses of Some γ-Lactone and Furofuran Natural Products** (Manat Pohmakotr)
10.00-10.30	**Coffee/tea break**
	Chairman: Manat Pohmakotr, Mahidol University
10.30-11.00	**IL-03: Novel Strategies toward Natural Product Synthesis** (Minoru Isobe)
11.00-11.30	**IL-04: Antimicrobial Secondary Metabolites from Marine-derived Fungi** (Vatcharin Rukachaisirikul)
11.30-12.00	**IL-05: Metal-catalyzed C-H Activation for the Synthesis of Isoquinolinium and Quinolizinium Salts and the Application in Natural Product Synthesis** (Chien-Hong Cheng)
12.00-13.00	**Lunch/informal discussion**
	Chairman: Biing-Jiun Uang, National Tsing Hua University
13.00-13.30	**IL-06: Acenes Generated from Soluble Precursors and Their Applications on OFET** (Tahsin J. Chow)
13.30-14.00	**IL-07: Carbazole Dendrimers** (Vinich Promarak)
14.00-14.30	**IL-08: Nanoparticle, Polymer, and Fullerene Ternary Hybrid Bulk Heterojunction Organic Photovoltaics: A Unified Investigation of the Influence of Nanoparticles Having Varied Conductivity, Surface Capping Agent, and Light Harvesting** (Chin-Ti Chen)
14.30-15.00	**IL-09: Surface Modification of Magnetic Nanoparticles with Functional Polymers** (Metha Rutnakornpituk)
15.00-15.30	**IL-10: Recent Advances of Small Molecule-based Organic Solar Cells** (Ken-Tsung Wong)
15.30-16.00	**Coffee/tea break**
	Chairman: Vinich Promarak, Suranaree University of Technology
16.00-16.30	**IL-11: Enzymatic Synthesis of Poly-LacNAc and Modified Poly-LacNAc** (Chun-Cheng Lin)
16.30-17.00	**IL-12: Synthesis of Cyclic Polyesters Catalyzed by Ligated Tin(II) Complexes** (Khamphee Phomphrai)

Surface Modification of Magnetic Nanoparticles with Functional Polymers

Metha Rutnakornpituk, Uthai Wichai, Boonjira Rutnakornpituk, Siraprapa Meerod, Pawinee Theamdee, Nipaporn Puangsin, Yingrak Prai-in, Bandit Thong-on, and Thapanapong Theppaleak

Department of Chemistry and Center of Excellence for Innovation in Chemistry, Faculty of Science, Naresuan University, Phitsanulok, 65000 Thailand

methar@nu.ac.th

Our work has focused on modification and functionalization of magnetite nanoparticle (MNP) surface with various polymers *via* atom transfer radical polymerization (ATRP). Different strategies, such as "grafting to" and "grafting from" methods, were employed to modify the particle surface. For example, active functional groups, e.g. azlactone (VDM) and acrylic acid groups, were successful functionalized onto the MNP surface for further attachments with amino acid and folic acid, respectively. In addition, surface functionalization of MNP with UV sensitive poly(azobenzene acrylate) and pH responsive poly(4-vinyl pyridine) was presented. Also, surface modification of MNP with polysiloxane in combination with poly(poly(ethylene glycol) methacrylate) to obtain polymeric bilayer surfactant was discussed. These surface modified and functionalized MNPs exhibit a great potential for uses in many areas, including biomedical and biotechnology.

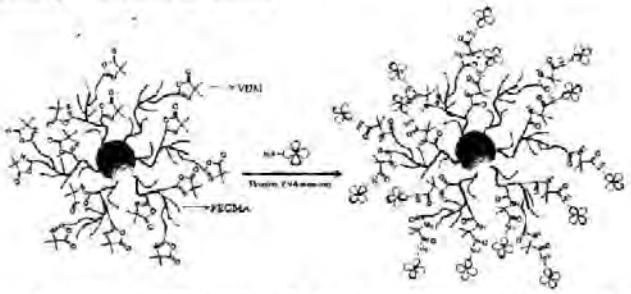

1. Prai-in, Y.; Tankanyu, K.; Rutnakornpituk, B.; Wichai, U.; Montembault, V.; Pascual, S.; Fontaine, L.; Rutnakornpituk, M. *Polymer* **2012**, *53*, 113.
2. Thong-On, B.; Rutnakornpituk, B.; Wichai, U.; Rutnakornpituk, M. *J. Nanopart. Res.* **2012**, *14*, 953.
3. Rutnakornpituk, M.; Puangsin, N.; Theamdee, P.; Rutnakornpituk, B.; Wichai, U. *Polymer* **2011**, *52*, 987.
4. Theamdee, P.; Traiphol, R.; Rutnakornpituk, B.; Wichai, U.; Rutnakornpituk, M. *J. Nanopart. Res.* **2011**, *13*, 4463.
5. Rutnakornpituk, B.; Wichai, U.; Vilaivan, T.; Rutnakornpituk, M. *J. Nanopart. Res.* **2011**, *13*, 6847.

METHA RUTNAKORNPITUK, Khon Kaen University (B.Sc. Hons. 1995), Virginia Tech (Ph.D. 2002), Associate Professor (2009-present). Research interests: synthesis of block copolymer, responsive polymers, surface modification of nanoparticle.

3.5) The 1st Thai-Taiwan Colloquium on “Frontier Research in Science and Technology” 30 November 2012 and 25 January 2013 at Naresuan University

Title: Surface modification of magnetic nanoparticle with functional polymers

We are invited to present our works representing the research team from Naresuan University to Prof. Dr. Chin-Ti Chen and Prof. Jason Dr. Chia-Seng Chang, Academia Sinica, Taiwan

4) Awards

4.1) Outstanding Research Award from The Office of National Research Council of Thailand, December, 2012. Title: “Synthesis and surface modification of magnetite nanoparticle with polymers”

4.2) Awards to the students in the project

4.2.1) นายบัณฑิต ทองอ่อน ได้รับรางวัลวิทยานิพนธ์ระดับปริญญาโทยอดเยี่ยม จากบัณฑิตวิทยาลัย มหาวิทยาลัยนเรศวร ประจำปี 2555 เรื่อง Synthesis of amphiphilic block copolymer via atom transfer radical polymerization as bilayer surfactant of magnetite nanoparticle

4.2.2) นางสาวภาวิณี เทียมดี ได้รับรางวัลการนำเสนอผลงานแบบโปสเตอร์ยอดเยี่ยมในงานการประชุมวิชาการระดับนานาชาติในงาน PACCON2009 ณ มหาวิทยาลัยนเรศวร เรื่อง Atom transfer radical polymerization of poly (ethylene glycol) methyl ether methacrylate (PEGMA) brush on magnetic nanoparticle surface

4.2.3) นายรฐนนท์ จันแก้ว ได้รับรางวัลการนำเสนอผลงานแบบโปสเตอร์ยอดเยี่ยมในงานการประชุมวิชาการระดับนานาชาติในงาน PERCH-CIC 2013 ณ โรงแรมจอมเทียนปาล์ม บีชแอนด์รีสอร์ท พัทยา ชลบุรี เรื่อง Temperature- and pH-Responsive Carboxymethylchitosan Hydrogel and a Controlled Release of Indomethacin

4.1) Outstanding Research Award from The Office of National Research Council of Thailand, December, 2012. Title: “Synthesis and surface modification of magnetite nanoparticle with polymers”

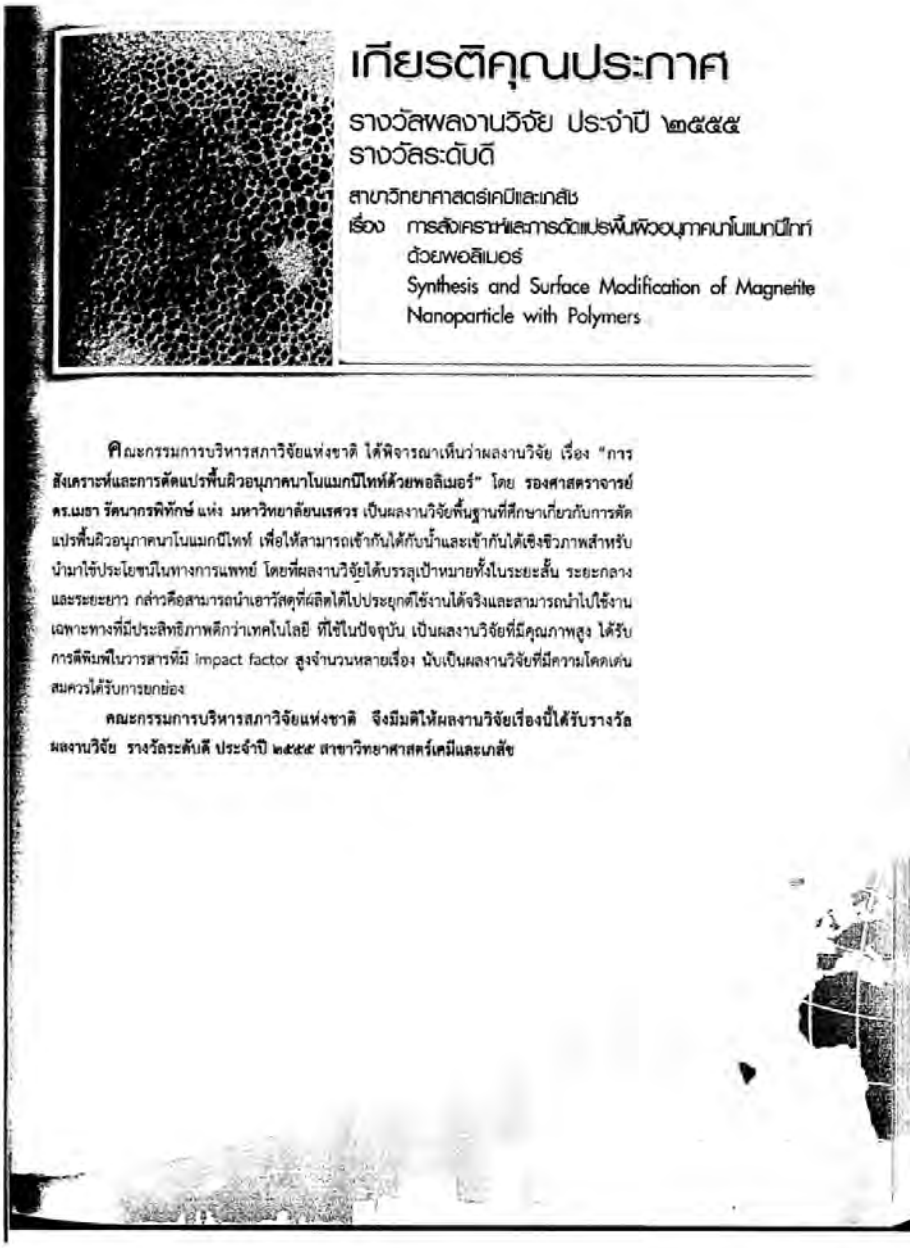

เกียรติคุณประกาศ

รางวัลผลงานวิจัย ประจำปี ๒๕๕๕
รางวัลระดับดี

สาขาวิทยาศาสตร์เคมีและเคมีสิ่ง

เรื่อง การสังเคราะห์และการดัดแปรพื้นผิวอนุภาคนาโนแมกนีไทท์ด้วยพอลิเมอร์

Synthesis and Surface Modification of Magnetite Nanoparticle with Polymers

คณะกรรมการบริหารสภาวิจัยแห่งชาติ ได้พิจารณาเห็นว่าผลงานวิจัย เรื่อง “การสังเคราะห์และการดัดแปรพื้นผิวอนุภาคนาโนแมกนีไทท์ด้วยพอลิเมอร์” โดย **รองศาสตราจารย์ ดร.เมธา รัตนากรพิทักษ์** แห่ง **มหาวิทยาลัยนเรศวร** เป็นผลงานวิจัยพื้นฐานที่ศึกษาเกี่ยวกับการดัดแปรพื้นผิวอนุภาคนาโนแมกนีไทท์ เพื่อให้สามารถเข้ากันได้กับน้ำและเข้ากันได้เชิงชีวภาพสำหรับนำมาใช้ประโยชน์ในทางการแพทย์ โดยที่ผลงานวิจัยได้บรรลุเป้าหมายทั้งในระยะสั้น ระยะกลาง และระยะยาว กล่าวคือสามารถนำเอาวัสดุที่ผลิตได้ไปประยุกต์ใช้งานได้จริงและสามารถนำไปใช้งานเฉพาะทางที่มีประสิทธิภาพดีกว่าเทคโนโลยี ที่ใช้ในปัจจุบัน เป็นผลงานวิจัยที่มีคุณภาพสูง ได้รับการตีพิมพ์ในวารสารที่มี impact factor สูงจำนวนหลายเรื่อง นับเป็นผลงานวิจัยที่มีความโดดเด่นสมควรได้รับการยกย่อง

คณะกรรมการบริหารสภาวิจัยแห่งชาติ จึงมีมติให้ผลงานวิจัยเรื่องนี้ได้รับรางวัลผลงานวิจัย รางวัลระดับดี ประจำปี ๒๕๕๕ สาขาวิทยาศาสตร์เคมีและเคมีสิ่ง

๑. ชื่อผลงาน

ชื่อผลงานวิจัย	การสังเคราะห์และการดัดแปรพื้นผิวอนุภาคนาโนแมกนีไทท์ด้วยพอลิเมอร์
หัวหน้าคณะ	รองศาสตราจารย์ ดร.เมธา รัตนากรพิทักษ์
สถานที่ติดต่อ	ภาควิชาเคมี คณะวิทยาศาสตร์ มหาวิทยาลัยนเรศวร จังหวัดพิษณุโลก ๖๕๐๐๐ โทรศัพท์ ๐ ๕๕๙๖ ๓๔๐๑ โทรศัพท์เคลื่อนที่ ๐๘ ๖๕๘๔ ๓๓๑๕ โทรสาร ๐ ๕๕๓๖ ๓๔๐๑
e-mail :	methar@nu.ac.th
ผู้วิจัยร่วม	นางสาวศิริประภา นิรอด นางสาวศิริรัก พรายดินทร์ นางสาวภาวิณี เพียมดี นายฐาปณพงศ์ เทพฤกษ์ นางสาวนิภาพร พวงศิลป์

๒. ความสำคัญและที่มาของการวิจัย

ในปัจจุบันได้มีการประยุกต์ใช้อนุภาคนาโนแมกนีไทท์ (Fe_3O_4) หลายด้านเนื่องจากสามารถตอบสนองต่อแม่เหล็กภายนอกได้ เช่น ในทางการแพทย์ ได้ถูกนำมาใช้เป็นตัวนำส่งยา (drug delivery) การสร้างภาพด้วยเรโซแนนซ์แม่เหล็ก (Magnetic Resonance Imaging, MRI) ทางด้านเทคโนโลยีได้ถูกนำมาใช้ทำฮีตบับทึกข้อมูลและเซนเซอร์ เป็นต้น

เนื่องจากอนุภาคนาโนแมกนีไทท์มีขนาดเล็กระดับนาโนเมตรจึงได้มีโอกาสที่จะเกิดการรวมตัวกัน (aggregation) เป็นตะกอนขนาดใหญ่ เนื่องจากแรงดึงดูดระหว่างอนุภาค ทำให้อนุภาคสูญเสียสมบัติการเป็นอนุภาคนาโนได้ ดังนั้นจึงต้องมีการเสถียรอนุภาคเหล่านี้ด้วยสารเสถียร (stabilizer) โดยกลไกการเสถียรอนุภาคอาจเกิดจากการเติมโมเลกุลที่มีประจุบนผิวอนุภาค เพื่อให้ประจุบนพื้นผิวของอนุภาคเกิดการผลักกับอนุภาคข้างเคียง (charge repulsion) หรือ เกิดจากการเติมโมเลกุลขนาดใหญ่ เช่น พอลิเมอร์ ลงบนผิวอนุภาคเพื่อเพิ่มความเกะกะระหว่างอนุภาค (steric repulsion) เป็นต้น

การดัดแปรพื้นผิวอนุภาคนาโนแมกนีไทท์ไม่เพียงทำให้อนุภาคมีความเสถียรและสามารถกระจายตัวได้ดีในตัวทำละลายแล้ว ยังทำให้อนุภาคมีความเข้ากันได้เชิงชีวภาพ ซึ่งมีความสำคัญอย่างมากในการนำอนุภาคไปใช้ทางการแพทย์ นอกจากนี้ การดัดแปรพื้นผิวอนุภาคนาโนแมกนีไทท์ยังทำให้เกิดความหลากหลายของชนิดของสารที่ใช้ในการดัดแปรพื้นผิวเพื่อให้ได้อนุภาคที่มีสมบัติเฉพาะตามต้องการได้ ดังนั้น การเลือกชนิดของสารดัดแปร รวมทั้งวิธีการดัดแปรพื้นผิวอนุภาคจึงมีความสำคัญเพราะจะส่งผลถึงสมบัติของอนุภาคที่เตรียมได้ด้วย ชนิดของสารที่ใช้ในการดัดแปรพื้นผิวอนุภาคนาโนแมกนีไทท์อาจเป็นโมเลกุลขนาดเล็ก พอลิเมอร์ หรือ สารชีวโมเลกุล

โดยงานวิจัยนี้ได้นำเสนอการออกแบบและสังเคราะห์พอลิเมอร์เพื่อดัดแปรพื้นผิวอนุภาคนาโนแมกนีไทท์ด้วยเทคนิคที่หลากหลาย เช่น เทคนิคการพอลิเมอไรเซชันออกจากพื้นผิว ("grafting from") และการตรึงสายโซ่พอลิเมอร์บนพื้นผิว ("grafting to") ด้วยพอลิเมอร์หลากหลายชนิด เช่น poly (ethylene glycol), (PEG), poly (acrylic acid) (PAA), poly (4-vinyl pyridine) (P4VP), poly (azlactone) นอกจากนี้งานวิจัยนี้ยังได้เสนอแนวคิดในการออกแบบพื้นผิวอนุภาค เพื่อให้มีสมบัติเฉพาะต่อการใช้งานทางด้านการแพทย์ เช่น การออกแบบพื้นผิวอนุภาคแบบสองชั้นเพื่อการกักเก็บยาไว้ในพอลิเมอร์ชั้นใน เพื่อใช้ในการควบคุมการปลดปล่อยยา การออกแบบพื้นผิวเพื่อให้มีหมู่ฟังก์ชันที่ตอบสนองต่อการเปลี่ยนแปลงสภาวะการเป็นกรดเบส (pH) หรือการกระตุ้นด้วยแสงยูวีเพื่อใช้เป็นกลไกในการควบคุมการปลดปล่อยยา การออกแบบพื้นผิวให้มีหมู่ฟังก์ชันเพื่อใช้ในการตรึงสารชีวโมเลกุลบนพื้นผิวอนุภาค ซึ่งความรู้เหล่านี้จะเป็นพื้นฐานในการออกแบบโครงสร้างบนพื้นผิวอนุภาคนาโนแมกนีไทท์ให้มีความหลากหลาย ความซับซ้อนและความเหมาะสมต่อการประยุกต์ใช้งานเฉพาะทางต่อไป

๓. แหล่งเงินทุนสนับสนุนในการทำวิจัย

สำนักงานกองทุนสนับสนุนการวิจัย (สกว.) ร่วมกับ สำนักงานคณะกรรมการการอุดมศึกษา (สกอ.) และมหาวิทยาลัยนเรศวร ศูนย์นาโนเทคโนโลยีแห่งชาติ (นาโนเทค) ศูนย์ความเป็นเลิศด้านนวัตกรรมทางเคมี และโครงการปริญญาเอกกาญจนาภิเษก (คปก.)

๔. วัตถุประสงค์ของการวิจัย

ออกแบบวิธีการเคลือบอนุภาคนาโนแมกนีไทท์ให้กระจายตัวได้ดีในน้ำและมีพื้นผิวที่มีสมบัติเฉพาะ เช่น ตอบสนองต่อการเปลี่ยนแปลงสภาวะความเป็นกรดเบสหรือต่อแสงยูวีและมีหมู่ฟังก์ชันบนพื้นผิวสำหรับการกักเก็บยาหรือการตรึงสารชีวโมเลกุลที่สนใจได้

๕. ระยะเวลาการทำวิจัย

๕ ปี ๘ เดือน (ตั้งแต่วันที่ ๑ มิถุนายน ๒๕๔๙ ถึงวันที่ ๓๑ มกราคม ๒๕๕๕)

๖. สรุปผลการวิจัย

๖.๑ การดัดแปรพื้นผิวอนุภาคนาโนแมกนีไทท์ด้วยพอลิเมอร์ทำให้อนุภาคสามารถกระจายตัวได้ดีในน้ำ (water dispersibility) เพราะหากจะต้องการนำเอาอนุภาคนี้ไปใช้ในทางการแพทย์ อย่างน้อยอนุภาคจะต้องกระจายตัวได้ดีในสารละลายที่มีน้ำเป็นตัวกลาง นอกจากนี้ การเคลือบอนุภาคด้วยพอลิเมอร์ ยังทำให้อนุภาคมีความเข้ากันได้เชิงชีวภาพได้ดีขึ้น ซึ่งงานวิจัยนี้ได้เลือกใช้ poly(ethylene glycol) (PEG) เพื่อให้อนุภาคกระจายตัวในน้ำได้ดีและมีความเข้ากันได้เชิงชีวภาพ (รูปที่ ๑)

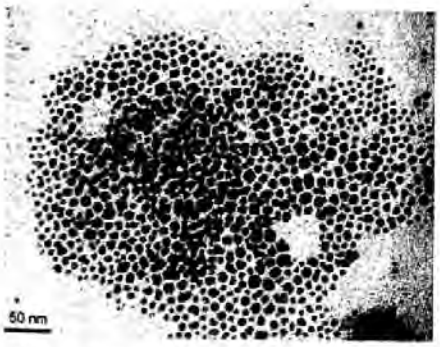

รูปที่ ๑ อนุภาคนาโนแมกนีไทท์ขนาดเส้นผ่าศูนย์กลาง ๑๐ นาโนเมตร ถ่ายด้วยกล้องจุลทรรศน์อิเล็คตรอนแบบส่องผ่าน (TEM)

๖.๒ เพื่อเคลือบอนุภาคนาโนแมกนีไทท์ด้วยพอลิเมอร์ที่มีสมบัติการตอบสนองต่อการเปลี่ยนแปลงสภาวะแวดล้อมภายนอก เช่น การเปลี่ยนแปลงสภาวะความเป็นกรดเบสหรือการตอบสนองต่อแสงยูวี โดยงานวิจัยนี้ได้ทำการเคลือบอนุภาคนาโนแมกนีไทท์ด้วย poly(4-vinyl pyridine)(P4VP) ซึ่งมีสมบัติเปลี่ยนแปลงตอบสนองต่อการเปลี่ยนแปลงสภาวะความเป็นกรดเบสของสารละลาย หรือ poly(azobenzene acrylateXABA) ซึ่งตอบสนองต่อการฉายแสงยูวี (รูปที่ ๒) ซึ่งการตอบสนองต่อสิ่งกระตุ้นภายนอกเหล่านี้ สามารถใช้เป็นกลไกในการกระตุ้นการปลดปล่อยยาที่ถูกกักเก็บไว้บนพื้นผิวอนุภาคได้

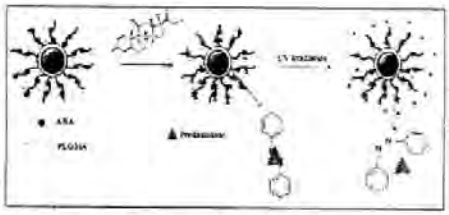

รูปที่ ๒ การดัดแปรพื้นผิวอนุภาคนาโนแมกนีไทท์ด้วย poly (azobenzene acrylate)(ABA) และกลไกการปลดปล่อยยาเมื่อกระตุ้นด้วยการฉายแสงยูวี

๖.๓ เพื่อเพิ่มหมู่ฟังก์ชันบนพื้นผิวอนุภาคนาโนแมกนีไทท์ ทำให้สามารถตรึงสารชีวโมเลกุลบนพื้นผิวอนุภาคได้ หรือ ออกแบบให้เกิดเป็นพอลิเมอร์แบบสองชั้น เพื่อสามารถกักเก็บยาบนพื้นผิวของอนุภาคได้ ซึ่งงานวิจัยนี้ได้ใช้หมู่แอซแลคโตนและอะคริลิกแอซิด เพื่อเป็นหมู่ฟังก์ชันที่สามารถทำปฏิกิริยาต่อได้กับสารชีวโมเลกุลที่สนใจ (รูปที่ ๓) นอกจากนี้ยังมีการสังเคราะห์พอลิเมอร์ร่วมแบบบล็อกระหว่าง mPEG-PCL และกรดโอเลอิกเพื่อเคลือบอนุภาคแบบสองชั้นเพื่อการกักเก็บยาอินโดเมทาซิน

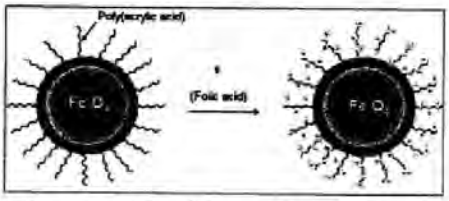

รูปที่ ๓ การตรึงกรดโฟลิกบนพื้นผิวอนุภาคนาโนแมกนีไทท์ที่มีการเคลือบด้วยพอลิอะคริลิกแอซิด

โดยผลกระทบขององค์ความรู้นี้ต่อความก้าวหน้าในเชิงวิชาการของสาขาที่ทำการวิจัย ได้แก่ หราบแนวทางการออกแบบและการสังเคราะห์พอลิเมอร์ชนิดใหม่บนพื้นผิวอนุภาคนาโนแมกนีไทท์ ซึ่งองค์ความรู้พื้นฐานเหล่านี้จะนำไปสู่การพัฒนาการสังเคราะห์และออกแบบโมเลกุลพอลิเมอร์

บนพื้นผิวอนุภาคนาโนซิลิกาหรือโครงสร้างระดับโมเลกุลแบบอื่นๆที่ซับซ้อนมากขึ้น และตอบสนองความต้องการในการประยุกต์ใช้งานเฉพาะด้านต่อไป

๗. ประโยชน์ที่ได้รับจากการวิจัย

- ประโยชน์ระยะสั้น คือ ความเข้าใจหลักการและเทคนิคการดัดแปรพื้นผิวทางเคมีของอนุภาคนาโนอย่างลึกซึ้ง เพื่อการพัฒนางานวิจัยขั้นสูงเพื่อการใช้งานเฉพาะทาง

- ประโยชน์ระยะกลาง คือ การตีพิมพ์ในวารสารระดับนานาชาติที่มีค่าอิมแพ็คแฟคเตอร์ (Impact factor) ๘ เรื่อง และการผลิตบัณฑิตปริญญาเอก สาขาเคมี จำนวน ๑ คน นิสิตปริญญาโท สาขาเคมีอุตสาหกรรม จำนวน ๖ คน และนิสิตปริญญาตรี สาขาเคมี จำนวน ๘ คน

ประโยชน์ระยะยาว คือ สามารถนำเอาวัสดุที่ผลิตได้ไปประยุกต์ใช้งานจริงและมีผลการใช้งานเฉพาะทางที่มีประสิทธิภาพดีกว่าเทคโนโลยีที่ใช้ในปัจจุบัน

๘. ศักยภาพในการพัฒนาไปสู่อุตสาหกรรม (การประยุกต์ในทางการแพทย์)

อนุภาคนาโนแมกนีไทท์ที่เคลือบด้วยพอลิเมอร์ที่มีสมบัติเฉพาะ มีศักยภาพในการนำไปประยุกต์ใช้งานทางการแพทย์ได้หลายแบบ เช่น

๑. เป็นวัสดุนำส่งยา ซึ่งยาสามารถบรรจุยาไว้ในวัสดุเดียวกันกับอนุภาคนาโนแมกนีไทท์ เราสามารถกำหนดอนุภาคให้อยู่ในตำแหน่งหรืออวัยวะที่ต้องการได้ (localization) โดยการเหนี่ยวนำด้วยสนามแม่เหล็กภายนอก ซึ่งจะทำให้ยาถูกปลดปล่อยออกมา ณ อวัยวะเป้าหมายได้อย่างมีประสิทธิภาพ

๒. การตรึงสารชีวโมเลกุลลงบนพื้นผิวอนุภาคนาโนแมกนีไทท์ เพื่อวัตถุประสงค์ต่างๆ เช่น การตรึงโปรตีนเพื่อช่วยในการนำสารเข้าสู่เซลล์ การติดฉลากเรืองแสงบนพื้นผิวอนุภาคเพื่อการตรวจสอบด้วยเทคนิคฟลูออเรสเซนส์ เป็นต้น นอกจากนี้ยังใช้ในการตรึงสารชีวโมเลกุลอื่นๆบนพื้นผิวอนุภาค เช่น ดีเอ็นเอ โมเลกุลยา เป็นต้น

การออกแบบและสังเคราะห์พอลิเมอร์บนพื้นผิวอนุภาคนาโนแมกนีไทท์จะทำให้ได้อนุภาคที่มีความเหมาะสมในการประยุกต์ใช้งานเฉพาะทางและมีประสิทธิภาพดีกว่าเทคโนโลยีที่ใช้ในปัจจุบัน ซึ่งจะนำไปสู่การพัฒนาทางด้านนาโนเทคโนโลยีของประเทศไทยให้สามารถแข่งขันได้ในระดับสากลได้

คณะวิทยาศาสตร์ มหาวิทยาลัยนเรศวร
FACULTY OF SCIENCE NARESUAN UNIVERSITY

วิทยาศาสตร์สร้างปัญญา

คณาจารย์คณะวิทยาศาสตร์ มหาวิทยาลัยนเรศวร เข้ารับรางวัลสภาวิจัยแห่งชาติ
ในงาน "วันนักประดิษฐ์" ประจำปี 2556

เมื่อวันที่ 2 กุมภาพันธ์ 2556 สำนักงานคณะกรรมการวิจัยแห่งชาติ (วช.) จัดงาน "วันนักประดิษฐ์" ประจำปี 2556 และพิธีมอบรางวัลสภาวิจัยแห่งชาติ : รางวัลผลงานวิจัย รางวัลวิทยานิพนธ์ ประจำปี 2555 รางวัลผลงานประดิษฐ์คิดค้น ประจำปี 2556 รางวัลผลงานด้านการวิจัยและพัฒนาระบบหุ่นยนต์กรรมไทย ประจำปี 2555 ณ ศูนย์การประชุม อิมแพ็ค ฟอรั่ม เมืองทองธานี จังหวัดนนทบุรี ในการนี้คณาจารย์คณะวิทยาศาสตร์ มหาวิทยาลัยนเรศวร เข้ารับรางวัลจาก ศ.สุรพงษ์ โตวิจักษณ์ชัยกุล ประธานสภาวิจัยแห่งชาติ จำนวน 3 ท่าน ได้แก่ รองศาสตราจารย์ ดร.เมธา รัตนาภรพิทักษ์ ได้รับรางวัลผลงานวิจัย ประจำปี 2555 ประเภทรางวัลระดับดี ผู้ช่วยศาสตราจารย์ ดร.ปริญญา มาสวัสดิ์ ได้รับรางวัลผลงานประดิษฐ์คิดค้น ประจำปี 2556 ประเภทรางวัลระดับดี และ ดร.อมรรัตน์ อัมวโรจน์วิทย์ ได้รับรางวัลวิทยานิพนธ์ ประจำปี 2555 ประเภทรางวัลระดับดี

งานธุรการ หน่วยประชาสัมพันธ์ โทร 0 5596 3119
วันที่ 4 กุมภาพันธ์ 2556

4.2.1) นายบัณฑิต ทองอ่อน ได้รับรางวัลวิทยานิพนธ์ระดับปริญญาโทยอดเยี่ยม จากบัณฑิตวิทยาลัย มหาวิทยาลัยนเรศวร ประจำปี 2555 เรื่อง Synthesis of amphiphilic block copolymer via atom transfer radical polymerization as bilayer surfactant of magnetite nanoparticle

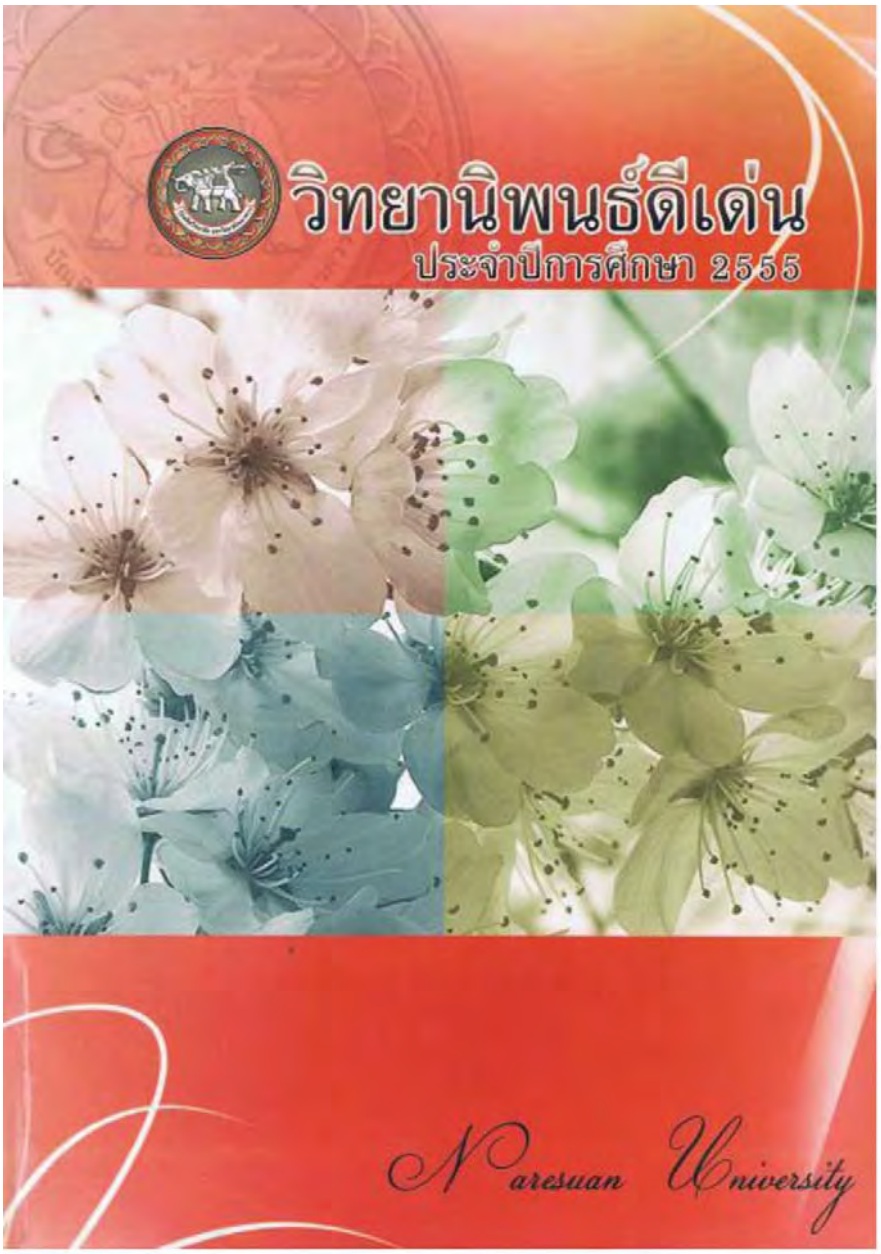

รางวัลวิทยานิพนธ์ดีเด่น (ระดับปริญญาโท)
ประเภทผลงานวิทยานิพนธ์ที่เป็นองค์ความรู้ใหม่และนำไปใช้ประโยชน์ได้
กลุ่มสาขาวิชาวิทยาศาสตร์และเทคโนโลยี

คณะวิทยาศาสตร์
สาขาวิชาเคมีอุตสาหกรรม

เรื่อง

SYNTHESIS OF AMPHIPHILIC BLOCK COPOLYMER VIA ATOM TRANSFER RADICAL POLYMERIZATION AS BILAYER SURFACTANT OF MAGNETITE NANOPARTICLE

ผู้วิจัย : นายบัณฑิต ทองอ่อน

ประธานที่ปรึกษา : รองศาสตราจารย์ ดร.เมธา รัตนากรพิทักษ์
กรรมการที่ปรึกษา : ดร.บุญจิรา รัตนากรพิทักษ์
กรรมการที่ปรึกษา : ผู้ช่วยศาสตราจารย์ ดร.ช.วยากรณ์ เพ็ชญไพศิษฏ์

Title	SYNTHESIS OF AMPHIPHILIC BLOCK COPOLYMER VIA ATOM TRANSFER RADICAL POLYMERIZATION AS BILAYER SURFACTANT OF MAGNETITE NANOPARTICLE
Author	Bandit Thong-On
Advisor	Associate Professor Metha Rutnakornpituk, Ph.D.
Co-Advisor	Boonjira Rutnakornpituk, Ph.D. Chor. Wayakron Phetphaisit, Ph.D.
Academic Paper	Thesis M.S. in Industrial Chemistry, Naresuan University, 2011
Keywords	Magnetite nanoparticle, polysiloxane, ATRP

ABSTRACT

We are here reporting the surface modification of magnetite nanoparticle (MNP) with amphiphilic copolymer of polydimethylsiloxane (PDMS) and poly (ethylene glycol) methyl ether methacrylate (PEGMA) to obtain the polymeric bilayer surfactant of PDMS inner shell and PEGMA periphery. PDMS was first prepared *via* acid-catalyzed ring-opening copolymerization of octamethylcyclo-tetrasiloxane (D_4) and tetramethylcyclotetrasiloxane (D_4H) using dihydroxypropyl tetramethyl disiloxane as an end capping agent and to control its molecular weight. Copolymerization of D_4 and D_4H was performed to gain the polysiloxane containing Si-H bonds for further functionalization and then coupling on MNP surface. The molecular weight of PDMS, estimated from ^{1}H NMR spectrum, was approximately 2,254 g/mol (m=19, n=14). Immobilization of the PDMS on the MNP surface was carried out through the hydrosillylation between Si-H-containing PDMS and allyl-grafted MNP. The PDMS-grafted MNP then served as a reactive macroinitiator for ATRP of PEGMA. The ATRP reaction was performed at room temperature in toluene using CuBr/Me_6Tren catalytic complex. Kinetics studies *via* proton-nuclear magnetic resonance spectrometer (^{1}H NMR) indicated the constant consumption of PEGMA during first 6 h of the ATRP reaction. Transmission electron microscopy (TEM) showed the average particle size about 7 nm in diameter. Fourier transform

infrared spectrophotometry (FTIR), thermogravimetric analysis (TGA) and vibrating sample magnetometry (VSM) indicated the increase of the copolymer in the complex when the ATRP reaction was prolonged. In addition, hydrodynamic size of the copolymer-coated MNP was significantly decreased when ATRP reaction was extended indicating the promotion of the particle dispersibility in water due to the better coating of hydrophilic PEGMA. VSM exhibited that the particles possessed superparamagnetic behavior at room temperature. TGA revealed the there was about 26% Fe_3O_4 core after 24 h of ATRP, signifying that there was high percentage of the polymer in the complexes.

4.2.2) นางสาวภาวิณี เทียมดี ได้รับรางวัลการนำเสนอผลงานแบบโปสเตอร์ยอดเยี่ยมในงานการประชุมวิชาการระดับนานาชาติในงาน PACCON2009 ณ มหาวิทยาลัยนเรศวร เรื่อง Atom transfer radical polymerization of poly (ethylene glycol) methyl ether methacrylate (PEGMA) brush on magnetic nanoparticle surface

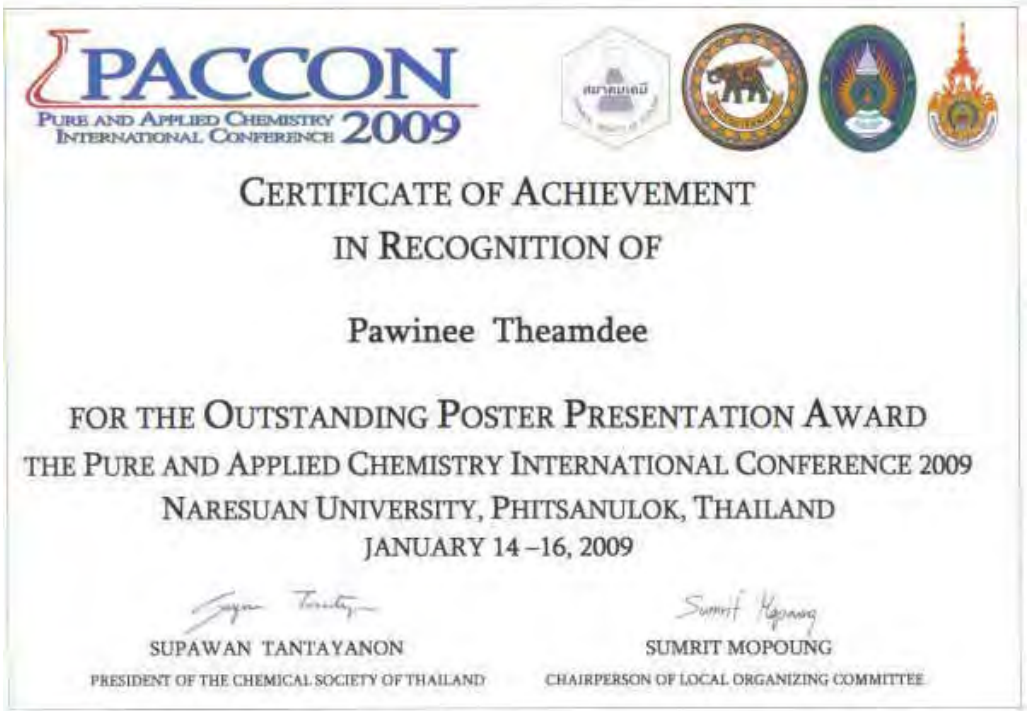

PACCON
PURE AND APPLIED CHEMISTRY INTERNATIONAL CONFERENCE 2009

CERTIFICATE OF ACHIEVEMENT
IN RECOGNITION OF

Pawinee Theamdee

FOR THE OUTSTANDING POSTER PRESENTATION AWARD
THE PURE AND APPLIED CHEMISTRY INTERNATIONAL CONFERENCE 2009
NARESUAN UNIVERSITY, PHITSANULOK, THAILAND
JANUARY 14 –16, 2009

SUPAWAN TANTAYANON
PRESIDENT OF THE CHEMICAL SOCIETY OF THAILAND

SUMRIT MOPOUNG
CHAIRPERSON OF LOCAL ORGANIZING COMMITTEE

4.2.3) นายรฐนนท์ จันแก้ว ได้รับรางวัลการนำเสนอผลงานแบบโปสเตอร์ยอดเยี่ยมในงานการประชุมวิชาการระดับนานาชาติในงาน PERCH-CIC 2013 ณ โรงแรมจอมเทียนปาล์มบีชแอนด์รีสอร์ท พัทยา ชลบุรี เรื่อง Temperature- and pH-Responsive Carboxymethylchitosan Hydrogel and a Controlled Release of Indomethacin

PERCH-CIC
PERDO

Center of Excellence for Innovation in Chemistry
Commission on Higher Education, Ministry of Education

In recognition and appreciation to

Rathanon Jankaew

for outstanding poster presentation in

The International Congress for Innovation in Chemistry
(PERCH-CIC Congress VIII)

May 5 - 8, 2013

Professor Vichai Reutrakul
Director, PERCH-CIC

5) International Collaboration

We have research collaboration with Prof.Dr.Laurent Fontaine from the Universite du Maine, Le Mans, France and we have received a collaborative funding from The Franco-Thai Cooperation Program in Higher Education and Research 2009-2010, supported by the Ministry of Foreign Affairs, Ministry of Higher Education and Research of France and the Commission on Higher Education of Thailand.

J Nanopart Res (2011) 13:4463–4477
DOI 10.1007/s11051-011-0399-7

RESEARCH PAPER

Surface modification of magnetite nanoparticle with azobenzene-containing water dispersible polymer

Pawinee Theamdee · Rakchart Traiphol · Boonjira Rutnakornpituk · Uthai Wichai · Metha Rutnakornpituk

Received: 11 January 2011 / Accepted: 26 April 2011 / Published online: 13 May 2011

Abstract We here report the synthesis of magnetite nanoparticle (MNP) grafted with poly (ethylene glycol) methyl ether methacrylate (PEGMA)-azobenzene acrylate (ABA) statistical copolymer via atom transfer radical polymerization (ATRP) for drug entrapment and photocontrolled release. MNP was synthesized via thermal decomposition of iron (III) acetylacetonate in benzyl alcohol and surface functionalized to obtain ATRP initiating sites. Molar compositions of the copolymer on MNP surface were systematically varied (100:0, 90:10, 70:30, and 50:50 of PEGMA:ABA, respectively) to obtain water dispersible particles with various amounts of azobenzene. The presence of polymeric shell on MNP core was evidenced by transmission electron microscopy (TEM). Drug loading and entrapment efficiencies as well as drug release behavior of the copolymer–MNP complexes were investigated. It was found that when percent of ABA in the copolymers was increased, entrapment and loading efficiencies of prednisolone model drug were enhanced. Releasing rate and percent of the released prednisolone of the complex exposed in UV light were slightly enhanced as compared to the system without UV irradiation. This copolymer–MNP complex with photocontrollable drug release and magnetic field-directed properties is warranted for further studies for potential uses as a novel drug delivery vehicle.

Keywords Atom transfer radical polymerization · Magnetite · Nanoparticle · Azobenzene · Coating · Drug delivery

Electronic supplementary material The online version of this article (doi:10.1007/s11051-011-0399-7) contains supplementary material, which is available to authorized users.

P. Theamdee · R. Traiphol · B. Rutnakornpituk · U. Wichai · M. Rutnakornpituk (✉)
Department of Chemistry and Center of Excellence for Innovation in Chemistry, Faculty of Science, Naresuan University, Phitsanulok 65000, Thailand
e-mail: methar@nu.ac.th

Introduction

In recent years, magnetite nanoparticle (MNP) coated with water dispersible polymeric surfactants have been intensively studied because it offers intriguing new opportunities for many biomedical applications such as magnetic resonance imaging (MRI) contrast enhancing agents (Pei et al. 2007; Sun et al. 2000; Teng and Yang 2003; Sellmyer 2002; Anders et al. 2002; Woo et al. 2004), hyperthermia treatment of tumors (Laurent et al. 2008), magnetic field-guided drug delivery (Zhang and Misra 2007), and biomolecular magnetic separation and diagnosis (Pinna et al. 2005). Surface coating of MNP is necessary when expected for use in vivo because it protects the particles from agglomeration, provides surface functionality for conjugation of biomolecules and prevents non-specific cell interaction (Veiseh et al.

2010). Therefore, surface modification of MNP is an important and challenging step for controlling chemical composition and function of the polymer on its surface.

A number of chemical approaches have been reported for coatings polymers on MNP surface such as physical adsorption, emulsion polymerization, and "grafting to" and "grafting from" methods (Fan et al. 2007; Hu et al. 2006; Marutani et al. 2004). Among these approaches, surface-initiated atom transfer radical polymerization (ATRP) has recently become a method of choice for coating organic polymeric shell on MNP core (Zhou et al. 2008; Fischer 2001; Sun et al. 2007). ATRP from the silanized surface of MNP has also been reported as an effective "grafting-from" method for surface modification. ATRP is a recently developed living/controlled radical polymerization method, which does not require stringent experimental conditions. It enables for the polymerization and block copolymerization of various functional monomers such as styrene (Zhao and Shipp 2003; Liu et al. 2005), methacrylate (Hermann High et al. 2007), and methacrylamide (Teodorescu and Matyjaszewski 1999) in a controlled condition, resulting in polymers with narrowly dispersed molecular weights. However, most of the researches on surface-initiated ATRP of MNP focused on the formation of hydrophobic polymeric shell on magnetite core, which limited its potential in biomedical applications (Moineau et al. 1998; Fischer 1999; Monteiro et al. 2005; Zhou et al. 2008).

In this study, we adopted a "grafting from" method to modify MNP surfaces with poly (ethylene glycol) methyl ether methacrylate (PEGMA)-azobenzeneacrylate (ABA) statistical copolymer via ATRP reaction (Fig. 1). Hydrophilic PEGMA allows the particles to well disperse in water, which is a requirement for biomedical uses. ABA was of particular interest in this study because azobenzene moiety can be switched from *trans* to *cis* forms by UV irradiation (Dokic et al. 2009; Maria et al. 2009; Yager and Barrett 2006; Nishimura et al. 1984). Isomerization from *trans* to *cis* of azobenzene moiety involves a structural rearrangement, resulting in a decrease in size from 9 to 5 Å (a distance between the para carbon atoms of azobenzene) and an increase in its dipole moment from 0 to 3.0 D (Archut et al. 1998). Taking advantage of the drastic change in its polarity, it was hypothesized that photocontrollable drug release should be gained due to *trans*-to-*cis* isomerizations of azobenzene units upon UV irradiation (Sin et al. 2005; Bucio et al. 2005; Liu et al. 2000; Sharma and Kimura 2003; Li et al. 2006; Aruna and Rao 2009; Kim et al. 2005; Park et al. 2001), resulting in an increase in polarity of the copolymer and acceleration of the expelling rate of the entrapped hydrophobic model drug from the complex (Fig. 2). It has been reported that azobenzene-modified mesoporous silica enhanced the releasing rate of molecules from inside to outside of the mesopore upon irradiated under UV and visible light (Fujiwara et al. 2008; Wang et al. 2009).

Hence, the primary aim of this study is to synthesize a well defined PEGMA-ABA statistical copolymer via surface-initiated ATRP of MNP. Molar ratio of PEGMA to ABA on MNP surface was systematically varied to obtain water dispersible MNP with photoresponsive properties. The existence of ABA in the structure was characterized by fourier transform infrared (FTIR) and UV–Visible spectrophotometry. Transmission electron microscopy (TEM) was studied to investigate the particle size and the presence of polymeric shell coated on MNP core. Magnetic properties of the complexes were determined via a vibrating sample magnetometer (VSM). Entrapment efficiency, loading efficiency, and releasing behavior of prednisolone model drug from the MNP complexes were also reported.

Experimental section

Materials

Unless stated otherwise, all reagents and solvents were used without further purification. Inhibitor-free PEGMA macromonomer ($\overline{M_n} \sim 300$ g/mol) was stored under N_2 at −5 °C until used. The following reagents were used as received: iron (III) acetylacetonate ($Fe(acac)_3$), 99+% (Acros), benzyl alcohol, 98% (Unilab), 3-aminopropyl triethoxysilane, 99% (Acros), 2-bromoisobutyryl bromide, 98% (Acros), copper (I) bromide, 98% (Acros), pentamethyldiethylenetriamine (PMDETA), 99% (Acros), dicyclohexyl carbodiimide (DCC), 99% (Acros), 4-phenylazophenol, 97% (Acros), acrylic acid 99.5% (Acros), ethyl-α-

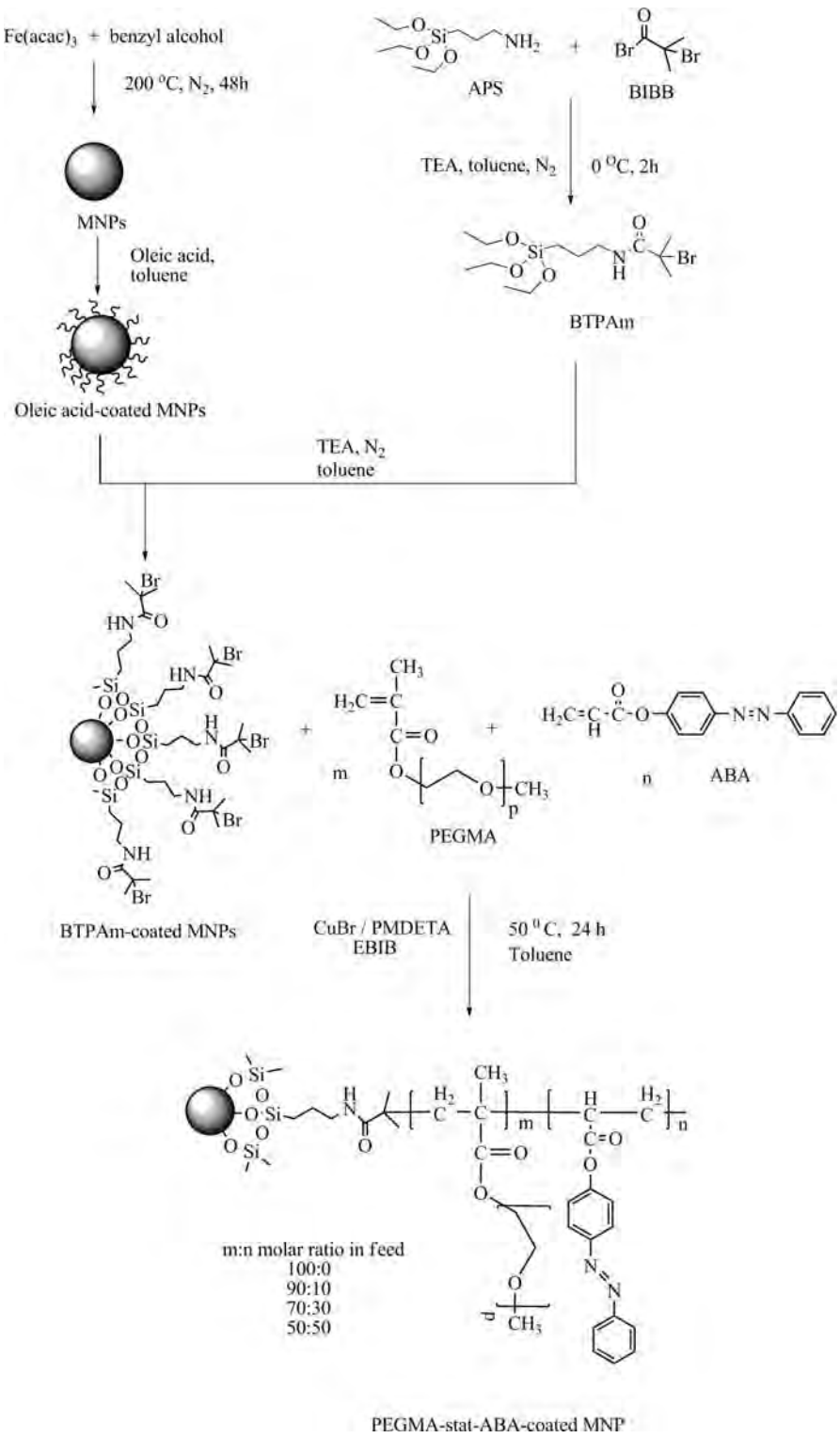

Fig. 1 An experimental overview

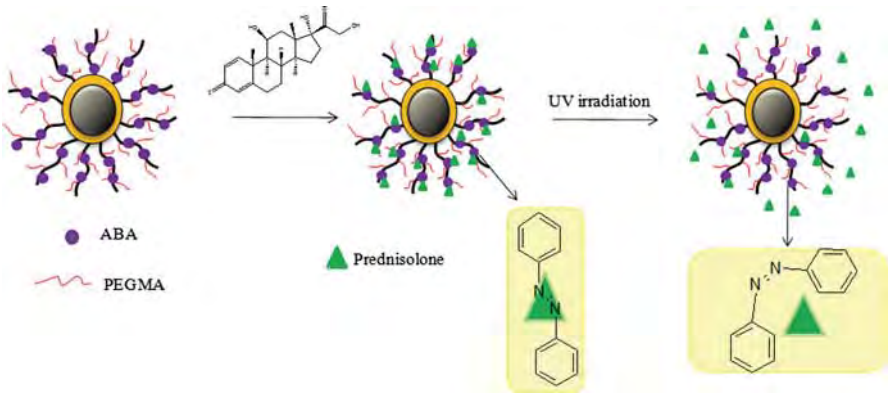

Fig. 2 Proposed mechanism of prednisolone-controlled release from PEGMA-ABA–magnetite complex

bromoisobutyrate (Aldrich) and oleic acid (Fluka). Triethylamine, 97% (Carto Erba) and toluene were stirred under CaH_2 and distilled prior to use. Cellulose dialysis tubing (Sigma–Aldrich) with molecular weight cutoff (MWCO) 12,400 was immersed in running water for 24 h before used.

Synthesis

Synthesis of oleic acid-coated MNP

MNP was prepared following the method previously reported by Nicola (Pinna et al. 2005). In a typical synthesis, iron (III) $(acac)_3$ (5.0 g, 14.05 mmol) was dissolved in benzyl alcohol (90 mL) in a three-neck round bottom flask. It was stirred at 200 °C for 48 h under nitrogen blanket. The precipitant was removed from the dispersion using an external magnet and washed with ethanol and CH_2Cl_2. This procedure was repeated three times and the particles were dried in vacuo. The dried particles (0.8 g) were re-suspended in dried toluene (30 mL) and sonicated for 1 h. Oleic acid (4 mL) was then added in the dispersion, followed by sonication for 3 h under nitrogen atmosphere. Finally, the aggregate was separated from the dispersion by centrifugation at 5,000 rpm for 15 min.

Synthesis of 2-bromo-2-methyl-N-(3-(triethoxysilyl) propanamide (BTPAm)

BTPAm was synthesized following the method previously reported by Yabin (Sun et al. 2007). The solution of 2-bromoisobutyrylbromide (BIBB) (0.1 mL, 0.8 mmol) in toluene (10 mL) was added dropwise to a cold solution of 3-aminopropyl triethoxysilane (APS) (0.18 mL, 0.8 mmol) in 10 mL of toluene containing triethoxylamine (TEA) (0.11 mL, 0.8 mmol) at 0 °C. The mixture was magnetically stirred for 2 h at 0 °C under nitrogen atmosphere. The reaction mixture was stirred for 24 h at room temperature. The mixture was filtered to remove salts, evaporated to remove the unreacted TEA and dried under reduced pressure. The resulting product, BTPAm, was yellowish thick liquid.

Synthesis of MNP coated with BTPAm, an ATRP initiator

To immobilize BTPAm on the oleic acid-coated MNP surfaces, the MNP-toluene dispersion (0.1 g of MNPs in 5 mL toluene) (30 mL), BTPAm (0.30 mL) and 2 M TEA in toluene (5 mL) were added into a round bottom flask. The mixture was stirred for 24 h at room temperature under nitrogen blanket. The particles were subsequently precipitated in methanol, following by magnet separation to obtain the BTPAm-coated MNP. Then, the MNP was re-dispersed in toluene and re-precipitated again in methanol. This procedure was repeated several times to completely remove unreacted BTPAm. The particles were finally dried in vacuo.

Synthesis of ABA monomer

ABA was prepared by a coupling reaction of 4-phenylazophenol and acrylic acid. To a 100 mL round-bottom flask containing an excess of 4-phenylazophenol (1.21 g, 0.0061 mol), acrylic acid (0.38 mL, 0.0054 mol), and dicyclohexylcarbodiimide (DCC) (1.24 g, 0.0061 mol) in distilled CH_2Cl_2 (20 mL) were slowly added. The solution was stirred at room temperature for 24 h under N_2 gas. The solution was

filtered and CH_2Cl_2 was then evaporated. The mixture was dissolved in diethyl ether, extracted with saturated $NaHCO_3$ (3 × 20 mL), dried with anh.$MgSO_4$, and then the solvent was evaporated until dryness.

(Co)polymerization of PEGMA and/or ABA via ATRP from MNP surface

Three different molar ratios of PEGMA-ABA copolymer (50:50, 70:30 and 90:10, respectively) and PEGMA homopolymer (100:0 of PEGMA-ABA molar ratio) grafted on MNP surface were prepared. An example for synthesizing 50:50 PEGMA-ABA-coated MNP was described herein. Other copolymer–MNP complexes were prepared in a similar fashion with proper amounts of reagents used. In a typical procedure, BTPAm-immobilized MNP (0.1 g) were sonicated in toluene (0.381 mL, 60% w/v) in a Schlenk tube. A solution of PEGMA (0.64 g, 2.13 mmol), ABA (0.56 g, 2.22 mmol) and ethyl-α-bromoisobutyrate (EBiB) as a sacrificial initiator (0.007 g, 0.35 mmol) were then syringed to the above Schlenk tube. The solution was degassed by three freeze–pump–thaw cycles before adding a solution of CuBr (0.064 g, 0.44 mmol) and PMDETA (0.009 g, 0.05 mmol) in DMF (0.032 mL, 5% v/v) filled with nitrogen. ATRP reaction was set at 50 °C for 24 h. The dispersions were removed periodically via a degassed syringe for determining reaction conversion and GPC analyses.

Characterization

Characterization of polymer and MNP

^{1}H NMR was performed on a 400 MHz Bruker NMR spectrometer using $CDCl_3$ as a solvent. FTIR was performed on a Perkin-Elmer Model 1600 Series FTIR Spectrophotometer. The solid samples were mixed with KBr to form pellets. Gel permeation chromatography (GPC) data was conducted on PLgel 10 μm mixed B2 columns and a refractive index detector. Tetrahydrofuran (THF) was used as a solvent with a flow rate of 1 mL/min at 30 °C. Magnetite concentrations in dispersions were analyzed via atomic absorption spectroscopy (AAS) and calculated from sample responses relative to those of standard and blank. Particles size and its distribution were observed from transmission electron microscopy (TEM). TEM images were taken using a Philips Tecnai 12 operated at 120 kV equipped with Gatan model 782 CCD camera. The particles were re-suspended in water with sonication before deposition on a TEM grid. Magnetic properties of the particles were measured at room temperature using a Standard 7403 Series, Lakeshore vibrating sample magnetometer (VSM). Magnetic moment of each sample was investigated over a range of ±10,000 G of applied magnetic fields using 30 min sweep time. Prednisolone concentrations were determined using Specord S100 UV–Visible spectrophotometer (Analytikjena AG) coupled with a photo diode array detector. A standard curve at $\lambda_{max} = 320$ nm UV absorbance was established using identical conditions to calculate the amount of the drug entrapped on and released from the particles.

Studies on drug entrapping and loading efficiencies of the surface-modified MNPs

Prednisolone was used as a model drug in the current studies. To incorporate the drug to the complex, the drug solution (6 mL, 0.375 mg/mL in THF) was added dropwise with sonication to the copolymer–magnetite complex dispersed in water (5 mL, 0.2–0.5 mg/mL MNP). The mixture was sonicated for 30 min to fully aggregate the drug in the hydrophobic ABA units presenting on the particle surface. The excess drug was precipitated out from the mixture and was removed by centrifugation at 2,000 rpm. Drug-loaded MNP was then separated using an external magnet. Due to a good solubility of prednisolone in a THF:ethanol solution (50:50%v/v), it was used to repeatedly extract the entrapped drug from the particle. After centrifugation to remove aggregated particle, the drug concentration in the supernatant, reflecting the amount of the entrapped drug in the complex, was determined using UV–Visible spectrophotometer. Entrapment efficiency (%EE) and drug loading efficiency (%DLE) were determined as following:

$$\%\ \text{Entrapment efficiency (\% EE)} = \frac{\text{Weight of the entrapped drug in nanoparticles}}{\text{Weight of loaded drug}} \times 100$$

$$\%\ \text{Drug Loading efficiency (\% DLE)} = \frac{\text{Weight of the entrapped drug in nanoparticles}}{\text{Weight of magnetite nanoparticles}} \times 100$$

Each experiment was repeated three times to obtain average values.

In vitro releasing studies of the entrapped prednisolone in the copolymer–magnetite complex

Prednisolone-loaded magnetite dispersions (5 mL) were dialyzed against 250 mL-phosphate buffer solution releasing media (pH 7.45) with consistently stirring at room temperature. Two experiments were performed simultaneously; under UV light irradiation and in the dark place as a control. At a given time, 5 mL aliquots of the aqueous solution were withdrawn from the releasing media and 5 mL of phosphate buffer solution was replaced into the releasing media. Concentrations of the released prednisolone were determined via UV–Visible spectrophotometer at 297 nm wavelength.

Results and discussion

MNPs were first synthesized via a thermal decomposition reaction of $Fe(acac)_3$ to obtain narrow-size distribution nanoparticles. To functionalize the particles surfaces, the initiator for ATRP was first covalently bonded onto the surface of the particles through the combination of ligand exchange reaction and condensation of triethoxysilane.

Synthesis of MNPs coated with BTPAm, an ATRP initiator

Figure 3 shows an FTIR spectrum of BTPAm-coated MNP (Fig. 3c) in comparison with those of bare magnetite (Fig. 3a) and BTPAm (Fig. 3b). In addition to a strong and broad signal of Fe–O bonds (578 cm^{-1}) observed in BTPAm-modified MNP, it also exhibited characteristic absorption signals of BTPAm; 1,643 cm^{-1} (–NH–CO– carbonyl stretching), 2,920 cm^{-1} (C–H stretching), 1,111–1,109 cm^{-1} (Si–O stretching), 1,532 cm^{-1} (N–H bending), and 3,346 cm^{-1} (N–H stretching) (Fig. 3c). It should be noted that an excess of BTPAm or unbound BTPAm was repeatedly removed from the particles.

Copolymerization of PEGMA and ABA via ATRP from MNP surface

Synthesis of ABA

ABA is a resultant product from a coupling reaction between 4-phenylazophenol and acrylic acid (Fig. 4a). The presence of sharp and strong signals of carbonyl group (1,736 cm^{-1}) and acrylate group (987 and 900 cm^{-1}) indicated the coupling reaction

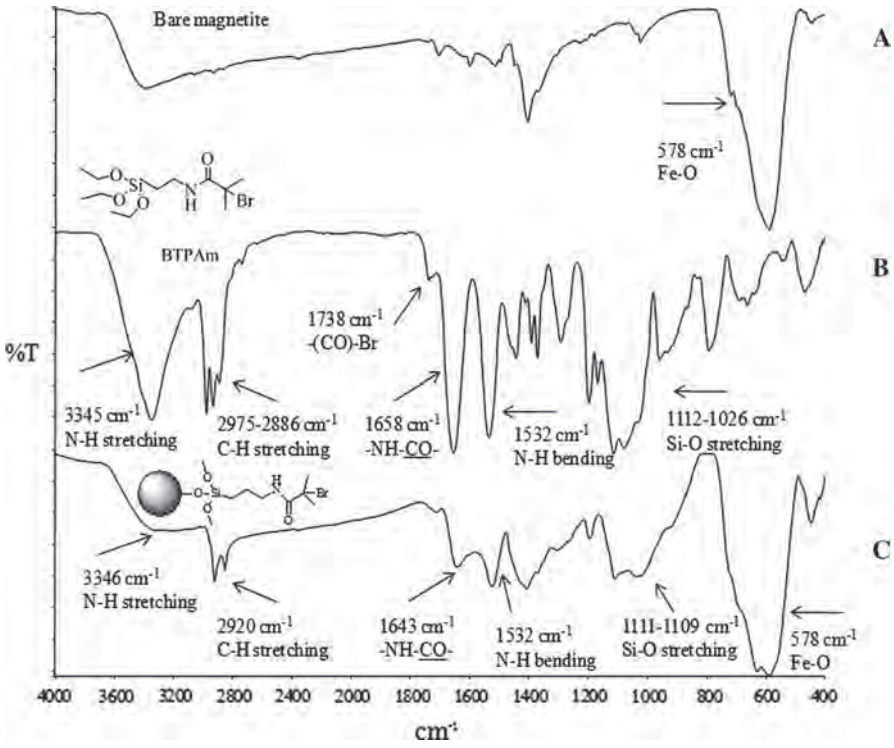

Fig. 3 FTIR spectra of (*a*) bare magnetite, (*b*) BTPAm, and (*c*) BTPAm-coated MNPs

between carboxylic acid of acrylic acid and hydroxyl group of 4-phenylazophenol. It should be noted once again that unreacted acrylic acid and 4-phenylazobenzene were removed from the final product. According to the ^{1}H NMR spectrum in Fig. 4b, characteristic signals of ABA were found as following: ^{1}H-NMR ($CDCl_3$, ppm): δ 7.98 (m, 4H (a), Ar*H*), 7.52 (d, 2H (b), Ar*H*), 7.30 (d, 2H (c), Ar*H*), 6.67 (d, $J = 17.3$ Hz, 1H (d), C*H*H = CH), 6.36 (dd, 1H, J = 17.3 and 10.50 Hz (e), C*H* = CH_2), 6.07 (d, 1H, J = 10.46 Hz (f), CH*H* = CH).

Figure 5 shows the representative UV–Visible absorption spectra of ABA solution in chloroform (0.01 mg/mL). The maximum absorption at 329 nm corresponds to the π–π* transition of *trans*-azobenzene chromophore and a weak band at 425 nm corresponds to the n–π* transition of *cis* isomer (Sin et al. 2005; Bucio et al. 2005; Liu et al. 2000; Sharma and Kimura 2003; Li et al. 2006; Aruna and Rao 2009; Kim et al. 2005; Park et al. 2001). *Trans* form of ABA, the energetically preferred ground state, can switch to the *cis* form via a photochemical isomerization process. Upon UV irradiation, the intensity of the *trans* peak at 329 nm decreased and broadened and, at the same time, the broad *cis* absorption band around 425 nm increased. This phenomenon was observed during the first 3 min of UV irradiation. When the time for UV exposure was extended, there was no significant change in UV spectra. Since the decrease of absorbance at 329 nm is a direct result of the *trans* to *cis* isomer conversion, the fraction of the *cis* isomer is estimated to be about 25 mol%.

Copolymerization of PEGMA and ABA from MNP surface via ATRP

In this study, PEGMA and ABA with various molar compositions (100:0, 90:10, 70:30, and 50:50, respectively) were statistically copolymerized on MNP surface via ATRP reaction. PEGMA on MNP surface allows the particles to well suspend in water, while ABA possesses photoisomerization upon UV light irradiation. Optimization of molar ratio of these two components was necessary to obtain dispersible particles in water with maximum UV light responsive properties.

In the ATRP reaction, a CuBr/PMDETA catalytic complex was used because it has been reported to

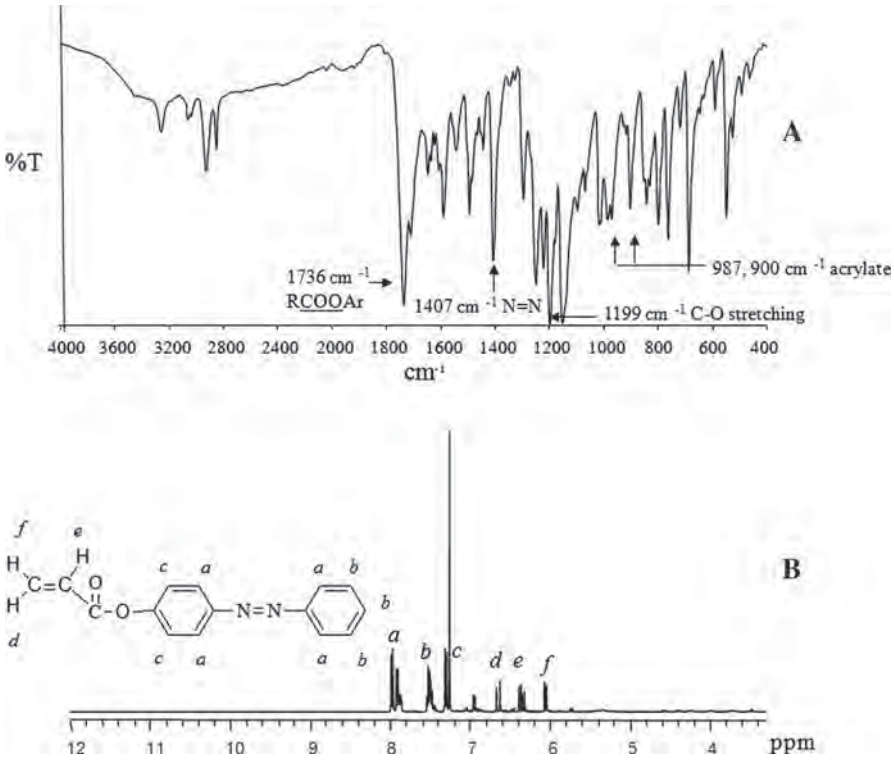

Fig. 4 **a** FTIR and **b** ^{1}H-NMR spectra of ABA

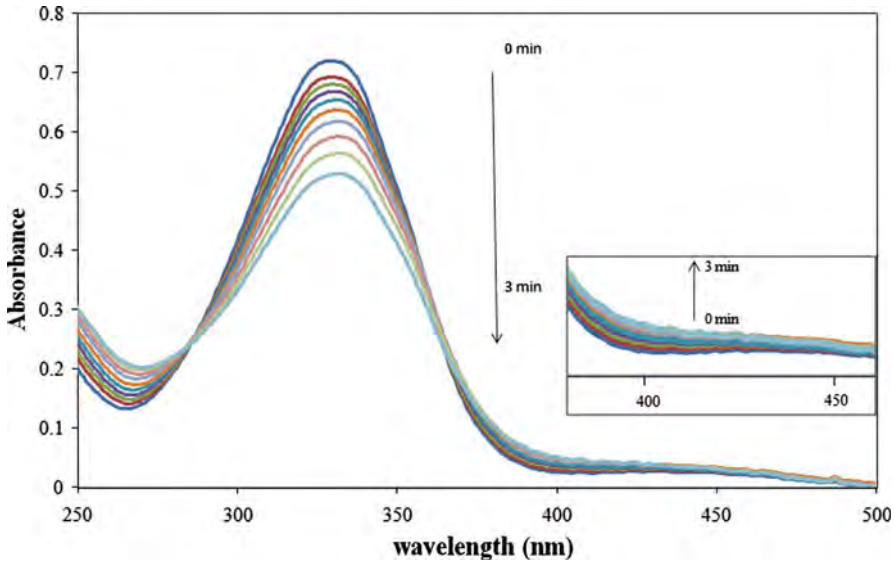

Fig. 5 Changes in UV–Visible spectra of ABA at different UV irradiation times, indicating the change from *trans* to *cis* forms

be an effective copper-mediated complex for a controlled living ATRP reaction of PEGMA (Neugebauer 2007). Ethyl-α-bromoisobutyrate (EBiB) was also added in the reaction solution as a "sacrificial" initiator. EBiB in the MNP dispersion can initiate free PEGMA-ABA copolymer in the solution. Because the MNP-supported copolymers were undetectable in NMR technique, therefore, the reaction conversions and copolymer compositions, discussed in the latter section, were investigated from the free copolymers via NMR spectrometry.

Figure 6 illustrates FTIR spectra of MNPs modified with various copolymer compositions (Fig. 6c–f) compared with those of PEGMA macromonomer and ABA (Fig. 6a and b, respectively). The spectra of PEGMA-ABA-coated MNPs exhibited characteristic absorption signals of PEGMA; 1,095 cm^{-1} (C–O–C stretching) and 1,720 cm^{-1} (O(C=O) stretching), and also those of azobenzene; 1,407 cm^{-1} (*trans* N = N). The drop of the intensity of ester (–O(C=O)– stretching, 1,720 cm^{-1}) and ether linkage signals (C–O–C stretching, 1,095 cm^{-1}) of PEGMA in relative to those of Fe–O bonds from MNP cores ($\sim$589 cm^{-1}) correspond to the decreased PEGMA compositions in the copolymer (Fig. 6c–f). In addition to that, the gradual increase of N=N signal of azobenzene (1,407 cm^{-1}) was also observed as percentage of ABA in the copolymer was increased. It should be noted that the signal corresponding to Fe–O bonds (578 cm^{-1}) from MNP cores were observed throughout the reactions without significant change in its intensity. The drastic decreases of the aliphatic signal around 3,000 cm^{-1} and the ester signal around 1,720 cm^{-1} upon addition only 10% of ABA into the copolymer (from Fig. 6c, d) were attributed to the low copolymer content in the complexes. PEGMA-ABA copolymerization having other copolymer compositions also exhibited similar FTIR patterns. TGA experiments showed a supportive result to FTIR results. Namely, the percent weight loss of the copolymer-coated MNPs, corresponding to the copolymer content in the complexes, was significantly lower than those of the PEGMA-coated MNP. Representative TGA thermograms of MNPs coated with PEGMA homopolymer and PEGMA-ABA copolymer were available in the supporting information.

Kinetic studies of the polymerization of PEGMA homopolymer (100:0 PEGMA-ABA) were first performed and followed by those of PEGMA-ABA copolymerization. In the PEGMA homopolymerization, the reaction rate was rapid at the beginning and dropped after 4 h (240 min) of the reaction (Fig. 7a). This was attributed to a decrease of radical concentration probably due to irreversible recombination of the active species. The first-order plot reveals a linear relationship during the course of first 4 h reaction, indicating a constant concentration of active radical species (supporting information). The rate of monomer conversion started to deviate from linearity at higher monomer conversion (after 4 h reaction).

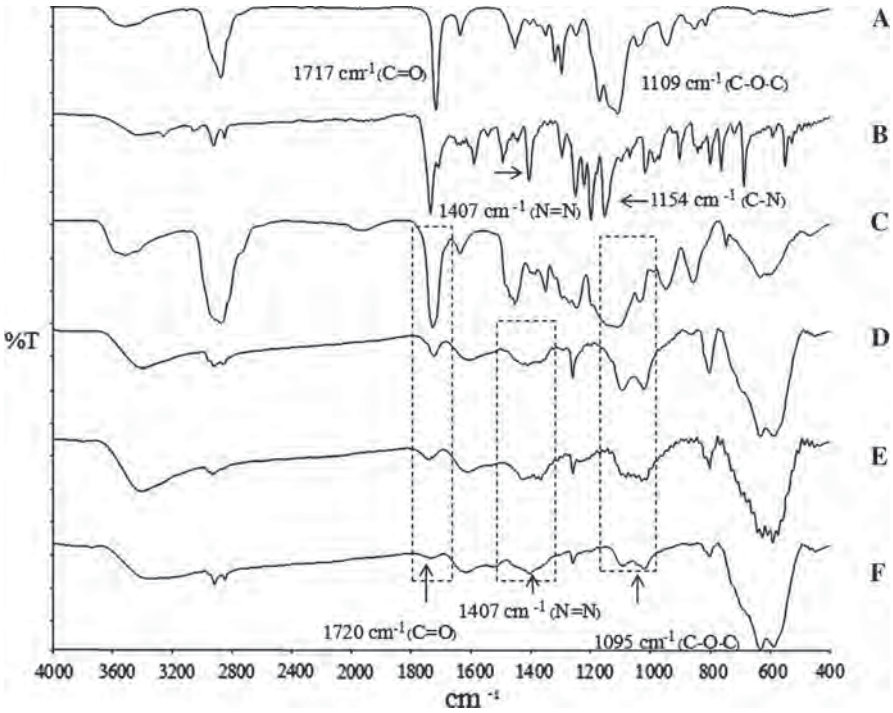

Fig. 6 FTIR spectra of (*a*) PEGMA macromonomer, (*b*) ABA, (*c*) 100:0, (*d*) 90:10, (*e*) 70:30, and (*f*) 50:50 PEGMA-ABA-coated MNPs

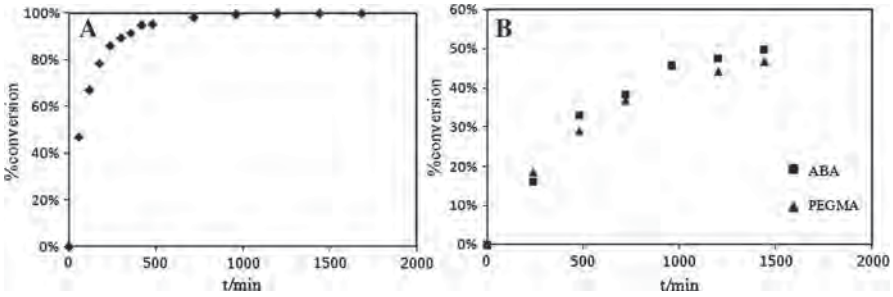

Fig. 7 Conversion vs. time plots of the polymerization of **a** PEGMA homopolymer and **b** 50:50 PEGMA-ABA copolymer

Figure 7b illustrates a conversion plot of 50:50 PEGMA-ABA copolymerization during 24 h of ATRP reaction. Conversion plots of the copolymerization having different PEGMA-ABA compositions (90:10 and 70:30, respectively) showed similar results to Fig. 7b (supporting information). Kinetic experiments indicate that the reaction rates of the PEGMA-ABA copolymerization gradually increased at the beginning and they were slower than that of PEGMA homopolymerization. This was attributed to the presence of ABA in the reaction, which essentially influenced the change in polarity of the system. Decreasing ABA molar ratio in the copolymer seemed to promote rate of the reaction. When the reactions further proceeded, the rate of polymerization decreased and ended at about 30–50% monomer conversion, suggesting feasible premature chain termination (Table 1). It was also found that ABA reacted more rapidly than PEGMA as indicated by the higher monomer conversion in all cases.

Table 1 summarizes % conversion and copolymer composition of PEGMA and ABA having various molar ratios. Copolymer compositions were estimated from the feed composition of the monomer and taking percent conversion into account. Percent ABA in the copolymer was calculated in a similar fashion. It was found that PEGMA-ABA molar ratio in the copolymer were comparable to the feed compositions. Interestingly, percentage of ABA in the copolymer was found to be slightly higher than percent feeding in every composition. This result agrees well with the conversion versus time plots indicating higher reaction

Table 1 A summary of reaction conversions and copolymer compositions of PEGMA-ABA copolymer at 24 h of ATRP reaction

Type of copolymer	% conversion[a]		% in the copolymer[b]	
	PEGMA	ABA	PEGMA	ABA
50:50 PEGMA-ABA	47	50	48	52
70:30 PEGMA-ABA	52	53	69	31
90:10 PEGMA-ABA	32	42	89	11
100:0 PEGMA-ABA	95	–	100	0

[a]Reaction conversions were calculated from ^{1}H NMR, [b] % PEGMA in the copolymer = [% $Conv._{PEGMA}$ × % $feed_{PEGMA}$]/[(% $Conv._{PEGMA}$ × % $feed_{PEGMA}$) + (% $Conv._{ABA}$ × % $feed_{ABA}$)]. % ABA in the copolymer was calculated in a similar fashion

reactivity of ABA than that of PEGMA. In addition, the relatively low percent monomer conversions in the copolymerization as compared to the PEGMA homopolymerization (100:0 PEGMA-ABA) were in good agreement with the FTIR and TGA results, which indicated that the polymer contents in the complexes in the case of the copolymerizations were lower than that of the PEGMA homopolymerization.

Characterization of PEGMA-ABA-coated MNP

According to TEM experiments, particles size and particle distribution of PEGMA-ABA-coated MNPs with various copolymer molar ratios were not significantly different from each other (Fig. 8). The particle size was in the range of 6–12 nm with the average diameter of 9.0 nm. In addition, the images also showed nanoscale agglomeration of multiple nanoparticles. This was attributed to in situ aggregation of hydrophilic PEGMA grafted on MNP surface during the ATRP copolymerizations in toluene. Even though nanoscale agglomeration was apparent, these particles were well re-suspended in water due to the presence of polymeric thin film on their surface (indicated by arrows). Furthermore, it was also observed that increasing PEGMA-to-ABA ratio in the copolymer enhanced dispersibility of the particles in water. Namely, 100:0 PEGMA-ABA-coated MNPs exhibited a good dispersibility in water without any aggregation observed, while 50:50 PEGMA-ABA-coated MNPs showed more aggregate than that of other copolymers after centrifugation. These complexes were stable in aqueous dispersions with insignificant aggregation after 1 month of preparation, indicating that these stable magnetite dispersions might be applicable for long-term uses.

Hysteresis curves of bare MNP, BTPAm-coated MNP and PEGMA-ABA-coated MNP were illustrated in Fig. 9. The particles showed superparamagnetic behavior at room temperature as indicated by the absence of remanence and coercitivity. Bare MNP and BTPAm-coated MNP showed relatively high saturation magnetization (M_s) (54–55 emu/g) due to a trace amount of organic component in the complexes (Fig. 9a, b). A slight decrease of Ms of PEGMA-ABA-coated MNP (39–45 emu/g) as compared to its precursors was attributed to the presence of the copolymers on MNP surface, reflecting a drop of magnetite content in the complex (Fig. 9c–e). Further decrease of M_s value was observed in PEGMA-coated MNP (31 emu/g) due to high content of PEGMA homopolymer in the complex (Fig. 9f). These results were in good agreement with the percent conversions of ATRP reactions shown in Table 1; high percent monomer conversions correspond to high amounts of the polymer in the complex.

Study in the configuration change of azobenzene moiety in PEGMA-ABA-coated MNP

Direct investigation of the isomerization of azobenzene grafted on the MNP was not detectable via UV–Visible spectrophotometry as performed in ABA monomer because the MNP blocked UV signals in the range of interest. In the present study, pyrene was thus used to investigate configuration change from *trans* to *cis* forms of azobenzene when it was exposed under UV light. Pyrene is typically used as a fluorescent probe to monitor the change in system polarity because its vibrational structure is sensitive to polarity of its environment (Winnik et al. 1987; Lee et al. 2004). Fluorescence of pyrene monomer possesses five predominant signals resulting from different vibrational levels, some of which are sensitive to the molecular solvent environment (Winnik et al. 1987). For instance, the I_1/I_3 ratio of pyrene is mostly dependent on solvent polarity as measured by the dielectric constant (Kalyanasundaram and Thomas 1977). In this study, we used 50:50 PEGMA-ABA-coated MNP coupled with pyrene as a probe to investigate polarity change of surrounding

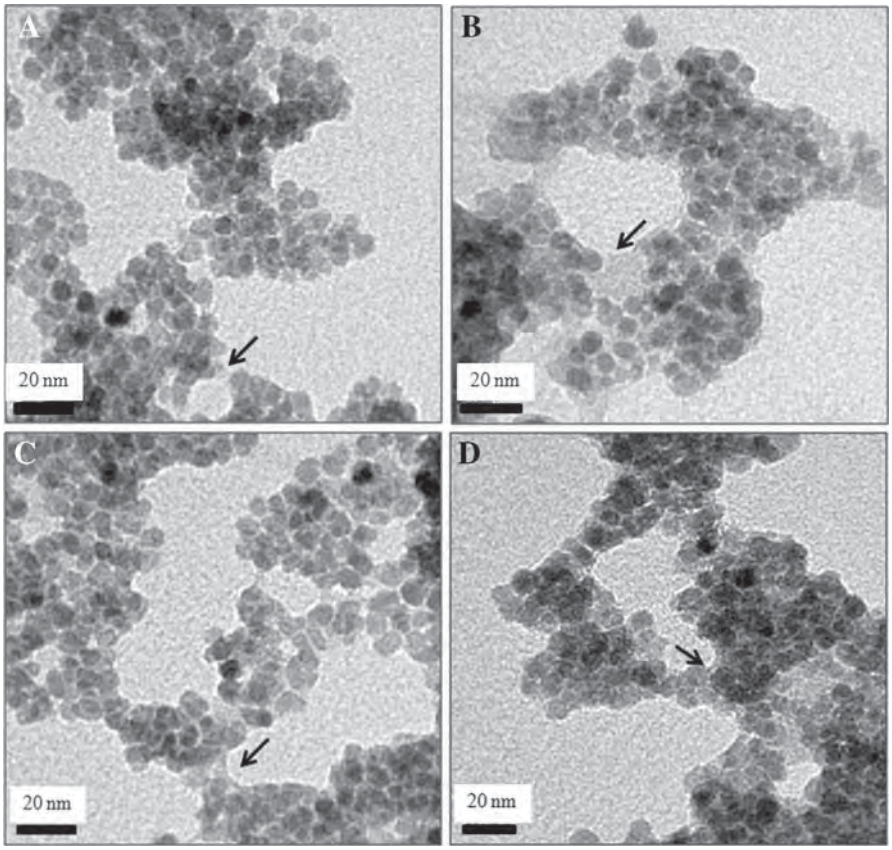

Fig. 8 TEM images of **a** 50:50, **b** 70:30, **c** 90:10, and **d** 100:0 PEGMA-ABA-coated MNPs

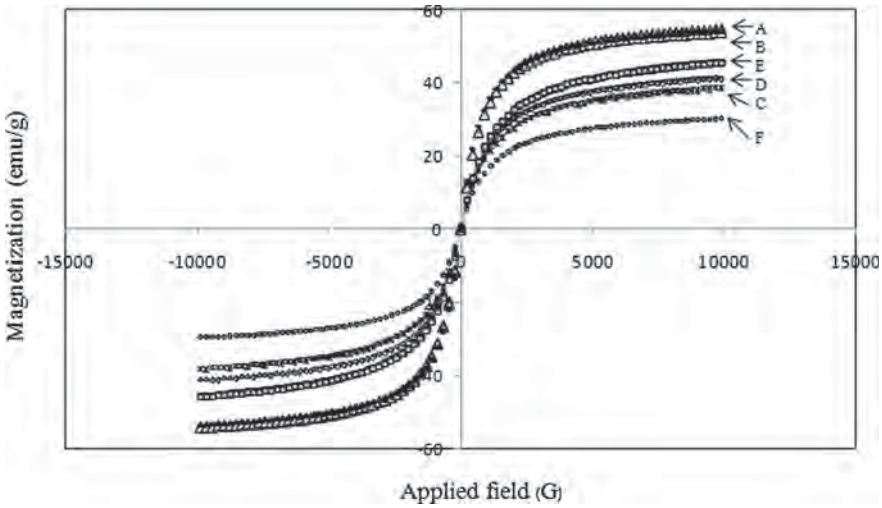

Fig. 9 Hysteresis curves of (*a*) bare MNP, (*b*) BTPAm-coated MNP, (*c*) 50:50, (*d*) 70:30, (*e*) 90:10, and (*f*) 100:0 PEGMA-ABA-coated MNPs

environment because it possessed high amount of azobenzene moieties in the complex. Figure 10 shows the fluorescence spectra of pyrene in the copolymer-coated MNP in DMSO excited at 330 nm before and after UV irradiations for 10–180 min. The change in fluorescence emission intensity ratio of pyrene (I_1/I_3) at 370 nm (I_1) and 376 nm (I_3) indicates the change in polarities of the surrounding

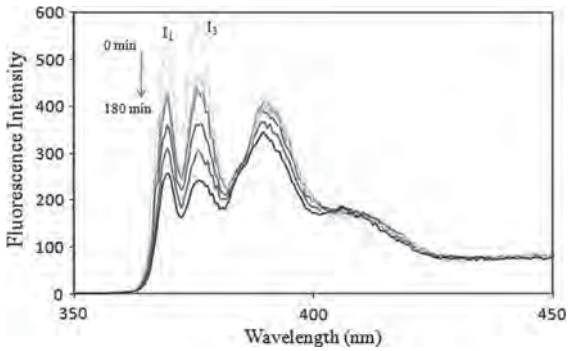

Fig. 10 Fluorescence spectra of pyrene in 50:50 PEGMA-ABA-coated MNP excited at 330 nm at various UV irradiation times

environment. Namely, the increase in I_1/I_3 value indicates the increase in polarity of the system, implying the change from *trans* to *cis* forms of azobenzene moiety. From the result shown in Fig. 10, I_1/I_3 values continuously increased when UV irradiation time was prolonged, indicating the increase of solvent polarity due to the change from *trans* to *cis* forms of azobenzene moiety. Since the *trans* to *cis* isomer conversion may also cause the reorientation of neighboring moieties, which additionally affects the polarity of pyrene local surrounding, it is not trivial to estimate the fraction of *cis* isomer from the change of I_1/I_3 value. The relatively long irradiation time of the copolymer-coated MNP ($\sim$180 min) as compared to that of the free ABA in solution ($\sim$3 min) was attributed to the restricted mobility of ABA grafted on the nanosolid support combined with the presence of PEGMA randomly copolymerized in the polymer chains, which might sterically inhibit the transformation from *trans* to *cis* forms of azobenzene on its surface.

Studies in prednisolone entrapment and loading efficiencies and releasing profile

It is known that UV irradiation of azobenzene groups enables to induce the switching of its *trans* to *cis* forms, resulting in an increase of its polarity. In the current study, drug control release application is of particular interest because we can take an advantage of this photoisomerization of azobenzene groups. It was envisioned that, once a hydrophobic model drug was added to the copolymer-coated MNP dispersion, it would somewhat partition to *trans*-azobenzene grafted on MNP surface due to similarity in their polarity. UV irradiation of the drug-loaded MNP complexes was thought to accelerate the releasing rate of the entrapped drug from their surface due to the switching from *trans* to *cis* forms of azobenzene moiety, resulting in the increase in the system polarity and repelling the drug from the MNP surface.

Prednisolone was selected as a model drug in the current studies because its λ_{max} in UV–Visible absorbance peaks did not overlap with those of ABA presenting in the copolymer–MNP complex. In addition, it shows fair solubility in phosphate buffer solution (PBS) which was used as a dialysis releasing media. It was hence hypothesized that prednisolone would partially precipitate in azobenzene grafted on MNP surface and was gradually expelled from the complex through dialysis membrane to PBS releasing media. Prednisolone releasing rate was thus expected to be accelerated upon UV irradiation due to photoisomerization of azobenzene moiety on MNP surface. To prepare prednisolone-entrapped copolymer–MNP complex, prednisolone solution in THF (0.375 mg/mL) was slowly added to the MNP complex resuspended in water with ultrasonicating. It is necessary

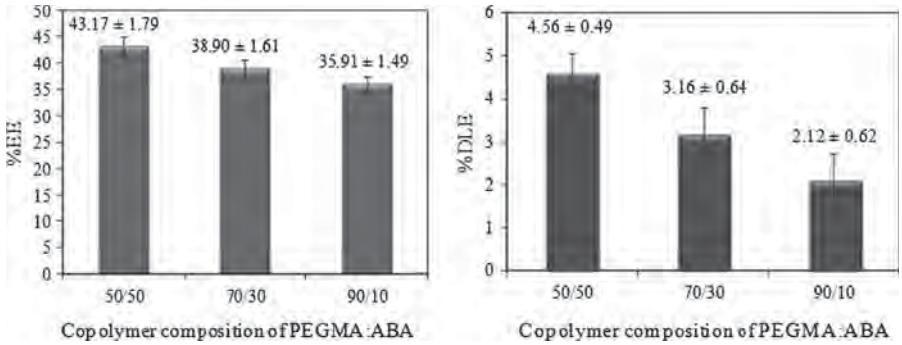

Fig. 11 Prednisolone entrapment efficiency (% EE) and loading efficiency (% DLE) of PEGMA-ABA-coated MNP in water

to resuspend the particles in aqueous base because a potential application of this complex is biomedical use, which essentially involves with aqueous base system.

Determination of prednisolone entrapment efficiency (%EE) and loading efficiency (%DLE)

%EE and %DLE of PEGMA-ABA-coated MNPs having various molar ratios of PEGMA to ABA were investigated (Fig. 11). Increasing ABA moiety in the copolymer seemed to promote both %EE and %DLE in every copolymer composition. This was rationalized that high percent of *trans*-azobenzene, reflecting high hydrophobic moiety, might enhance degrees of prednisolone aggregation in ABA, resulting in the increase in entrapment and loading capacities of the complex.

Investigation of prednisolone releasing behavior

Drug releasing profiles of the drug-entrapped particles exposed under UV light was established and compared with that of a control experiment (the sample was kept in the dark place). The percentage of the released drug was calculated based on the amount of the entrapped drug in each complex. It was found that the drug concentration released at equilibrium in the case of exposure under UV light was slightly higher than those without UV irradiation (Fig. 12). Predinisolone released from the complex was primarily attributed to desorption of the hydrophobic drug from azobenzene moiety in the copolymer. Under UV irradiation, photoisomerization from *trans* to *cis* forms of azobenzene moiety led to an additional driving force to expel the drug from the particle surface due to the increase in its polarity. The slight enhancement of the drug-released amounts at equilibrium of the samples exposed under UV light was attributed to the statistical architecture of the copolymer, which might inhibit the *trans*-to-*cis* transformation of azobenzene moiety. Formation of block structure having ABA inner block and PEGMA outer shell on the particle surface might improve the transformation efficiency and percent drug loading of this complex. Synthesis of the PEGMA-ABA block copolymer grafted on MNP surface and its photo-controlled drug release are warranted for a future studies. In addition, it was also found that increasing

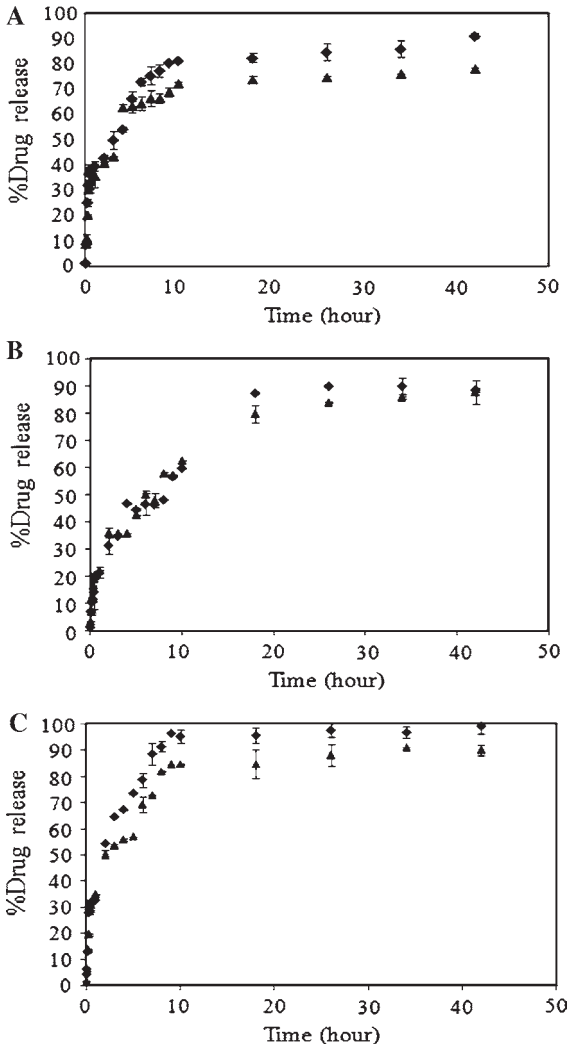

Fig. 12 Prednisolone-releasing profiles of **a** 50:50, **b** 70:30, and **c** 90:10 PEGMA-ABA-coated MNPs in PBS releasing media, (*filled diamond*) under UV and (*filled triangle*) without UV irradiation

percentage of PEGMA in the copolymer seemed to slightly enhance % prednisolone released at equilibrium. This was attributed to the good dispersibility in water of the particles with high loading of PEGMA, which thus promoted releasing competency of the entrapped drug from the particle surface.

Conclusions

This study presented a "grafting-from" method to modify MNP surfaces with PEGMA and ABA

statistical copolymer via ATRP reaction and a study on its application for photocontrolled drug release. The originality of this study is that this is the first report on conjugating photoresponsive azobenzene on MNP surface. It was hypothesized that the change in configuration from *trans* to *cis* in azobenzene moiety renders the system more polar, resulting in acceleration of the repelling rate of prednisolone, the hydrophobic model drug, entrapped in azobenzene in the particle surface. Increasing percentage of azobenzene in the copolymer seemed to promote %EE and %DLE of the complex. Under UV irradiation, the percentage of the released drug was slightly higher than the system without UV irradiation. This complex was hypothetically applicable to load any other hydrophobic drug by partitioning to azobenzene moiety on the particle surfaces. Improvement of drug loading efficiency and releasing behavior of the complex is warranted for future studies for potential uses as magnetic field-directed drug delivery vehicle with photocontrollable drug release.

Acknowledgments The authors thank the Thailand Research Fund (TRF) (DBG5380001) and Naresuan University for financial funding. The National Research Council of Thailand (NRCT) is also acknowledged. The Center of Excellence for Innovation in Chemistry (PERCH-CIC), Commission on Higher Education, Ministry of Education is gratefully acknowledged for financial supports.

References

Anders S, Sun S, Murray CB, Rettner CT, Best ME, Thomson T, Albrecht M, Thiele J-U, Fullerton EE, Terris BD (2002) Lithography and self-assembly for nanometer scale magnetism. Microelectron Eng 61–62:569–575

Archut A, Azzellini GC, Balzani V, Cola LD, Vgtle F (1998) Toward photoswitchable dendritic hosts Interaction between azobenzene-functionalized dendrimers and erosin. J Am Chem Soc 120:12187–12191

Aruna P, Rao BS (2009) Ionomeric poly(urethane semicarbazides) with azobenzene groups in the main chain-studies on photoswitching behavior and mechanical properties. React Funct Polym 69:20–26

Bucio E, Skewes P, Burillo G (2005) Synthesis and characterization of azo acrylates grafted onto polyethylene terephthalate by gamma irradiation. Nucl Instrum Methods Phys Res 236:301–306

Dokic J, Gothe M, Wirth J, Peters MV, Schwarz J, Hecht S, Saalfrank P (2009) Quantum chemical investigation of thermal *cis*-to-*trans* isomerization of azobenzene derivatives: substituent effects, solvent effects, and comparison to experimental data. J Phys Chem A 113:6763–6773

Fan QL, Neoh KG, Kang ET, Shuter B, Wang SC (2007) Solvent-free atom transfer radical polymerization for the preparation of poly (poly(ethyleneglycol) monomethacrylate)-grafted Fe_3O_4 nanoparticles: synthesis, characterization and cellular uptake. Biomaterials 28:5426–5436

Fischer H (1999) The persistent radical effect in controlled radical polymerizations. J Polym Sci A 37:1885–1901

Fischer H (2001) The persistent radical effect: a principle for selective radical reactions and living radical polymerizations. Chem Rev 101:3581–3610

Fujiwara M, Akiyama M, Hata M, Shiokawa K, Nomura R (2008) Photoinduced acceleration of the effluent rate of developing solvents in azobenzene-tethered silica gel. ACS Nano 2:1671–1681

Hermann High LR, Holder SJ, Penfold HV (2007) Synthesis of star polymers of styrene and alkyl (Meth)acrylates from a porphyrin initiator core via ATRP. Macromolecules 40: 7157–7165

Hu F, Neoh KG, Cen L, Kang ET (2006) Cellular response to magnetic nanoparticles "PEGylated" via surface-initiated atom transfer radical polymerization. Biomacromolecules 7:809–816

Kalyanasundaram K, Thomas JK (1977) Environmental effects on vibronic band intensities in pyrene monomer fluorescence and their application in studies of micellar systems. J Am Chem Soc 99:2039–2044

Kim SY, Lee YM, Kang JS (2005) Indomethacin-loaded methoxy poly(ethylene glycol)/poly(D, L-lactide) amphiphilic diblock copolymericnanospheres: pharmacokinetic and toxicity studies in rodents. J Biomed Mater Res A 74A:581–590

Laurent S, Forge D, Port M, Roch A, Robic C, Elst LV, Muller RN (2008) Magnetic iron oxide nanoparticles: synthesis, stabilization, vectorization, physicochemical characterizations, and biological applications. Chem Rev 108:2064–2110

Lee JH, Carraway ER, Schlautman MA, Yim S, Herbert BE (2004) Characterizing pyrene-Ag+ exciplex formation in aqueous and ethanolic solutions. J Photochem Photobiol A 167:141–148

Li Y, Deng Y, Tong X, Wang X (2006) Formation of photoresponsive uniform colloidal spheres from an amphiphilic azobenzene-containing random copolymer. Macromolecules 39:1108–1115

Liu KW, Bian S, Li L, Samuelson L, Kumar J, Tripathy S (2000) Enzymatic synthesis of photoactive poly(4-phenylazophenol). Chem Mater 12:1577–1584

Liu G, Yan X, Lu Z, Curda SA, Lal J (2005) One-Pot synthesis of block copolymer coated cobalt nanocrystals. Chem Mater 17:4985–4991

Maria PD, Fontana A, Gasbarri C, Siani G, Zaniratob P (2009) Kinetics of the Z–E isomerization of monosubstituted azobenzenes in polar organic and aqueous micellar solvents. Arkivoc 8:16–29

Marutani E, Yamamoto S, Ninjbadgar T, Tsujii Y, Fukuda T, Takano M (2004) Surface-initiated atom transfer radical polymerization of methyl methacrylate on magnetite nanoparticles. Polymer 45:2231–2235

Moineau G, Granel C, Dubois Ph, Jerome R, Teyssie P (1998) Controlled radical polymerization of methyl methacrylate

initiated by an alkyl halide in the presence of the wilkinson catalyst. Macromolecules 31:542–544
Monteiro MJ, Adamy MM, Leeuwen BJ, Herk AM, Destarac M (2005) "Living" radical ab initio emulsion polymerization of styrene using a fluorinated xanthate agent. Macromolecules 38:1538–1541
Neugebauer D (2007) Graft copolymers with hydrophilic and hydrophobic polyether side chains. Polymer 48:4966–4973
Nishimura N, Kosako S, Sueishi Y (1984) The thermal isomerization of azobenzenes. III. Substituent, solvent, and pressure effect on the thermal isomerization of push-pull azobenzenes. Bull Chem Soc Jpn 57:1617–1625
Park EK, Lee SB, Lee YM (2001) Preparation and characterization of methoxy poly(ethylene glycol)/poly(e-caprolactone) amphiphilic block copolymeric nanospheres for tumor-specific folate-mediated targeting of anticancer drugs. Biomaterials 26:1053–1061
Pei W, Kumada H, Natusma T, Saito H, Ishio S (2007) Study on magnetite nanoparticles synthesized by chemical method. J Mag Magn Mater 310:2375–2377
Pinna N, Grancharov S, Beato P, Bonville P, Antonietti M, Niederberger M (2005) Magnetite nanocrystals: nonaqueous synthesis characterization and solubility. Chem Mater 17:3044–3049
Sellmyer DJ (2002) Strong magnets by self-assembly. Nature 420:374–375
Sharma L, Kimura T (2003) FT-IR investigation into the miscible interactions in new materials for optical devices. Polym Adv Technol 14:392–399
Sin SL, Gan LH, Hu X, Tam KC, Gan YY (2005) Photochemical and thermal isomerizations of azobenzene-containing amphiphilic diblock copolymers in aqueous micellar aggregates and in film. Macromolecules 38:3943–3948
Sun S, Murray CB, Weller D, Folks L, Moser A (2000) Monodisperse FePt nanoparticles and ferromagnetic FePt nanocrystal superlattices. Science 287:1989–1992
Sun Y, Ding X, Zheng Z, Cheng X, Hu X, Peng Y (2007) Surface initiated ATRP in the synthesis of iron oxide/polystyrene core/shell nanoparticles. Eur Polym J 43:762–772
Teng X, Yang H (2003) Synthesis of face-centered tetragonal FePt nanoparticles and granular films from $Pt@Fe_2O_3$ core–shell nanoparticles. J Am Chem Soc 125:14559–14563
Teodorescu M, Matyjaszewski K (1999) Atom transfer radical polymerization of (Meth)acrylamides. Macromolecules 32:4826–4831
Veiseh O, Gunn JW, Zhang M (2010) Design and fabrication of magnetic nanoparticles for targeted drug delivery and imaging. Adv Drug Deliv Rev 62:284–304
Wang Y, Zhang M, Moers C, Chen S, Xu H, Wang Z, Zhang X, Li Z (2009) Block copolymer aggregates with photoresponsive switches: towards a controllable supramolecular container. Polymer 50:4821–4828
Winnik FM, Winnik MA, Tazuke S (1987) Interaction of hydroxypropylcellulose with aqueous surfactants: fluorescence probe studies and a look at pyrene-labeled polymer. J Phys Chem 91:594–597
Woo K, Hong J, Choi S, Lee HW, Ahn JP, Kim CS, Lee SW (2004) Easy synthesis and magnetic properties of iron oxide nanoparticles. Chem Mater 16:2814–2818
Yager KG, Barrett CJ (2006) Novel photo-switching using azobenzene functional materials. J Photochem Photobiol A 182:250–261
Zhang J, Misra RDK (2007) Magnetic drug-targeting carrier encapsulated with thermo sensitive smart polymer: core–shell nanoparticle carrier and drug release response. Acta Biomater 3:838–850
Zhao H, Shipp DA (2003) Preparation of poly(styrene-block-butyl acrylate) block copolymer-silicate nanocomposites. Chem Mater 15:2693–2695
Zhou Y, Wang S, Ding B, Yang Z (2008) Modification of magnetite nanoparticles via surface-initiated atom transfer radical polymerization (ATRP). Chem Eng J 138:578–585

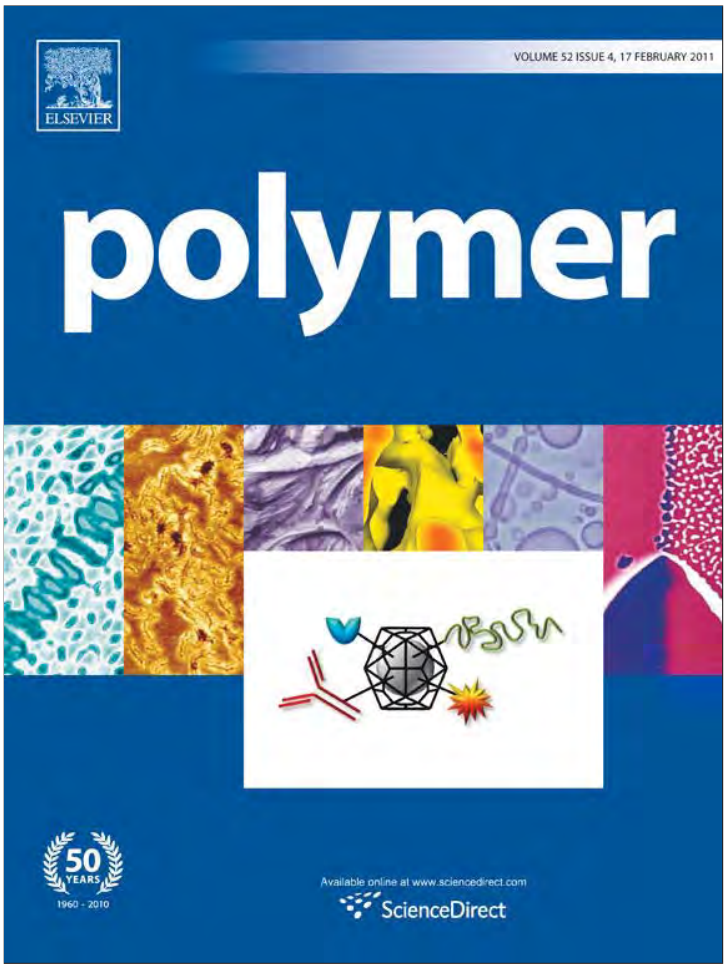

Polymer 52 (2011) 987–995

Contents lists available at ScienceDirect

Polymer

journal homepage: www.elsevier.com/locate/polymer

Poly(acrylic acid)-grafted magnetic nanoparticle for conjugation with folic acid

Metha Rutnakornpituk*, Nipaporn Puangsin, Pawinee Theamdee, Boonjira Rutnakornpituk, Uthai Wichai

Department of Chemistry and Center of Excellence for Innovation in Chemistry, Faculty of Science, Naresuan University, Phitsanulok 65000, Thailand

ARTICLE INFO

Article history:
Received 7 October 2010
Received in revised form
22 December 2010
Accepted 24 December 2010
Available online 9 January 2011

Keywords:
Nanoparticle
poly(acrylic acid)
ATRP

ABSTRACT

Poly(acrylic acid) (poly(AA))-grafted magnetite nanoparticles (MNPs) prepared *via* surface-initiated atom transfer radical polymerization (ATRP) of *t*-butyl acrylate, followed by acid-catalyzed deprotection of *t*–butyl groups, is herein presented. In addition to serve as both steric and electrostatic stabilizers, poly(AA) grafted on MNP surface also served as a platform for conjugating folic acid, a cancer cell targeting agent. Fourier transform infrared spectroscopy (FTIR) was used to monitor the reaction progress in each step of the syntheses. The particle size was 8 nm in diameter without significant aggregation during the preparation process. Photocorrelation spectroscopy (PCS) indicated that, as increasing pH of the dispersions, their hydrodynamic diameter was decreased and negatively charge surface was obtained. According to thermogravimetric analysis (TGA), up to 14 wt% of folic acid (about 400 molecules of folic acid per particle) was bound to the surface-modified MNPs. This novel nanocomplex is hypothetically viable to efficiently graft other affinity molecules on their surfaces and thus might be suitable for use as an efficient drug delivery vehicle particularly for cancer treatment.

1. Introduction

Synthesis of magnetite nanoparticles (MNPs) coated with a thin film of organic polymer has recently attracted much attention due to their potential biomedical applications such as magnetic resonance imaging [1–6], magnetic separation, controlled drug release [7] and hyperthermia treatment of tumor cells [8]. A thin shell of polymeric coating on the particle surface is necessary to prevent nanometer-sized particle aggregation due to their inherent anisotropic dipolar interaction, resulting in losing the specific properties associated with their nanometer dimensions [9,10]. In addition, the polymers on their surface can provide a platform for incorporating biological functional molecules, such as amino acid [11], protein [12,13] and DNA [14–16], for particle labeling with fluorescent molecules [10,17] and for attaching folic acid [18,19], a receptor for tumor cells.

Recently, atom transfer radical polymerization (ATRP) has been reported as a potential "grafting-from" method for surface modification [20,21,27]. ATRP is a living/controlled radical polymerization method, which does not require stringent experimental conditions [22,23]. ATRP enables for the polymerization and block copolymerization of a wide range of functional monomers such as styrene [24–26], methacrylate [27], acrylate [28,29] and methacrylamide [30], yielding polymers with narrowly dispersed molecular weights. Surface modification of nanoparticles *via* ATRP has attracted a great attention in recent years. As compared to a conventional radical polymerization, surface-initiated ATRP from nanoparticles produced polymers with narrow polydispersity index (PDI) and proceeded in a controlled fashion [31]. In addition, the advantage of ATRP technique as compared to other controlled radical polymerization (CRP) techniques is that the polymerization can be initiated at low reaction temperature, while other CRP techniques such as reversible addition-fragmentation chain transfer (RAFT) and nitroxide-mediated polymerizations require relatively high reaction temperature to generate radicals from azo or peroxide initiators. Moreover, functionalization of the particle surface with alkyl halide, the ATRP initiating species, can be easily carried out either by physical absorption of acid-containing halides [36] or covalent bonding of ATRP initiating halides *via* silanization [32]. The "grafting from" strategy *via* ATRP has thus been mostly adopted for MNP surface modification with a variety of polymeric surfactants such as polystyrene [27], poly(methyl methacrylate) [33], poly(ethylene glycol) methacylate [34,35] and poly(acrylamide) [36].

The aim of the current work is to adopt a "grafting from" method to modify MNP surfaces with poly(*t*-butyl acrylate) (poly(*t*-BA)) *via* ATRP, followed by acid-catalyzed deprotection of *t*-butyl groups to obtain poly(AA)-grafted MNP. It is thought that ATRP can offer well-defined water dispersible poly(AA) stabilizers with low molecular weight distribution on the particle surface. The carboxylic acid groups overexpressed on its surface are readily reactive toward molecules containing functional groups such as amine and alcohol. It has thus gained our attention because, not only serving as steric and electrostatic surfactants [37], poly(AA) can also be used as a key intermediate

* Corresponding author. Tel.: +66 5596 3464; fax: +66 5596 1025.
E-mail address: methar@nu.ac.th (M. Rutnakornpituk).

0032-3861/$ – see front matter © 2011 Elsevier Ltd. All rights reserved.
doi:10.1016/j.polymer.2010.12.059

for grafting a large range of functional molecules [38,39]. Folic acid (FA) is of particular interest in this work because it can specifically conjugate with folate receptors overexpressed on cancer cell membranes [40]. Precedents have reported the immobilization of FA on the outermost surface of MNPs coated with other polymeric surfactants [41–44]. Therefore, it is expected that the multifunctional FA-grafted MNPs prepared in this work should bind to cancer cell membranes specifically and consequently improve uptake efficiency of the MNP to the cells. The detail studies on the efficiency on treating cancer cells of this complex are warranted for a future investigation.

In the present work, poly(AA)-coated MNPs were thus prepared *via* surface-initiated ATRP of *t*-BA, followed by acid-catalyzed hydrolysis of *t*-butyl groups. FTIR was used to monitor the reaction progress in each step. Thermogravimetric analysis (TGA) was used to investigate percent of each composition in the polymer-MNP complex. Transmission electron microscopy (TEM) technique was also used to monitor the particle size and the presence of the polymer in the complex. Vibrating sample magnetometry (VSM) was performed to reveal their magnetic properties. In combination with UV–visible spectrophotometry and FTIR, TGA technique was conducted to evidence the existence of FA in the complexes.

2. Experimental section

2.1. Materials

Unless otherwise stated, all reagents were used without further purification: iron (III) acetylacetonate ($Fe(acac)_3$), 99% (Acros), benzyl alcohol (Unilab), 3-aminopropyl triethoxysilane (APS), 99% (Acros), triethylamine (TEA) (Carto Erba), 2-bromoisobutyryl bromide (BIBB), 98% (Acros), copper (I) bromide (CuBr), 98% (Acros), *N,N,N′,N″,N″*-pentamethyldiethylenetriamine (PMDETA), ethyl-α-bromoisobutyrate (Aldrich), 99% (Acros), folic acid, 97% (Fluka), N-hydroxyl succinamide (NHS), 98% (Acros), dicyclohexyl carbodiimide (DCC), 99% (Acros), di-*t*-butyl dicarbonate (Boc_2O), 99% (Aldrich), ethylene diamine (EDA), 99.5% (Fluka), trifluoroacetic acid (TFA), 99.5% (Fluka). *t*-Butyl acrylate (*t*-BA), 99% (Fluka), was distilled under vacuum prior to use.

2.2. Synthesis

2.2.1. Synthesis of oleic acid-coated magnetite nanoparticles (MNPs)

MNPs were prepared *via* thermal decomposition following the method previously described [45]. In a typical procedure, $Fe(acac)_3$ (1.0 g, 2.81 mmol) and benzyl alcohol (20 ml) were mixed by magnetic stirring in a three-neck flask with nitrogen flow. The mixture was heated to 200 °C for 48 h. The precipitant was then removed from the dispersion using an external magnet and washed with ethanol and CH_2Cl_2 repeatedly to remove benzyl alcohol. The particles were then dried at room temperature under reduced pressure. To prepare oleic acid-coated MNPs, the dried MNPs (0.6 g) were introduced into an oleic acid solution in dried toluene (4 ml oleic acid in 30 ml THF) and ultrasonicated for 3 h.

2.2.2. Synthesis of 2-bromo-2-methyl-N-(3-(triethoxysilyl) propanamide (BTPAm))

To a stirred solution of 3-aminopropyl triethoxysilane (APS) (0.18 ml, 0.8 mmol) and triethylamine (TEA) (0.12 ml, 0.8 mmol) in dried toluene (10 ml), 2-bromoisobutyryl bromide (BIBB) (0.1 ml, 0.8 mmol) in dried toluene (10 ml) was added dropwise at 0 °C for 2 h under nitrogen. The reaction mixture was warmed to room temperature and stirred for 24 h. The mixture was passed through a filter paper to remove salts and the filtrate was evaporated to remove the unreacted TEA under reduced pressure. The resulting product, BTPAm, was yellowish thick liquid (78% yield). ^{1}H NMR (400 MHz, $CDCl_3$) δ_H: 0.60 [m, 2H, Si–$\underline{CH_2}$, 1.20 [t, 9H, O–CH_2–$\underline{CH_3}$], 1.65 [m, 2H, Si–CH_2–$\underline{CH_2}$], 1.95, [s, 6H, $\underline{CH_3}$–C–Br], 3.25 [m, 2H, $\underline{CH_2}$–NH], 3.80 [m, 6H, CH_3–$\underline{CH_2}$–O]. FT-IR (KBr disc) υ_{max}: 3345 cm^{-1} (NH stretching), 2975–2889 cm^{-1} (C–H stretching), 1738 cm^{-1} (C=O of acid bromide stretching), 1658 cm^{-1} (C=O of amide stretching), 1532 cm^{-1} (NH bending), 1442 cm^{-1} (C–N stretching), 1286 cm^{-1} (C–Br stretching), 1112–1026 (Si–O stretching).

2.2.3. Immobilization of 2-bromo-2-methyl-N-(3-(triethoxysilyl) propanamide (BTPAm)) onto MNP surface (BTPAm-coated MNPs) (Fig. 1)

To immobilize BTPAm on the oleic acid-coated MNP surface, the MNP-toluene dispersion (0.1 g of oleic acid-coated MNPs in 5 ml toluene) (30 ml), BTPAm (0.90 ml) and 2 M TEA in toluene (6 ml) were added into a round bottom flask. The mixture was stirred for 24 h at room temperature under nitrogen. The particles were subsequently precipitated in methanol, following by magnet separation to obtain the BTPAm-modified MNPs. Then, the MNPs were re-dispersed in toluene and re-precipitated in methanol. This procedure was repeated several times to completely remove unreacted BTPAm. The particles were finally dried *in vacuo*.

2.2.4. Synthesis of poly(t-butyl acrylate)-coated MNPs (poly(t-BA)-coated MNPs) via ATRP reaction

To a schlenk tube containing dioxane (1 ml), CuBr (0.3 g, 0.0021 mol), and PMDETA (0.42 ml, 0.0021 mol) were added under nitrogen blanket. The mixture was stirred until homogenous blue color was observed. Then, *t*-butyl acrylate (*t*-BA) (3 ml, 0.021 mol) monomer and BTPAm-immobilized MNPs (0.3 g) were added *via* a syringe. The mixture was degassed and nitrogen-purged by three freeze-thaw cycles. The solution was then heated to 90 °C for 24 h to commence ATRP reaction. At a given time, the reactions were ceased and poly(*t*-BA)-grafted MNPs were magnetically separated and washed thoroughly with methanol and dried *in vacuo*.

2.2.5. Synthesis of poly(acrylic acid)-coated MNPs (poly(AA)-coated MNPs) via hydrolysis of poly(t-butyl acrylate)-coated MNPs

Poly(*t*-BA)-coated MNPs were hydrolyzed to obtain acrylic acid functional groups on MNP surfaces. Briefly, poly(*t*-BA)-coated MNPs (0.05 g) were hydrolyzed in a 20-ml TFA solution (0.1 M of TFA in THF) at room temperature for 24 h. The solution was concentrated under reduced pressure, diluted with CH_2Cl_2, and repeatedly precipitated in cold hexane. The precipitate was separated by a permanent magnet and dried *in vacuo*. The possible reactions between TFA and polymers coated on MNP surface are illustrated in supplementary data.

2.2.6. Synthesis of N-(2-aminoethyl) folic acid (EDA-FA) (Fig. 2)

2.2.6.1. Protection of an amino group of ethylene diamine (EDA) with t-butyl carbamate (Boc). A solution of di-*t*-butyl dicarbonate (Boc_2O) (0.23 ml, 1 mmol) in anhydrous CH_2Cl_2 (10 ml) was added dropwise to a cold solution of ethylene diamine (EDA) (0.67 ml, 10 mmol) in anhydrous CH_2Cl_2 (10 ml) at 0 °C under nitrogen atmosphere. The mixture was magnetically stirred at 0 °C for 2 h and at room temperature for 24 h. Then, distilled water (5 ml) was added into the mixture to dissolve the precipitate. The organic layer was washed with brine (15 ml) 5 times, dried over anhydrous Na_2SO_4, and then concentrated under reduced pressure to give *t*-butyl *N*-(2-aminoethyl) carbamate (EDA-Boc), appearing as thick oil (82% yield). ^{1}H NMR (400 MHz, $CDCl_3$) δ_H: 1.40 [s, 9H, $\underline{CH_3}$ Boc], 2.80 [m, 2H, $\underline{CH_2}$–NH_2], 3.20[m, 2H, CH_2–$\underline{CH_2}$–NH-Boc]. FTIR (KBr disc) υ_{max}: 3360 cm^{-1} (NH stretching), 2955–2923 cm^{-1} (C–H stretching), 1693 cm^{-1} (C=O of amide stretching), 1525 cm^{-1} (NH bending), 1366-1277 cm^{-1} (C–N bending), 1172 cm^{-1} (C–O stretching).

2.2.6.2. Coupling folic acid with the amino-protected EDA. To a stirred solution of FA (0.275 g, 6.25 10^{-4} mol) in anhydrous DMSO (5 ml) and pyridine (4 ml), the solution of EDA-Boc (0.10 g, 6.25 10^{-4} mol) and DCC (0.21 g, 7.5 10^{-4} mol) in anhydrous DMSO (5 ml) were added. The mixture was stirred at room temperature for 18 h under nitrogen blanket. After the reaction completed, the mixture was gradually poured into a vigorously stirred diethyl ether (20 ml) at 0 °C. The yellow precipitate was collected and washed with cold diethyl ether several times and dried under high vacuum to obtain {*t*-butyl N-(2-aminoethyl) carbamate} folic acid (Boc-EDA-FA), appearing as a yellow solid (85% yield). ^{1}H NMR (400 MHz, DMSO-d_6) δ_H: 1.40 [s, 9H, CH_3 Boc], 2.0 [m, 2H, CH_2–CH_2–CO–NH], 2.40 [m, 2H, CH_2–CO–NH], 2.90 [m, 2H, CH_2–NH–CO], 3.10 [m, 2H, CH_2–NH–Boc], 4.30 [m, 1H, HOOC–CH–NH], 4.50 [d, 2H, phenyl-NH-CH_2 folic acid], 6.60 [d, J = 8 Hz, 2H, 2CH=CH phenyl folic acid], 6.90 [t, 1H, phenyl-NH-CH_2], 7.60 [d, J = 8 Hz, 2H, 2CH=CH phenyl folic acid], 8.60 [s, 1H, N=CH Ar folic acid]. FTIR (KBr disc) υ_{max}: 3360–2600 cm^{-1} (OH and NH stretching), 1700 cm^{-1} (C=O of amide stretching), 1605 cm^{-1} (C–O of acid stretching), 1168 cm^{-1} (C–O stretching).

TFA (2 ml) was then added to Boc-EDA-FA and stirred at room temperature. After 2 h stirring, TFA was removed under reduced pressure and the resulting residue was dissolved in anhydrous DMF. Pyridine was added until a formation of yellow precipitate and it was subsequently washed with diethyl ether and dried to give *N*-(2-aminoethyl) folic acid (EDA-FA) (80% yield, T_m 290 °C). ^{1}H NMR (400 MHz, DMSO-d_6) δ_H: 2.0 [m, 2H, CH_2–CH_2–CO–NH], 2.40 [m, 2H, CH_2–CO–NH], 2.60 [m, 2H, CH_2–NH–CO], 3.30 [m, 2H, CH_2–NH_2], 4.20 [m, 1H, HOOC-CH-NH], 4.40 [d, 2H, phenyl-NH-CH_2 folic acid], 6.60 [d, J = 8 Hz, 2H, 2CH=CH phenyl folic acid], 6.90 [t, 1H, Phenyl-NH-CH_2], 7.70 [d, J = 8 Hz, 2H, 2CH=CH phenyl folic acid], 8.60 [s, 1H, N=CH Ar folic acid]. FTIR (KBr disc) υ_{max}: 3600–2800 cm^{-1} (OH and NH stretching), 1684 cm^{-1} (C=O of amide stretching), 1605 cm^{-1} (C–O of acid stretching), 1532–1335 cm^{-1} (C–N bending), 1202–1132 cm^{-1} (C–O stretching).

2.2.7. Immobilization of folic acid on the surfaces of poly(AA)-coated MNPs

Poly(AA)-coated MNPs were dispersed in a 10 ml aqueous solution containing NHS (40 mg) and EDC·HCl (20 mg) and the mixture was kept in a dark place for 2 h. The particles were recovered, washed with water and dried *in vacuo*. Then, the particles were added in a solution of 200 mg of EDA-FA and 50 mg of EDC in 10 ml anhydrous DMSO. The suspension was agitated overnight at 37 °C in dark. The particles were then recovered, washed with DMSO and methanol several times and dried *in vacuo*.

2.3. Characterization

FTIR was performed on a Perkin–Elmer Model 1600 Series FTIR Spectrophotometer. The solid samples were mixed with KBr to form pellets. Nuclear magnetic resonance spectroscopy (NMR) was performed on a 400 MHz Bruker NMR spectrometer using $CDCl_3$ as a solvent. Gel permeation chromatography (GPC) data was conducted on PLgel 10 μm mixed B2 columns and a refractive index detector. Tetrahydrofuran (THF) was used as a solvent with a flow rate of 1 ml/min at 30 °C. TEM were performed using a Philips Tecnai 12 operated at 120 kV equipped with Gatan model 782 CCD camera. TGA was performed on SDTA 851 Mettler-Toledo at the temperature ranging between 25 and 600 °C at a heating rate of 20 °C/min under oxygen atmosphere. VSM was performed at room temperature using a Standard 7403 Series, Lakeshore vibrating sample magnetometer. The magnetic moment was investigated over a range of applied magnetic fields from −10,000 to +10,000 G using 30 min sweep time. Hydrodynamic diameter of the particles was measured *via* PCS using NanoZS4700 nanoseries Malvern

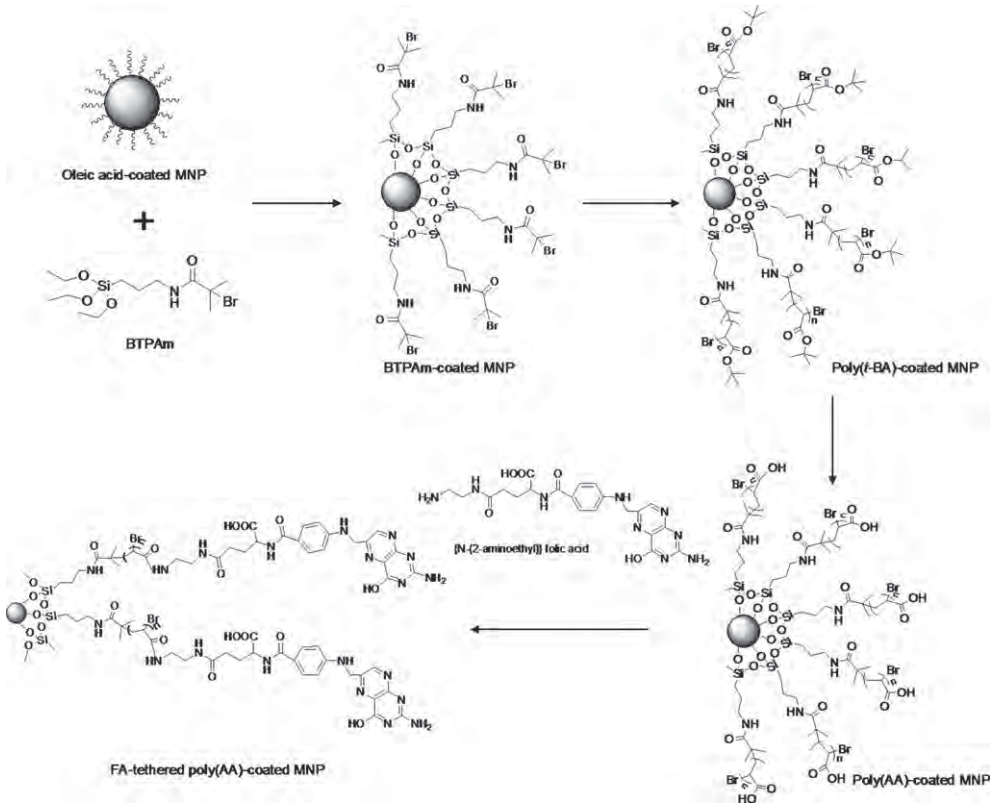

Fig. 1. Synthesis of poly(AA)-coated MNPs *via* ATRP reaction and immobilization of folic acid.

instrument. The sample dispersions were sonicated for 10 min before the measurement at 25 °C. The presence of FA was investigated using SPECORD S100 UV–Visible spectrophotometer (Analytikjena AG) coupled with a photo diode array detector at $\lambda_{max} = 371$ nm.

3. Results and discussion

The aim of this work is to modify MNP surfaces with poly(AA) and immobilize folic acid on their surfaces. Poly(AA) grafted on the particle surfaces is thought to provide steric and electrostatic stabilizations and dispersibility of the particles in aqueous media. Another major advantage of this system was that the carboxylic acid-enriched surfaces of poly(AA)-grafted MNPs provided a platform for efficient surface immobilization of any functional molecules such as DNA, drugs, protein and fluorescent molecules. Hence, the novelty of this current work is that this is the first report on synthesizing multifunctional poly(AA)-coated MNPs for attaching folic acid (FA), a model molecule in this work. Precedents have reported the immobilization of biomolecules on the distal ends of MNPs coated with other polymeric surfactant [41–44]. This novel system is hypothesized to increase the loading efficiency of FA on the MNP surfaces.

To perform surface-initiated ATRP from MNPs, BTPAm, a molecule containing an ATRP initiating site was first synthesized through amidization between APS and BIBB, followed by silanization of triethoxysilane of BTPAm on MNP surface. The results of the synthesis of BTPAm including FTIR and ^{1}H NMR are illustrated in supplementary data. To immobilize BTPAm on MNP surfaces, bare MNPs were first coated with oleic acid to form well dispersed MNPs in toluene. The advantage of this procedure was that the MNPs were well dispersible in the media before reacting with BTPAm, allowing BTPAm to effectively silanize to their surfaces due to its greater surface approaching ability in the dispersed MNPs.

Fig. 3 displays FTIR spectra of poly(*t*-BA)-coated MNPs withdrawn from the dispersions at 1, 6, 12 and 24 h of ATRP reaction. Because ATRP is known as a controlled radical polymerization, the time period for the ATRP reaction is thus crucial for tuning the molecular weight of the polymers. A progressive growth of ester linkage signals (–O(C=O)- stretching, ~1724 cm^{-1} and C–O stretching, ~1147 cm^{-1}) of *t*-BA repeating units in relative to those of a Si–O signal of the linker (~1100–1020 cm^{-1} and ~800 cm^{-1}) indicated that the molecular weights of poly(*t*-BA) on MNP surfaces increased as increasing ATRP reaction time. It should be noted that the signal corresponding to Fe-O bonds from MNP core (~589 cm^{-1}) were observed throughout the reactions without significant change in its intensity.

Weight loss from TGA technique of poly(*t*-BA)-coated MNPs at various ATRP reaction times was investigated to determine the relative amount of poly(*t*-BA) that can be grafted on the particle surface. It should be noted that the particles were separated from the uncoordinated species using an external magnet. Using an assumption that % char yield was the weight of magnetite remaining at 600 °C, the weight loss of the surface-modified MNPs was thus attributed to the decomposition of organic components including BTPAm and poly(*t*-BA) that complexed to the particle surface. Hence, percent char yield of bare MNP and MNP coated with BTPAm were determined to obtain percent of BTPAm in the complexes in each sample. According to TGA results, percent of BTPAm in the complexes was about 2 wt%, while percents of poly(*t*-BA) were 3 wt%, 15 wt%, 26 wt% and 43 wt% of the complexes at 1, 6, 12 and 24 h ATRP reaction times, respectively (Fig. 4). This was a supportive result to FTIR that poly(*t*-BA) chain length was prolonged when ATRP reaction time was extended.

To investigate the molecular weight and the molecular weight distribution of poly(*t*-BA), small amount of ethyl bromoisobutylate (EBiB) was added in the dispersion as a "sacrificial initiator" to form free poly(*t*-BA) along with poly(*t*-BA) grafted on MNP. After 24 h of

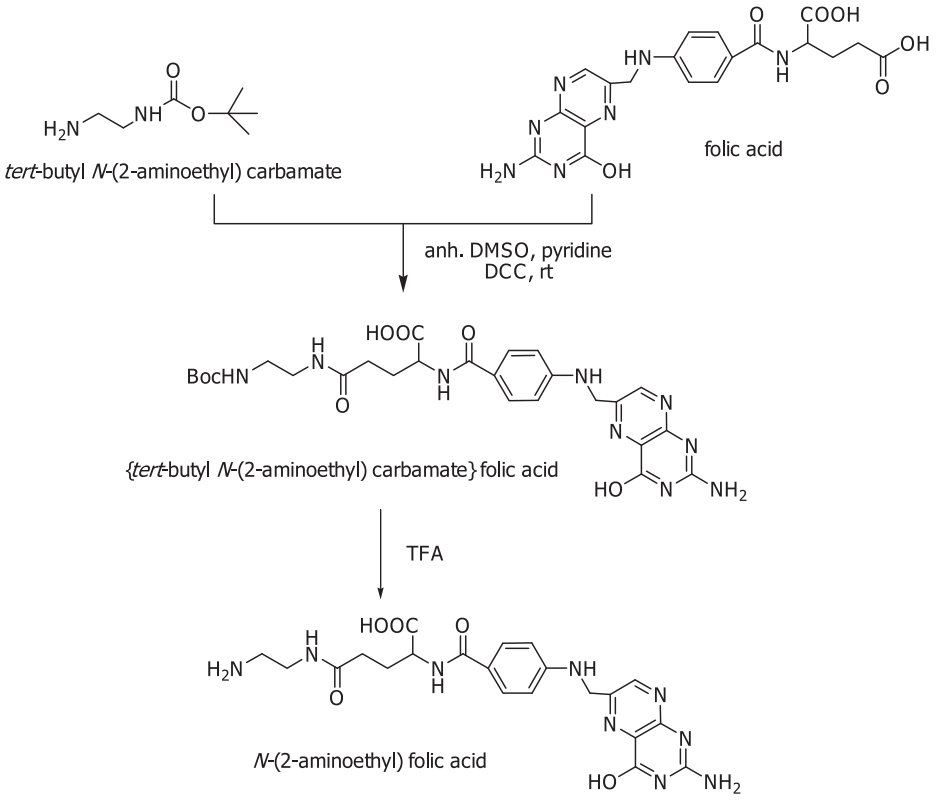

Fig. 2. Synthesis of *N*-(2-aminoethyl) folic acid (EDA-FA).

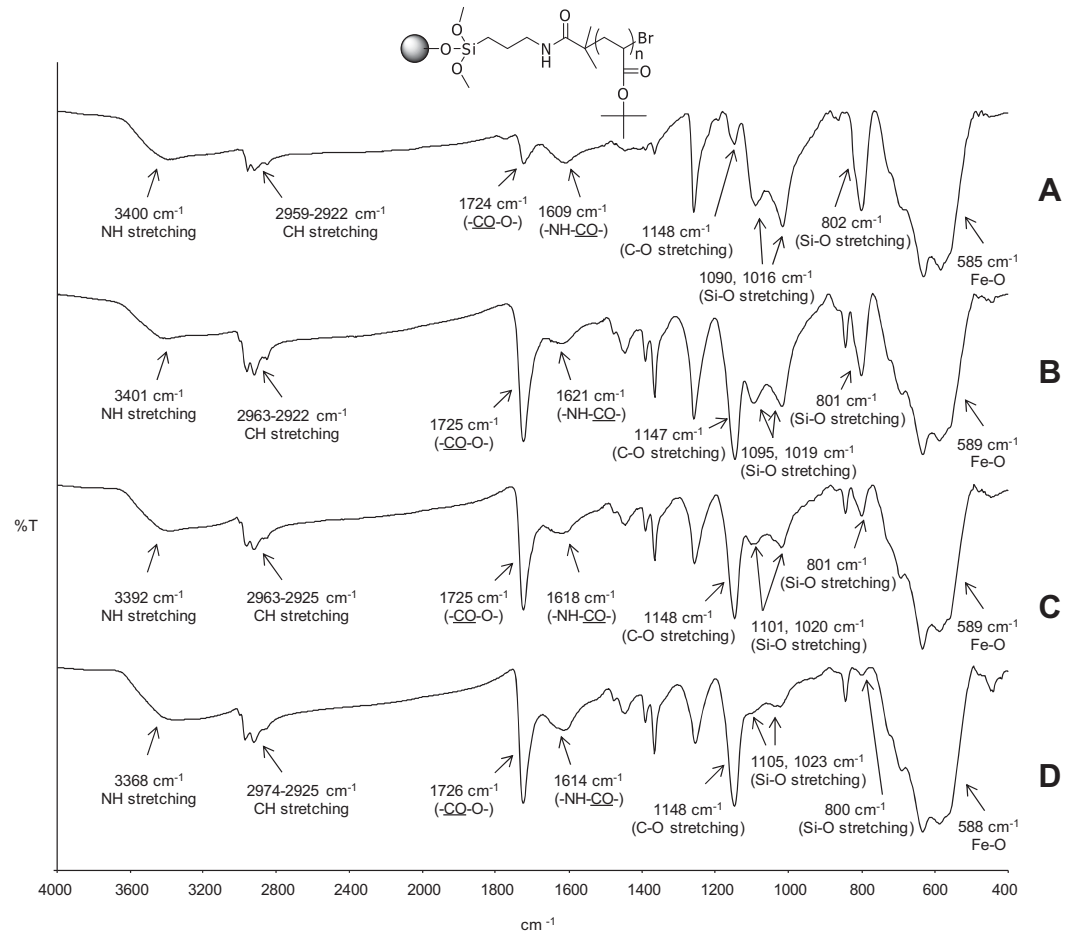

Fig. 3. FTIR spectra of poly(*t*-BA)-coated MNP at various ATRP reaction times, A) 1 h, B) 6 h, C) 12 h and D) 24 h.

the reaction, the free poly(*t*-BA) was removed from the MNP complex using an external magnet. According to GPC results, molecular weight of poly(*t*-BA) was about 18,600 g/mol and its molecular weight distribution was about 1.22. This narrow molecular weight distribution indicated the living mechanism of controlled radical polymerization. ^{1}H NMR spectrum of free poly(*t*-BA) is shown in supplementary data.

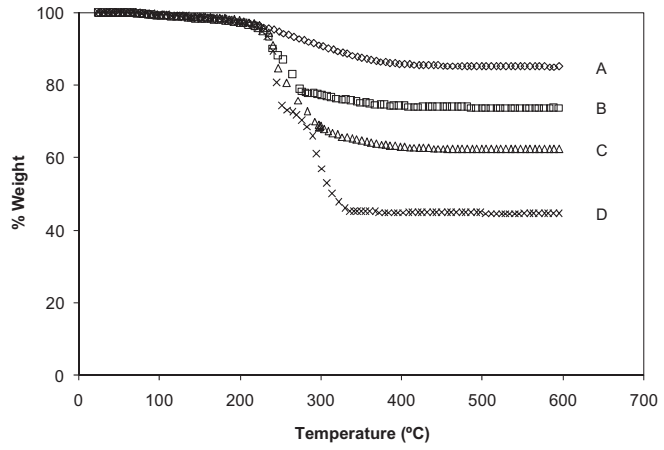

Fig. 4. TGA thermograms of poly(*t*-BA)-coated MNPs at various ATRP reaction times, A) 1 h, B) 6 h, C) 12 h and D) 24 h.

TEM images of MNP complexes at each step of the reaction are illustrated in Fig. 5. Bare MNPs observed in Fig. 5A were well organized because they were somewhat uniformed in size, which was in the range of 6–10 nm in diameter with the average of about 8 nm. Surface modification of the MNPs resulted in a slightly broader size distribution due to the presence of organic compounds coated on their surface (Fig. 5B–D). However, the average particle size was not significant difference from those of bare MNPs. It should be noted that poly(*t*-BA)-coated MNPs were well dispersed in toluene due to the existence of hydrophobic poly(*t*-BA) on their surface (Fig. 5C), while poly(AA)-coated MNPs were well dispersed in water because of the presence of hydrophilic and charge surfactants of poly(AA) (Fig. 5D).

The *M-H* curves of bare MNP, BTPAm-coated MNP, poly(*t*-BA)-coated MNPs and poly(AA)-coated MNP were illustrated in Fig. 6. They showed superparamagnetic behavior at room temperature as indicated by the absence of reminance and coercivity upon removing an external applied magnetic field. According to the results in Table 1, the decrease of saturation magnetization (M_s) from 59 emu/g of bare MNPs to 27 emu/g of poly(*t*-BA)-coated MNPs was attributed to the presence of the organic surfactant on their surface, resulting in the decrease of percent of magnetite in the complexes. After the hydrolysis of poly(*t*-BA) to form poly(AA)-coated MNP, its M_s value increased from 27 to 39 emu/g sample due to the removal of *t*-BA groups in poly(*t*-BA), which subsequently increased percent of magnetite in the complexes. Interestingly, when taking percent of magnetite in the complex into account, the M_s values in emu/g magnetite basis of these complexes were not

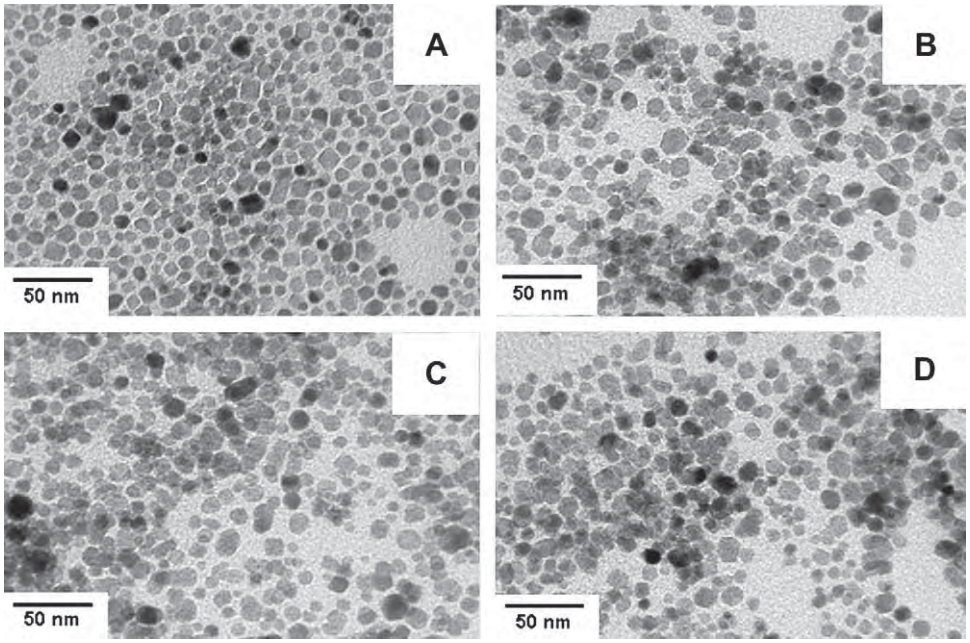

Fig. 5. TEM images of A) bare MNPs, B) BTPAm-coated MNPs, C) poly(*t*-BA)-coated MNPs, D) poly(AA)-coated MNPs. In the TEM sample preparation, MNPs in Figure A–C were dispersed in toluene and those in Figure D were dispersed in water.

significantly different from each other, indicating that magnetic properties of the particles were not considerably affected upon ATRP of poly(*t*-BA) and hydrolysis to form poly(AA)-coated MNPs.

After the hydrolysis reaction, it was conceived that MNPs having carboxylic acid-enriched surfaces were obtained. These carboxylic acid functional groups are readily reactive toward coupling reactions with other molecules having affinity functional groups such as amine and alcohol. In the current work, folic acid (FA) was chemically immobilized on the surface-modified MNPs. FA has two carboxylic acid groups at the α and γ positions, which can covalently react with amino functional groups of EDA. However, it has already been verified that γ-COOH is more accessible to covalently react with amino groups due to its high reactivity [46,47]. FA needs to be first activated with ethylene diamine (EDA) to obtain primary amine-terminated FA (*N*-(2-aminoethyl) folic acid or EDA-FA). This logical strategy enhanced the reactivity of FA to efficiently react with carboxylic acid overexpressed on the surface of poly(AA)-coated MNPs through amidization reaction. Results of the synthesis of EDA-FA including FTIR and ^{1}H NMR spectra were detailed in supplementary data.

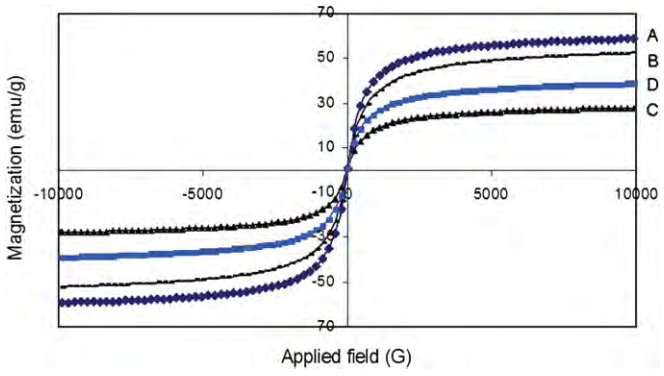

Fig. 6. *M-H* curves of A) bare MNP, B) BTPAm-coated MNP, C) poly(*t*-BA)-coated MNP and D) poly(AA)-coated MNP.

In the grafting reaction between poly(AA)-coated MNPs and EDA-FA, *N*-hydroxyl succinimide (NHS) was used to activate the dangling carboxylic acid groups. FTIR spectra of the products in each step were thus illustrated in comparison with the starting compounds (Fig. 7). Fig. 7A showed the FTIR spectrum of poly(AA)-coated MNPs and those of NHS was depicted in Fig. 7B. In Fig. 7C, the sharp and strong characteristic signal of ester linkages appeared at 1723 cm^{-1}, indicating the coupling reaction between carboxylic acid of poly(AA)-coated MNPs and NHS. In addition, Fe-O linkages of magnetite core were also observed at 586 cm^{-1}. After the coupling reaction with EDA-FA (Fig. 7D), the characteristic signals of FA, such as 1700–1500 cm^{-1} and 1153–1069 cm^{-1}, appeared in the FA-bound MNPs (Fig. 7E), indicating the successful conjugation of FA on the MNP surfaces.

UV–visible spectrophotometry was also applied to confirm the presence of FA in the conjugated MNP complex. FA showed a λ_{max} value at 371 nm (Fig. 8A), whilst those of FA-conjugated MNPs also exhibited a weak absorbance signal at the same wavelength (Fig. 8B). It is worth to mention that poly(AA)-coated MNPs before FA loading did not show any absorbance signal at the same wavelength (Fig. 8C). This result implied that FA was, to some extent, covalently conjugated to the MNP surfaces.

To determine percentage of magnetite core and organic shell in the complexes in each step of the reactions, the complexes were characterized *via* TGA to investigate their mass loss. Bare MNPs manifested a drastic weight loss between 200 and 350 °C with 90%

Table 1
Percentage of magnetite in the complex and their magnetic properties.

Sample	emu/g sample[a]	% Fe_3O_4[b]	emu/g Fe_3O_4
Bare MNP	59	90	65
BTPAm-coated MNP	53	88	60
Poly(*t*-BA)-coated MNP	27	45	61
Poly(AA)-coated MNP	39	63	62

[a] Estimated from the saturation magnetization (M_s) at 10,000 G from VSM technique.
[b] Estimated from % char yield at 600 °C from TGA technique.

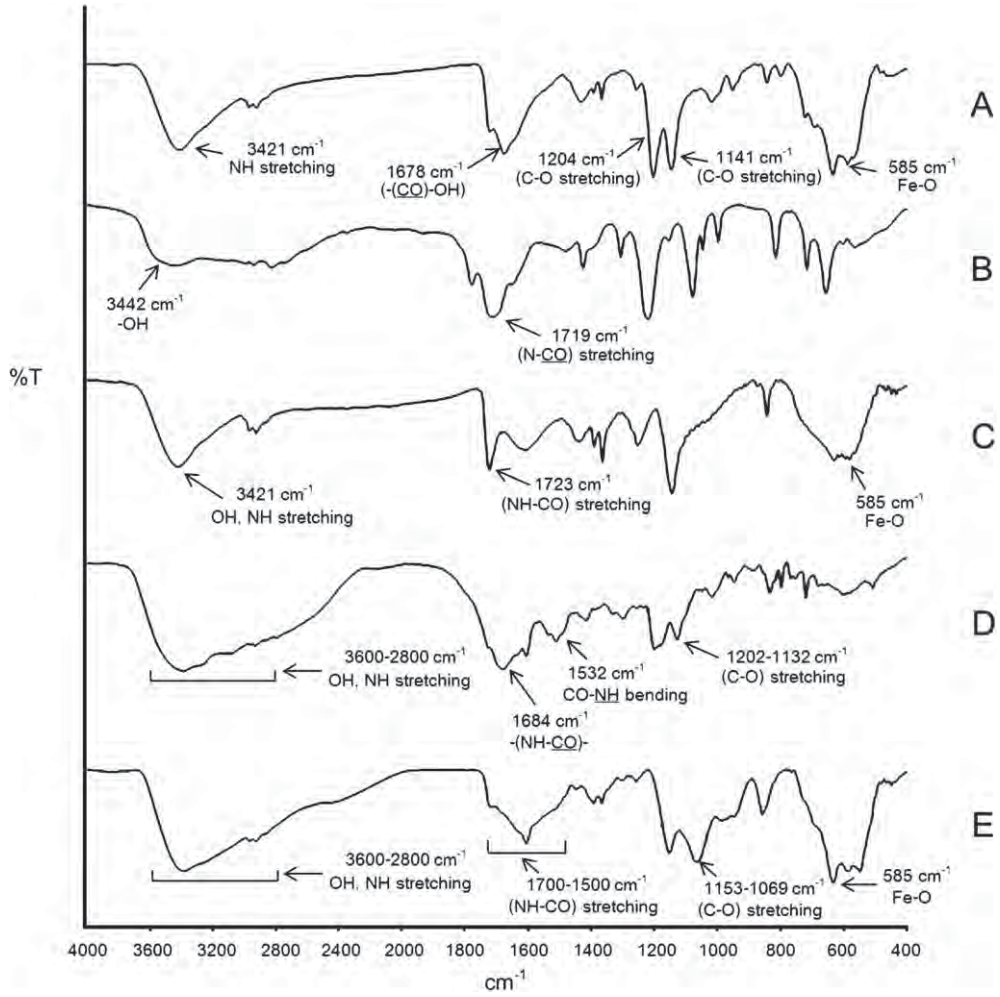

Fig. 7. FTIR spectra of (A) poly(AA)-coated MNP, (B) NHS, (C) NHS-poly(AA)-coated MNP, (D) EDA-FA and (E) FA-poly(AA)-coated MNP.

char yield (Fig. 9A). This was attributable to the decomposition or desorption of the absorbed ammonium salt at elevated temperature and eventually loss some weight [48,49]. The weight loss of MNPs coated with BTPAm, poly(*t*-BA) and poly(AA) were attributed to the decomposition of organic components complexing to the particle surface and % char yields were the weight of magnetite core. From TGA thermograms in Fig. 9B,C, there was about 2 wt% of BTPAm and 49 wt% of poly(*t*-BA) in poly(*t*-BA)-coated MNPs. The

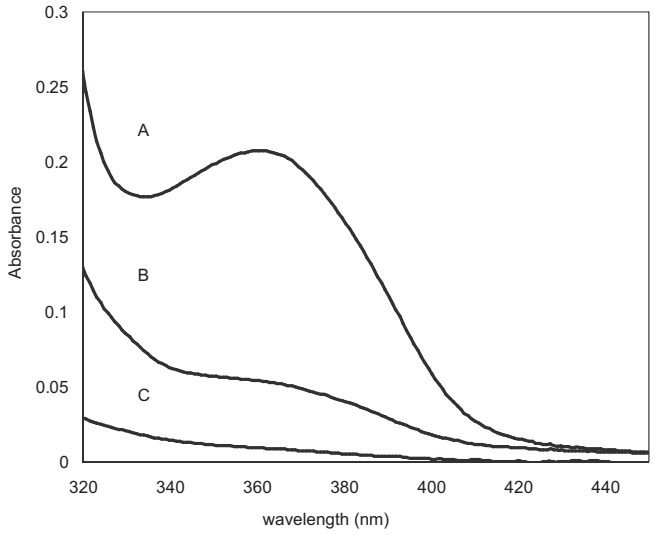

Fig. 8. UV–visible spectra of (A) folic acid (FA), (B) FA-conjugated MNP and (C) poly (AA)-coated MNP without FA.

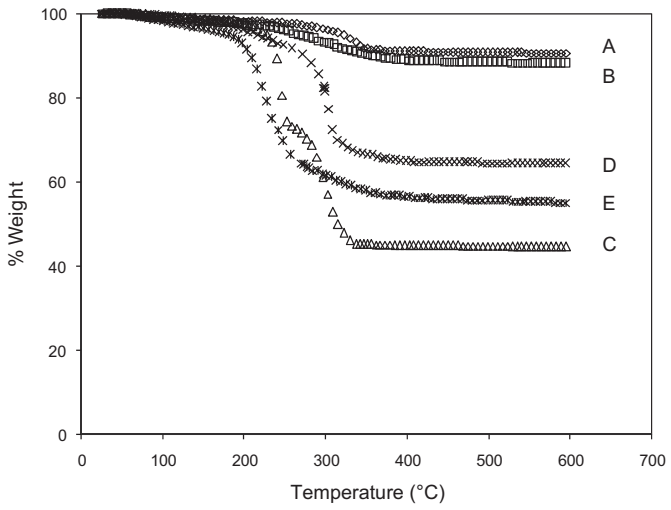

Fig. 9. TGA thermograms of (A) bare MNP, (B) BTPAm-coated MNP, (C) poly(*t*-BA) coated MNP, (D) poly(AA)-coated MNP and (E) FA-poly(AA)-coated MNP.

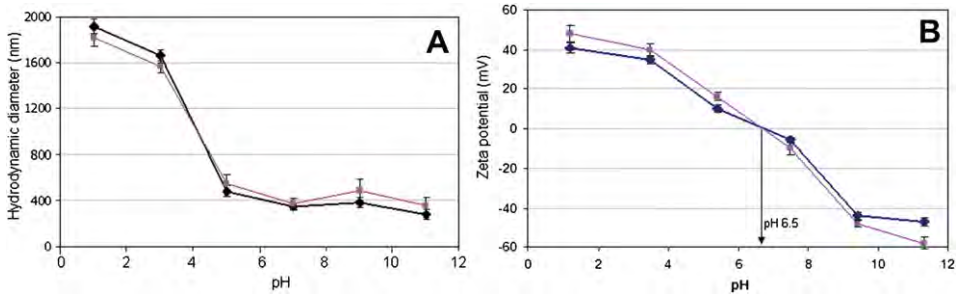

Fig. 10. The effect of pH of the aqueous dispersions containing poly(AA)-coated MNP (◆) and FA-poly(AA)-coated MNP (■) on their hydrodynamic diameter and zeta potential. The experiments were performed at 25 °C.

grafting density of BTPAm, the initiating site for ATRP on the particle, can be calculated and it was found that there was about 0.8 molecule/nm^2 (150 molecules/particle). Examples of the calculation are illustrated in supplementary data. The grafting density of poly(*t*-BA) were comparable to that of BTPAm on the surface.

After the hydrolysis of poly(*t*-BA), percent of organic components in the case of poly(AA)-coated MNPs significantly dropped (from 49 to 27 wt%) due to the removal of *t*-BA groups from the polymeric layer of the particles (Fig. 9D). The 27 wt% of poly(AA) corresponded to 23 carboxylic acid/nm^2 (4600 acid/particle). From Fig. 9E, there was about 14 wt% of FA in the complex, corresponding to about 2 FA molecules/nm^2 (400 FA molecules/particle). Therefore, percent conversion of carboxylic acid to FA was about 8%. The lowering temperature of TGA curve in Fig. 9E (FA-poly (AA)-coated MNP) as compared to that in Fig. 9D (poly (AA)-coated MNP) was attributed to the weight loss of FA component in the complex. The decomposed TGA thermogram of free FA has been investigated and shown in supplementary data. In addition, it was also found that there was about 2.7 FA molecules/site of the ATRP initiator (400 FA molecule/150 sites of BTPAm in a single particle). The limited number of the % conversion and grafting density of FA on the particle surface was attributed to limited accessibility of bulky FA to react with steric poly (AA). However, the grafting density of FA might be improved by copolymerization of poly(AA) with other polymers to lessen steric hindrance of the compact poly(AA), so that FA con be more effectively conjugated. Also, utilization of spacer from the particle surface is another approach that can diminish steric hindrance on the dense surface.

Because carboxylic acid functional groups can be easily ionized in an aqueous solution, it is thus interesting to understand how pH of the dispersions affect hydrodynamic diameter and surface charge of poly(AA)-coated MNPs and FA-poly(AA)-coated MNP. pH of the aqueous dispersions containing the complexes (0.2 mg/ml) were varied from approximately 1–11 and their hydrodynamic diameters were determined *via* PCS technique. In both samples, as pH of the dispersions increased, their hydrodynamic diameters rapidly decreased at acidic pH (ranging between pH 1.2–5.4) and gradually decreased at pH ranging between 5.4 and 11.3 (Fig. 10). It was hypothesized that as increasing pH of the dispersions, ionization of carboxylic acid on the surface of poly(AA)-coated MNPs took place, resulting in the formation of carboxylate ions on their surfaces. The negative charges of carboxylate ions led to additional electrostatic repulsion toward neighboring particles and thus prevented massive flocculation.

The results from zeta potential measurements also supported this assumption. The surface charges of poly(AA)-coated MNPs were positive at the pH ranging between 1.2 and 6.5 and negative at the pH range of 6.5–11.3, implying that point of zero charge (PZC) of this complex was pH 6.5 (Fig. 10). It was also found that FA-containing complex showed a slightly higher zeta potential than the other at pH ranging between 1.2 and 6.5. This was attributed to the presence of amines in FA structure, resulting in protonated amino groups. Similarly, the enriched amines in the complex might also influence the lower zeta potential in FA-containing complex at basic pH.

The large size of the particles in DLS as compared to those from TEM measurements (8 nm in diameter) might come from the fact that there were some nano-clusters of particles in the dispersions. These nano-clusters of the particles can be observed in TEM measurements from the first step of the particle synthesis (shown in supplementary data). When poly(AA) was chemically grafted on their surface, these clusters still presented. Although these nano-clusters existed in the dispersions, the particles were well dispersible in aqueous dispersions without macroscopic aggregation visibly observed because there were poly(AA) coated on their surface.

Cytotoxicity testings of poly(AA)-coated MNP and FA-poly(AA)-coated MNP were also performed. According to our preliminary results, it was found that the dispersions were not toxic against Vero cell line up to 50 μg/ml concentration of the sample (sulforhodamine B (SRB) assay method). Detail studies regarding the toxicity of the magnetite complexes are warranted for future studies.

4. Conclusions

This work presented a “grafting from” strategy to modify MNP surfaces with poly(*t*-BA) *via* ATRP, followed by a hydrolysis of *t*-BA groups to obtain poly(AA) and finally immobilization of folic acid on their surfaces. The originality of this work is that this is the first report on modifying MNP surface with poly(AA) which serves as a platform for folic acid immobilization. Because the folate receptor is overexpressed on the surface of cancer cells, it is for this reason that folic acid is of particular interest in the current work in an attempt to facilitate the intracellular uptake by specific cancer cells for cancer therapy. Folic acid was successfully activated with ethylene diamine (EDA) to obtain primary amine-terminated folic acid derivative. This logical strategy enhanced the reactivity of folic acid to be efficiently immobilized on MNP surfaces through amidization reaction.

In addition to the use of binding affinity of carboxylic acid functional groups, poly(AA) on their surface can also provide stabilization mechanisms through both steric repulsion due to the long chain polymers and electrostatic repulsion owing to the formation of negative charges in basic pH dispersions. Furthermore, poly(AA) on their surfaces also promoted particle dispersibility in water, which is a minimum requirement for biomedical uses. This novel magnetically guidable nanocomplex might be suitable for use as an efficient drug delivery vehicle particularly for cancer treatment.

Acknowledgement

The authors thank the Thailand Research Fund (TRF) and Naresuan University (DBG5380001) for financial funding. The Center of Excellence for Innovation in Chemistry (PERCH-CIC), Commission on Higher Education, Ministry of Education is also gratefully acknowledged for financial support.

Appendix. Supplementary data

Proposed reaction mechanisms of trifluoroacetic acid (TFA) with the polymers on MNP surface. FTIR and ^{1}H NMR spectra of 2-bromo-2-methyl-*N*-(3-(triethoxysilyl) propanamide (BTPAm)) and *N*-(2-aminoethyl) folic acid (EDA-FA). ^{1}H NMR spectrum of poly(t-BA), TEM images showing some nano-aggregation. Examples of calculation of grafting density. TGA thermogram of folic acid.

Appendix. Supplementary data

Supplementary data associated with this article can be found in the online version, at doi:10.1016/j.polymer.2010.12.059.

References

[1] Pei W, Kumadaa H, Natusmea T, Saitoa H, Ishio S. J Magn Magn Mater 2007;310:2375–7.
[2] Sun S, Murray CB, Weller D, Folks L, Moser A. Science 2000;287:1989–92.
[3] Teng X, Yang H. J Am Chem Soc 2003;125:14559–63.
[4] Casula MF, Floris P, Innocenti C, Lascialfari A, Marinone M, Corti M, et al. Chem Mater 2010;22:1739–48.
[5] Anders S, Sun S, Murray CB, Rettner CT, Best ME, Thomson T, et al. Microelectron Eng 2002;61-62:569–75.
[6] Woo K, Hong J, Choi S, Lee HW, Ahn JP, Kim CS, et al. Chem Mater 2004;16:2814–8.
[7] Zhang J, Misra RDK. Acta Biomater 2007;3:838–50.
[8] Laurent S, Forge D, Port M, Roch A, Robic C, Elst LV, et al. Chem Rev 2008;108:2064–110.
[9] Veiseh O, Gunn JW, Zhang M. Adv Drug Deliv Rev 2010;62:284–304.
[10] Sahoo Y, Goodarzi A, Swihart MT, Ohulchanskyy TY, Kaur N, Furlani EP. J Phys Chem 2005;109:3879–85.
[11] Hayashi K, Ono K, Suzuki H, Sawada M, Moriya M, Sakamoto W, et al. Chem Mater 2010;22:3768–72.
[12] Feng PB, Gao F, Gu HC. J Colloid Interface Sci 2005;284:1–6.
[13] Liu X, Xing J, Guan Y, Shan G, Liu H. Colloids Surf A Physicochem Eng 2004;238:127–31.
[14] Mornet S, Vekris A, Bonnet J, Duguet E, Grasset F, Choy JH, et al. Mater Lett 2000;42:183–8.
[15] Cheng G, Zhao J, Tu Y, He P, Fang Y. Anal Chem Acta 2005;533:11–6.
[16] Lellouche J, Senthil G, Joseph A, Buzhansky L, Bruce I, Bauminger ER, et al. J Am Chem Soc 2005;127:11998–2006.
[17] Corr SA, Rakovich YP, Gun'ko YK. Nanoscale Res Lett 2008;3:87–104.
[18] Zhang Y, Kohler N, Zhang M. Biomaterials 2002;23:1553–61.
[19] Sonvico F, Mornet S, Vasseur S, Dubernet C, Jaillard D, Degrouard J, et al. Bioconjug Chem 2005;16:1181–8.
[20] Zhoua Y, Wang S, Ding B, Yang Z. Chem Eng J 2008;138:578–85.
[21] Fischer H. Chem Rev 2001;101:3581–610.
[22] Pyun J, Jia S, Kowalewski T, Patterson GD, Matyjaszewski K. Macromolecules 2003;36:5094–104.
[23] Hu B, Fuchs A, Huseyin S, Gordaninejad F, Evrensel C. Polymer 2006;47:7653–63.
[24] Zhao H, Shipp DA. Chem Mater 2003;15:2693–5.
[25] Liu G, Yan X, Lu Z, Curda SA, Lal J. Chem Mater 2005;17:4985–91.
[26] Sun Y, Ding X, Zheng Z, Cheng X, Hu X, Peng Y. Euro Polym J 2007;43:762–72.
[27] Hermann High LR, Holder SJ, Penfold HV. Macromolecules 2007;40:7157–65.
[28] Shipp DA, Wang JL, Matyjaszewski K. Macromolecules 1998;31:8005–8.
[29] Xia J, Gaynor SG, Matyjaszewski K. Macromolecules 1998;31:5958–9.
[30] Teodorescu M, Matyjaszewski K. Macromolecules 1999;32:4826–31.
[31] Raghuraman GK, Rühe J, Dhamodharan R. Nanopart Res 2008;10:415–27.
[32] Czaun M, Hevesi L, Takafuji M, Ihara H. Chem Commun; 2008:2124–6.
[33] Marutanil E, Yamamoto S, Ninjbadgar T, Tsujii Y, Fukuda T, Takano M. Polymer 2004;45:2231–5.
[34] Zhou Y, Wang S, Ding B, Yang Z. Chem Eng J 2007;40:6217–23.
[35] Fan QL, Neoh KG, Kang ET, Shuter B, Wang SC. Biomaterials 2007;28:5426–36.
[36] Frimpong RA, Hilt JZ. Nanotechnology 2008;19:1–7.
[37] Si S, Kotal A, Mandal TK, Giri S, Nakamura H, Kohara T. Chem Mater 2004;16:3489–96.
[38] Zhang M, Breiner T, Mori H, Muller AHE. Polymer 2003;44:1449–58.
[39] Wan S, Zheng Y, Liu Y, Yan H, Liu KJ. Mater Chem 2005;15:3424–30.
[40] Sauzedde F, Elaïssari A, Pichot C. Colloid Polym Sci 1999;277:846–55.
[41] Ng V, Lee YV, Chen BT, Adeyeye AO. Nanotechnology 2002;13:554–8.
[42] Hayashi K, Moriya M, Sakamoto W, Yogo T. Chem Mater 2009;21:1318–25.
[43] Kohler N, Fryxell GE, Zhang M. J Am Chem Soc 2004;126:7206–11.
[44] Landmark KJ, DiMaggio S, Ward J, Kelly C, Vogt S, Hong S, et al. ACS Nano 2008;2:773–83.
[45] Pinna N, Grancharov S, Beato P, Bonville P, Antonietti M, Niederberger M. Chem Mater 2005;17:3044–9.
[46] Mohapatra S, Mallick SK, Maiti TK, Ghosh SK, Pramanik P. Nanotechnology 2007;18:385102.
[47] Park EK, Lee SB, Lee YM. Biomaterials 2005;26:1053–61.
[48] Rutnakornpituk M, Meerod S, Boontha B, Wichai U. Polymer 2009;50:3508–15.
[49] Tao K, Dou H, Sun K. Chem Mater 2006;18:5273–8.

J Nanopart Res (2012) 14:953
DOI 10.1007/s11051-012-0953-y

RESEARCH PAPER

Magnetite nanoparticle coated with amphiphilic bilayer surfactant of polysiloxane and poly(poly(ethylene glycol) methacrylate)

Bandit Thong-On · Boonjira Rutnakornpituk · Uthai Wichai · Metha Rutnakornpituk

Received: 3 October 2011 / Accepted: 25 May 2012

Abstract We are here reporting the surface modification of magnetite nanoparticle (MNP) with amphiphilic steric stabilizer of polydimethylsiloxane (PDMS) and poly(poly(ethylene glycol) methacrylate) (PPEGMA). The main purpose of this work is to obtain the polymeric bilayer surfactant of hydrophobic PDMS inner shell and hydrophilic PPEGMA brush corona on MNP core. Functionalized PDMS was first synthesized and then covalently grafted on the functionalized MNP surface. The PDMS-coated MNP served as a reactive macroinitiator for atom transfer radical polymerization (ATRP) of PPEGMA. Kinetics studies indicated the constant consumption of PEGMA during first 7 h of the ATRP. Transmission electron microscopy showed the average particle size of 7 nm in diameter. Fourier transform infrared spectrophotometry, thermogravimetric analysis, and vibrating sample magnetometry indicated the increase of the percentage of the copolymer in the complex when the ATRP was prolonged. The decrease in its hydrodynamic size from 446 to 162 nm when the ATRP was extended indicated the improvement in its dispersibility in water. In addition, it was found that percent entrapment efficiency and loading efficiency of indomethacin model drug in the PPEGMA-coated MNP was 62 and 27 %, respectively.

Keywords Magnetite · Bilayer · ATRP

Introduction

During these recent years, magnetite nanoparticle (MNP) (Fe_3O_4) has widely been of scientific and technological interest because of its magnetically guidable and nanoscale-related properties. The broad applications of MNP include magnetic resonance imaging (MRI) enhancement (Lee et al. 2009; Park et al. 2003; Pei et al. 2007; Hong et al. 2008; Jaffer et al. 2006), drug delivery (Jain et al. 2009; Meerod et al. 2008; Rutnakornpituk et al. 2009), magnetic separation and diagnosis of biological molecules such as DNA and antibodies (Pich et al. 2004; Öisjöen et al. 2009; Brestovac et al. 2005). MNP is usually stabilized either by charge repulsion of electrical surface or steric repulsion of long-chain polymeric surfactants (Chorny et al. 2010; Storm et al. 2002; Zhang and Zhang 2005) grafted on their surfaces to prevent particle aggregation. Several methods have been investigated to prepare polymer-coated MNP, such as physical adsorption of polymers on the particle surfaces, emulsion polymerization in the presence of nanoparticles and the so-called "grafting to" and

Electronic supplementary material The online version of this article (doi:10.1007/s11051-012-0953-y) contains supplementary material, which is available to authorized users.

B. Thong-On · B. Rutnakornpituk · U. Wichai · M. Rutnakornpituk (✉)
Department of Chemistry and Center of Excellence for Innovation in Chemistry, Faculty of Science, Naresuan University, Phitsanulok 65000, Thailand
e-mail: methar@nu.ac.th

Published online: 12 June 2012

"grafting from" strategies (Fan et al. 2007; Galeotti et al. 2011; Kralj et al. 2010; Cao et al. 2009).

Many attempts have recently been made on preparing core/shell MNP that possessed polymer-coated surfaces. Atom transfer radical polymerization (ATRP) has been successfully applied to surface-initiated grafting polymerization in order to prepare a dense polymeric layer with controlled structure on the surface of MNP (Galeotti et al. 2011; Rutnakornpituk et al. 2011; Neugebauer 2007; Sun et al. 2007). ATRP is one of a controlled radical polymerization method that has widely applied for (co)polymerization of homo- and block (co)polymers because it allows for a good control in the molecular weight and polydispersity of the (co)polymers. ATRP has been used for polymerizations of a wide range of functional monomers such as styrene (Brown and Price 2001; Yi et al. 2007; Reining et al. 2002; Qiang et al. 2006), (meth)acrylates (Semsarzadeh et al. 2003; Yin et al. 2005; Wootthikanokkhan et al. 2001), and (meth)acrylamides (Monge and Haddleton 2004; Jiang et al. 2008). It was found that reasonable $\overline{M_n}$ and narrow polydispersity index (PDI) of the polymers were obtained.

The primary aim of this work was to coat MNP surface with amphiphilic surfactant of PPEGMA and PDMS to obtain the particles with bilayer surface of hydrophobic PDMS inner shell and hydrophilic PPEGMA corona. Precedents have reported the stabilization of MNP with a variety of amphiphilic copolymers, such as poly(ethylene oxide) (PEO)–poly(propylene oxide) (PPO) copolymer (Jain et al. 2009), poly(ethylene glycol) methyl ether (mPEG)–poly(ε-caprolactone) (PCL) copolymer (Meerod et al. 2008; Rutnakornpituk et al. 2009), polyurethane (PU)–PEO copolymer (Harris et al. 2003), and PDMS–poly(lactide) (PLA) copolymer (Ragheb and Riffle 2008), to obtain stable MNP dispersions in water. Physical adsorption (Jain et al. 2009; Meerod et al. 2008; Rutnakornpituk et al. 2009) or ionic interactions (Harris et al. 2003; Ragheb and Riffle 2008) of one block of the copolymers to MNP surface was mostly proposed for the particle stabilization mechanism. Because of their weak interactions, dissolution of the copolymers from MNP surface when used for a long period of time was concerned. The advantage of our present work is that the PDMS hydrophobic block was covalently bound onto the MNP surface, which might diminish the stabilization limitation for long-term applications. In addition, the hydrophobic PDMS inner layer can be used as a reservoir for entrapment of hydrophobic compounds, while the hydrophilic PPEGMA provides steric repulsion and water dispersibility to the particles.

In this report, PDMS was first synthesized via an acid-catalyzed ring-opening copolymerization of D_4 and D_4H, followed by ATRP of PPEGMA brush from the polysiloxane macroinitiator. Kinetic studies of the ATRP of PEGMA from the PDMS macrointiator were investigated via nuclear magnetic resonance spectroscopy (^{1}H NMR). TEM was conducted to determine the particle size and its distribution and photocorrelation spectroscopy (PCS) was performed to determine hydrodynamic size of the copolymer–MNP complex. Magnetic properties of the complex were investigated via VSM. The percentages of the composition in the copolymer–MNP complex were also determined via thermogravimetric analysis (TGA). In addition, the preliminary studies on the entrapment and loading efficiencies of indomethacin as a model drug in this complex are also reported.

Experimental

Materials

Unless otherwise stated, all reagents were used without further purification: iron(III) acetylacetonate ($Fe(acac)_3$), 99.9 % (Acros), benzyl alcohol, 98 % (Unilab), oleic acid (Fluka), CuBr, 99.999 % (Aldrich), triethylamine, 97 % (Carto Erba), 3-aminopropyl triethoxysilane, 99 % (Acros), 2-bromoisobutyryl bromide (BIBB), 98 % (Acros) and allyl glycidyl ether, 99 % (Acros). D_4, 99 % (Fluka) and D_4H, 95 % (Fluka) were stirred in CaH_2 and distilled prior to use. 1,1,3,3-Tetramethyldisiloxane, 97 % (Acros) and allyl alcohol, 99C % (Acros) were fractionally distilled and stored under N_2 until used. Poly(ethylene glycol) methacrylate (PEGMA) (Aldrich) with average $\overline{M_n}$ of 300 g mol^{-1} was purified by passing through basic and neutral alumina, respectively, and stored at −4 °C after purification. Me_6Tren was prepared according to the previously reported procedure and the details of the syntheses have been provided in the Supporting information. *N,N*-Dimethyl formamide (Acros), toluene (Acros), and $CDCl_3$ (Euriso-Top) were used as received.

Syntheses

Synthesis of PDMS via acid-catalyzed ring-opening polymerization

Synthesis of 3-dihydroxypropyl tetramethyl disiloxane (disiloxane diol) as an endcapper Allyl alcohol (4.2 ml, 0.06 mol), toluene (15 ml), and platinum (0)-1,3-divinyl-1,1,3,3-tetramethyldisiloxane complex (0.046 ml, 0.5 %v/v) were charged into a reaction flask with consistently stirring at 50 °C. 1,1,3,3-Tetramethyldisiloxane (5 ml, 0.025 mol) was then slowly introduced into the reaction flask via a dropping funnel. The reaction temperature was set at 65 °C for 4 h. After the reaction was complete, an excess of allyl alcohol was removed from the mixture under reduced pressure at 65 °C for at least 3 h.

Synthesis of hydroxyl-terminated polydimethylsiloxane (PDMS-OH) PDMS-OH was prepared through an equilibrium acid-catalyzed ring-opening copolymerization of D_4 and D_4H. 1:1 Molar ratio of D_4 to D_4H (D_4, 1 g, 3.4 mol and D_4H, 0.81 g, 3.4 mol) was used in the reaction with the use of the disiloxane diol (0.19 g, 0.722 mol) end capping agent. After the reaction temperature was raised to 50 °C, trifluoromethane sulfonic acid (triflic acid) (0.001 ml, 0.65 %v/v) was slowly added into the solution via a syringe. The reaction was equilibrated at 55 °C for 48 h. The acidic mixture was cooled to room temperature, dissolved in diethyl ether, and neutralized by extraction with water. The mixture was dried over sufficient anhydrous magnesium sulfate with continuously stirring for 30 min and subsequently filtered through a filter paper. Diethyl ether was evaporated via a rotary evaporator and monomers remaining from the equilibration were removed under reduced pressure at 60 °C overnight.

Synthesis of allyl-grafted MNP

APS (2.734 ml, 0.012 mol) was slowly introduced into a mixture of sulfamic acid (SA) (0.1 g, 1.03 mmol) and allyl glycidyl ether (1.175 g, 0.010 mol) under nitrogen atmosphere. The reaction was set at room temperature for 12 h with stirring. After reaction was complete, SA was removed by filtration and the product was washed with diethyl ether (3 × 10 ml) and evaporated until dryness. The as-synthesized allyl-containing silane compound (0.1 ml) and 2 M TEA in toluene (1 ml) were added into the dispersion of oleic acid-coated MNP (0.1 g oleic acid-coated MNP in 5 ml toluene) and the details of the synthesis of oleic acid-coated MNP have been provided in the Supporting information. The mixture was stirred at room temperature for 24 h under nitrogen blanket. The particles were precipitated in ethanol, following by external magnet separation to obtain the allyl-grafted MNP. Then, the MNP were re-dispersed in toluene and re-precipitated in ethanol. This procedure was repeated three times to remove unreacted species from the particles.

Immobilization of the PDMS onto surface of the allyl-grafted MNP and ATRP of PPEGMA from the particle surface

The PDMS-OH (1 g, 0.476 mol) was slowly introduced into the reaction mixture of the allyl-grafted MNP dispersion (0.1 g of the MNP in 10 ml toluene) and Pt catalyst (Platinum (0)-1,3-divinyl-1,1,3,3-tetramethyldisiloxane complex). The reaction temperature was set at 70 °C for 6 h. After the reaction was complete, the precipitants were removed from the dispersion using an external magnet and washed with ethanol and toluene, respectively. BIBB (0.15 ml, 0.05 mol) was slowly introduced into the reaction mixture of the PDMS-OH-coated MNP dispersion (0.1 g of the PDMS-coated MNP in 10 ml toluene) and 2 M TEA in toluene (0.25 ml) at 0 °C under nitrogen atmosphere. A white precipitate was formed upon the addition. The reaction temperature was set at room temperature for 24 h with stirring. After the reaction was complete, the precipitants of PDMS-Br-coated MNP were removed from the dispersion using an external magnet and washed with ethanol and toluene, respectively.

The mixture of the PDMS-Br-coated MNP (0.1 g) and PEGMA (3 ml, 0.01 mol) dispersed in toluene (2 ml, 60 % w/v) was sonicated for 1 h and purged with nitrogen gas for 15 min. After the addition of CuBr (0.014 g, 0.1 mol), Me6-Tren (0.025 ml, 0.1 mol) and dialkyl bromide disiloxane (0.055 ml, 0.1 mol) as a sacrificial initiator (the synthesis has been provided in the Supporting information), ATRP reaction was carried out at room temperature for 24 h with nitrogen gas purging and magnetically stirring. After the polymerization, the particles were precipitated in ethanol and the aggregate was repeatedly

washed with ethanol to remove unreacted PEGMA, CuBr, and the ligand. The as-synthesized PPEGMA-coated MNP was finally dried under reduced pressure.

Characterization

^{1}H NMR spectra were performed on a 400 MHz Bruker NMR spectrometer using $CDCl_3$ as a solvent. FTIR was performed on a Perkin-Elmer Model 1600 Series FTIR Spectrophotometer in the wavenumber range of 4,000–400 cm^{-1}. Liquid samples were directly cast onto potassium chloride plates. Solid samples were made by the pressed disk method after mixing dried solid samples with KBr. TEM was performed on Philips Tecnai 12, operated at 120 kV equipped with Gatan model 782 CCD camera. The sample solution in water or toluene was directly cast onto carbon-coated copper grids and let to slowly evaporate at room temperature. Magnetic properties of the particles were measured at room temperature using a Standard 7403 Series, Lakeshore vibrating sample magnetometer (VSM). Magnetic moment of each sample was investigated over a range of ±10,000 G of applied magnetic fields using 30-min sweep time. TGA was performed on SDTA 851 Mettler-Toledo at the temperature ranging between 25 and 600 °C at a heating rate of 20 °C/min under oxygen atmosphere. Hydrodynamic size of the particles was measured by PCS using NanoZS4700 nanoseries Malvern instrument. DI water used as a dispersing media was filtered through 0.22-μm nylon syringe filters before used. The aqueous dispersions of the particles were sonicated for 10 min before the measurement without filtration.

Investigation of entrapping and loading efficiencies of indomethacin in PPEGMA-coated MNP

To incorporate indomethacin, the model drug, to the particles, the drug solution (2 ml, 25 mg/ml in THF) was added dropwise with stirring to an aqueous dispersion of PPEGMA-coated MNP (5 ml). The mixture was stirred for 30 min to remove THF and to allow fully partitioning the drug into the hydrophobic shell of the particles. Drug-loaded magnetite was then separated using an external magnet. The concentration of the excess drug in the supernatant was determined using UV–Visible spectrophotometer. The amount of the entrapped drug in the particles was determined from the difference of the weights of the loaded drug and the excess of the drug remaining dispersible in the solution. The details of the calculation are provided in the Supporting information. Entrapment efficiency and drug loading efficiency (DLE) were determined as followed:

$$\text{Entrapment efficiency } (\%\text{EE}) = \frac{\text{Weight of the entrapped drug in the particles}}{\text{Weight of loaded drug}} \times 100$$

$$\text{Drug loading efficiency } (\%\text{DLE}) = \frac{\text{Weight of the entrapped drug in the particles}}{\text{Weight of the particles}} \times 100$$

Results and discussion

The primary aim of this work was to coat MNP with a novel amphiphilic surfactant to obtain bilayer surface of hydrophobic PDMS inner shell and hydrophilic PPEGMA corona. It was envisioned that the hydrophobic PDMS inner layer can be used as a reservoir for entrapment of hydrophobic entities and the hydrophilic PPEGMA brush provided steric repulsion and water dispersibility to the particles. Polysiloxane was first synthesized via an acid-catalyzed ring-opening copolymerization of D_4 and D_4H to obtain the Si–H-containing PDMS. This reaction was designed such that the PDMS can be covalently grafted onto the MNP surface through hydrosilylation. The PDMS-coated MNP can be then used as a macroinitiator for ATRP of PPEGMA to form water dispersible particles with double-layer surface.

Synthesis of difunctionalized PDMS via an acid-catalyzed ring-opening polymerization

Synthesis of dihydroxypropyl tetramethyl disiloxane (disiloxane diol)

Disiloxane diol was synthesized through a hydrosilylation between 1,1,3,3-tetramethylsiloxane and allyl alcohol to obtain the hydroxyl-terminated endcapper. ^{1}H NMR indicated the formation of the linkages corresponding to the coupling reaction of Si–H bond to allyl alcohol: methylene protons (–CH_2–) of propyl

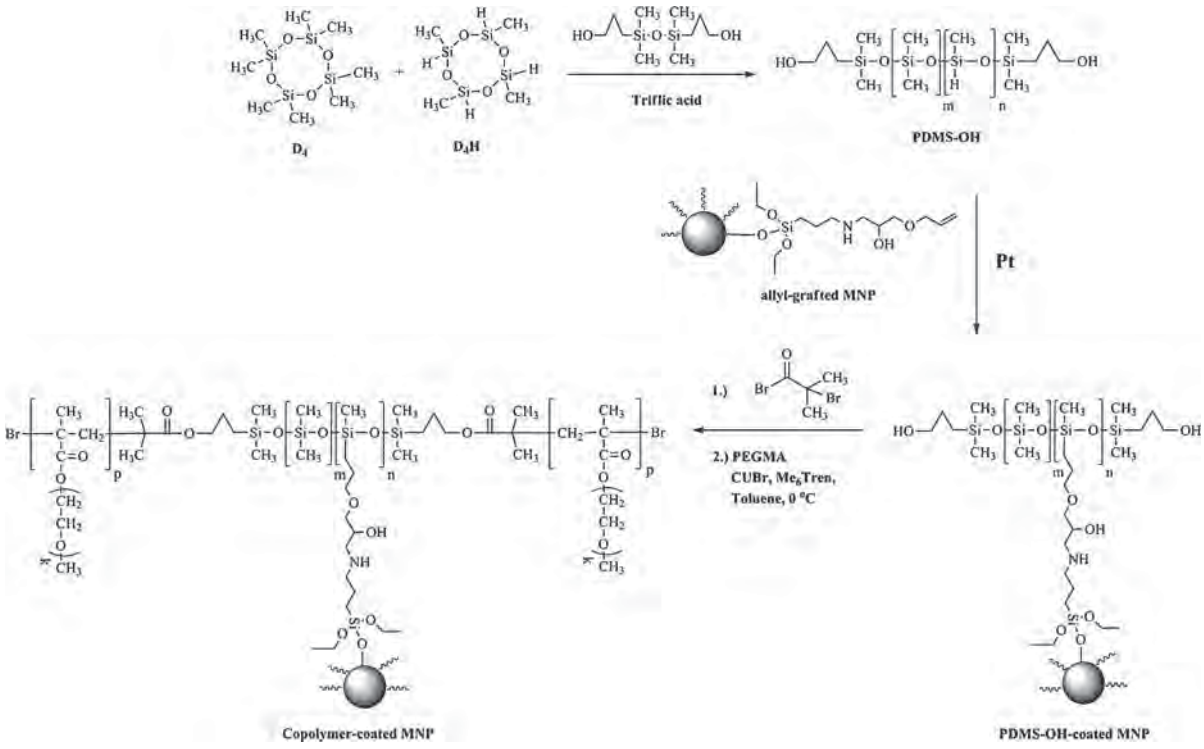

Fig. 1 Surface modification of MNP with amphiphilic steric surfactant of PDMS and PPEGMA

alcohol at 0.5, 1.5, and 3.6 ppm. In addition, the disappearance of Si–H signal (4.7 ppm) signified the formation of the disiloxane diol. The resultant product appeared as transparent oil (70.5 % yield). The FTIR and ^{1}H NMR spectra of the product have been provided in the Supporting information. ^{1}H NMR (400 MHz, $CDCl_3$) δ_H: 0.05 [m, 12H, Si–C*H*$_3$], 0.50 [m, 4H, Si–C*H*$_2$], 1.60 [m, 4H, CH$_2$–C*H*$_2$–CH$_2$], 2.00 [s, 1H, CH$_2$–O*H*], 3.60 [m, 4H, CH$_2$–C*H*$_2$–OH]. FTIR (thin film) υ_{max}: 3369 cm^{-1} (O–H stretching), 2958 cm^{-1} (C–H stretching), 1411 cm^{-1} (CH$_2$ stretching), 1260 cm^{-1} (Si-CH$_3$ stretching), 1078 cm^{-1} (Si–O stretching), and 800 cm^{-1} (Si–C stretching) (Fig. 1).

Synthesis of hydroxyl-terminated polydimethylsiloxane (PDMS-OH)

PDMS-OH was synthesized via a ring-opening polymerization of D_4/D_4H mixture. 1:1 Molar ratio of D_4 to D_4H was used in this reaction in order to introduce Si–H linkages in the polysiloxane chain for further functionalization. The signal at 4.7 ppm corresponding to the hydrogen on Si (Si–*H*) indicated the presence of Si–H thoroughly dispersed in the polysiloxane chain. The ^{1}H NMR spectra of the product have been provided in the Supporting information. In good agreement with ^{1}H NMR, FTIR spectrum manifested the presence of Si–H bond (2,160 cm^{-1}), Si–O bond (1,038 cm^{-1}), and Si–CH$_3$ bond (1,261 cm^{-1}) of the PDMS-OH (Fig. 2A). The 2,500 g/mol-targeted $\overline{M_n}$ of the PDMS-OH were controlled by adjusting the molar ratio of the cyclic monomers to the disiloxane diol endcapper. The methyl protons on Si (Si–C*H*$_3$, 0.06 ppm) relative to the methylene protons at the chain terminals (Si–CH$_2$CH$_2$C*H*$_2$OH, 3.60 ppm) were used to calculate its $\overline{M_n}$ using an endgroup analysis method via ^{1}H NMR. The $\overline{M_n}$ of the as-synthesized PDMS-OH was approximately 2,254 g/mol ($m = 19$, $n = 14$).

Synthesis of allyl-grafted MNP

To prepare allyl-grafted MNP, allyl-containing silane was first synthesized. It was prepared through a ring-opening reaction of epoxide ring of allyl glycidyl ether with an amino group of aminopropyl triethoxysilane to obtain allyl-containing silane compound. The

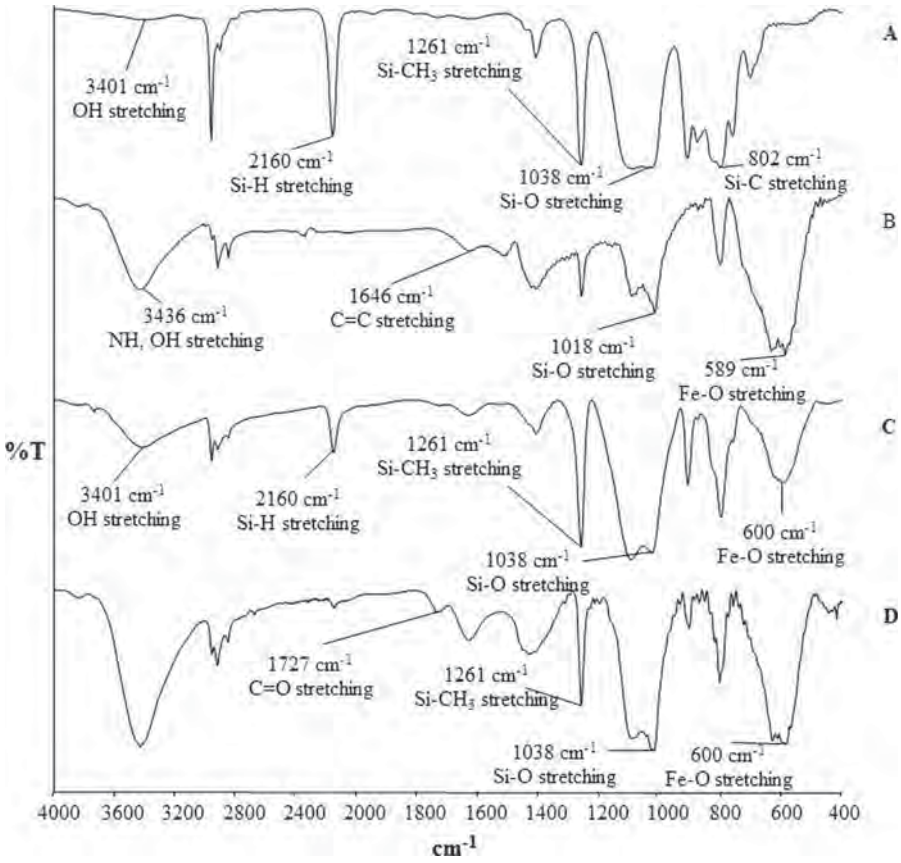

Fig. 2 FTIR spectra of (*A*) PDMS-OH, (*B*) allyl-grafted MNP, (*C*) PDMS-OH-coated MNP, and (*D*) PDMS-Br-coated MNP

resultant product appeared as yellowish oil (87 % yield). The ^{1}H NMR spectrum of the product is shown in the Supporting information. In combination with the disappearance of the signals of the epoxide ring, the presence of the signals at 5.3–5.8 ppm (allyl protons), 1.2, and 3.8 ppm (ethoxy protons) indicated the formation of allyl-containing silane product. In addition, the C=C signal of allyl functional groups (1,647 cm^{-1}) in the resultant product was apparent in FTIR spectrum. FTIR: 3412 cm^{-1} (NH, O–H stretching), 2927 cm^{-1} (C–H stretching), 1647 cm^{-1} (C=C stretching), 1490 cm^{-1} (CH_2 stretching), 1103 cm^{-1} (C–O–C, Si–O stretching), and 800 cm^{-1} (Si–C stretching). ^{1}H NMR (400 MHz, $CDCl_3$) δ_H: 0.50 [m, 2H, CH_2–CH_2–Si], 1.15 [t, 9H, O–CH_2–CH_3], 1.50 [m, 2H, CH_2–CH_2–CH_2], 2.50 [m, 4H, CH_2–NH–CH_2], 3.40 [m, 2H, –O–CH_2–(CH–OH)–], 3.75 [m, 1H, CH_2–(C*H*–OH)–CH_2, 2H, O–CH_2–CH_3], 4.00 [d, 2H, –CH_2–O–CH_2–], 5.20 [m, 1H, CH_2=C*H*–CH_2–] and 6.80 [m, 2H, CH_2=CH–CH_2–]. FTIR (thin film) υ_{max}: 3412 cm^{-1} (N–H, O–H stretching), 2927 cm^{-1} (C–H stretching), 1647 cm^{-1} (C=C stretching), 1490 cm^{-1} (CH_2 stretching), 1103 cm^{-1} (C–O–C, Si–O stretching), and 800 cm^{-1} (Si–C stretching).

The allyl-containing silane compound was then covalently bonded onto the oleic acid-coated MNP through the combination of ligand exchange reaction and condensation of triethoxysilane to obtain allyl-grafted MNP resultant product. FTIR exhibited characteristic absorption signals of the allyl-grafted MNP: 3436 cm^{-1} (N–H, O–H stretching), 1018 cm^{-1} (Si–O stretching), and 800 cm^{-1} (Si–C– stretching) (Fig. 2B). In combination with a strong and broad signal of Fe–O bonds (634 cm^{-1}), this evidenced that allyl-containing silane compound was immobilized onto the MNP surface.

Immobilization of the PDMS onto surface of the allyl-grafted MNP and ATRP of PPEGMA from the particle surface

To immobilize PDMS onto the surface of MNP, hydrosilylation between Si–H of the as-synthesized PDMS-OH and C=C of the allyl-grafted MNP was

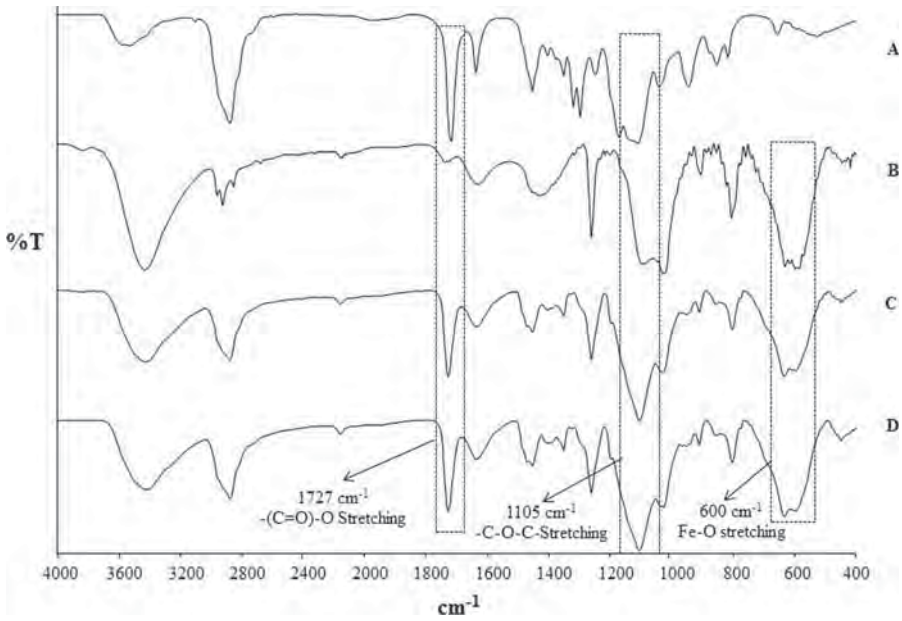

Fig. 3 FTIR spectra of (*A*) PEGMA oligomer, PPEGMA-coated MNP after (*B*) 0 h, (*C*) 6 h, and (*D*) 24 h of ATRP

accomplished to obtain PDMS-coated MNP. FTIR spectrum of the PDMS-OH-coated MNP exhibited characteristic absorption signals of both PDMS-OH and MNP core: 3401 cm^{-1} (O–H stretching), 1261 cm^{-1} (Si–CH_3 stretching), 1038 cm^{-1} (Si–O stretching), and 600 cm^{-1} (Fe–O) (Fig. 2C). After the hydrosilylation, the decrease of the signal intensity of Si–H (2,160 cm^{-1}) relative to that of Si–CH_3 (1,261 cm^{-1}) indicated the depletion of Si–H linkages in the PDMS. The presence of the Si–H signal in ^1H NMR signified the remaining of unreacted Si–H bonds after the reaction. Even though there was some Si–H trace in the PDMS, the as-synthesized PDMS-OH-coated MNP exhibited an improvement in its dispersibility in toluene when compared to the MNP without PDMS coating. TGA and VSM techniques also showed supportive results to FTIR that PDMS was bound to the MNP complexes and they have been discussed in details in the later sections.

BIBB, an active ATRP initiator, was then immobilized on the surface of PDMS-OH-coated MNP to obtain PDMS-Br-coated MNP. After the reaction, alkyl bromide groups, functioning as active ATRP initiators for PPEGMA, should present on the MNP surface. FTIR exhibited characteristic absorption signals of the PDMS-Br-coated MNP: 1727 cm^{-1} (O–(C=O) carbonyl stretching), 1261 cm^{-1} (Si–CH_3 stretching), 1038 cm^{-1} (Si–O stretching), and 600 cm^{-1} (Fe–O) (Fig. 2D). The disappearance of Br–C=O (1,767–1,807 cm^{-1}) of BIBB and the presence of –OC=O (1,727 cm^{-1}) of the resultant product indicated the occurrence of the coupling reaction.

ATRP reactions of PPEGMA from the PDMS-Br-coated MNP surface were set for 24 h at room temperature. The samples were withdrawn from the reaction mixture after 1, 6, and 24 h of the reaction, ultracentrifuged to precipitate the particles, thoroughly washed with ethanol, dried in vacuo and characterized via FTIR. Figure 3 shows FTIR spectra of PEGMA oligomer and PPEGMA-coated MNP after 0, 6, and 24 h of ATRP. A progressive growth of −O(C=O)– stretching signals (1,727 cm^{-1}) and C–O–C stretching signals (1,105 cm^{-1}) of PPEGMA repeating units indicated that $\overline{M_n}$ of PPEGMA on MNP surfaces increased as increasing ATRP reaction time. In addition, Fe–O bond signals at 600 cm^{-1} were also observed throughout the reaction.

In the ATRP reaction, the as-synthesized dialkyl bromide disiloxane was also added into the reaction mixture as a sacrificial initiator. After ultracentrifugation of the dispersion to precipitate the particle, the supernatant containing free PPEGMA brush initiated from the sacrificial initiator was analyzed via ^1H NMR to monitor the reaction progress using DMF as an internal standard. Due to the structural similarity between alkyl bromide grafted on the particle surface and the sacrificial initiator, it was assumed that the reaction reactivities of these two initiator systems were similar.

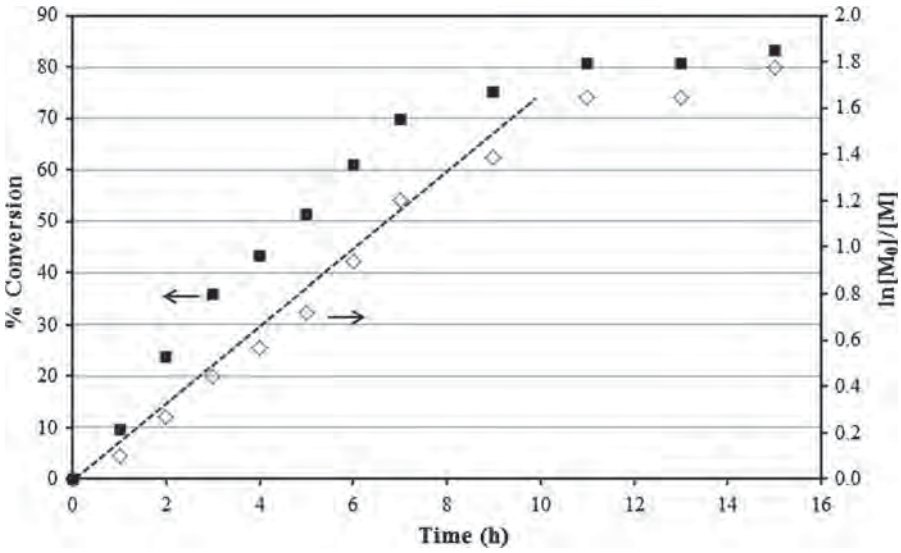

Fig. 4 Conversion versus time plot and first-order kinetic plot of ATRP of PPEGMA

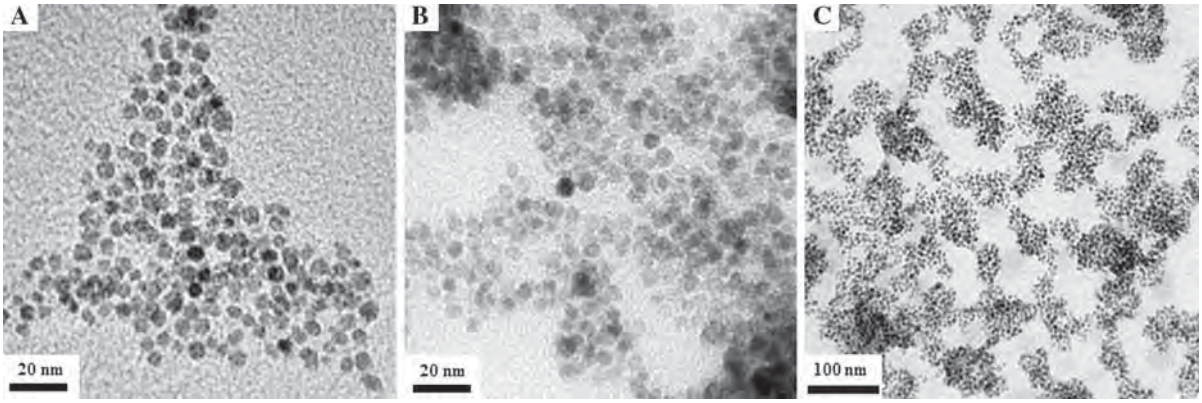

Fig. 5 TEM images of **a** PDMS-OH-coated MNP prepared from toluene dispersion; **b**, **c** PPEGMA-coated MNP after 24 h of ATRP prepared from aqueous dispersion at different magnifications

The monomer conversion versus time plot of the ATRP of PPEGMA shows that the reaction rate was constant during first 7 h of the reaction and it was slowed down when the reaction was prolonged (Fig. 4). In good agreement with this, the first-order plot reveals a linear relationship during the course of first 7 h of the reaction, indicating the constant consumption rate of the monomer at initial state of the reaction. After 7 h of the reaction, the rate of the reaction started to deviate from linearity at high percent monomer conversion. This was probably due the premature termination of active radicals during the polymerization due to the depletion of PEGMA concentration.

According to the TEM measurements, the particles show narrow size distribution with the size ranging between 4 and 9 nm and the average of 7 nm in diameter (Fig. 5). Figure 5b, c illustrates the particle distribution of the PPEGMA-coated MNP prepared from aqueous dispersions in comparison with that of the PDMS-OH-coated MNP prepared from toluene dispersion (Fig. 5a). Hydrophobic PDMS in the PDMS-OH-coated MNP promoted their good dispersibility in toluene, while hydrophilic PPEGMA in the PPEGMA-coated MNP rendered them well dispersible in water. It was also noticed that dispersibility of the PPEGMA-coated MNP in water was greatly improved when ATRP reaction time was prolonged

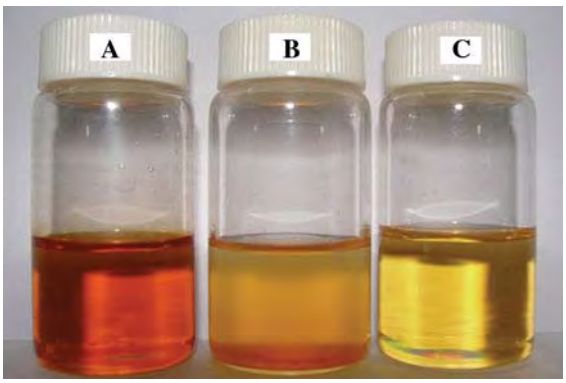

Fig. 6 Appearance of (*A*) PDMS-OH-coated MNP in toluene and PPEGMA-coated MNP dispersed in H_2O after (*B*) 6 h and (*C*) 24 h of ATRP

from 6 to 24 h as indicated by the more transparent yellowish dispersion in Fig. 6C (12 h) than that in Fig. 6B (6 h). This implied a better coating of hydrophilic PPEGMA on MNP surface. The slight difference in colors of the dispersions in Fig. 6A, C was probably due to the interaction of MNP complexes in different solvents (toluene and water), which might influence the appearance of the dispersion colors. One might wonder that the color change of these dispersions may arise from the phase transformation of magnetite during the ATRP step. Selected area electron diffraction (SAED) technique was thus performed to obtain the crystal structure information of the complexes from each step of the reactions (bare MNP, PDMS-coated MNP, and PPEGMA-coated MNP). Their SAED patterns revealed that the particles were crystalline and their *d* values were in good agreement with those observed in Fe_3O_4 (Moisescu et al. 2008; Prai-in et al. 2012), indicating that there was no major phase transformation of magnetite core in each step. The SAED patterns of each complex are shown in the Supporting information.

PCS was conducted to investigate the hydrodynamic diameters (D_H) of PDMS-OH-coated MNP dispersed in toluene and PPEGMA-coated MNP dispersed in water (Table 1). The hydrodynamic size of bare MNP in toluene was not measured because it was not well redispersible in the solvent, resulting in aggregation of the particles. In the particles stabilized with the polymers, the large D_H ranging between 162 and 446 nm was attributed to the size of their complexes with some nanoscale particle aggregation. This nanoaggregate was also apparent in the TEM experiments (Fig. 5c). It was also observed that D_H of the PPEGMA-coated MNP after 24 h of ATRP was significantly smaller than those of the other two complexes. This was devoted to the better coating of hydrophilic PPEGMA on the particle surface, resulting in the enhancement in water dispersibility and the decrease in D_H of the aggregate.

The rather large size of D_H (162 nm) even after ATRP (PPEGMA-coated MNP) was probably due to the limited accessibility of PEGMA to react with the pre-formed aggregated PDMS-coated MNP. Therefore, the stability of the particles in the solvents was concerned when dispersed for long period of time. Stability studies of PDMS-coated MNP (before ATRP) in toluene and PPEGMA-coated MNP (after ATRP) in water were performed. At a given time, the dispersions were centrifuged to remove large aggregate and the concentrations of MNP remaining dispersible in the media were measured via atomic absorption spectroscopy (AAS). It was found that, in both samples, percentages of the dispersible particles

Table 1 Hydrodynamic diameter (D_H), composition and magnetic properties of the MNP complexes

Type of complex	D_H (nm)[a]	% Char yield[b]	% in the complex[b]			emu/g of complex[c]	emu/g of Fe_3O_4[b,c]
			Fe_3O_4	PDMS	PPEGMA		
Bare MNP	–	88	100	–	–	44	44
PDMS-OH-coated MNP	446 ± 1	80	91	9	–	35	38
PPEGMA-coated MNP after 6 h of ATRP	295 ± 1	58	66	7	27	25	38
After 24 h of ATRP	162 ± 1	23	26	3	71	10	38

[a] Measured at room temperature via PCS technique

[b] Estimated from % char yield at 600 °C via TGA technique

[c] Estimated from M_s values at 10,000 G via VSM technique

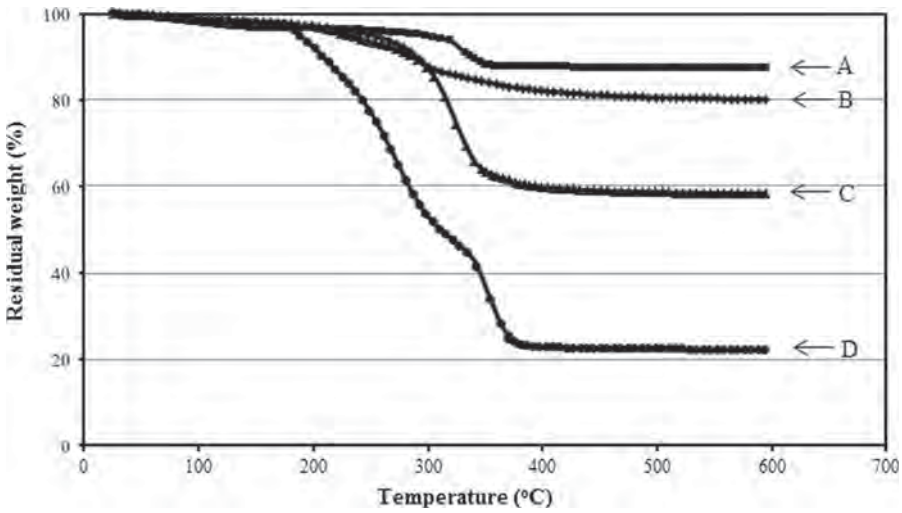

Fig. 7 TGA thermograms of (*A*) bare MNP, (*B*) PDMS-OH-coated MNP and PPEGMA-coated MNP after (*C*) 6 h and (*D*) 24 h of ATRP

in the solvents gradually decreased and there were about 30–50 % MNP remaining dispersible in the media after 5 weeks (the plot is shown in the Supporting information). One possible explanation is that the polymers might not be completely coated on the surface of the particles, which essentially influenced their stability in the dispersions. Improvement in dispersibility of PDMS-coated MNP in toluene should also enhance dispersibility and stability of PPEGMA-coated MNP in water. This can be achieved by optimization of the reaction conditions in the PDMS coating step of MNP such as the reaction temperature, solvent and catalyst, and this is warranted for a future study.

Figure 7 shows the TGA thermograms of bare MNP, PDMS-OH-coated MNP and PPEGMA-coated MNP after 6 and 12 h of ATRP. The samples from each step of the reactions exhibited distinctive TGA curves giving rise to the information of the amount of PDMS and PPEGMA in the complexes. The slight drop in the weight of bare MNP was attributable to the residual benzyl alcohol used as the solvent in the MNP preparation step. According to the TGA results, there were about 9 wt % PDMS in the PDMS-OH-coated MNP and 3–7 wt% PDMS in the PPEGMA-coated MNP (Table 1). The drop in the percentage of PDMS was attributed to the increase of PPEGMA component in the complexes. The PPEGMA-coated MNP showed the weight loss stage ranging between 200 and 380 °C (Fig. 7C, D), which was attributed to the decomposition of PPEGMA in the complexes. When the time periods of ATRP reaction were extended from 6 to 24 h, the percentage of PPEGMA increased from 27 to 71 % and the percentage of magnetite core decreased from 66 to 26 %, indicating the progressive increase of PPEGMA in the complexes. This was a supportive result to FTIR (Fig. 3) and PCS experiments (Table 1) that PPEGMA chain length on their surface was extended when ATRP reaction time was prolonged.

Hysteresis curves of bare MNP, PDMS-OH-coated MNP, PPEGMA-coated MNP after 6 h and 24 h of ATRP were illustrated in Fig. 8. They showed superparamagnetic behavior at room temperature as indicated by the absence of remanence and coercivity upon removing an external applied magnetic field. The saturation magnetization values (M_s) ranged between 10 and 44 emu/g complex (Table 1). As expected, the M_s values decreased as the percentage of magnetite core in the complexes, determined via TGA technique, decreased. When taking the percentage of magnetite in the complex into account, the M_s in emu/g magnetite basis of PDMS-OH-coated MNP slightly dropped from 44 to 38 emu/g magnetite. This was attributed to the use of high reaction temperature in the PDMS-coating step of MNP (hydrosilylation of PDMS-OH and allyl-grafted MNP), which might affect the magnetic properties of MNP core. Interestingly, magnetic properties of the PDMS-coated and PPEGMA-coated MNPs were not significantly different from each other, indicating that the ATRP grafting step of PPEGMA from MNP surface did not deteriorate magnetic properties of the complexes.

The studies on drug entrapping and loading efficiencies were performed to confirm the formation of bilayer surface of MNP with a hydrophobic inner shell. Indomethacin was selected as a hydrophobic

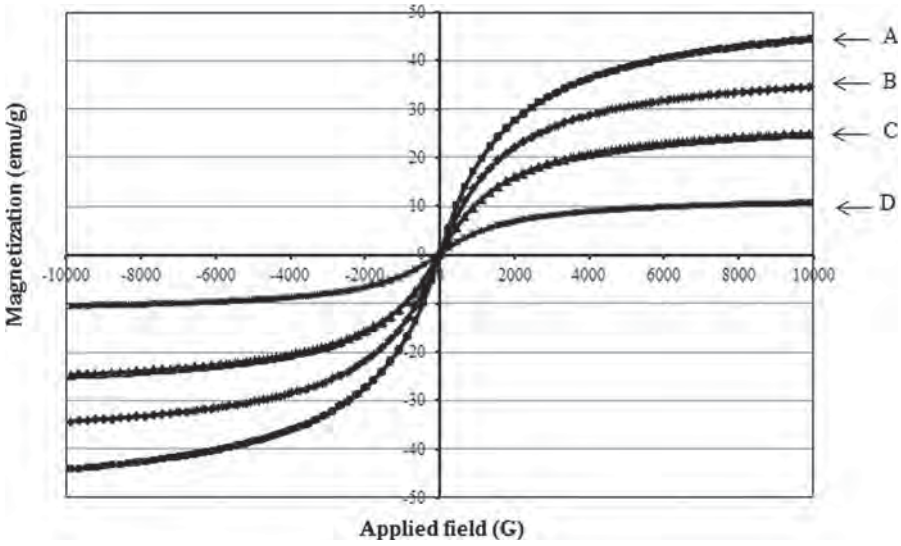

Fig. 8 Magnetization curves of (*A*) bare MNP, (*B*) PDMS-OH-coated MNP and PPEGMA-coated MNP after (*C*) 6 h and (*D*) 24 h of ATRP

model drug in this study because its concentration can be measured via UV–vis spectrophotometry. It was envisioned that indomethacin should somewhat partition into the hydrophobic PDMS layer on the particle surface. It was found that percent drug entrapment efficiency (%EE) of the complex was 62 % and drug loading efficiency (%DLE) was 27 % (an example of the calculation is illustrated in the Supporting information). This signified the formation of bilayer structure with hydrophobic PDMS inner shell on MNP surface.

Conclusions

Surface modification of MNP with PDMS–PPEGMA amphiphile via a "grafting from" strategy to obtain polymeric bilayer surfactant has been reported. The hydrophilic PPEGMA provided steric repulsion and water dispersibility to the particles, while hydrophobic PDMS inner layer might serve as a reservoir for entrapment of hydrophobic entities. PDMS was synthesized via acid-catalyzed ring-opening copolymerization of D_4 and D_4H. This reaction was designed such that the as-synthesized PDMS possessed Si–H bonds in the chain for further functionalization and subsequently coupling with MNP surface. After the immobilization of the PDMS on the MNP surface, it was then used as a macroinitiator for ATRP of PPEGMA. According to the kinetic studies, the propagating rate of PPEGMA was constant during first 7 h of the reaction. Increasing time periods of ATRP of PPEGMA further enhanced the percentage of the polymer in the complex, resulting in the enhancement in its dispersibility in water. These novel magnetic field-guidable complexes might be used as nanovehicles for loading hydrophobic entities, such as drugs, fluorophores and biomolecules, by partitioning to the hydrophobic inner shell on the particle surface.

Acknowledgments The authors thank the Thailand Research Fund (TRF) and Naresuan University (DBG5380001) for financial funding. The Center of Excellence for Innovation in Chemistry (PERCH-CIC), Commission on Higher Education, Ministry of Education is also gratefully acknowledged for financial support.

References

Brestovac B, Harnett GB, Smith DW, Frost F, Shellam GR (2005) Multiplex nested PCR (MNP) assay for the detection of 15 high risk genotypes of human papillomavirus. J Clin Virol 33:116–122

Brown DA, Price GJ (2001) Preparation and thermal properties of block copolymers of PDMS with styrene or methyl methacrylate using ATRP. Polymer 42:4767–4771

Cao H, He J, Deng L, Gao X (2009) Fabrication of cyclodextrin-functionalized superparamagnetic Fe_3O_4/amino-silane core–shell nanoparticles via layer-by-layer method. Appl Surf Sci 255:7974–7980

Chorny M, Hood E, Levy RJ, Muzykantov VR (2010) Endothelial delivery of antioxidant enzymes loaded into non-polymeric magnetic nanoparticles. J Controlled Release 146:144–151

Fan Q-L, Neoh K-G, Kang E-T, Shuter B, Wang S-C (2007) Solvent-free atom transfer radical polymerization for the preparation of poly(poly(ethyleneglycol) monomethacrylate)-grafted Fe_3O_4 nanoparticles: synthesis, characterization and cellular uptake. Biomaterials 28:5426–5436

Galeotti F, Bertini F, Scavia G, Bolognesi A (2011) A controlled approach to iron oxide nanoparticles functionalization for magnetic polymer brushes. J Colloid Interface Sci 360: 540–547

Harris LA, Goff JD, Carmichael AY, Riffle JS, Harburn JJ, Pierre TG, Saunders M (2003) Magnetite nanoparticle dispersions stabilized with triblock copolymers. Chem Mater 15:1367–1377

Hong RY, Feng B, Chen LL, Liu GH, Li HZ, Zheng Y, Wei DG (2008) Synthesis, characterization and MRI application of dextran-coated Fe_3O_4 magnetic nanoparticles. Biochem Eng J 42:290–300

Jaffer FA, Libby P, Weissleder R (2006) Molecular and cellular imaging of atherosclerosis: emerging applications. J Am Coll Cardiol 47:1328–1338

Jain TK, Foy SP, Erokwu B, Dimitrijevic S, Flask CA, Labhasetwar V (2009) Magnetic resonance imaging of multifunctional pluronic stabilized iron-oxide nanoparticles in tumor-bearing mice. Biomaterials 30:6748–6756

Jiang J, Lu X, Lu Y (2008) Stereospecific preparation of polyacrylamide with low polydispersity by ATRP in the presence of Lewis acid. Polymer 49:1770–1776

Kralj S, Makovec D, Campelj S, Drofenik M (2010) Producing ultra-thin silica coatings on iron-oxide nanoparticles to improve their surface reactivity. J Magn Magn Mater 322: 1847–1853

Lee K, Park C, Moon H-Y, Ahn E, Park HE, Ihm S-H, Seung K-B, Yoon T-J, Chang K, Lee C, Cheong C, Hong KS (2009) Magnetic resonance tracking of multifunctional nanoparticle-labeled mouse mesenchymal stem cells in a mouse model of myocardial infarction. Curr Appl Phys 9:12–14

Meerod S, Tumcharern G, Wichai U, Rutnakornpituk M (2008) Magnetite nanoparticles stabilized with polymeric bilayer of poly(ethylene glycol) methyl ether–poly(ε-caprolactone) copolymers. Polymer 49:3950–3956

Moisescu C, Bonneville S, Tobler D, Ardelean I, Benning LG (2008) Controlled biomineralization of magnetite (Fe_3O_4) by *Magnetospirillum gryphiswaldense*. Miner Mag 72: 333–336

Monge S, Haddleton DM (2004) Synthesis of precursors of poly(acryl amides) by copper mediated living radical polymerization in DMSO. Eur Polym J 40:37–45

Neugebauer D (2007) Graft copolymers with hydrophilic and hydrophobic polyether side chains. Polymer 48:4966–4973

Öisjöen F, Schneiderman JF, Astalan AP, Kalabukhov A, Johansson C, Winkler D (2009) A new approach for bioassays based on frequency- and time-domain measurements of magnetic nanoparticles. Biosens Bioelectron 25:1008–1013

Park NH, Park JK, Choi Y, Yoo C-I, Lee CR, Lee H, Kim HK, Kim S-R, Jeong T-H, Park J, Yoon CS, Kim Y (2003) Whole blood manganese correlates with high signal intensities on T1-weighted MRI in patients with liver cirrhosis. NeuroToxicology 24:909–915

Pei W, Kumada H, Natusme T, Saito H, Ishio S (2007) Study on magnetite nanoparticles synthesized by chemical method. J Magn Magn Mater 310:2375–2377

Pich A, Bhattacharya S, Boyko V, Adler H-JP (2004) Temperature-sensitive hybrid microgels with magnetic properties. Langmuir 20:10706–10711

Prai-in Y, Tankanya K, Rutnakornpituk B, Wichai U, Montembault V, Pascual S, Fontaine L, Rutnakornpituk M (2012) Azlactone functionalization of magnetic nanoparticles using ATRP and their bioconjugation. Polymer 53:113–120

Qiang R, Fanghong G, Bibiao J, Dongliang Z, Jianbo F, Fudi G (2006) Preparation of hyperbranched copolymers of maleimide inimer and styrene by ATRP. Polymer 47: 3382–3389

Ragheb RT, Riffle JS (2008) Synthesis and characterization of poly(lactide-b-siloxane-b-lactide) copolymers as magnetite nanoparticle dispersants. Polymer 49:5397–5404

Reining B, Keul H, Hcker H (2002) Amphiphilic block copolymers comprising poly(ethylene oxide) and poly (styrene) blocks: synthesis and surface morphology. Polymer 43:7145–7154

Rutnakornpituk M, Meerod S, Boontha B, Wichai U (2009) Magnetic core-bilayer shell nanoparticle: a novel vehicle for entrapment of poorly water-soluble drugs. Polymer 50:3508–3515

Rutnakornpituk M, Puangsin N, Theamdee P, Rutnakornpituk B, Wichai U (2011) Poly(acrylic acid)-grafted magnetic nanoparticle for conjugation with folic acid. Polymer 52:987–995

Semsarzadeh MA, Mirzaei A, Vasheghani-Farahani E, Nekoomanesh Haghighi M (2003) Atom transfer radical polymerization of (meth)acrylates and their novel block copolymers with vinyl acetate. Eur Polym J 39:2193–2201

Storm PB, Moriarity JL, Tyler B, Burger PC, Brem H, Weingart J (2002) Polymer delivery of camptothecin against 9L gliosarcoma: release, distribution, and efficacy. J Neuro-Oncol 6:209–217

Sun Y, Ding X, Zheng Z, Cheng X, Hu X, Peng Y (2007) Surface initiated ATRP in the synthesis of iron oxide/polystyrene core/shell nanoparticles. Eur Polym J 43:762–772

Wootthikanokkhan J, Peesan M, Phinyocheep P (2001) Atom transfer radical polymerizations of (meth)acrylic monomers and isoprene. Eur Polym J 37:2063–2071

Yi Z, Pan K, Jiang L, Zhang J, Dan Y (2007) Copper-based reverse ATRP process of styrene in mixed solvents. Eur Polym J 43:2557–2563

Yin M, Habicher WD, Voit B (2005) Preparation of functional poly(acrylates and methacrylates) and block copolymers formation based on polystyrene macroinitiator by ATRP. Polymer 46:3215–3222

Zhang Y, Zhang J (2005) Surface modification of monodisperse magnetite nanoparticles for improved intracellular uptake to breast cancer cells. J Colloid Interface Sci 283:352–357

Polymer 53 (2012) 113–120

Contents lists available at SciVerse ScienceDirect

Polymer

journal homepage: www.elsevier.com/locate/polymer

Azlactone functionalization of magnetic nanoparticles using ATRP and their bioconjugation

Yingrak Prai-in [a], Kritsada Tankanya [a], Boonjira Rutnakornpituk [a], Uthai Wichai [a], Véronique Montembault [b], Sagrario Pascual [b], Laurent Fontaine [b,**], Metha Rutnakornpituk [a,*]

[a] Department of Chemistry and Center of Excellence for Innovation in Chemistry, Faculty of Science, Naresuan University, Muang, Phitsanulok 65000, Thailand
[b] UCO2M, LCOM-Chimie des Polymères, UMR CNRS 6011, Université du Maine, Avenue O. Messiaen, 72085 Le Mans Cedex 9, France

ARTICLE INFO

Article history:
Received 22 August 2011
Received in revised form
9 November 2011
Accepted 13 November 2011
Available online 19 November 2011

Keywords:
Magnetite
Azlactone
ATRP

ABSTRACT

Surface modification of magnetite nanoparticle (MNP) with poly(poly(ethylene glycol) methyl ether methacrylate-*stat*-2-vinyl-4,4-dimethylazlactone) copolymers (Poly(PEGMA-*stat*-VDM)) *via* atom transfer radical polymerization (ATRP) and its application to anchor thymine peptide nucleic acid (PNA) monomer are reported. ATRP of PEGMA and VDM was first performed in a solution system to optimize the reaction condition and the optimal condition was then applied in the surface-initiated ATRP of MNP. Fourier transform infrared spectroscopy (FTIR) indicated the presence of the copolymer in the MNP complexes. After immobilization of thymine PNA monomer, thermogravimetric analysis (TGA) results indicated that there were 4 wt% of the PNA monomer in the complex (1.2 μmol/g complex). The existence of the PNA monomer in the complex was also confirmed *via* FTIR and vibrating sample magnetometry (VSM). The MNP complex with active surface might be efficiently used as magnetically guidable nano-solid support for PNA oligomers and other molecules containing affinity functional groups.

1. Introduction

Magnetite iron oxide nanoparticles (MNP, Fe_3O_4) are widely studied in the present days. MNP have been used for many biomedical applications such as magnetic resonance imaging [1–3], drug delivery system [4,5], enzyme and protein immobilization [6–8], RNA and DNA purification [9–11], and gene therapy [12–14]. The minimum requirements of MNP for these applications are that it should be chemically stable, biocompatible, non-toxic, well dispersible in liquid media and able to be bound with biological molecules such as peptides, hormones, nucleotides or drugs [1–14]. Therefore, surface modification of MNP with various polymers becomes a good choice to obtain biocompatible MNP and to enhance the interaction between MNP and biological species.

Several methods, including physical adsorption of polymers to MNP surface, emulsion polymerization in the presence of MNP and so-called "grafting-to" and "grafting-from" methods have been developed to prepare polymer-coated MNP [15–18]. Among these methods, the "grafting-from" technique has been preferable because polymer chains are grown from initiator-functionalized MNP surface by *in situ* polymerization to obtain a permanent linkage of the polymers on its surface. Recently, several groups have applied atom transfer radical polymerization (ATRP) based on a "grafting-from" method to prepare polymeric layers on surface of MNP [19–21]. The advantages of this method are that the as-synthesized polymer possesses low polydispersity index, controllable molecular weight, functionality, composition distribution and desired polymer architecture [19–21].

In this work, we have applied a copper-mediated ATRP technique to synthesize grafted statistical copolymer of poly(ethylene glycol) methacrylate (PEGMA) and 2-vinyl-4,4-dimethylazlactone (VDM) onto MNP containing an ATRP initiator immobilized on its surface. The azlactone ring of 4,4-dimethyl-5-oxazolone displays a high reactivity toward nucleophilic molecules such as primary amines, alcohol and thiols by means of a ring-opening addition reaction without the use of catalysts. In addition, there is no by-product eliminated from the ring-opening reaction between VDM and nucleophiles [22–28]. Moreover, the azlactone functionality shows a good resistance to hydrolysis at neutral pH: this is a considerable advantage compared to other activated acid forms [29].

We have previously studied the dependence of the molecular architecture of VDM-styrene copolymer on accessibility of

* Corresponding author. Tel.: +66 5596 3464; fax: +66 5596 3401.
** Corresponding author.
E-mail addresses: laurent.fontaine@univ-lemans.fr (L. Fontaine), methar@nu.ac.th, mrutnako@hotmail.com (M. Rutnakornpituk).

0032-3861/$ – see front matter © 2011 Elsevier Ltd. All rights reserved.
doi:10.1016/j.polymer.2011.11.021

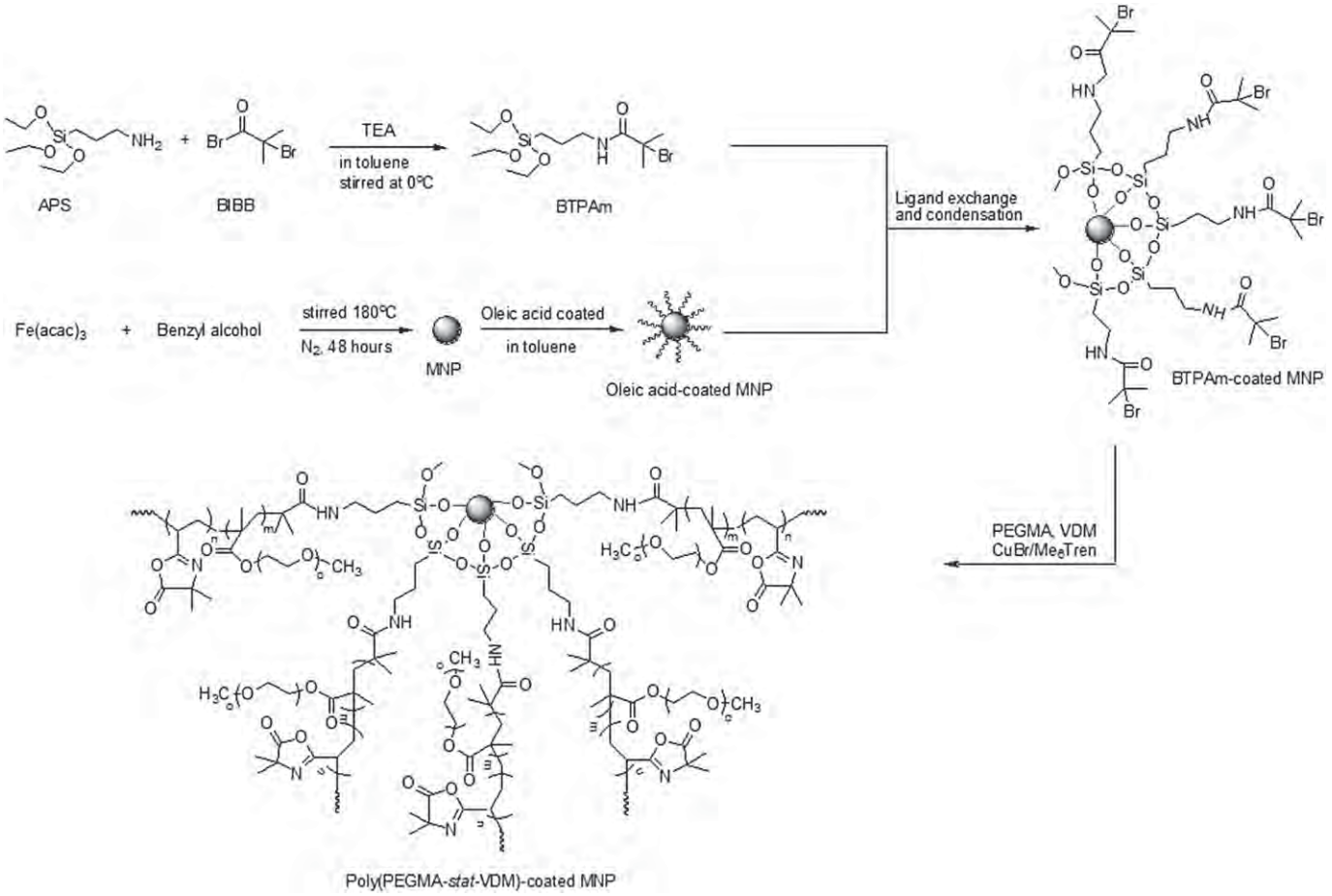

Scheme 1. Surface modification of MNP with poly(PEGMA-*stat*-VDM) copolymer *via* ATRP reaction.

benzylamine as a model nucleophilic compound to react with the azlactone rings grafted on a solid support. It was found that the statistical architecture of VDM-styrene copolymer exhibited a good result in terms of reactivity and efficiency in the azlactone -ring-opening reaction due to the existence of styrene spacers resulting in the open access to VDM units [24]. In the present work, water dispersibility of MNP could be greatly improved by introducing a thin layer of PEGMA to its surface and the presence of the azlactone rings of VDM serves as a site for immobilization of biological nucleophilic molecules, such as enzymes [30] or proteins [31] on its surface. In this work, thymine PNA monomer was used as a model compound for immobilization onto the VDM-grafted particles (Scheme 1). FTIR, VSM and TGA techniques were used to verify the existence of thymine PNA monomer on its surface.

Table 1
ATRP of mixtures of PEGMA and VDM using various molar ratios of EBiB initiator and CuBr/Me_6Tren catalytic complexes in toluene.

Entry	EBiB/CuBr/ Me_6Tren	Temp (°C)	Time (min)	Conv[a] (%)		$\overline{M}_{n,th}$[b] (g/mol)	$\overline{M}_{n,SEC}$[c] (g/mol)	PDI[c]
				PEGMA	VDM			
1	1/1/1	50	30	83	90	18,705	29,400	2.17
2	1/0.5/0.5	30	90	70	82	16,199	18,600	1.72
3	1/0.2/0.2	30	90	52	61	12,039	14,400	1.35

[a] Calculated *via* ^{1}H NMR spectroscopy.
[b] $\overline{M}_{n,th} = ([PEGMA]_0/[EBiB]_0 \times conv_{PEGMA} \times M_{PEGMA}) + ([VDM]_0/[EBiB]_0 \times conv_{VDM} \times M_{VDM})$.
[c] Measured *via* SEC (calibrated with polystyrene standard).

2. Experimental

2.1. Materials

Unless otherwise stated, all reagents were used without further purification: iron (III) acetylacetonate ($Fe(acac)_3$, 99.9%, Acros), benzyl alcohol (98%, Unilab), oleic acid (Fluka), copper(I)bromide (99.999%, Aldrich), triethylamine (TEA, 97%, Carto Erba), ethyl-2-bromoisobutyrate (EBiB, 98%, Aldrich), and thymine PNA (Acros). Poly(ethylene glycol) methyl ether methacrylate (PEGMA, Aldrich)

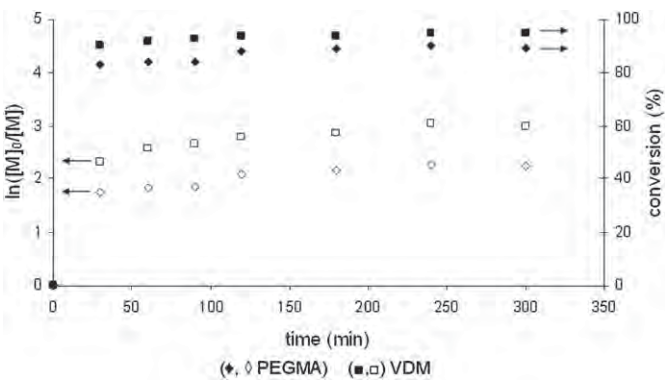

Fig. 1. The $\ln([M]_0/[M])$ *vs* time plot and monomers conversions *vs* time plot of ATRP of PEGMA and VDM using $[PEGMA]_0/[VDM]_0/[EBiB]_0/[CuBr]_0/[Me_6Tren]_0$ molar ratio = 50/50/1/1/1, in toluene at 50 °C.

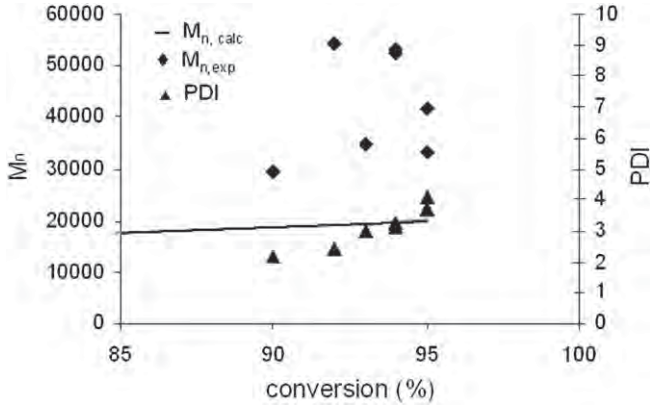

Fig. 2. Dependence of $\overline{M}_n$ and $\overline{M}_w/\overline{M}_n$ (PDI) with monomer conversion of ATRP of PEGMA and VDM using $[PEGMA]_0/[VDM]_0/[EBiB]_0/[CuBr]_0/[Me_6Tren]_0$ molar ratio = 50/50/1/1/1, in toluene at 50 °C.

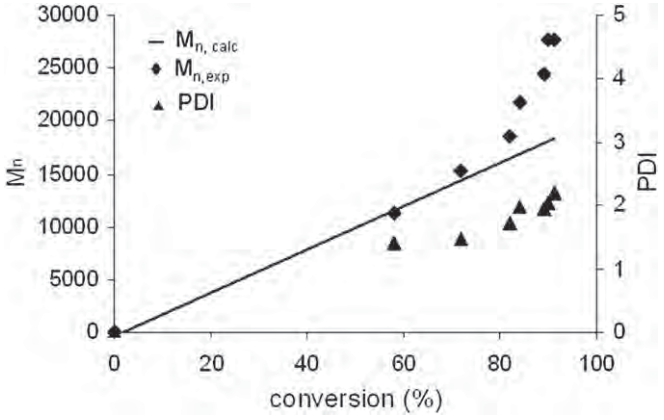

Fig. 4. Dependence of $\overline{M}_n$ and $\overline{M}_w/\overline{M}_n$ (PDI) with monomer conversion of ATRP of PEGMA and VDM using $[PEGMA]_0/[VDM]_0/[EBiB]_0/[CuBr]_0/[Me_6Tren]_0$ molar ratio = 50/50/1/0.5/0.5, in toluene at 30 °C.

with average molecular weight $\overline{M}_n = 300\ g\ mol^{-1}$ was purified by passing through basic alumina and stored at −4 °C after purification. 2-Vinyl-4,4-dimethylazlactone (VDM, 99.4%, ISOCHEM), was distilled *in vacuo* and stored at −15 °C after purification. Tris-[2-(dimethylamino) ethyl]amine (Me_6Tren) [32] and 2-bromo-2-methyl-*N*-(3-(triethoxysilyl)propyl)propanamide (BTPAm) [21] were prepared according to previously reported procedures. CH_2Cl_2 and diethyl ether were dried with P_2O_5 and distilled prior to use. *N*,*N*-dimethylformamide (DMF, Acros), toluene (Acros) and $CDCl_3$ (99%, Euriso-Top) were used as received.

2.2. Characterization

^1H NMR spectra were obtained from a Bruker AC 200-MHz spectrometer using $CDCl_3$ as a solvent. Molar masses and molar mass distributions were determined *via* size exclusion chromatography (SEC) at 35 °C on a system equipped with a Spectra System AS1000 autosampler with a guard column (Polymer Laboratories, PL gel 5 μm guard, 50 × 7.5 mm) followed by two columns (Polymer Laboratories, two PL gel 5 μm Mixed-D columns, 2 × 300 × 7.5 mm). Polystyrene standards (580–483 × 10 g mol^{-1}) were used to calibrate the SEC. Fourier transform infrared (FTIR) analyses were recorded using a Nicolet Avatar 370 DTGS spectrometer in the attenuated total reflection (ATR) mode. Elemental analysis was performed by the Service Central d'Analyses du Centre National de Recherche Scientifique, Gif-sur-Yvette (France). TEM images were taken using a Philips Tecnai 12 operated at 120 kV equipped with Gatan model 782 CCD camera. The particles were re-suspended in toluene or DMF with sonication before deposition on a TEM grid. Magnetic properties of the particles were measured at room temperature using a Standard 7403 Series, Lakeshore vibrating sample magnetometer (VSM). Magnetic moment of each sample was investigated over a range of ±10,000 G of applied magnetic fields using 30 min sweep time. Thermogravimetric analysis (TGA) was performed on SDTA 851 Mettler-Toledo at the temperature ranging between 25 and 600 °C at a heating rate of 20 °C/min under oxygen atmosphere. XRD patterns of the particles were collected on a Philips X'pert X-ray diffractometer under CuK_α radiation ($\lambda = 1.540598$ Å) operated at 30 kV and 2θ ranging from 0 to 90°.

2.3. General procedure for the synthesis of poly(PEGMA-stat-VDM) copolymers via ATRP in solution

An example of the synthesis of poly(PEGMA-*stat*-VDM) using EBiB/CuBr/Me_6Tren/PEGMA/VDM of 1/1/1/50/50 is illustrated. CuBr (0.0287 g, 0.2 mmol) was added to a Schlenk tube equipped with a stir bar. After sealing with a rubber septum, the Schlenk tube was deoxygenated with three vacuum/argon fill cycles. A degassed solution of PEGMA (6 g, 20 mmol), VDM (2.78 g, 20 mmol), toluene (70% v/v, 6 mL), EBiB (0.039 g, 0.2 mmol) and DMF (5% v/v, 0.4 mL) (used as an internal standard) was added to the Schlenk tube containing CuBr *via* a cannula. The resulting solution was further degassed using freeze/pump/thaw cycles *in vacuo*. Degassed Me_6Tren (0.046 g, 0.2 mmol) was added ($t = 0$) to the Schlenk tube and it was then placed in an oil bath preheated to a desired

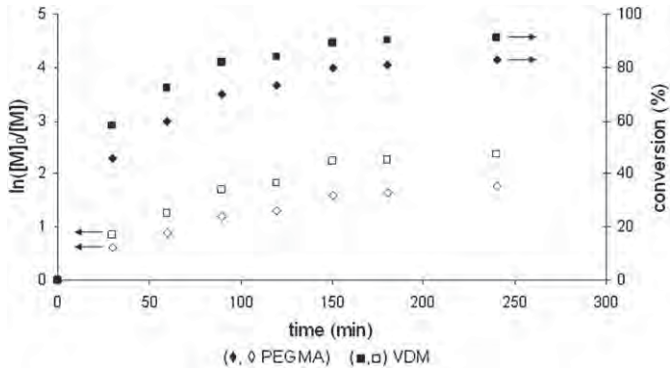

Fig. 3. The $\ln([M]_0/[M])$ *vs* time plot and monomers conversions *vs* time plot of ATRP of PEGMA and VDM using $[PEGMA]_0/[VDM]_0/[EBiB]_0/[CuBr]_0/[Me_6Tren]_0$ molar ratio = 50/50/1/0.5/0.5, in toluene at 30 °C.

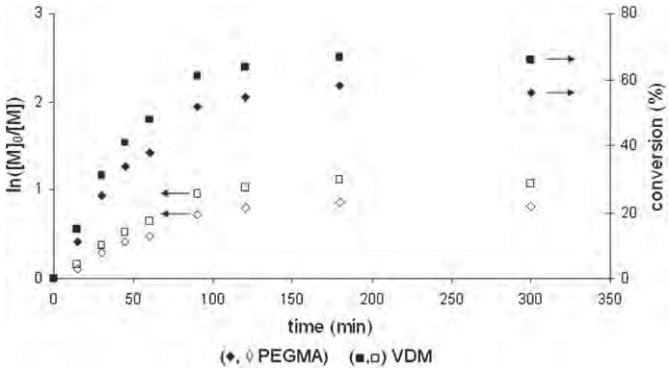

Fig. 5. The $\ln([M]_0/[M])$ *vs* time plot and monomers conversion *vs* time plot of ATRP of PEGMA and VDM using $[PEGMA]_0/[VDM]_0/[EBiB]_0/[CuBr]_0/[Me_6Tren]_0$ molar ratio = 50/50/1/0.2/0.2, in toluene at 30 °C.

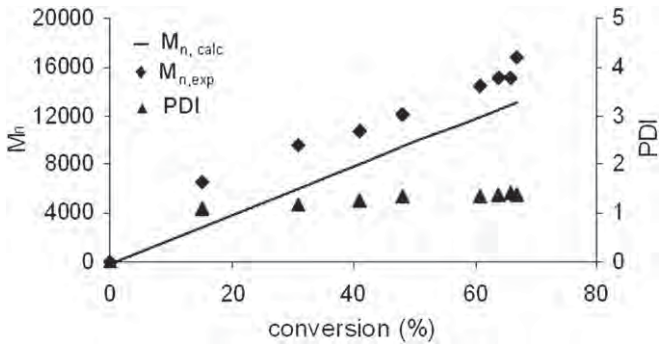

Fig. 6. Dependence of $\overline{M}_n$ and $\overline{M}_w/\overline{M}_n$ (PDI) with monomer conversion of ATRP of PEGMA and VDM using $[PEGMA]_0/[VDM]_0/[EBiB]_0/[CuBr]_0/[Me_6Tren]_0$ molar ratio = 50/50/1/0.2/0.2, in toluene at 30 °C.

temperature. The samples were withdrawn periodically *via* a degassed syringe for conversion measurements and SEC analyses.

2.4. Synthesis of MNP coated with ATRP initiators (BTPAm-coated MNP)

BTPAm-coated MNP was prepared *via* a three-step reaction; (1) synthesis of MNP core, (2) coating the MNP with oleic acid and (3) grafting BTPAm onto the oleic acid-coated MNP. MNP was synthesized *via* a thermal decomposition reaction according to the procedure previously reported [33]. Namely, $Fe(acac)_3$ (5 g, 14.05 mmol) and benzyl alcohol (90 mL) were mixed in a three-necked round bottomed flask equipped with a mechanical stirrer and septum. The mixture was set at 180 °C for 48 h with nitrogen flow. After the reaction, the precipitant was removed from the dispersion using an external magnet and washed with ethanol and CH_2Cl_2 repeatedly to remove benzyl alcohol. The particles were then dried at room temperature under reduced pressure. To prepare oleic acid-coated MNP, and MNP-toluene dispersion (0.8 g of dried MNP in 30 mL of toluene) was sonicated for 1 h. Oleic acid (4 mL) was then slowly dropped into the dispersion and sonicated for 3 h under nitrogen atmosphere. To immobilize BTPAm onto the MNP surface, the oleic acid-coated MNP dispersed in toluene was mixed with BTPAm using TEA as a catalyst. The reaction was carried out at room temperature for 24 h under nitrogen atmosphere. The dispersion was precipitated in methanol and washed with toluene to remove oleic acid and ungrafted BTPAm from the dispersion. The Br loading calculated from elemental analysis (%Br = 0.71%) was estimated to 8.89×10^{-2} mmol g^{-1}.

2.5. Synthesis of poly(PEGMA-stat-VDM)-coated MNP via ATRP

BTPAm-coated MNP dispersed in toluene was sonicated for 20 min and degassed using argon. This suspension was then added to a degassed Schlenk tube containing CuBr, PEGMA, VDM, EBiB (used as a free initiator), and DMF (used as an internal standard) *via* a cannula. Degassed Me_6Tren ligand was added to the above dispersion ($t = 0$) and the mixture was set in an oil bath preheated at 30 °C. The samples were withdrawn periodically *via* a degassed syringe to monitor the monomer conversions *via* ^1H NMR spectroscopy and to determine molecular characteristics of the copolymer *via* SEC analyses. At the end of the copolymerization, the surface-modified MNP were separated from the mixture by external magnet, precipitated into diethyl ether and dried *in vacuo*. The as-synthesized poly(PEGMA-*stat*-VDM)-coated MNP resulted as a fine black powder.

2.6. Immobilization of thymine PNA monomer on the poly(PEGMA-stat-VDM)-coated MNP

The synthesis procedure of thymine PNA monomer is explained in details in the supporting information. Thymine PNA monomer (10 mg) was added into a dispersion of poly(PEGMA-*stat*-VDM)-coated MNP (10 mg) in DMF (10 mL). The mixture was sonicated at room temperature for 6 h under argon atmosphere. The particle was then collected using an external magnet and washed with DMF repeatedly to remove ungrafted thymine PNA monomer from the particle surface.

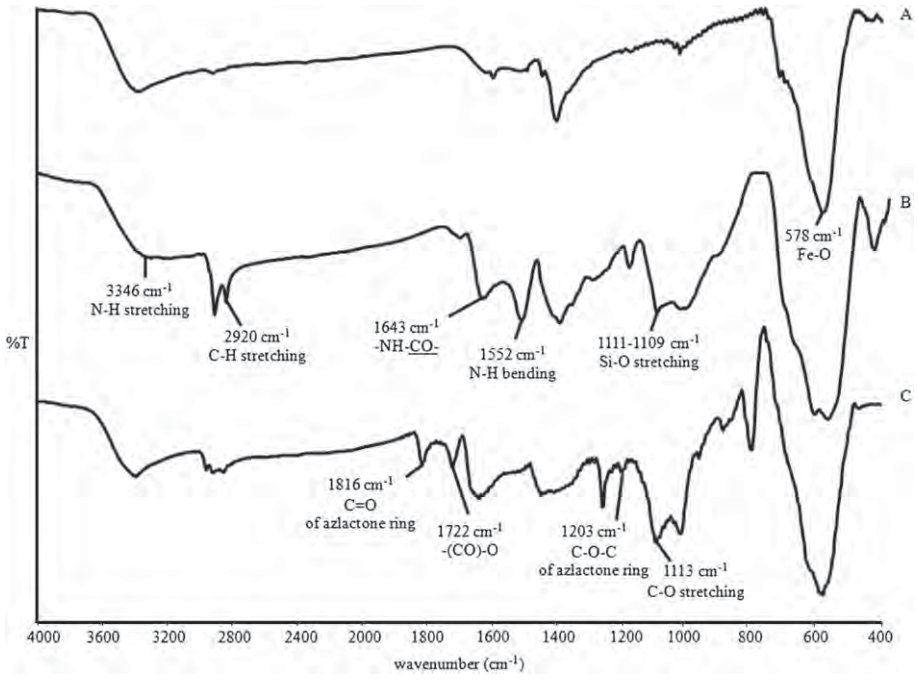

Fig. 7. FTIR spectra of (A) bare MNP, (B) BTPAm-coated MNP and (C) poly(PEGMA-*stat*-VDM)-coated MNP.

Table 2
Summary of monomers conversions, $\overline{M}_n$, and PDIs of poly(PEGMA-*stat*-VDM) copolymers using 100/100/1/0.4/0.4 molar ratio of $[PEGMA]_0/[VDM]_0/[EBiB]_0/[CuBr]_0/[Me_6Tren]_0$, respectively, in toluene at 30 °C.

Time (min)	Conv[a] (%)		$\overline{M}_{n,th}$[b] (g/mol)	$\overline{M}_{n,SEC}$[c] (g/mol)	PDI[c]
	PEGMA	VDM			
0	0	0	0	0	0
30	13	16	3062	3800	1.20
45	14	17	3282	4100	1.21
60	15	20	3640	5400	1.19
90	18	22	4229	7700	1.14
120	18	25	4438	7900	1.13
150	20	24	4668	8000	1.13
180	22	28	5246	8100	1.13
1440	24	29	5616	8300	1.09

[a] Determined *via* ^{1}H NMR spectroscopy (monomer depletion monitored relative to DMF used as an internal standard).
[b] $\overline{M}_{n,th} = ([PEGMA]_0/[EBiB]_0 \times conv_{PEGMA} \times M_{PEGMA}) + ([VDM]_0/[EBiB]_0 \times conv_{VDM} \times M_{VDM})$.
[c] Measured by SEC (calibrated with polystyrene standard).

3. Results and discussion

3.1. Synthesis of poly(PEGMA-stat-VDM) via ATRP in solution

In the present work, a statistical copolymer of PEGMA and VDM was first synthesized in toluene using CuBr/Me_6Tren catalytic complex in the presence of EBiB as an initiator. CuBr and Me_6Tren were selected as a catalytic complex in the present work. Fontaine et al. have reported that using Me_6Tren ligand led to a good control in polymerization of VDM: the experimental molecular weights were comparable to the theoretical values and narrow polydispersities were obtained [34]. Molar ratio of CuBr/Me_6Tren/EBiB was studied in order to determine the best experimental conditions to obtain a good control in molecular weight and molecular weight distribution. The selected reaction conditions would then be used for surface-initiated ATRP of PEGMA and VDM from magnetite nanoparticles, which would be then used for immobilizing thymine PNA monomer on their surface.

A EBiB/CuBr/Me_6Tren molar ratio of 1/1/1 has successfully been used in our group to synthesize well-defined (co)polymers based on VDM in solution [34]. Therefore, in this work, poly(PEGMA-*stat*-VDM) was synthesized *via* ATRP of PEGMA and VDM monomers using the same catalytic/initiator system and similar catalyst/ligand ratios. Table 1 shows the summary of the statistical copolymerizations of 50/50/1 molar ratio of PEGMA/VDM/EBiB at various CuBr/Me_6Tren ratios.

A preliminary experiment was performed in toluene at 50 °C using $[EBiB]_0/[CuBr]_0/[Me_6Tren]_0$ ratio of 1/1/1 (entry 1, Table 1). Fig. 1 shows that conversions of PEGMA and VDM reached 83% and 90%, respectively, after 30 min of polymerization time. Moreover, the $\ln([M]_0/[M])$ *vs* time plot shows a curvature and reaches a plateau after 30 min of the reaction, indicating the presence of irreversible terminations. This phenomenon is confirmed by the relative broad polydispersity indices obtained (PDIs = 2.17) (Fig. 2). A decrease of $[EBiB]_0/[CuBr]_0/[Me_6Tren]_0$ ratio to 1/0.5/0.5 and a decrease of the reaction temperature to 30 °C resulted in a decrease of PEGMA and VDM conversion to 70% and 82%, respectively (after 90 min, entry 2, Table 1 and Fig. 3). However, the polydispersity indices were still high (PDIs = 1.40–2.19) for a controlled radical polymerization (Fig. 4). In addition, the $\ln([M]_0/[M])$ *vs* time plot again shows a decrease of active species concentration, which is compatible with the presence of irreversible terminations (Fig. 3).

When a 1/0.2/0.2 molar ratio of $[EBiB]_0/[CuBr]_0/[Me_6Tren]_0$ was used, the $\ln([M]_0/[M])$ *vs* time plot was linear at the beginning, indicating that the concentration of active species was constant in the first step of the polymerization (Fig. 5). At 90 min, 52% of PEGMA conversion and 61% of VDM conversion were reached (entry 3, Table 1). The polydispersity index in this case decreased to 1.35 and the $\overline{M}_n$ values increased with the monomer conversion, and they are somewhat closed to the theoretical values (Fig. 6). This experiment clearly shows that a decrease of the catalytic complex-to-initiator ratio allows a better control of the ATRP of PEGMA and VDM in toluene.

3.2. Preparation of poly(PEGMA-stat-VDM)-coated MNP via ATRP

To perform ATRP from MNP surface, 2-bromo-2-methyl-*N*-(3-(triethoxysilyl)propyl)propanamide (BTPAm), a molecule containing an ATRP initiating site, was first immobilized onto the particle surface *via* silanization reaction using the triethoxy silane group of BTPAm. FTIR spectrum of BTPAm-coated MNP shows characteristic absorption signals of BTPAm: C–O (1111–1109 cm^{-1}), N–H (3346 cm^{-1}), NH–CO (1643 cm^{-1}), indicating the anchorage of BTPAm (Fig. 7B). Elemental analysis indicated the presence of 0.71% Br in the MNP, corresponding to 8.89×10^{-2} mmol Br per gram of MNP.

Then, to prepare statistical copolymers based on PEGMA and VDM grafted onto MNP surface, the optimal condition established previously for ATRP in solution were used. Because the MNP-supported copolymers were undetectable in NMR technique, the free initiator EBiB (also called "sacrificial" initiator) was added to the reaction to easily monitor the reaction progress. Such a strategy was previously applied to VDM monomer by our group [24]. Therefore, monomer conversions and copolymer compositions, discussed in the latter section, were investigated from the free copolymers *via* NMR spectroscopy. The reaction was carried out in toluene at 30 °C using $[PEGMA]_0/[VDM]_0/[EBiB]_0/[BTPAm\text{-coated MNP}]_0/[CuBr]_0/[Me_6Tren]_0$ in a 100/100/1/1/0.4/0.4 molar ratio. This molar ratio was adjusted in accordance with the fact that there were both ATRP initiating sites (BTPAm) grafted on particle surface and a free initiator (EBiB) in this system. After the ATRP reactions, the particles in the dispersion were magnetically separated from the mixture. The aggregate was used in FTIR and VSM characterizations, and the supernatant containing the free copolymers was used in SEC and NMR analyses.

Fig. 7C shows FTIR spectrum of poly(PEGMA-*stat*-VDM)-coated MNP compared with those of bare MNP (Fig. 7A) and BTPAm-coated MNP (Fig. 7B). Poly(PEGMA-*stat*-VDM)-coated MNP exhibited a characteristic signal of azlactone rings of VDM units at 1816 cm^{-1} (–CaO stretching), 1203 cm^{-1} (C–O–C stretching) and that of PEGMA at 1722 cm^{-1} (–CaO stretching) (Fig. 7C), indicating the presence of the copolymer in the complex. A broad and strong band of Fe-O from MNP cores was also observed at 578 cm^{-1}.

Table 2 shows the monomer conversion, $\overline{M}_n$ and polydispersity indices (PDI) of poly(PEGMA-*stat*-VDM) produced by the free initiator. It was found that the monomer conversions of PEGMA and VDM in BTPAm-coated MNP reached 24% and 29%, respectively, after 24 h of reaction, while those in the solution system with the same reaction conditions proceeded in a much shorter time (25% and 31%, respectively, in 30 min reaction) (see Table S3 in the supporting information). This phenomenon has been previously observed in the surface-initiated ATRP of VDM from the Wang resin solid support [24]. $\overline{M}_n$ gradually increased when the reaction conversions increased, indicating the growth of the copolymer chains. In all cases, the $\overline{M}_{n,SEC}$ values were higher than the theoretical ones and their distributions were narrow (PDIs = 1.09–1.21) throughout the reaction (Table 2).

3.3. Immobilization of thymine PNA monomer on poly(PEGMA-stat-VDM)-coated MNP

The as-synthesized poly(PEGMA-*stat*-VDM)-coated MNP containing active azlactone functional groups were then used as

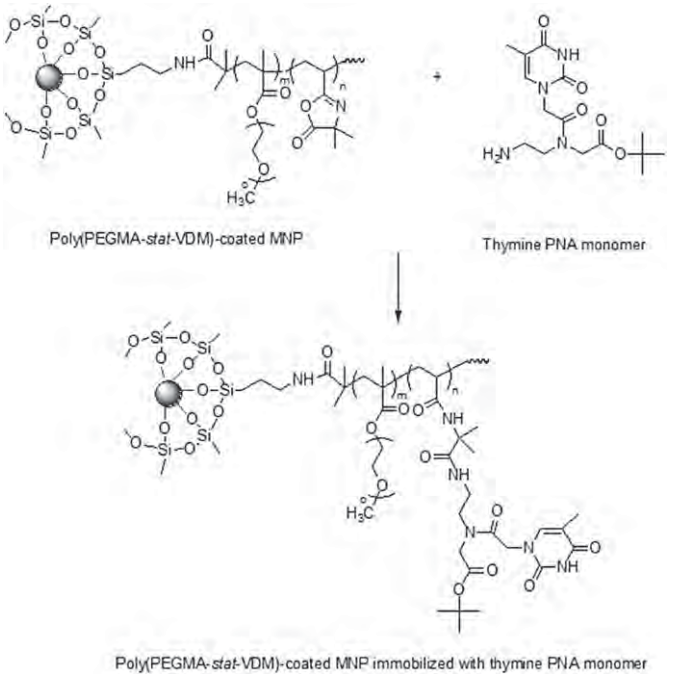

Scheme 2. Immobilization of thymine PNA monomer onto poly(PEGMA-*stat*-VDM)-coated MNP.

a magnetically guidable-nanoscale amine support. In this study, thymine PNA monomer was selected as a model compound for grafting onto the particle surface. It is anticipated that these novel copolymer-coated MNPs can be used as a nanosolid support for PNA oligomer immobilization. Because precedents have reported the utilization of PNA oligomer as a probe for detection of DNA sequences [35–38], the attachment of PNA oligomers on these copolymer-coated MNP is warrant for further studies.

The immobilization process of thymine PNA monomer on the particle surface was performed in anhydrous DMF at room temperature for 6 h (Schemes 1 and 2). Fig. 8C shows the disappearance of cyclic carbonyl of azlactone rings at 1816 cm^{-1} [24] and the appearance of a signal at 1159 cm^{-1} corresponding to a C–H stretching of thymine [39], indicating the presence of thymine PNA monomer in the complex.

TEM images of MNP complexes at each step of the reaction are shown in Fig. 9. Bare MNP was not well dispersible in any solvent due to the lack of polymer coating; TEM experiments were not performed on bare MNP sample. After coating with oleic acid, the particles were well dispersible in toluene. Therefore, the TEM image shown in Fig. 9A was prepared from the particle dispersion in toluene. The particle size was in the range of 7–14 nm with the average diameter of 9 nm. After surface modification of the particle with poly(PEGMA-*stat*-VDM) in DMF, there was some nanoscale aggregation of about 30–50 particles/cluster (Fig. 9B). After immobilization of thymine PNA monomer on their surface, more aggregation of the particles was observed (about 100 particles/cluster) (Fig. 9C). The presence of hydrophobic thymine PNA monomer units on surface of the complexes might promote the particle aggregation in DMF. Although there was some nano-aggregation observed in TEM, these complexes were still visually re-dispersible in various solvents, such as THF, DMF and toluene, probably due to the presence of the polymeric thin film on their surface. A TEM image showing the presence of polymeric thin films on the particle surface was illustrated in the supporting information.

TGA studies were carried out to determine the mass loss of the organic components in the grafted-MNP. The MNP complexes in each step of the reaction showed their distinctive TGA curves, giving rise to the information of the amount of BTPAm, poly(-PEGMA-*stat*-VDM) and thymine PNA monomer in the grafted-MNP (Fig. 10). The slight loss in mass of bare MNP was attributed to the residual benzyl alcohol used as the reaction solvent in the MNP preparation step. According to the TGA results, there were about 6 wt% of BTPAm and 17 wt% of poly(PEGMA-*stat*-VDM) copolymer in the complexes. After the immobilization step of thymine PNA monomer, an increase in weight loss as compared to the one before the grafting reaction was observed (Fig. 10D), indicating that there were about 4 wt% thymine PNA monomer grafted to the

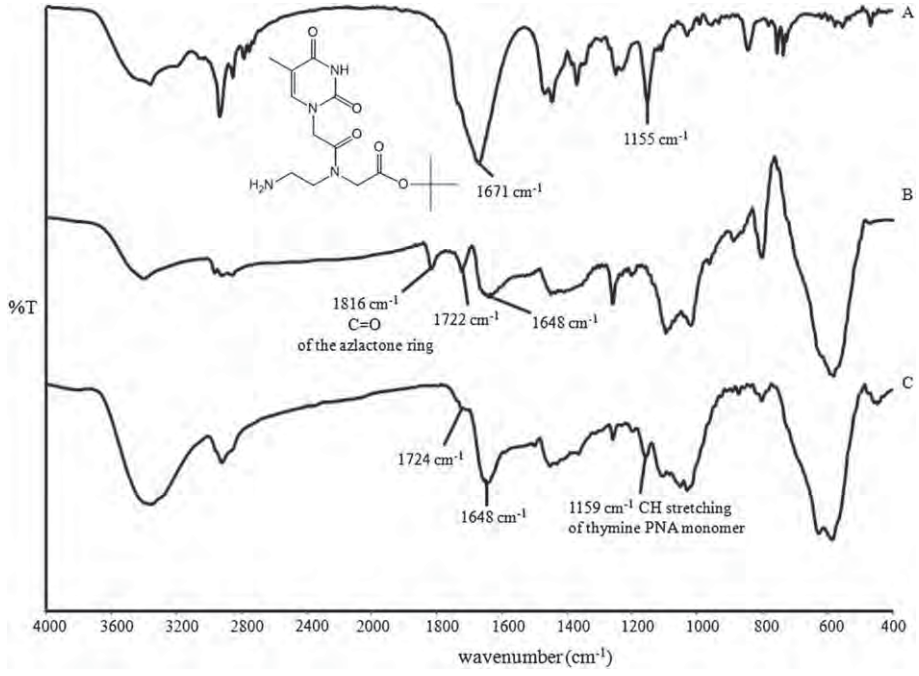

Fig. 8. FTIR spectra of (A) thymine PNA monomer, (B) poly(PEGMA-*stat*-VDM)-coated MNP and (C) poly(PEGMA-*stat*-VDM)-coated MNP immobilized with thymine PNA monomer.

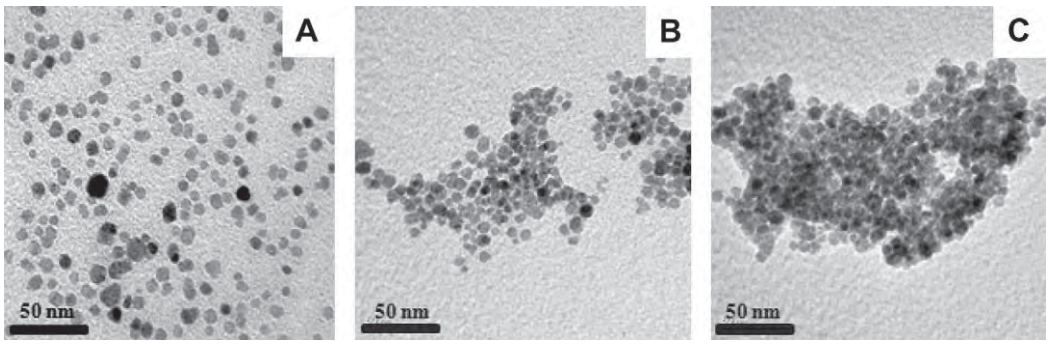

Fig. 9. TEM images of (A) oleic acid-coated MNP (prepared from toluene dispersion), (B) poly(PEGMA-*stat*-VDM)-coated MNP (prepared from DMF dispersion) and (C) poly(PEGMA-*stat*-VDM)-coated MNP immobilized with thymine PNA monomer (prepared from DMF dispersion).

grafted-MNP. This number corresponds to about 1.2 μmol of thymine PNA monomer per gram of the grafted-MNP (An example of the calculation is show in the supporting information). This was a supportive result to FTIR that thymine PNA monomer existed in the copolymer-coated MNP.

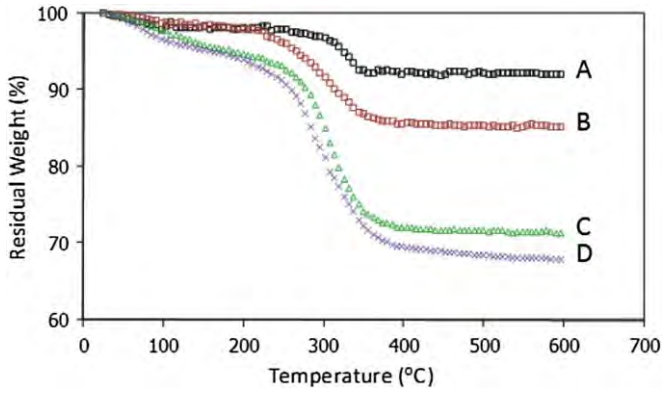

Fig. 10. TGA curves of (A) bare MNP, (B) BTPAm-coated MNP, (C) poly(PEGMA-*stat*-VDM)-coated MNP and (D) poly(PEGMA-*stat*-VDM)-coated MNP immobilized with thymine PNA monomer.

The *M*–*H* curves measured at room temperature of the particles in each step of the reaction are illustrated in Fig. 11. As illustrated in the inset, all samples showed no hysteresis at room temperature. The decrease of saturation magnetization (M_s) from 56 emu/g of bare MNP to 49 emu/g of BTPAm-coated MNP was attributable to the presence of BTPAm thin layer on the particle surface, resulting in the decrease of the percentage of MNP core in the complex (Fig. 11). Likewise, the M_s values of poly(PEGMA-*stat*-VDM)-coated MNP (36 emu/g) and poly(PEGMA-*stat*-VDM)-coated MNP immobilized with thymine PNA monomer (34 emu/g) were significantly lower than those of the BTPAm-coated MNP, which was again devoted to the decrease of MNP content in the complexes owing to the copolymer/thymine coating. This was in good agreement with the FTIR result indicating the presence of the copolymer in the complex. When taking the percentage of magnetite in the complex into account, the M_s values in emu/g magnetite basis were in the range of 46–56 emu/g magnetite (see Table S4 in the supporting information). The slight drop in the M_s values in emu/g magnetite basis was attributed to the use of organic solvents, e.g. DMF, in surface modification reactions, which might, to some extent, affect the magnetic properties of MNP core.

The crystal structures of each complex were also investigated. From XRD studies, the position and relative intensities of all diffraction signals of bare MNP and poly(PEGMA-*stat*-VDM)-coated

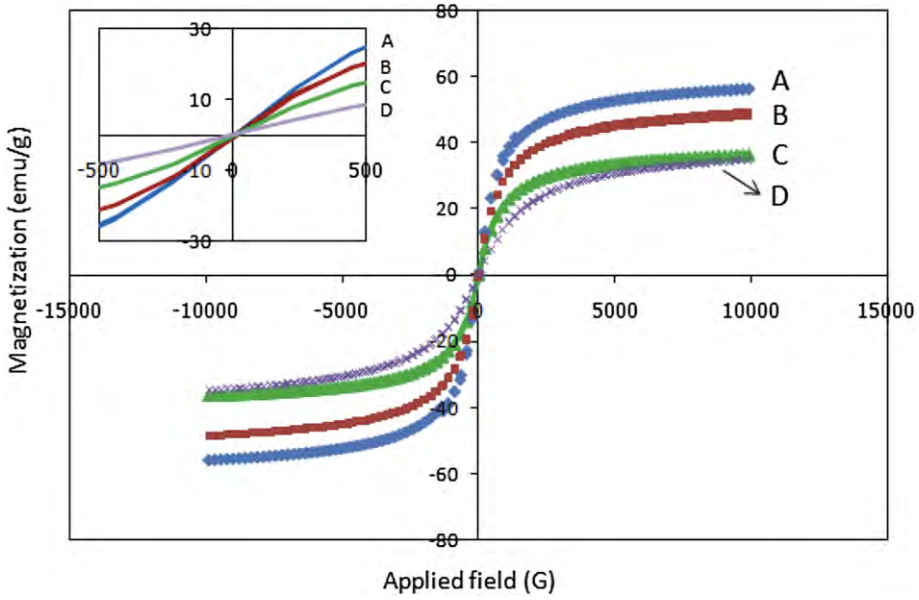

Fig. 11. *M*–*H* curves of A) bare MNP, B) BTPAm-coated MNP, C) poly(PEGMA-*stat*-VDM)-coated MNP and D) poly(PEGMA-*stat*-VDM)-coated MNP immobilized with thymine PNA monomer. The expansion in the range of ±500 G of applied filed is shown in the inset.

MNP matched well with the characteristic peaks of magnetite crystal [40] ($2\theta = 30.2^\circ$, 35.6°, 43.3°, 53.7°, 57.2° and 62.7°) obtained from the standard Fe_3O_4 powder diffraction data (see Figure S10 in the supporting information). Due to the limited amount of the as-synthesized poly(PEGMA-*stat*-VDM)-coated MNP immobilized with thymine PNA monomer, determination of its crystal structure *via* the XRD technique was not possible. Selected area electron diffraction (SAED) was thus performed to study the crystal structure information of the MNP immobilized with thymine PNA monomer (see Figure S11 in the supporting information). Its SAED pattern revealed that the particles were crystalline and the *d*-values of the SAED were in good agreement with those observed in Fe_3O_4 [41].

4. Conclusions

This work presented the surface modification of MNP with the statistical copolymer between PEGMA and VDM *via* ATRP to obtain the particles containing active functional groups on its surface. Hydrophilic PEGMA promoted good dispersibility to the particle in polar solvents and azlactone rings served as active functional groups for further chemical attachment with nucleophiles of interest. Surface-initiated ATRP of the copolymer *via* a "grafting-from" strategy from the particle produced the active polymer layer with a predicable and controllable fashion. The nanosolid supports were successfully used for immobilization of thymine PNA monomers on its surface. The results signified the feasibility to functionalize the surface of these novel azlactone-based nanoparticles with a broad range of other nucleophilic scavengers such as hydroxyl- and thiol-containing compounds.

Acknowledgment

The authors thank the Thailand Research Fund (TRF) and Naresuan University (DBG5380001) for financial funding. We also thank the Franco-Thai Cooperation Program in Higher Education and Research 2009–2010, supported by the Ministry of Foreign Affairs, Ministry of Higher Education and Research of France and the Commission on Higher Education of Thailand and PHC grant (PHC 2009–2010 n° 20609UF). YP specially acknowledges the Royal Golden Jubilee for the scholarship (PHD/0207/2551). The Center of Excellence for Innovation in Chemistry (PERCH-CIC), Commission on Higher Education, Ministry of Education is also gratefully acknowledged for financial support.

Appendix. Supplementary material

Supplementary data related to this article can be found online at doi:10.1016/j.polymer.2011.11.021.

References

[1] Singh A, Dilnawaz F, Mewar S, Sharma U, Jagannathan NR, Sahoo SK. ACS Appl Mater 2011;3:842–56.
[2] Chen HH, Josephson L, Josephson DE. WIREs Nanomed Nanobiotechnol 2011; 3:86–99.
[3] Valero E, Tambalo S, Marzola P, Ortega-Muñoz M, López-Jaramillo FJ, Sanoyo-González F, et al. J Am Chem Soc 2011;133:4889–95.
[4] Yu C, YunPeng B, Bao T, ZhaoLong L. Chin Sci Bull 2009;54:1190–6.
[5] Ruiz-Hernández E, Baeza A, Vallet-Regí M. ACS Nano 2011;5:1259–66.
[6] Ponvel KM, Lee DG, Woo EJ, Ahn IS, Lee CH. Korean J Chem Eng 2009;26: 127–30.
[7] Johnson AK, Zawadzka AM, Deobald LA, Crawford RL, Paszczynski AJ. J Nanopart Res 2008;10:1009–25.
[8] Park HJ, McConnell JT, Boddohi S, Kipper MJ, Johnson PA. Colloids Surf B 2011; 83:198–203.
[9] Sarkar TR, Irudayaraj J. Anal Biochem 2008;379:130–2.
[10] Kang K, Choi J, Nam JH, Lee SC, Kim KJ, Lee SW, et al. J Phys Chem B 2009;113: 536–43.
[11] Park ME, Chang JH. Mater Sci Eng C 2007;27:1232–5.
[12] Ito A, Matsuoka F, Honda H, Kobayashi T. Cancer Gene Ther 2003;10:918–25.
[13] Morishita N, Nakagami H, Morishita R, Takeda S, Mishima F, Terazono B, et al. Biochem Biophys Res Commun 2005;334:1121–6.
[14] Hayashi K, Moriya M, Sakamoto W, Yogo T. Chem Mater 2009;21:1318–25.
[15] Beyaz S, Tanrisever T, Kockar H. Macromol Res 2010;18:1154–9.
[16] Ko SW, Hong MK, Choi HJ, Ryu BH. IEEE Trans Magn 2009;45:2503–6.
[17] Cai J, Guo J, Ji M, Yang W, Wang C, Fu S. Colloid Polym Sci 2007;285:1607–15.
[18] Wan S, Huang J, Yan H, Liu K. J Mater Chem 2006;16:298–303.
[19] Marutani E, Yamamoto S, Ninjbadgar T, Tsujii Y, Fukuda T, Takano M. Polymer 2004;45:2231–5.
[20] Zhou Y, Wang S, Ding B, Yang Z. Chem Eng J 2008;138:578–85.
[21] Sun Y, Ding X, Zheng Z, Cheng X, Hu X, Peng Y. Eur Polym J 2007;43: 762–72.
[22] Heilmann SM, Rasmussen JK, Krepski LR. J Polym Sci A Polym Chem 2001;39: 3655–77.
[23] Guyomard A, Fournier D, Pascual S, Fontaine L, Bardeau J-F. Eur Polym J 2004; 40:2343–8.
[24] Fournier D, Pascual S, Montembault V, Haddleton DM, Fontaine L. J Comb Chem 2006;8:522–30.
[25] Lucchesi C, Pascual S, Dujardin G, Fontaine L. React Funct Polym 2008;68: 97–102.
[26] Drtina GJ, Heilmann SM, Moren DM, Rasmussen JK, Krespski LR, Smith HK, et al. Macromolecules 1996;29:4486–9.
[27] Tripp JA, Stein JA, Svec F, Fréchet JMJ. Org. Lett 2000;2:195–8.
[28] Tripp JA, Svec F, Fréchet JMJ. J Comb Chem 2001;3:216–23.
[29] Messman JM, Lokitz BS, Pickel JM, Kilbey II SM. Macromolecules 2009;42: 3933–41.
[30] Cullen SP, Mandel IC, Gopalan P. Langmuir 2008;24:13701–9.
[31] Coleman PL, Walker MW, Milbrath DS, Stauffer DM, Rasmussen JK, Krepski LR, et al. J Chromatogr A 1990;512:345–63.
[32] Ciampolini M, Nardi N. Inorg Chem 1966;5:41.
[33] Rutnakornpituk M, Puangsin N, Theamdee P, Rutnakornpituk B, Wichai U. Polymer 2011;52:987–95.
[34] Fournier D, Pascual S, Fontaine L. Macromolecules 2004;37:330–5.
[35] Ananthanawat C, Vilaivan T, Hoven VP, Su X. Biosens Bioelectron 2010;25: 1064–9.
[36] Huang B, Hou J, Lin S, Chen J, Hong H. Harmful Algae 2008;7:495–503.
[37] Masuko M. Nucleic Acids Res 2003;3:145–6.
[38] Perry-O'Keefe H, Rigby S, Oliveira K, Sørensen D, Stender H, Coull J, et al. J Microbiol Methods 2001;47:281–92.
[39] Singh JS. J Mol Struct 2008;876:127–33.
[40] Bomat-Miguel O, Tartaj P, Morales MP, Bonville P, Golla-Schindler U, Zhao XQ, et al. Small 2006;2:1476–83.
[41] Moisescu C, Bonneville S, Tobler D, Ardelean I, Benning LG. Mineral Mag 2008; 72:333–6.